Discovery and Characterization of a Novel Family of Human Ubiquitin Ligases termed Membrane Associated RING-CH (MARCH) Proteins

By

Eric Carter Bartee

A Dissertation Presented to the

Department of Molecular Microbiology and Immunology

And the

Oregon Health and Sciences University School of Medicine

In partial fulfillment of the requirements for the degree of

Doctor of Philosophy

June 2007

Oregon Health and Sciences University

School of Medicine

Certificate of Approval

This is to certify that the dissertation of

Eric Carter Bartee

Has been approved

Dr. Klaus Früh

Dr. Jay Nelson

Dr. Ann Hill

Dr. Svetlana Lutsenko

Dr. Mary Stenzel-Poore

Table of Contents

Acknowledgements

So many people and so little space.

I have to thank Klaus for being a wonderful mentor. You gave me the freedom to play around in science and discover my own way. No mentor could have done a better job, or been more enjoyable to work for. For that I sincerely thank you. I'd also like to thank the members of the Früh lab and our collaborators, who have created a wonderful work environment and managed to put up with my singing for six years.

However, not everything in this dissertation came about due to science, and I would never have been able to come this far without the loving support of my family Moo, Doo, and Loo as well as Granny and Grampa. You put up with me when I was not easy to put up with, and still managed to help me turn out…something less than evil. Now I've grown into a successful man for myself. I have to thank you for that, because it never would have happened with out you.

And of course, there is Mee. Six years of graduate school and you are the best thing to happen to me. You were always there when I needed a shoulder to cry on, or someone to listen to me vent. Always know that any success I might have could never happen without your love.

Abstract

Both poxviruses and γ2-herpesviruses share the K3-family of viral immune evasion proteins. These proteins are characterized by an amino-terminal RING-CH domain followed by two transmembrane domains. We analyzed several human homologues of the K3-family termed membrane-associated RING-CH (MARCH) proteins. All MARCH proteins localized to subcellular membranes while several reduced surface levels of known K3-family substrates. Thus, MARCH proteins appear to be structurally and functionally homologous to viral K3 proteins. One of the major challenges in determining the function of this family is the identification of their physiological substrates. To overcome this we created a quantitative proteomics approach which can be used to identify novel substrates for both the K3- and MARCH-families. Using stable isotope labeling by amino acids in cell culture, we compared the proteome of plasma membrane, golgi, and endoplasmic reticulum membranes in the presence and absence of K5 and MARCH-VIII. Quantitative mass spectrometric protein identification from these fractions revealed that CD316 (bone marrow stromal antigen 2), CD166 (activated leukocyte cell adhesion molecule) and syntaxin-4 were consistently underrepresented in the plasma membrane of K5 expressing cells, while CD44, CD81 (TAPA-1) and B-cell receptor-associated protein 31kDa (Bap31) were consistently underrepresented in the plasma membrane of MARCH-VIII expressing cells. Furthermore, downregulation of each of these proteins was independently confirmed. Our results both identify and characterize a novel family of human ubiquitin ligase enzymes and elucidate a novel technique which can analyze this family and be easily adapted to the analysis of other cellular enzymes viral immune modulators.

Chapter 1: Introduction

Viral Immune Evasion

Viruses are obligate intracellular parasites, which survive by infecting host cells and utilizing host machinery to proliferate and disperse. Host organisms have evolved a wide variety of defense mechanisms to counter these infections, including the innate and adaptive immune systems. In order to survive, viruses have developed an arsenal of immune evasions mechanisms to neutralize these defenses. While all viruses have some method of immune evasion, one family which is particularly efficient is the Herpesviridae. Herpesviruses are defiend by their structure (1). These viruses contain large dsDNA genomes which are contained inside a capsid in mature virions. These capsids are then encased in an amorphous tegument and surrounded by a lipid envelop. In addition to these structural characteristics, all examined herpesviruses share four additional properties: they all encode a significant number of enzymes, new synthesis of viral DNA occurs in the nucleus, production of viral progeny results in destruction of the infected cell, and all are able to exstablish a persistant or latent infection in their hosts (1). Herpesviruses are extremely common in nature with virtually every species infected with at least one herpesvirus. The family herpesviridae is divided into three subfamilies α- β- and γ-herpesviruses. α-herpesviruses are characterized by a wide species host range, short reproductive cycle and rapid spread in culture. Examples of human α-herpesviruses include HSV-1, HSV-2 (Herpes Simplex) and ZSV (Varicella-zoster). β-herpesviruses are characterized by a limited by non-exclusive host range and slow growth cycle. The major exmple of a human β-herpesvirus is HCMV (Human Cytomegalo Virus). γ-

herpesviruses are characterized by a host range exclusive to a single species. Two good examples of human γ-herpesviruses include EBV (Epstein Barr) and KSHV (Kaposis Sarcoma Associated Herpes) (1).

Herpesviruses use a variety of mechanisms to evade the host's immune response, including modulation of the major histocompatibility complex class I (MHC-I) pathway, evasion of natural killer (NK) cells, alteration of cytokine expression, and circumvention of the humoral response (2-4). Due to their efficient immune evasion, herpesviruses are able to establish long-term persistent or latent infections in the face of extremely robust immune responses. For example, human cytomegalovirus (HCMV) is able to establish a persistent/latent infection in humans despite 10% of all CD4+ and CD8+ memory T cells being specific to this single pathogen (5).

Evasion of the MHC-I antigen presentation pathway is particularly important to viral immune evasion. This pathway displays antigenic peptides from infecting viruses on the cell surface, allowing cytotoxic T-lymphocytes (CTL's) to monitor cells for viral infection. MHC-I is a dimer consisting of a heavy chain and light chain. The heavy chain is a 42kDa type-1 glycoprotein containing three Ig folds and two anti-parallel beta sheets, while the light chain is a 12kDa soluble protein known as beta-2 microglobulin (β_2M). The MHC-I pathway begins following proteolysis of proteins into 8-10 amino acid antigenic peptides in the cytoplasm. These peptides are translocated into the lumen of the endoplasmic reticulum (ER) via the TAP (transporter of antigenic peptides) complex, which consists of TAP1 and TAP2, and loaded onto MHC-I with the help of the molecular chaperones tapasin, protein disulfide isomerase, calnexin and calreticulin. Following peptide loading, MHC-I interacts with the B-cell receptor-associated protein

31kDa (Bap31) and traffics from the ER to the plasma membrane (6,7). Antigenic peptides, in the context of MHC-I, are then recognized by CD8+ CTL's which lyse infected cells, thus inhibiting viral spread.

Herpesviruses have evolved diverse mechanisms which inhibit MHC-I presentation. For example, EBNA-1, the major latent nuclear protein from Epstein-Barr virus, contains a 239 amino acid Gly-Ala repeat which inhibits EBNA-1's protealysis into antigenic peptides (8). In contrast, the ICP47 protein, from Herpes Simplex virus-1, inhibits antigenic peptide translocation through the TAP complex (9). The best examples of the diverse mechanisms herpesviruses use to evade MHC-I antigen presentation, however, are those found in the related viruses HCMV and MCMV (murine cytomegalovirus). HCMV encodes four related proteins, US2, US3, US6, and US11, which inhibit MHC-I antigen presentation via different mechanisms (US6 inhibits TAP (10), US3 retains MHC-I in the ER (11), US2 and US11 degrade MHC-I via the proteosome (12). In contrast to HCMV, the related mouse herpesvirus, MCMV, encodes three unrelated proteins, m4, m6 and m152, which also inhibit MHC-I presentation (m6 targets MHC-I for lysosomal destruction, (13), m152 retains MHC-I in the ER (14,15), and m4 traffics to the cell surface with MHC-I and inhibits CTL recognition by an unknown mechanism (16,17). Despite the different mechanisms used, both viruses successfully subvert the MHC-I pathway, inhibiting detection within host cells (18).

K3 and K5

Recently, several groups observed that cells infected with a γ2-herpesvirus, termed KSHV, displayed reduced surface expression of MHC-I (19,20). KSHV, also

known as HHV-8, is a fairly recently discovered human γ-herpesvirus which infects a variety of cell types, including endothelial cells, B cells, macrophages and hematopoeitic stems cells (21). KSHV is the etiological agent of several B cell proliferative disorders, including primary effusion lymphoma (PEL) and multicentric Castleman's disease (CD) (22), as well as a multifocal neoplasm known as Kaposi's sarcoma (KS) (22,23).

The mechanism of KSHV induced B cell disorders are fairly well understood. In B cell infections, KSHV exists mainly in a latent state. The viral DNA is maintained as an episome while only limited genes are highly expressed (24). CD is a polyclonal B cell proliferative disorder presumably driven by the secretion of vIL-6. In contrast, PELs are monoclonal B cell lymphomas derived from an individual B cell which is transformed by expression of viral genes including LANA (latency associated nuclear antigen) and the kaposins (25,26). LANA is a multifunctional protein which maintains the KSHV genome in an episomal state by tethering the viral DNA to the host chromosomes (27-29), inhibits cell death by altering p53 function (30), controls latent vs lytic infection by inhibiting the KHSV lytic activation Rta (31), and drives cells towards the S1 phase of the cell cycle (32,33).

Unlike KSHV induced B cell disorders, KS is an extremely complex disorder whose molecular mechanism are not yet completely understood. There are several known forms of KS, including classic KS which affects mainly elderly Mediterranean men, endemic KS which is found in sub-Saharan Africa and is more severe then classic KS, post transplant KS which occurs following treatment with immunosurppressive drugs, and epidemic KS which is extremely aggressive and found mainly in AIDS patients who have compromised immune systems. KS is normally characterized by the

formation of highly vascularized bruise-like lesions in the mouth or on the extremities (34). KS lesions contain a wide variety of cell types, including endothelial cells, infiltrating inflammatory cells, and KS spindle cells (34-37). The KS spindle cells, named for their distinctive spindle morphology, are considered to be the true tumor cells in KS (23,34,35). While the nature of KS spindle cells is still under debate, they are probably derived from several sources, including vascular endothelial cells and spindle shaped macrophagic cells (34-39). Spindle cells are the most common infected cells in KS tumors (40). At late stages of KS development, almost 60% of spindle cells stain positive for latent markers of KSHV infection such as LANA-1, v-flip, and v-cyclin (41). While almost no spindle cells stain positive for lytic KSHV markers, treatment with the viral inhibitor ganciclovir reduced the occurance of KS in patients infected with AIDS (42) suggesting that lytic KSHV infection plays a key role in KS tumor formation (43).

The reduction of MHC-I in KSHV infected cells was subsequently determined to be caused by expression of two KSHV open reading frames (ORFs), K3 and K5 (also known as MIR1 and MIR2), which are 40% identical to each other (19,20,44,45). Although K3 and K5 localize primarily to the ER (19,45,46), their expression did not alter synthesis of the MHC-I heavy chain, association of the heavy chain with β_2M, or loading of MHC-I with antigenic peptide (19,20,44). Instead, K3 and K5 directly bound to MHC-I in a post Golgi compartment (47). This interaction was mediated by the transmembrane domains of both K3/K5 and MHC-I and catalyzed the ubiquitination of lysines in the cytoplasmic tail of the MHC-I heavy chain (20,47-50) resulting in the rapid clathrin dependent endocytosis of MHC-I from the cell surface (19,20,47,51). Depletion of tsg101 (tumor susceptibility gene 101), which functions to sort ubiquitinated proteins

down the multivesicular body pathway (MVB), restored surface expression of MHC-I (47). Following endocytosis, internalized MHC-I colocalized with the lysosomal marker LAMP-2 and inhibition of lysosomal acidification restored MHC-I to the cell surface (19,20,45,52). These data led to the conclusion that, in the presence of K3 or K5, MHC-I was ubiquitinated, endocytosed, targeted down the MVB pathway, and degraded via lysosomal proteases.

Both the K3 and K5 genes encode type-3 integral membrane proteins, which contain two membrane spanning domains with the amino- and carboxy-Termini located in the cytoplasm (48). The amino-terminus of both K3 and K5 contains a series of conserved cysteines and histidines which form a RING-CH (really interesting new gene) domain (46,53). Hybrid molecules, in which the RING-CH domain and transmembrane domains of K3 were exchanged with those of K5, downregulated MHC-I (48), however, mutation of the conserved cysteines in the RING-CH domain or deletion of the transmembrane domains resulted in constructs which failed to downregulate MHC-I (45,47,48,54). These data suggest that the RING-CH domain and transmembrane domains of K3 and K5 are absolutely required to downregulate MHC-I and play a similar role in both proteins.

A role for the RING-CH domains of K3 and K5 as ubiquitin ligase (E3) domains was suggested following the observation that the purified RING-CH domain of K5 catalyzed the formation of high molecular weight ubiquitinated products *in vitro* (49). E3s provide specificity to the ubiquitin pathway by interacting with both substrates and ubiquitin conjugating (E2) enzymes. This interaction brings E2s into proper spatial orientation with each substrate, as well as catalyzing the transfer of ubiquitin from the E2

to the substrate via an unknown mechanism. K5 interacts with two E2s, UbcH5 and Ubc13. Depletion of UbcH5 completely inhibits ubiquitination and downregulation of MHC-I. In contrast, depletion of Ubc13 results in the addition of a monoubiquitin onto the MHC-I heavy chain, but not multiple ubiquitins (50). This monoubiquitinated MHC-I is removed from the cell surface and stored in intracellular vesicles. These data led to the hypothesis that K5 interacts with both UbcH5 and Ubc13 in a sequential fashion. An initial interaction, between K5 and Ubc13, catalyzes the monoubiquitination of MHC-I. This monoubiquitination leads to removal of MHC-I from the cell surface and storage in intracellular vesicles. A second interaction, between K5 and UbcH5, then catalyzes the addition of polyubiquitin onto intracellular MHC-I, resulting in lysosomal degradation.

While the carboxy-termini of K3 and K5 are largely divergent from one another, deletion of this region results in constructs which are unable to downregulate MHC-I (48,52). This effect was mapped to several small conserved regions, including two clusters of acidic amino acids, a potential tyrosine based sorting motif, and a small cluster of four conserved amino acids termed a NTRV motif (48,52). The acidic clusters of K5 likely function as binding sites for the adapter proteins PACS1 and PACS2 (52,55) which mediate retrograde trafficking from the endosomes to the transgolgi network (TGN), and from the TGN to the ER, respectively (56,57). This interaction is important for K5 function since overexpression of a PACS2 dominant negative inhibits some functions of K5 (55). While a function has not been proposed for either the putative tyrosine based sorting signal or the NTRV motif, mutation of either domain results in constructs which are unable to downregulate MHC-I (52), implying that these regions play vital roles in K5 function.

While both K3 and K5 degrade MHC-I, these genes likely play significantly different roles during viral infection. K3 is very efficient at removing all three MHC-I alleles (HLA-A, HLA-B, and HLA-C) from the cell surface, while K5 is generally less efficient and downregulates only HLA-A and HLA-B (19,20,54). Since removal of all MHC-I alleles from the cell surface can lead to activation of natural killer (NK) cells (58), the observation that K5 did not downregulate HLA-C led to the hypothesis that K5 played a role in evasion of NK cells (54). While cells expressing K5 could not be lysed by NK cells, surprisingly, cells expressing both K3 and K5 were equally resistant (54), suggesting that NK cell resistance was not due to the failure of K5 to downregulate HLA-C. This observation led to the discovery that, in addition to MHC-I, K5 degrades the T cell and NK cell costimulatory molecules ICAM-1 and B7.2 (49,51,54). Restoration of ICAM-1 and B7.2 surface expression, using dominant negative constructs of clathrin and dynamin or addition of the lysosomal inhibitor NH_4Cl, allowed for efficient NK mediated lysis of cells expressing K5 (51). These data suggest that K5 inhibits NK cell activation by downregulating ICAM-1 and B7.2 via the same mechanism as MHC-I (51,54).

The observation that K5 downregulated proteins besides MHC-I led to the hypothesis that K5 might have additional targets. In fact, a series of antibody-based screens which demonstrated that, in addition to MHC-I, K5 downregulated CD31 (55), while both K3 and K5 downregulated the interferon-γ receptor (Ifnγ-R) (59) and CD1d (60). The ability of K3 and K5 to downregulate their unique substrates is determined by each proteins transmembrane domains. However, each substrate must also contain a cytoplasmic lysine as a target for ubiquitination (47,60). The substrates extracellular region does not appear to play a significant role in substrate selection, since replacement

of the extracellular region of ICAM-1 or B7.2 with the extracellular region of the nonsubstrate protein CD8 did not alter K5 mediated downregulation (54).

While the observations above outline a basic mechanism for the function of K3 and K5 (51), many questions remain unanswered. For example, K5's downregulation of CD31 occurs through two distinct pathways (55). CD31 present on the cell surface prior to K5 expression is ubiquitinated and targeted down the MVB pathway for destruction in the lysosome. CD31 synthesized following K5 expression, however, is ubiquitinated in the ER and destroyed via a proteosomal mechanism. Treatment of cells with the proteosomal inhibitor lactacystin restored CD31 to the cell surface (55), suggesting that both mechanisms play a role in K5's ability to inhibit CD31 surface expression. Likewise, cleavage intermediates of the MHC-I heavy chain caused by expression of K3, could be stabilized by the addition of proteosome inhibitors (61) suggesting that the proteosome might play a role in K3 mediated degradation of MHC-I. The reason for this two-pronged approach, however, is currently unknown.

A second part of the K3/K5 mechanism which is not well understood is substrate selection. While this selection appears to be mediated mainly through the transmembrane domains, conserved features or motifs within these domains have not been determined which could mediate this selection. Additionally, other factors, such as proper subcellular localization also appear to play a critical role. For example, disrupting K5 localization using Brefeldin A or a dominant negative version of PACS2 inhibits downregulation of CD31 but not MHC-I (55). These data suggest that the substrate selection of K5 is influenced by PACS2 mediated localization.

Since an animal model does not exist for KSHV, K3 and K5's effect *in vivo* is difficult to determine. Both K3 and K5, however, are expressed in KSHV infected endothelial cells and B cells (44,46). *In vitro*, K5 expressing endothelial cells display a decreased ability to migrate during wound healing (55), while K5 expressing B cells fail to stimulate MHC-I or CD1d restricted T cells and do not respond to interferon-γ (51,59,60). Thus, K3 and K5 are likely to play a critical role in KSHV pathogenesis, this hypothesis has not yet been formally proven.

Homologues of K3 and K5 in other Viruses

Around the time that K3 and K5 were characterized, it was also observed that the KSHV homologue, murine γ2-herpesvirus 68 (MHV-68) downregulated the murine MHC-I molecule H2-D^b (62). This downregulation was caused by expression of the MHV-68 ORF MK3. Interestingly, MK3 shares limited homology with KSHV-K3. MK3 contains both an amino-terminal RING-CH domain and two transmembrane domains, and expression of MK3 results in the direct ubiquitination and destruction of H2-D^b molecules (63). However, while MK3 appears to be a structural and functional homologue of KSHV-K3, the mechanism MK3 uses to downregulate MHC-I appears to be very different. For instance, the carboxy-terminus of MK3 interacts with several proteins involved in MHC-I peptide loading including TAP1, TAP2, and Tapasin (64-67). Since MK3 mutants which fail to associate with TAP/Tapasin are unable to degrade H2-D^b (66,67), and H2-D^b mutants which fail to interact with TAP/Tapasin are not degraded by MK3 (66), the peptide loading complex appears to act as a bridge between MK3 and H2-D^b (66). Additionally, MK3 mediated ubiquitination of H2-D^b can occur

on serine, threonine, or lysine residues (68), and MK3 degrades H2-D^b molecules via the proteosome before they traffic through the Golgi (62,63,66). MK3 also interacts with several proteins in the ER associated degradation (ERAD) pathway, including Derlin1, VIMP, and p97(69). The ERAD pathway functions to degrade terminally misfolded proteins. Proteins unable to fold properly in the ER are ubiquitinated and translocated back to the cytoplasm, primarily through the SEC61 translocon, where these proteins are degraded via the proteosome (70-72). Inhibition of the ERAD pathway inhibits MK3 mediated degradation of H2-D^b (69), suggesting that, despite structural homology to KSHV-K3, MK3 degrades MHC-I via a mechanism closer to US2 and US11 (12,73).

While most viral ORF's targeting MHC-I are highly virus specific, homologues of K3 and K5 are found in several members of the γ2-herpesviridae as well as the unrelated poxviridae (74). Like herpesviruses, poxviruses are large ssDNA viruses encoding a variety of enzymes and surrounded by a amorphous tegument and host derived envelope. Unlike herpesviruses, however, poxviruses replicate exclusively in the cytoplasm and infection results exclusively in an extremely rapid lytic replication cycle (1). In fact, despite both being dsDNA viruses, herpesviruses and poxviruses are relatively unrelated to each other (75). Like MK3, these ORF's share limited primary homology but contain an amino-terminal RING-CH domain and two predicted transmembrane domains. Only one of these homologues, the ORF M153R encoded by the rabbit poxvirus myxoma, has been analyzed. Expression of M153R downregulated MHC-I, CD4 and Fas via the same mechanism as K5 (76,77), while deletion of M153R from myxoma resulted in decreased viral virulence *in vivo.* Thus, several unrelated viral families encode structural and

functional homologues of K3. These proteins define the K3-family of viral immune evasion molecules.

The Ubiquitin System and the Multivesicular Body Pathway

Ubiquitin is a 76 amino acid soluble protein named for its ubiquitous expression. The ubiquitin system was originally characterized for playing a role in protein degradation (78,79). There are four basic components of the ubiquitin system: ubiquitin, a single ubiquitin activating enzyme (E1), a series of E2s and a wide array of E3s. Upon initiation of the ubiquitin pathway, ubiquitin forms a thioester linkage with the active cysteine on E1. This activated ubiquitin is then transferred via a trans(thio)esterification reaction onto the active cysteine of a cellular E2. An E3 then links this E2:ubiquitin conjugate to a specific substrate and catalyzes the transfer of ubiquitin from the E2 onto lysine residues in the substrate. This initial conjugation of ubiquitin then frequently leads to the formation of large polyubiquitin chains (80-83) (reviewed in (84)).

Historically, modification with ubiquitin was proposed to result in proteolysis of the modified protein by the 26S proteosome. Recently evidence, however, suggests that ubiquitination plays an important role in a variety of cellular processes, including cell cycle control (85), DNA repair (86), signaling (87), and protein destruction via the lysosome (88-90). Ubiquitinated transmembrane proteins destined for lysosomal destruction are frequently targeted down the MVB pathway (reviewed in (91)). Targeting down this pathway is mediated by a series of three multiprotein ESCRT (endosomal sorting complex required for transport) complexes. ESCRT-I, in conjunction with the ubiquitin interacting proteins, Vps27/HRS and Hse1, binds directly to

ubiquitinated transmembrane proteins through ubiquitin interacting motifs in both Vps27/HRS and Hse1. ESCRT-I then recruits ESCRT-II whose main function appears to be the recruitment and organization of ESCRT-III. ESCRT-III catalyzes the invagination and pinching off of the limiting endosomal membrane to form a small vesicle within a larger vesicle, or a multivesicular body. Following release of ESCRT-I, -II, and –III from the MVB membrane by the AAA-type ATPase Vps4, the outer MVB membrane fuses with a lysosome, allowing for degradation of the inner vesicle by lysosomal proteases.

Ubiquitin Ligases (E3)

Due to the complexity of the ubiquitin system proper ubiquitin regulation is critical to cell survival. Due to the lack of variety in ubiquitin, E1 and E2s (92), most of this regulation is carried out by E3s (93). There are around 500 known E3s. This makes E3s one of the most numerous enzymes families. The importance of E3s is clearly demonstrated by the number of diseases resulting from misregulation of these enzymes, including Parkinsons (94), Fanconi Anemia (95), prion diseases (96), as well as numerous examples in a wide variety of cancers (97-99). Most E3s fall into one of three families: Fbox/SCF complexes, HECT (Homologous to E6-Associated Protein carboxy-Terminus) domain containing proteins, and RING domain containing proteins. Fbox/SCF complexes are multiprotein complexes which function as single E3s (100). In contrast, HECT domains and RING domains are individual protein domains defined by a unique amino acid sequence. The HECT domain is a large 336 amino acid domain with a defined tertiary fold (Uniprot), while the RING domain is a small (20-50 amino acid) zinc binding domain characterized by a series of conserved cysteines and histidines (53).

While HECT domains are not very common, the RING domain is extremely widespread with over 500 known human RING containing proteins (Uniprot).

HECT domains are always found at a proteins carboxy-terminus and contain two large loops connected by a flexible linker (101-103). The first loop contains a low affinity E2 binding site while the second loop contains an active cysteine. The remaining amino-terminus of the HECT domain containing protein is involved in substrate selection and recruitment. The low affinity of the HECT domain E2 binding site suggests that several rounds of E2-E3 interaction are probably required for successful ubiquitination (104). HECT domain containing E3s catalyze ubiquitination directly by enzymatically transferring ubiquitin from a bound E2 to the active cysteines on the second loop of the HECT domain. This ubiquitin is then transferred from the HECT domain E3 enzymes to the substrate.

RING domains, which can be found at any location in a protein, coordinate two zinc ions with a cross braced structure (53). RING domain containing E3s bind E2s through a groove formed by this coordination of zinc. However, unlike HECT domain containing E3s, RING domain containing E3s do not appear to form a ubiquitin-E3 intermediate. The mechanism by which RING domain containing E3s catalyze ubiquitination is still unknown. One possiblility is that these E3s merely serve as a bridge to bring substrates into the proper spacial orientation for ubiquitination to occur. Mutations in several RING E3s which abolish substrate selection, however, only moderately reduce these E3s catalytic activitiy (105,106). Thus, the exact mechanism by which RING domains catalyze ubiquitination is currently only poorly understood.

Statement of Purpose & Hypothesis

This work was initiated to identify the origins of the K3-family of genes found in the herpesviridae and poxviridae. Since the K3-family of genes is conserved across multiple members of two diverse viral families, it is unlikely that each virus evolved these genes separately (46,74,107,108). Since the K3-family of genes is limited to distinct subgroups within each viral family, however, it is equally unlikely that these genes represent remnants of a common viral ancestor. Since both the herpesviridae and poxviridae are known to acquire genes, including E3s, from their hosts (106,109-115) (reviewed in (116)), and K3 and K5 are found in a region of the KSHV genome which is rich in cellular homologues (110), we hypothesized that each virus had acquired its K3-family gene from its host. This hypothesis predicted the existence of previously uncharacterized cellular homologues of the K3-family in the genomes of viral hosts, such as humans. The purpose of this work was to identify these cellular homologues and characterize their function.

Chapter 2: Relevant Techniques

Proteomics and the Ubiquitin Pathway

The sequencing of the human genome has simplified the identification of proteins containing HECT and RING domains. Novel proteins containing these domains are frequently involved in ubiquitination. Additionally, well characterized *in vitro* assays allow investigators to rapidly establish if a HECT or RING domain containing protein is an active E3. Identifying the substrates recognized by these E3s, however, is much more difficult. Despite a wide range of techniques being used to link novel E3s with their physiological substrates, numerous examples now exist of E3s being proposed without the identification of a corresponding substrate (117-120). The most common methods to identify E3 substrates center on purifying each potential substrate via its direct interaction with the E3. These techniques, however, require the substrate:E3 interaction be strong enough and abundant enough to survive the purification process (121),(122). Along with potential substrates, these studies also occasionally discover non-substrate proteins which interact with an individual E3 enzyme (69). While identification of these proteins helps determine the mechanism used by a specific E3, such identifications do not usually help determine direct substrates.

Recently, proteomics has been used to discover potential E3 substrates. For example, Su et al used a prokaryotic ubiquitination screen to determine that RhoGDI was a novel substrate for the E3 enzyme GRAIL (Gene Related to Anergy In Lymphocytes) (122). This technique reconstituted the entire ubiquitin system in bacterial cells and then screened a cDNA library for ubiquitinated proteins. In contrast, Ayad et al elucidated

novel substrates for the Anaphase Promoting Complex by reconstituting the entire ubiquitin system *in vitro* (123). These techniques, however, can only analyze soluble E3s and require a proper E3:substrate interaction to occur outside of a physiological setting.

Two Dimensional-PAGE

Ideally, screens for novel E3 substrates allow each E3 to remain in a physiological setting while still analyzing large portions of the proteome simultaneously. One technique that fits these criteria is two-dimensional polyacrylamide gel electrophoresis (2D-PAGE) (124,125). Originated in 1975 (126), 2D-PAGE separates complex protein samples based on two sequential criteria. First, 2D-PAGE separates proteins based on their isoelectric point (pI), the pH at which a protein does not contain a net charge. Following this initial separation, 2D-PAGE then separates proteins based on their molecular weight (MW). Most uses of 2D-PAGE fall into one of two categories. Individual 2D-PAGE gels can fully separate complex protein samples allowing for identification of hypothetical proteins (127) and mapping of novel proteomes (128-131). In contrast, replicate 2D-PAGE gels can be used to analyze differential protein expression. This comparative 2D-PAGE is particularly powerful since due to the simultaneous analysis of protein expression and post-translational modifications (132). Comparative 2D-PAGE has been used to discover cellular changes induced by a wide variety of stimuli, including responses to drug treatment and viral infection (133-135), as well as changes induced by certain cancers (136,137). Additionally, several groups have used 2D-PAGE to analyze the ubiquitin pathway by identifying novel E3 substrates (138-140), and modification of proteins in the ubiquitin cascade (141,142).

Quantitative Mass Spectroscopy

A second method to analyze complex protein samples is to link the separating power of liquid chromatography (LC) with the analyzing power of the mass spectrometer (reviewed in (143,144)). LC is a general term for any separation chemistry which takes place in the liquid state including anion and cation exchange, reverse phase, and size exclusion (145). Each type of LC separates samples using different chemical properties, allowing researchers to tailor sample separation to their specific needs. Since all LC occurs in the liquid phase, multiple forms of LC can be run sequentially (LC/LC) (145). The resolving power of LC/LC is roughly equal to the product of the resolving powers of the two individual LC steps used, allowing for comprehensive separation of extremely complex samples (145,146).

The mass spectrometer is a name given to a family of instruments which measure the mass/charge (m/z) ratio of ionized molecules. Computer programs then match the observed m/z ratio of each particle to m/z's predicted for known peptides (147), allowing for identification of individual peptides contained within the analyzed sample (146). Mass spectrometers consist of two basic parts; an ionization source which creates ionic particles, and a mass analyzer which determines the m/z ratio of these particles (148). Since some of the ionization sources used in mass spectrometers are compatible with LC, samples separated via LC/LC can be directly analyzed via mass spectroscopy (MS) (146). The combination of liquid chromatography followed by mass spectroscopy (LC/MS) has been widely successful in analyzing complex biological processes including ubiquitination (149-154).

Recent advances also allow MS to determine the relative abundance of individual proteins identified in two protein samples (155-157) (reviewed in (158)). This quantitative MS relies upon the incorporation of isotopic labels into each protein sample. The mass spectrometer can identify each differential label, and computer programs can quantitate the amount of each peptide present. These data can then be used to determine the relative amounts of a specific protein present in each sample (159,160). The major difference between methods utilizing this technique is how they incorporate the isotopic label. ICAT (isotope coded affinity tagging), and the related technique iTraq, use reactive chemistry within each protein to incorporate the isotopic label (156). ICAT and iTraq have the advantage that they add a label onto preformed proteins, allowing these techniques to be used on samples which cannot be easily manipulated, such as tissue or serum. ICAT has been employed to analyze differential protein expression in many systems, including Huntington's disease (161), sickle cell anemia (162), pancreatic cancer (163), and breast cancer (164). However, ICAT is limited to proteins that can be labeled with the chosen chemistry (165). The most common chemistry used in ICAT is cysteine reactive, which excludes proteins without available reactive cysteines. iTraq is a relatively new technique which overcomes this problem by using an amine reactive chemistry to bind an isotopic label onto the amino-Terminus of all tryptic peptides (157).

Both ICAT and iTraq are best utilized in systems where proteins are not synthesized or turned over during the course of the experiment. For experiments done in cell culture, however, the preferred method of isotopic labeling is SILAC (stable isotope labeling with amino acids in cell culture) (155). In SILAC, one sample of cells is grown in media spiked with isotopically 'heavy' amino acids (C^{13} and N^{15}), while a second

sample is grown in isotopically 'light' amino acids (C^{12} and N^{14}). These amino acids are metabolically incorporated into cellular proteins as they are synthesized. Each protein labeled with SILAC contains an endogenous isotopic label, eliminating the need to label samples with reactive chemistry. SILAC has been used to determine relative protein abundance in yeast, plant and human systems (166-168).

2D-PAGE has two major advantages over LC/MS. The first is that the ability of 2D-PAGE to analyze post-translational modifications. Since many post-translational modifications do not significantly alter a proteins MW, it can be difficult to analyze these modifications using standard 1D-PAGE analysis. However, the ability of 2D-PAGE to analyze both MW and pI simultaneously allows it to detect many modifications which might otherwise be missed. In contrast, MS analyzes only select peptides from each protein. This incomplete coverage limits MS analysis of post-translational modifications to peptides recovered peptides which frequently represent less than 20% of the total protein. Additionally, since MS based peptide identification works using a 'best fit' model, it is impossible for MS to analyze unknown or unanticipated post-translational modifications, even if these modifications occur on recovered peptides. The second advantage of 2D-PAGE is that this technique is far more accurate for protein quantitation. Analysis of proteins displaying differential expression using 2D-PAGE results in different intensity spots which each represent a significant amount of protein. The differences between these spots can be easily analyzed and quantified using either the naked eye or commercially available analysis software. In contrast, LC/MS quantitation relies on complex software algorithms which cannot be easily confirmed. Additionally,

the minute quantities of peptide which is quantitated during MS analysis results in extremely inaccurate quantitation.

Despite the power of 2D-PAGE in analyzing complex samples, this technique is limited by several inherent restrictions. First is that 2D-PAGE requires proteins to remain soluble through both the first and second dimension separation steps (169). Unfortunately, many large or hydrophobic proteins are not soluble under the conditions required for 2D-PAGE. The lack of protein solubility during 2D-PAGE is particularly problematic when attempting to use 2D-PAGE to identify ubiquitinated proteins, since the addition of polyubiquitin tends to make proteins large and highly insoluble. A second limitation is that 2D-PAGE is useful over only a small dynamic range of protein expression. Regardless of protein input, only the most abundant proteins in a sample are observed in 2D-PAGE (170), largely due to the requirement that proteins separated via 2D-PAGE must be visualized before they can be analyzed. Silver staining, the most common method used to visualize proteins separated by 2D-PAGE, detects linear protein expression over less than one order of magnitude (171). A final constraint is that the fist dimension separation step of 2D-PAGE is unable to resolve highly acidic or basic proteins, which is particularly problematic when analyzing post-translational modifications, which often shift a protein to a more acidic pI. These limitations restrict most 2D-PAGE experiments to highly soluble, highly abundant proteins, with an isoelectric point between 3 and 9 (172).

Like 2D-PAGE, LC/MS analysis has several inherent advantages. The first is that LC/MS analysis results in the direct identification of each protein analyzed. In contrast, 2D-PAGE requires researchers to identify each spot in their analysis separately. Since

2D-PAGE can analyze from several hundred to a thousand spots simultaneously this separate identification step can represent a significant investment of both time and resources. A second advantage of LC/MS is that it has a much larger dynamic range than 2D-PAGE. By using exhaustive separation of samples prior to analysis it is possible to analyze virtually every protein in samples as complex as a yeast whole cell extract. This level of proteome coverage is simply not available using 2D-PAGE analysis. Finally, LC/MS is not subject to the solubility or acidity issues which plague 2D-PAGE. Since the separation steps for most MS analysis occurs in the liquid phase, virtually any protein which can be made soluble can be analyzed using LC/MS. One caveat to this is that certain peptides will be incompatible with certain forms of LC separation. For example, highly hydrophobic peptides, such as those deriving from with a proteins transmembrane region, are extremely difficult to remove from a reverse phase column. In general, however, many fewer proteins and peptides are excluded during LC/MS analysis then would be excluded during standard 2D-PAGE.

Most quantitative proteomics techniques are designed to monitor global changes in protein expression. While braod analysis has led to a better understanding of certain cellular processes, such as the general role of ubiquitin, it does not necessarily lend itself to analysis of individual enzymes, such as E3s. Since individual E3s have limited substrate specificity, using proteomic techniques to identify these substrates can prove extremely challenging. No technique is currently available which has proven successful in identifying substrates for a wide variety of novel E3s.

Chapter 3: Discovery of MARCH proteins[1]

Introduction

Ubiquitination plays a central role in diverse cellular functions, many of which are the consequence of ubiquitin-mediated proteosomal degradation (173). However, ubiquitination also regulates the sorting of proteins along the endocytic route to lysosomes (174). Protein targets are selected for ubiquitination by ubiquitin-ligases (E3s). E3s simultaneously interact with a substrate and an ubiquitin conjugating enzyme (E2s), which receive activated ubiquitin from the ubiquitin activating enzyme (E1). Two major families of E3s contain HECT-domains (homologous to E6 AP c-terminus) and RING-domains (really interesting new gene) (175). The RING-domain belongs to a large class of zinc finger motifs that is characterized by a conserved series of cysteines and histidines: the RING-finger (C3HC4), the RING-H2-finger (C3H2C3), the LIM-finger (C2HC5) and the TRIAD-finger (C6HC). A motif structurally related to the RING-finger is the plant homeo domain (PHD) or leukemia-associated protein domain (LAP) (176,177) which is characterized by the C4HC3-sequence. A subfamily of the PHD/LAP domain, termed BKS domain, was discovered in γ2-herpesviruses and poxvirus as well as several eukaryotic genomes (110). Yeast contains a single protein with this motif, SSM4 or Doa10. SSM4 is responsible for the ER-associated degradation of a subclass of

[1] This chapter has been previously published under the following reference:
Bartee E, Mansouri M, Hovey Nerenberg BT, Gouveia K, Früh K. Downregulation of cell surface glycoproteins by a family of human ubiquitin ligases homologous to viral immune evasion proteins. J Virol. 2004 Jan;78(3):1109-1120.
All data included in this thesis is my work except where noted by footnote.

hydrophobic proteins by the proteosome (178). The BKS-domain of this protein was further shown to act as an ubiquitin ligase *in vitro*. Given both the sequence and functional similarity to the RING- and RING-H2 domain, it has been proposed to rename the BKS subtype of PHD/LAP motifs as RING-CH (178), a nomenclature adopted in this thesis.

The two RING-CH proteins, K3 and K5, in the genome of Kaposi's sarcoma associated herpesvirus (KSHV), as well as the single K3-gene of murine γ2-herpesvirus 68 (MHV68) were determined by several groups to encode proteins that inhibit the surface expression of major histocompatibility complex class I (MHC-I) molecules (19,20,62). In addition to MHC-I, K5 was found to downregulate surface expression of the co-stimulatory molecules ICAM-1 and B7.2 (51,54). Sequences homologous to the γ2-herpesvirus RING-CH proteins are present in poxvirus genomes (110) and the myxomavirus homologue M153R downregulates MHC-I and CD4 by a similar mechanism as the herpesviral proteins (76,77). Thus γ2-herpesviruses and poxvirus share a family of immune evasion proteins. Several names have been suggested for this family such as modulators of immune recognition (MIR) (49), Scrapins (76), or K3-family (74).

Target molecules for the K3-family are rapidly internalized from the cell surface and destroyed in the lysosomes (19,20,77). A notable exception is MK3 which associates with MHC-I during peptide loading and causes MHC-I to be degraded by the proteosome (63,66,179). K3-family proteins require lysines in the cytoplasmic tail of their target molecules for downregulation and MHC-I, CD4 and B7.2 are ubiquitinated in cells transfected with K3 proteins (47,49,63,77). Moreover, since the isolated RING-CH-domain of several K3-family protein was shown to display ubiquitin ligase activity *in*

vitro, it was proposed that this family of RING-CH proteins act as E3s that mediate the ubiquitination of the cytosolic tails of target transmembrane proteins (49,63,77).

The viral RING-CH proteins likely originated from eukaryotic hosts since poxviruses and herpesviruses are unrelated viral families. Several examples exist for host-related immune evasion genes shared between herpesviruses and poxviruses (180). Moreover, the existence of genes homologous to K3 and K5 in the genomes of lower eukaryotes was noted by Nicholas et al upon completion of the sequence for the corresponding region of the KSHV genome (110). Furthermore, several investigators described K3-related genes in mammalian genomes that are related to K3 family of viral proteins (109). One of these homologous proteins, termed c-Mir, was recently shown to downregulate B7.2 in a manner very similar to K5 (181). In contrast to the viral K3-family proteins, however, c-Mir was unable to reduce the surface expression of MHC-I (181). In addition to c-MIR, I identified eight additional RING-CH proteins related to the viral proteins. The characterization of several members of this family, termed membrane associated RING-CH proteins (MARCH) revealed that MARCH-IV and -IX effectively reduced the surface expression of MHC-I but not B7.2. I further report that MHC-I is ubiquitinated and internalized in a lysine-dependent manner in the presence of MARCH-IV and -IX. To our knowledge these are the first cellular gene products identified that downregulate surface expression of MHC-I. These data suggest that the viral K3-family was derived from MARCH-related proteins, a protein family that seems to regulate endocytosis of cell surface receptors via ubiquitination.

Materials and Methods

Reagents

Conanamycin A (Sigma) and lactacystin (Boston Biochem) were used at 50nM and 20 μM, respectively. Protein A/G beads were from Santa Cruz Biotechnology. Antibodies: AP-1 (Sigma), K455 (from Per A. Peterson), anti-Fas (Pharmingen), anti-TfR (US Biologicals), anti-B7.1 (Pharmingen), anti-B7.2 (Pharmingen), anti-FLAG (Sigma), P4D1 (Santa Cruz), anti-EEA-1 (BD Transduction Labs), anti-Golgin-97 (Molecular Probes), anti-Calnexin (Stressgen), anti-Flag:FitC (Sigma), anti-LAMP-1 (University of Iowa). Hybridomas for W6/32, BB7.2 and OKT4 were obtained from ATCC and grown in house. HeLa cells used in this study were stably transfected with tet-transactivator (Clontech).

Plasmids:

CDNA for B7.1 was isolated from B7.1/pRMHa3 (from Lars Karlsson) and inserted into pUHD10.1. B7.2 (181) was obtained from Satoshi Ishido, A2.1 and CD4 wildtype and lysine mutants were described in (77), vps4 wildtype and vps4-EQ mutant were obtained from Phillip Woodman (182). MARCH-I cDNA was a gift from Sumio Sugano (cDNA FLJ20668, clone KAIA585). cDNAs for MARCH-II, MARCH-V, MARCH-VII, MARCH-VIII and both splice variants of MARCH-IX were obtained via the IMAGE consortium (clone IDs 24525, 3905766, 3449089, and 4830278, 4811410, 3936171 respectively). MARCH-IV cDNA was obtained from the Kazusa DNA Research Institute (clone KIAA1399). Each MARCH gene was amplified via PCR both with and without a carboxy-terminal FLAG epitope tag using suitable primers. The PCR products were digested with appropriate restriction enzymes and ligated into either the

pUHD10-1 or tet-regulatable pUHG10-3 vector (183). The amino-terminal portions including the RING-CH domains of selected MARCH-I, II, IV, VIII, and IX were fused to GFP using pGEX-4T-1 vector (AP Biotech).

Deletion constructs of MARCH-IV were created by amplifying the corresponding region of the MARCH-IV mRNA via PCR using suitable primers both with and without a carboxy-Terminal FLAG epitope tag. PCR products were digested with appropriate restriction enzymes and ligated into the pUHD10-1 vector.

Real-Time PCR

Short (50-100bp) fragments from MARCH-I, MARCH-II, MARCH-IV, MARCH-VIII and two splice variants of MARCH-IX cDNA were amplified via PCR using appropriate primers. The PCR reaction was carried out in the following buffer: 1x SYBR Green PCR Buffer (PE Biosystems), 3mM $MgCl_2$, .8mM dNTP's, .625U Amplitaq Gold (PE Biosystems), .01µl Amperase (PE Biosystems), and 50nM primers. 23µl buffer was added to 2µl template cDNA and run under the following conditions: 95^0C for 10min, followed by 40 cycles of 95^0C for 15 seconds, 60^0C for 1 minute. Amplification was tracked via CYBR-Green (PE Biosystems) incorporation using an ABI-PRISM 7700 Sequence Detection System (Applied Biosystems, Foster City, CA). Absolute standards were generated using known quantities of cloned MARCH cDNA's.

Uptake Assay

Uptake of MHC-I was measured as previously described (77). In short, 24 hours post-transfection, HeLa cells were washed and the polyclonal anti- human MHC-I

antiserum K455 (1:100) was allowed to bind for 30min at 4^0C. Cells were washed with PBS and either fixed immediately in 2% paraformaldehyde or incubated in fresh growth media at 37^0C for 120 minutes to allow uptake of antibody bound MHC-I. K455 was visualized with Alexaflour:594 conjugated goat anti-rabbit secondary antibody (Molecular Probes).

Immune Fluorescence and flowcytometry

For flowcytometry, cells were trypsinized, washed with ice-cold PBS, and incubated with appropriate antibodies for 30 min at 4^oC. After washing several times in PBS, cells were incubated with PE-conjugated goat anti-mouse secondary antibody (DAKO) and washed again before analysis with a FACScalibur flowcytometer (BD Biosciences).

Immune fluorescence was described previously (77). In short, cells were plated on glass coverslips (Fisher), transfected for 24 hours, fixed with 2% paraformaldehyde, permeabilized with 0.2% triton and blocked with 3% BSA and 0.5% fish gelatin. After staining with primary antibody and secondary antibodies for at least 30 min at 37^0C, coverslips were mounted on slides and covered with Vectashield H-1200 + DAPI (Vector Laboratories). All pictures were taken in monochrome; contrast enhanced, and artificially colored using Openlab software (Improvision).

Metabolic labeling, Immunoprecipitation and Western Blotting

After starving in methionine-free medium for 30 minutes, HeLa transfectants were metabolically labeled with ^{35}S-cysteine/^{35}S-methionine (250 μCi, Amersham) for 15

min. Labeled cells were washed twice with PBS and either lysed immediately in PBS containing 1% Triton X-100 and protease inhibitors (Roche), or the label was chased with excess (2mM) unlabeled cysteine and methionine for the indicated time. Lactacycstine or ConA were present throughout starvation, labeling and chase. Lysates were precleared with protein A/G agarose beads and incubated with 3μg of antibody for 1 hr and followed by 2 hours incubation with protein A/G beads. Immunoprecipated proteins were washed five times with 0.1% Triton X-100 in PBS. Samples were treated with Endoglycosidase H (Roche) according to manufacturer's instructions prior to boiling in SDS buffer and analyzed by SDS-PAGE gel electrophoresis. Re-immunoprecipitation experiments were as described (77).

For immunoblotting of unlabeled immunoprecipitates, I used the WesternBreeze Chemiluminescent Detection System (Invitrogen) following Semi-dry transfer to PVDF membranes (Millipore).

Ubiquitination assay

UbcH2 and UbcH3 were obtained from Boston Biochem. $(His)_6$-UbcH5a was obtained from Roger Everettt, expressed in BL21-DE3 cells (Stratagene) and purified as previously described (115). Purified E2 proteins were stored at -80^0C. E3 proteins were purified as described (77) and stored at 4^0C. *In vitro* reaction mixtures (20μl total) included: 50nM rabbit E1 (Boston Biochem), 28μM Ubiquitin, 5mM ATP, 50mM Tris-HCl pH 7.5, 50mM NaCl, and 2mM DTT. E2 enzymes were used at concentrations varying from 0.1 to 2.3μM, and E3 concentrations ranged from 3 to 30μM. After 90 minutes of incubation at 30^0C, reactions were stopped by boiling in SDS sample buffer.

Samples were electrophoresed through 12% polyacrylamide SDS gels and immunoblotted using anti-ubiquitin antibody P4D1.

Results

Mammalian K3-family homologues

Hallmarks of the viral K3-family are an amino-terminal RING-CH domain followed by two transmembrane domains. Using the RING-CH domain of K3 and K5 I searched the Genbank database using BLAST 2.0. Nine hypothetical human proteins of unknown function were identified that display RING-CH domains followed by two or more predicted transmembrane domains (Fig. 1). We propose to name this mammalian gene family Membrane Associated RING-CH (MARCH) proteins. MARCH-VI, also called TEB-4, contained twelve predicted TM-domains and is the predicted homologue of yeast SSM4/Doa10 (178). MARCH-V is predicted to contain four transmembrane domains. In the remaining seven predicted proteins, the RING-CH domain is followed by two predicted transmembrane domains. MARCH-VII has an aminoterminal extension of about 500 amino-acids prior to the RING-CH-domain and is only distantly related to the other MARCH-proteins. Phylogenetic analysis reveals that the remaining six two-transmembrane proteins occur as three pairs that are closely related: MARCH-I and -VIII, MARCH-II and -III, MARCH-IV and -IX. MARCH-VIII is identical to the previously characterized c-MIR (181). The primary structure and topology of the viral K3-proteins, which all display short amino-termini containing the RING-CH domain succeeded by two transmembrane domains, is thus most closely related to these six MARCH proteins.

Tissue specific expression of MARCH proteins

To investigate whether MARCH protein expression is ubiquitous or tissue-specific, I performed real-time RT-PCR using primers specific for MARCH-I, -II, -IV, and -VIII and both splice variants of -IX on a panel of human tissue samples (Fig. 2). The most abundant expression was observed for MARCH-II and -IX which were expressed in every tissue analyzed at high copy numbers (note the different scale). The most restricted expression was observed for MARCH-IV which was mainly expressed in brain and placenta. Transcripts for the other three MARCH proteins tested were detected in only some tissues and at generally lower levels. These data indicate both a tissue-specific and a wide-spread expression of MARCH proteins.

Subcellular localization of MARCH proteins

The predicted transmembrane domains implied that MARCH proteins localize to membranous compartments. To determine their subcellular localization I transfected HeLa cells with FLAG-tagged cDNA constructs for MARCH-I, -II, -III, -IV, -V, -VIII, and -IX. Cells were analyzed by immunofluorescence using anti-FLAG together with antibodies to various markers of subcellular compartments (Fig. 3). MARCH-I, -III, and -VIII showed a distinct punctuate staining pattern that partially overlapped with endocytic or lysosomal vesicles. MARCH-II and -V showed an ER-like staining pattern that overlapped with calnexin staining (staining a). In some cells however, MARCH-II showed a vesicular staining that did not overlap with calnexin but co-stained partially with Lamp (staining b). The reason for these mutually exclusive patterns is currently not

known. MARCH-IV and -IX co-stained with the Golgi-markers Golgin or the trans-Golgi marker AP-1, respectively. The staining pattern observed for most of the MARCH proteins is thus quite distinct from the ER-staining observed for the γ2-herpesvirus and poxvirus proteins (45,49,77) but is consistent with MARCH proteins being associated with subcellular membranes.

Ubiquitin-ligase activity of the RING-CH domains of MARCH proteins

The predicted RING-CH domain implies ubiquitin ligase activity of MARCH proteins. RING-E3s are known to catalyze the formation of ubiquitin-adducts *in vitro* when co-incubated with ubiquitin, ATP, E1, and an appropriate E2 (175). Using purified GST-fusion proteins, I examined if the RING-CH domains of MARCH-I, -II, -IV, -VIII and -IX act as ubiquitin ligases *in vitro.* These RING-CH domains were selected because the corresponding MARCH proteins downregulated cell surface glycoproteins as discussed in the next paragraph. The purified proteins were incubated with ubiquitin, ATP, and E1 together with E2. Immunoblotting with antibodies against ubiquitin revealed that the RING-CH-GST fusion proteins of four MARCH proteins were able to catalyze the formation of high-molecular weight molecular ubiquitin complexes in the presence of ubcH2, ubcH3 or ubcH5a (Fig. 4). Despite its high homology to MARCH-IV, MARCH-IX did not mediate ubiquitination with any of the E2s shown in Fig. 4 or with UbcH6, UbcH7, MmUbc6 or MmUbc7 (data not shown). However, since MARCH proteins showed a distinct specificity for individual E2 enzymes even when their RING-CH domains were closely related (e.g. MARCH-I and -VIII), the latter observation does not contradict a ubiquitin ligase function for MARCH-IX. More likely, MARCH-IX was

unable to function with the panel of E2 tested. Ubiquitin complexes were not detected in the absence of MARCH proteins or in the presence of purified GST (Fig. 4). The finding that four out of five RING-CH-domains examined in this assay demonstrated E3 activity strongly suggests that all MARCH proteins act as ubiquitin ligases but differ in their E2 specificity.

Downregulation of surface receptors by MARCH-proteins

All viral K3-family members downregulate expression of MHC-I. Additional substrates are ICAM-1 and B7.2 (but not B7.1) for K5 as well as Fas and CD4 for M153R. To examine if MARCH proteins affected MHC-I or any of these other glycoproteins I transiently transfected HeLa cells with expression plasmids for all two-transmembrane MARCH proteins (except MARCH-VII) and the four-transmembrane MARCH-V, and monitored surface expression of selected glycoproteins. The following known substrates for viral K3-family members were tested: Fas (CD95) and MHC-I, both of which are endogenously expressed in HeLa cells, as well as transfected HLA-A2.1, CD4 and B7.2. I used endogenously expressed transferrin receptor (TfR) and transfected B7.1 as controls, neither of which is downregulated by the viral proteins. The results are plotted as fluorescence of the respective surface markers versus fluorescence of co-transfected GFP (Fig. 5A). Interestingly and unexpectedly, the expression of every surface glycoprotein was affected by at least one of the MARCH-proteins with the notable exception of B7.1. The four-transmembrane MARCH-V as well as the two-transmembrane MARCH-III did not downregulate any of the protein tested although these proteins were clearly expressed as revealed by immuno-precipitation and

immunoblot of their FLAG-tagged versions (Fig. 5B,C). MARCH-II, which is approximately 60% identical to MARCH-III, downregulated TfR and B7.2. For the remaining four proteins a distinct pattern emerged whereby MARCH-I and -VIII downregulated TfR, B7.2 and Fas whereas MARCH-IV and -IX downregulated MHC-I and CD4. The downregulation of B7.2 by MARCH-VIII is consistent with previous reports (181). Our results indicate an intrinsic substrate specificity correlating with sequence homology (Fig. 1). Some overlap in substrate specificity, however, seems to exist between these two pairs of proteins since surface levels of transfected A2.1 was also weakly reduced by MARCH-VIII and transfected B7.2 was weakly reduced by MARCH-IV. Downregulation of TfR was not previously reported for any of the viral proteins and TfR is the only type II transmembrane protein included in our panel. Taken together, these data suggest that the human homologues of viral immune evasion proteins downregulate a distinct, partially overlapping, panel of cell surface glycoproteins.

Functional domains of MARCH-IV and MARCH-IX

The distinct substrate specificity of MARCH-I/VIII and MARCH-IV/IX correlates with homologies in their primary structure. MARCH-I and -VIII are closely related (>90% identity) in their RING-CH domains and transmembrane domains, whereas their amino-terminal and carboxy-terminal regions are less than 20% identical. A similar relationship is also observed between MARCH-IV and -IX which are more than 90% identical in their RING-CH domain and TM-domain but generally less than 20% in the remaining sequence (Fig. 6). In contrast, the RING-CH and TM domains of MARCH-II and -III, which differ in their ability to downregulate surface molecules, are only about

60% identical. Thus it seems that the substrate specificities are largely determined by the RING-CH and TM-domains. To test this assumption I performed deletion analysis of MARCH-IV. Expression of the predicted full-length MARCH-IV yields four different protein bands of which the full-length protein (product 4) is only a minor fraction. In contrast, protein bands of the same size as those observed in a construct that lacks 63 amino acids in the amino-terminal region are predominant (Fig. 5). Since both full-length and truncated version downregulate MHC-I (Fig. 5), and since MARCH-IX does not display an amino-terminal extension, it seems that the truncated version of MARCH-IV is the functional form with respect to MHC-I and CD4 downregulation. Therefore, the truncated form was used and denoted as MARCH-IV in all other experiments. Interestingly, the observed molecular weight (MW) of (truncated) MARCH-IV is 55kDa (Fig. 5) whereas the predicted MW is 38kDa. In contrast, the observed MW of all other MARCH-proteins, including MARCH-IX, is as predicted (Figs. 5, 6). I deleted the amino-terminal and carboxy-terminal domains of MARCH-IV to map substrate-determining regions as well as to determine the region of MARCH-IV responsible for this shift in apparent MW. MHC-I downregulation was monitored by flowcytometry using non-tagged versions of the truncated proteins whereas the apparent molecular weight was determined by immunoblot using FLAG-tagged constructs. Truncation of the amino-terminal region preceding the RING-CH domain or deletion of the carboxy-terminal end following the transmembrane regions did not abolish the ability to downregulate MHC-I (Fig. 6). Therefore the amino-terminal or carboxy-terminal regions, including small stretches conserved between MARCH-IV and -IX, are not essential for MHC-I downregulation consistent with the hypothesis that substrate specificity is

determined by the RING-CH and TM-domains. However, a truncated version of MARCH-IV lacking both the amino-terminus and the carboxy-terminus was unable to downregulate MHC-I (Fig. 6). Thus, at least parts of the non-conserved regions are required for a functional molecule but not for substrate specificity. The apparent MW of the shortest MARCH-IV construct containing only the RING-CH and TM-domains corresponded to the predicted MW. In contrast, constructs that contained the MARCH-IV carboxy-terminus showed an increase in apparent size of approximately 5kDa. Furthermore, each of the two amino-terminal regions seemed to shift the MW by 5kDa suggesting that MARCH-IV contains three modifications each of which is approximately 5kDa. Since the truncation experiments rule out trivial explanations such as read-throughs or alternative start codons for this increase in size, we conclude that MARCH-IV is post-translationally modified. At present, we do not know the nature of this modification, but we ruled out N-linked glycosylation or ubiquitination (data not shown). Additional experiments to identify this modification are currently in progress. Mutations in the RING-CH domains also established that this domain is essential for MHC-I downregulation by MARCH-IV and -IX. MARCH-IX occurs in two splice variants, one lacking the RING-CH domain. Forced expression of this RING-CH-deleted form does not downregulate MHC-I (Fig. 6). Likewise, point mutations in the RING-CH domain of MARCH-IV abolish MHC-I downregulation (Fig. 6) consistent with an essential role of the E3 activity for MHC-I downregulation.

Comparison of MHC-I downregulation by MARCH-IV and KSHV-K5

We were wondering if MHC-I downregulation by MARCH-IV was only observed at very high expression levels. MARCH-IV is expressed only at a very low level in HeLa cells, (data not shown). Therefore, I compared MHC-I expression at different expression levels of MARCH-IV or K5 by taking advantage of the tetracycline-regulatable system to partially express either protein (183). Tet-off HeLa cells were transfected with either MARCH-IV or with K5 in the presence of increasing amounts of tetracycline to shut off transcription. After 48 hours, surface expression of MHC-I molecules was analyzed by flowcytometry (Fig. 7A) and expression of MARCH-IV and K5 (both FLAG-tagged) was determined by immunoblot (Fig. 7B). In both cases I observed partial MHC-I downregulation below the detectable level of RING-CH protein expression. MARCH-IV was consistently expressed at lower levels compared to K5 which might indicate that high levels of MARCH-IV expression are not well tolerated by transfected cells. A lower percentage of MARCH-IV transfectants showed reduced MHC-I expression levels compared to K5, which could be explained by the lower expression levels of MARCH-IV. The efficient downregulation of MHC-I at low expression levels suggested an efficient MHC-I downregulation by MARCH-IV comparable to K5.

MHC-I downregulation by MARCH-IV and MARCH-IX occurs via endocytosis

MHC-I downregulation of MARCH-IV is as efficient as that of K5 at comparable expression levels (Fig. 7). Thus, the MARCH proteins are not only structurally but also functionally related to the viral K3-family of immune evasion proteins. Most members of the viral K3-family reduce expression of their target substrates by inducing a rapid internalization from the cell surface. The only known exception is MK3 which mediates

proteosomal degradation of MHC-I prior to its exit from the ER (63). To study if MHC-I was internalized by MARCH-IV and -IX, I compared the internalization of MHC-I in MARCH-IV or -IX transfected and non-transfected cells. After incubation with anti-MHC-I antibody at 4^0C, cells were either fixed immediately or transferred to 37^0C for 2 hours to allow uptake of MHC-I. After fixation and visualization with a secondary antibody, a distinct punctuate staining was observed in MARCH-IV or -IX transfected cells consistent with rapid uptake of MHC-I (Fig. 8A). In contrast, uniform surface staining was observed in non-transfected cells. These results suggest that MHC-I traffics to the cell surface prior to endocytosis.

A role of the endocytic pathway in the removal of MHC-I from the cell surface by MARCH-IV and -IX was also suggested by experiments using inhibitors of endosome acidification such as concanamycin A (ConA). Treatment of MARCH-IV or –IX with ConA restored MHC-I surface expression measured by flowcytometry (Fig. 8C). Moreover, pulse-chase analysis and immunoprecipitation of HLA-A2.1 in MARCH-IV transfected cells revealed that the acquisition of EndoH-resistance by HLA-A2.1 occurred with the same kinetics in the presence or absence of MARCH-IV (Fig. 8B) which argues against and interference with MHC-I exocytosis. However, MHC-I degradation was accelerated in MARCH-IV transfected cells, a process that was slowed down by ConA, whereas the proteosome inhibitor lactacystin had no stabilizing effect (Fig. 8B). These results are consistent with HLA-A2.1 exiting the ER, being transported to the cell surface and then rapidly internalized by endocytosis and ultimately destroyed, most likely in lysosomes.

The proposed function of this protein family as ubiquitin ligases implies a role for ubiquitination in the internalization process. Ubiquitinated cell surface receptors are internalized and sorted to lysosomes via MVBs, a process that is regulated by several sequential multiprotein ESCRT complexes (184). After completion of the MVB sorting, the AAA-type ATPase vps4 (vacuolar protein sorting protein 4) is required for the dissociation of the ESCRT complexes from the membrane (184). Using an ATPase-deficient, GFP-tagged form of vps4 (GFP-Vps4-E228Q) which is dominant-negative (182) I examined whether the internalization of MHC-I in MARCH-IV and –IX transfected cells involves MVB formation. Surface expression of MHC-I was monitored on HeLa cells, co-transfected with MARCH-IV and either WT or DNvps4. Neither DN- nor WTvps4 changed the surface levels of MHC-I in HeLa cells in the absence of MARCH-IV or -IX (data not shown). In contrast, co-transfection of DNvps4 with MARCH-IV or -IX partially restored surface MHC-I expression as shown by an increase in the mean fluorescence of transfected cells (Fig.9A). In a separate line of experiments, I studied the subcellular localization of internalized MHC-I in cells transfected with DNvps4. It was shown previously that DNvps4 generated and bound to aberrant vacuolated endosomes whereas WTvps4 stained the cytosol (182). Uptake of MHC-I molecules in MARCH-IV and –IX transfected cells was assayed as above except that cells were also co-transfected with DNvps4. MHC-I remained at the cell surface in cells that stained brightly for GFP indicating large amounts of DNvps4 (Fig. 9B) consistent with the FACS-analysis. However, MHC-I and DNvps4 colocalized in MARCH-IV- and -IX transfected cells that expressed low levels of DNvps4. We interpret this observation as evidence that MHC-I is taken up by endocytosis and sorted via the MVB pathway.

Ubiquitination is essential for MHC-I internalization

To examine if MHC-I molecules are ubiquitinated in the presence of MARCH-IV and -IX, I co-transfected HeLa cells with an HA-tagged truncated version of HLA-A2.1, d331 (45), together with MARCH-IV or -IX. For control, I also transfected the RING-CH mutants of MARCH-IV and -IX described above. To slow down MHC-I turnover, cells were also treated with ConA. HLA-A2.1 molecules were immunoprecipitated with antibody-BB7.2 (not shown) and re-precipitated either with anti-HA or with ubiquitin-specific antibody P4D1 (Fig. 10A). A single higher-molecular weight species of approximately 49kDa was precipitated by P4D1 from the ConA-treated cells transfected with wildtype MARCH-IV and -IX but not with their mutant forms. The size of this protein band is approximately equivalent to the 50kDa expected for mono-ubiquitinated HLA-A2.1d331 (note that the heavy chain of antibody P4D1 migrates to a similar position thus slightly displacing the labeled protein). The observed stabilization of the ubiquitinated intermediate by ConA is also consistent with our previous observations in M153R-transfected cells (77). The most likely targets for ubiquitination on transmembrane glycoproteins are lysines in the cytoplasmic tail. To examine the role of lysines for substrate downregulation by MARCH-IV and -IX I used a panel of constructs derived from HLA-A2.1 and a lysine-deleted version of CD4 (77). Flowcytometry revealed that removal of lysines from the tail of HLA-A2.1 renders these molecules resistant to MARCH-IV or -IX downregulation (Fig. 8B). Removal of cytoplasmic lysines also renders CD4 resistant to downregulation by MARCH-IV (Fig. 10C). To rule out the possibility that these mutations changed the target molecules in such a way that

they are unable to be recognized by MARCH-IV or -IX, we introduced a lysine residue into a HA-tag at the carboxy-terminal end of HLA-A2.1. This re-introduction of a lysine residue into a sequence not related to HLA-A2.1 restored downregulation both by MARCH-proteins. Therefore, we conclude that lysines in the tail are an absolute requirement for MHC downregulation by MARCH-IV and -IX suggesting that ubiquitination is essential for internalization.

Discussion

We addressed the question whether MARCH family proteins were functionally related to viral immune evasion proteins of the K3-family. The overall sequence homology of these predicted proteins is rather low and limited mostly to the RING-CH domain (Fig. 1). The primary structure was thus suggestive but insufficient to conclude which of these proteins were functionally related to the viral immunomoldulators. Using a panel of potential substrates selected as known substrates of viral K3-family proteins, I observed an efficient and specific downregulation of various cell surface glycoproteins by the cellular homologues. The partially overlapping, partially distinct substrate specificity observed for the MARCH proteins is also typical of the viral proteins. The molecular reason for this specificity is unknown, but substrates seem to interact transiently with the viral proteins (47) and substrate recognition seems to reside in the transmembrane regions of the targets (49). Consistently, I observed that sequence correlation in the RING-CH domains and TM-domains correlated with substrate specificity whereas deletion of the amino-terminal or carboxy-terminal domains did not affect substrate downregulation.

My results also confirm the previously reported downregulation of B7.2 by MARCH-VIII (c-MIR) (181). However, I also observed that MARCH-I which is homologous to MARCH-VIII efficiently downregulated B7.2 and that both MARCH-I and -VIII downregulated Fas and Tfr. Moreover, the unrelated MARCH-II also downregulated B7.2. Different from Goto et al I did not observe a preferential expression of MARCH-VIII in lymphnodes. Rather, MARCH-VIII mRNA was found at low levels in most tissues examined (Fig. 2). Also different was our observation of a moderate, but significant downregulation of transfected HLA-A2.1 by MARCH-VIII. Our observed downregulation of HLA-A2.1 could be caused by a higher level of expression achieved in our study using the tetracycline-inducible system which might facilitate a weak interaction. In general, however, a pattern emerged whereby MARCH-I and -VIII targeted a distinct set of surface glycoproteins compared to MARCH-IV and -IX. This pattern mimics the dichotomy of function for the K3 and K5 genes of KSHV. While K3 downregulates a broader spectrum of MHC-I alleles compared to K5 (20), K5 but not K3 also downregulates B7.2 and ICAM-1 (51,54).

The essential, sequence-independent role of lysines in the cytoplasmic tails of substrates together with ubiquitinated HLA-A2.1 strongly suggests that ubiquitination is required for downregulation by the MARCH-family. In contrast to Goto et al who reported multiple ubiquitination of B7.2, I observed only a single species of ubiquitinated HLA-A2.1. This difference could be caused by the fact that B7.2 contains eleven lysines in its cytoplasmic tail (Coscoy et al, 2001), whereas the HA-tagged A2.1 form used in our experiments contained only two lysines (45). Recent data showed that multiply ubiquitinated receptor tyrosine kinases did not contain poly-ubiquitin but were mono-

ubiquitinated at multiple sites (185). Thus it is possible that B7.2 contains mono-ubiquitins at multiple sites whereas only one of the two lysines is used for ubiquitination of the HA-tagged version of HLA-A2.1. Notably, only two ubiquitinated forms of the murine MHC-I molecule H2-D^b, which contains three lysines, where found in MK3 transfected cells (63). A central role for ubiquitin is further corroborated by the observed ubiquitin-ligase activity of the RING-CH domain *in vitro* and by the partial restoration of MHC-I surface expression by DNvps4. Very similar observations were reported for both herpesviral and poxviral K3-family proteins which were shown to require at least one lysine in the tail (49,63,77) and substrate internalization was inhibited by interference with the MVB pathway (47,77). The isolated RING-CH domains of both K5 and M153R also act as ubiquitin ligases (49,77). The current model for the function of the viral proteins is that they transiently interact with their substrates and mediate the ubiquitination of the cytosolic tail. Our data, as well as the observations by (181), are consistent with the cellular homologues acting in a manner very similar to their viral relatives.

While MARCH proteins induced the internalization of glycoproteins at the cell surface, subcellular localization studies revealed that they all localize to intracellular membrane compartments. Similarly, all members of the viral K3-family localize to intracellular membranes, mostly the ER. Therefore, the stage of intracellular transport at which target glycoproteins become ubiquitinated is currently unclear. It is possible that ubiquitination occurs en route to the cell surface or target proteins could be ubiquitinated during recycling. The localization of MARCH-IV and -IX in the Golgi and TGN, respectively, is consistent with either possibility.

The MARCH-family represents a novel family of ubiquitin ligases with a non-canonical RING-domain for which we adopted the name RING-CH-domain as previously proposed for the SSM4/Doa10 protein (178). A close relationship between the RING-CH domain and other RING-domains is also suggested by structural predictions whereas other PHD-domains are predicted to fold into structures that are clearly distinct from the RING-domain (53). The RING-CH domain thus expands the RING-E3 family, already the most abundant E3 family with potentially several hundred members (175). Different from the MARCH-family, however, most RING-E3s are either cytosolic, nuclear or peripheral transmembrane proteins (175). To our knowledge, only two non-MARCH-family transmembrane RING-E3s have been described: Der3/Hrd1 (186,187) and p78 (188). These E3s have all been shown to be involved in the degradation of misfolded proteins in the ER or ER-associated protein degradation (ERAD). MARCH-VI, the human homologue of SSM4/Doa10, is also likely to be involved in ERAD. In contrast, MARCH-IV and -IX (this study) and MARCH-VIII (181) direct the internalization of their substrates. Since most two-TM MARCH-proteins localize to the endosomal/lysosomal compartment, endocytosis, rather than proteosomal degradation, will likely be the major mechanism of MARCH mediated protein degradation.

The membrane association of MARCH proteins implies that their corresponding ubiquitin-conjugating enzymes are also membrane associated or need to be recruited to membranes. Indeed, experimental evidence suggests that SSM4/Doa10, p78 and Der3/Hrd1 cooperate with ubc6 and ubc7 (178,186-188). Ubc6 and ubc7 are bound to the ER-membrane via a transmembrane domain or by interacting with another protein respectively (189,190). MARCH-VI might therefore interact with the human homologues

of ubc6 or ubc7. MARCH proteins that leave the ER and regulate internalization, however, are more likely to interact with different E2s *in vivo*. While the E2s interacting with MARCH proteins *in vivo* have yet to be identified, our *in vitro* ubiquitination experiments suggest that the amino-terminal regions of each MARCH protein dictate a preference for certain E2s.

At present we can only speculate about the physiological role of the MARCH proteins. Results obtained with forced expression of MARCH proteins in our experiments strongly suggest that several members of this family regulate the degradation of glycoproteins at the cell surface. MARCH-IV and -IX could be involved in the internalization of free heavy chains upon dissociation of peptide and β_2M. However, gene knockdown of MARCH-IX by siRNA did not affect the turnover of MHC heavy chains in HeLa cells (data not shown). Alternatively, MARCH-IV and -IX might have to be upregulated by external stimuli before they affect MHC-I turnover whereas they are involved in the turnover of other cell surface protein at basal levels. Since I only screened a small number of cell surface proteins, MARCH proteins will probably be involved in the internalization of other, yet to be identified transmembrane proteins. Many cell surface receptors are internalized upon engagement with ligands, either soluble or bound to the surface of neighboring cells (175). The involvement of ubiquitin in these processes is just beginning to emerge and the regulation of ubiquitination is not known. We therefore speculate that MARCH-proteins will be involved in regulating receptor internalization as well as protein turnover.

The functional relationship between MARCH-family and the viral K3-family suggests that the viral proteins were derived from their cellular homologues. Ample

precedence exists for common host-related immunomodulators in both herpesviral and poxviral genomes (180). These host-derived proteins, however, often assume a new or modified function, possibly even acting as inhibitors of their host counterparts. Whereas in most of these cases the known function of the host-protein served as a roadmap to elucidate the function of the viral protein, the reverse strategy has been used here to discover the function of a novel eukaryotic protein family.

Figure 1: Human homologues of viral K3 family proteins

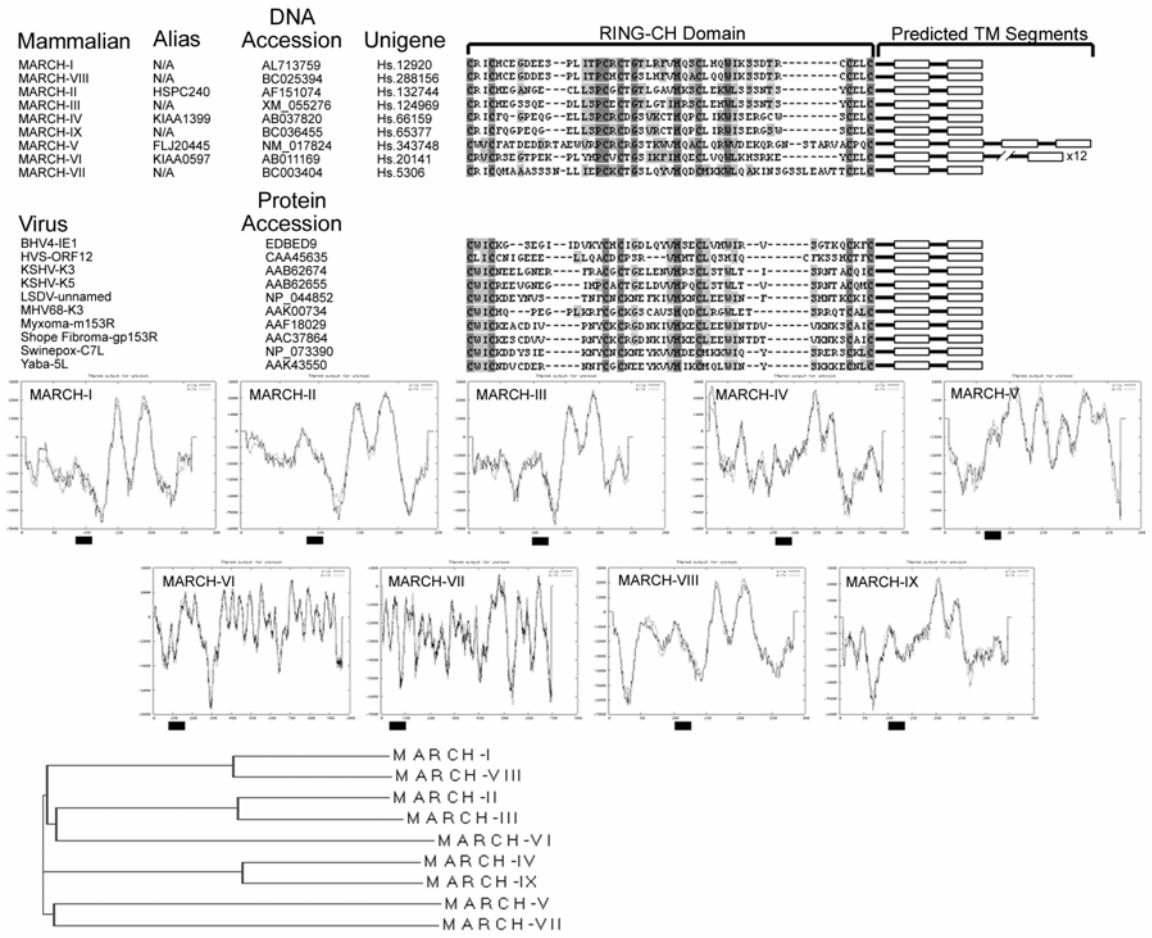

Figure 1: Human homologues of viral K3 family proteins

The RING-CH domain from the nine identified human MARCH proteins (I-IX) and the known viral K3-family proteins were aligned using Vector NTI 7.0 software. The RING-CH-domain is shown boxed in dark gray, while other conserved amino acids are shown boxed in light gray. The hydropathy plots (middle panel) for each MARCH protein were generated using TMPRED (www.ch.embnet.org). The location of the RING-CH domain is shown by a black box under the hydropathy plot, while the number of transmembrane domains predicted is shown to the right of the RING-CH alignment. Phylogenetic relationships (bottom) were generated using Vector NTI suite 7 software.

Figure 2: Tissue Distribution of MARCH proteins

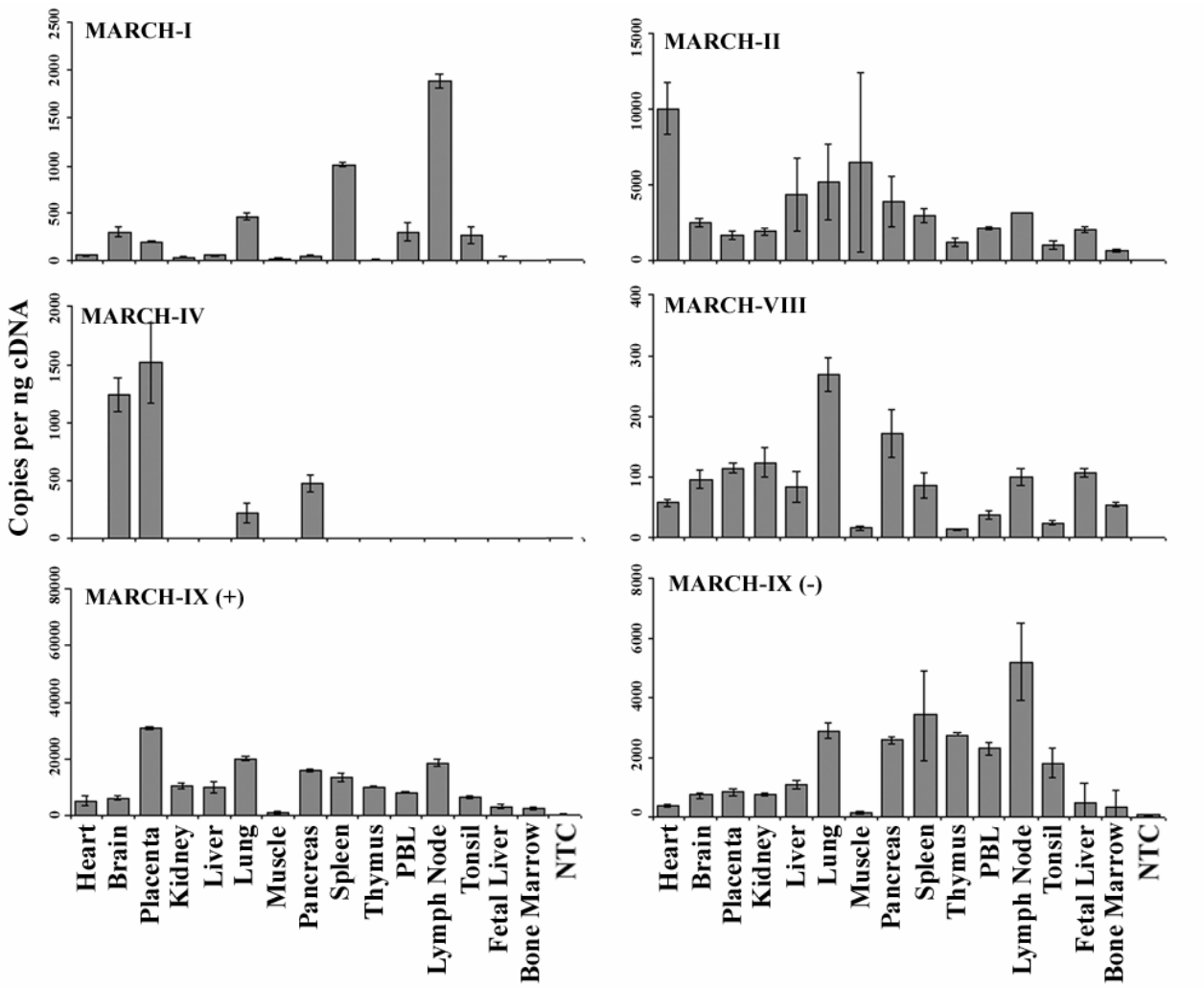

Figure 2: Tissue Distribution of MARCH proteins

Expression of MARCH-I, II, IV, VIII, and both variants of IX was measured by real-time PCR in a panel of human tissue cDNAs (Clonetech). Expression of each gene was quantified using absolute standards created from plasmid DNA. Concentrations of cDNAs were normalized using the housekeeping genes GAPDH and β-actin.

Figure 3: Localization of MARCH proteins to intracellular membranous organelles.

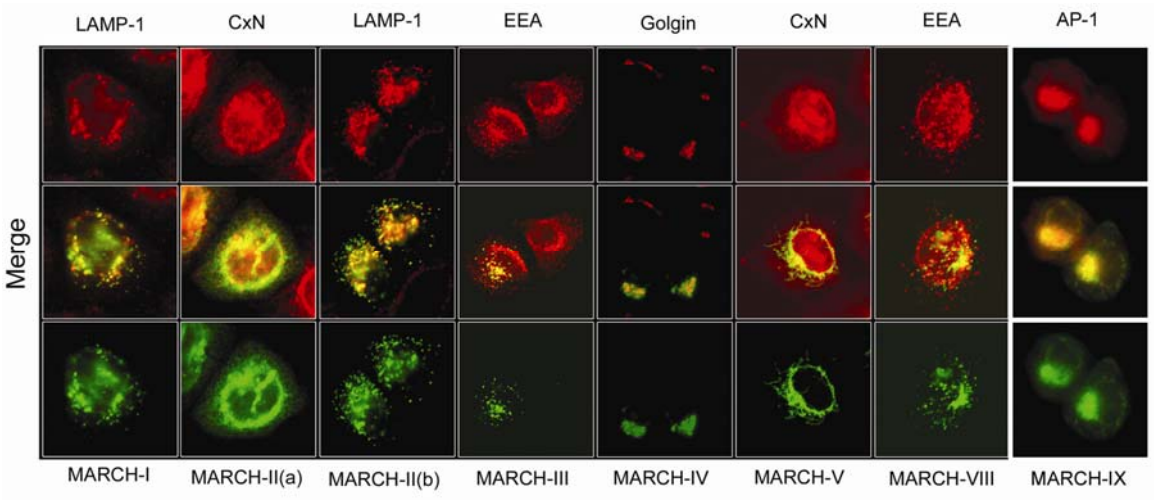

Figure 3: Localization of MARCH proteins to intracellular membranous organelles.

HeLa cells were transfected with plasmids encoding carboxy-terminally Flag-tagged versions of the indicated MARCH proteins. 20 hours post-transfection cells were stained with antibodies against indicated cellular markers (top panel in red) or anti-FLAG (bottom panel in green). Colocalization is visualized as yellow in the merged panel (middle). All cellular markers were examined against all MARCH-proteins. However, only those results are shown which indicated a significant overlap. Markers of subcellular compartments were: calnexin (Cxn) for ER, Golgin-97 for Golgi, Adaptor protein 1 (AP-1) for TGN, early endosomal antigen (EEA) for endosomes, LAMP-1 for lysosomes.

Figure 4: MARCH proteins act as ubiquitin ligases *in vitro*.

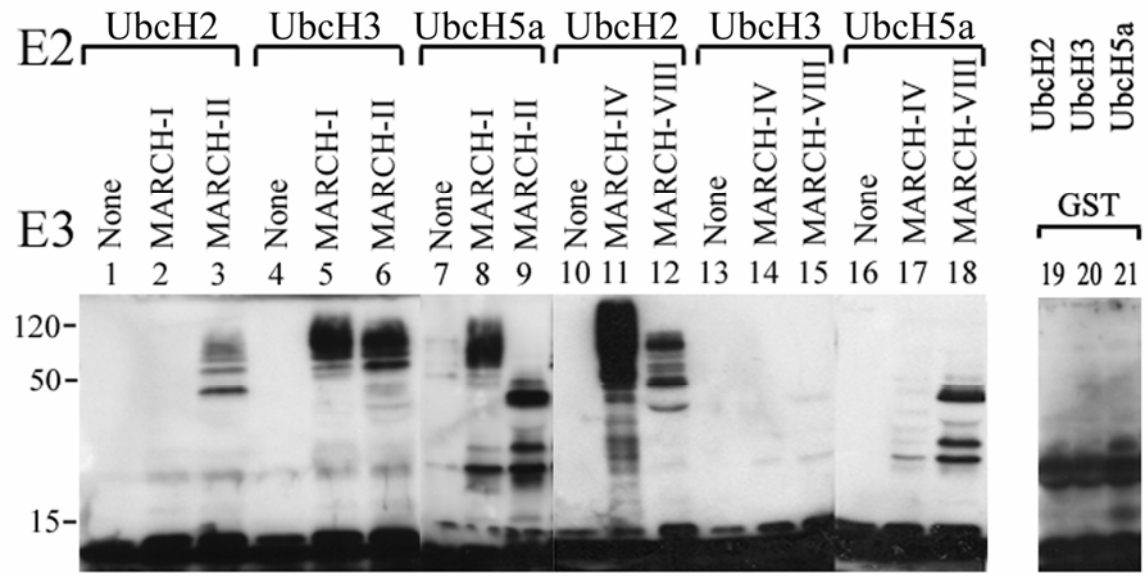

Figure 4: MARCH proteins act as ubiquitin ligases *in vitro*.

GST fusion proteins of the amino-terminal domains of individual MARCH proteins were incubated with ubiquitin, ATP, E1 and the indicated ubiquitin-conjugating enzymes (ubc, E2) and separated by SDS-PAGE prior to immunoblotting with the ubiquitin-specific antibody P4D1. Ubiquitin ligase activity is indicated by the appearance of high molecular weight ubiquitinated species. Ubiquitinated proteins were not detected in the absence of E3s (None) or with GST alone.

Figure 5: Downregulation of surface glycoproteins by the MARCH-family.

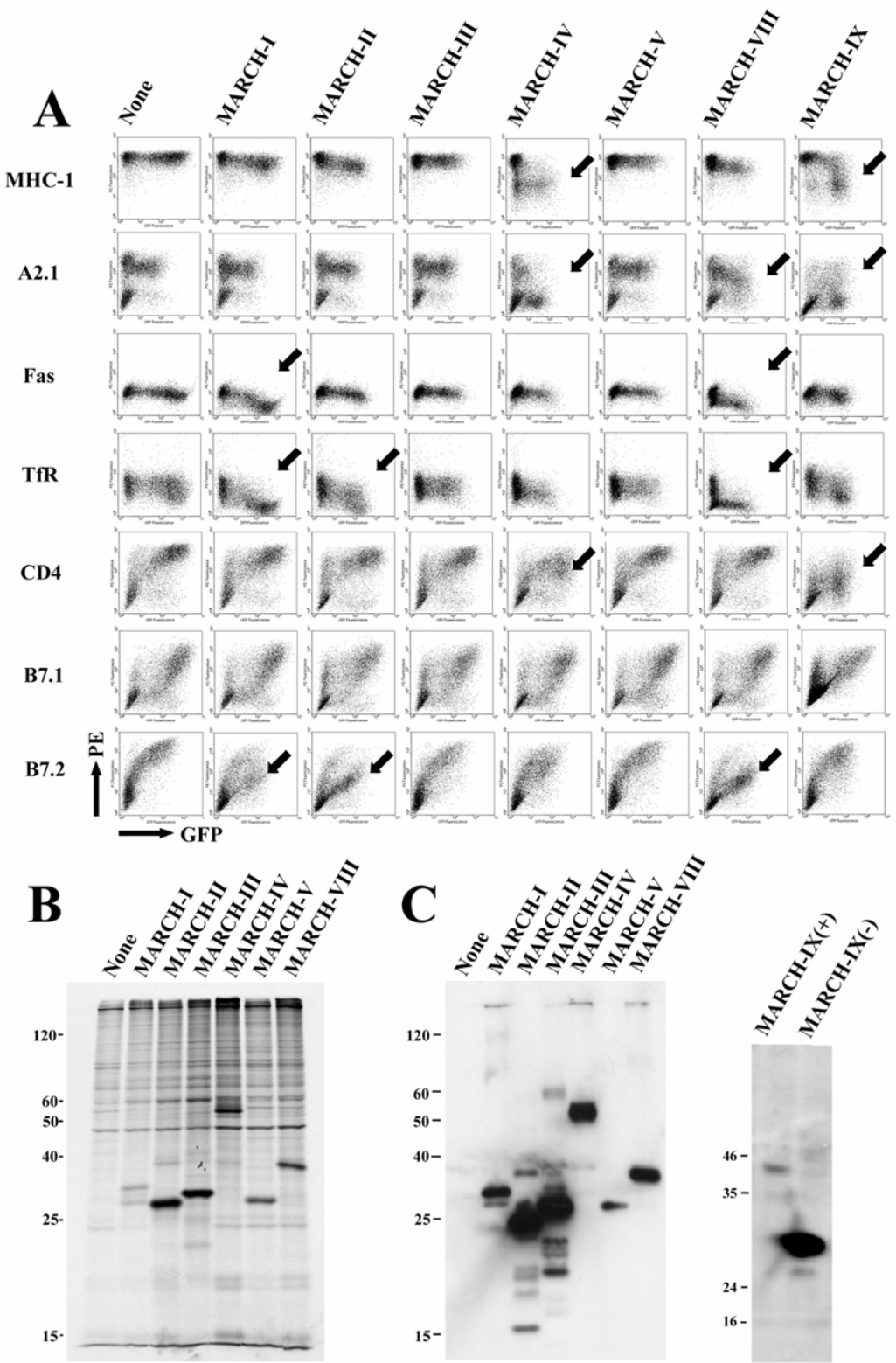

Figure 5: Downregulation of surface glycoproteins by the MARCH-family.

(A) HeLa cells were transfected with the respective MARCH expression plasmid and GFP. Surface expression of indicated surface proteins was measured via flow-cytometry using specific primary antibodies and a PE conjugated secondary at 24 hours post-transfection. Black arrows indicate significant downregulation. Expression of FLAG-tagged versions of MARCH proteins was confirmed with anti-FLAG antibody by immunoprecipitation (B) while steady state levels were measured by immunoblot (C). Introduction of the FLAG-tag at the carboxy-terminus of MARCH-proteins did not affect the ability of these proteins to downregulate their substrates (data not shown).

Figure 6: Functional domains of MARCH-IV and MARCH-IX

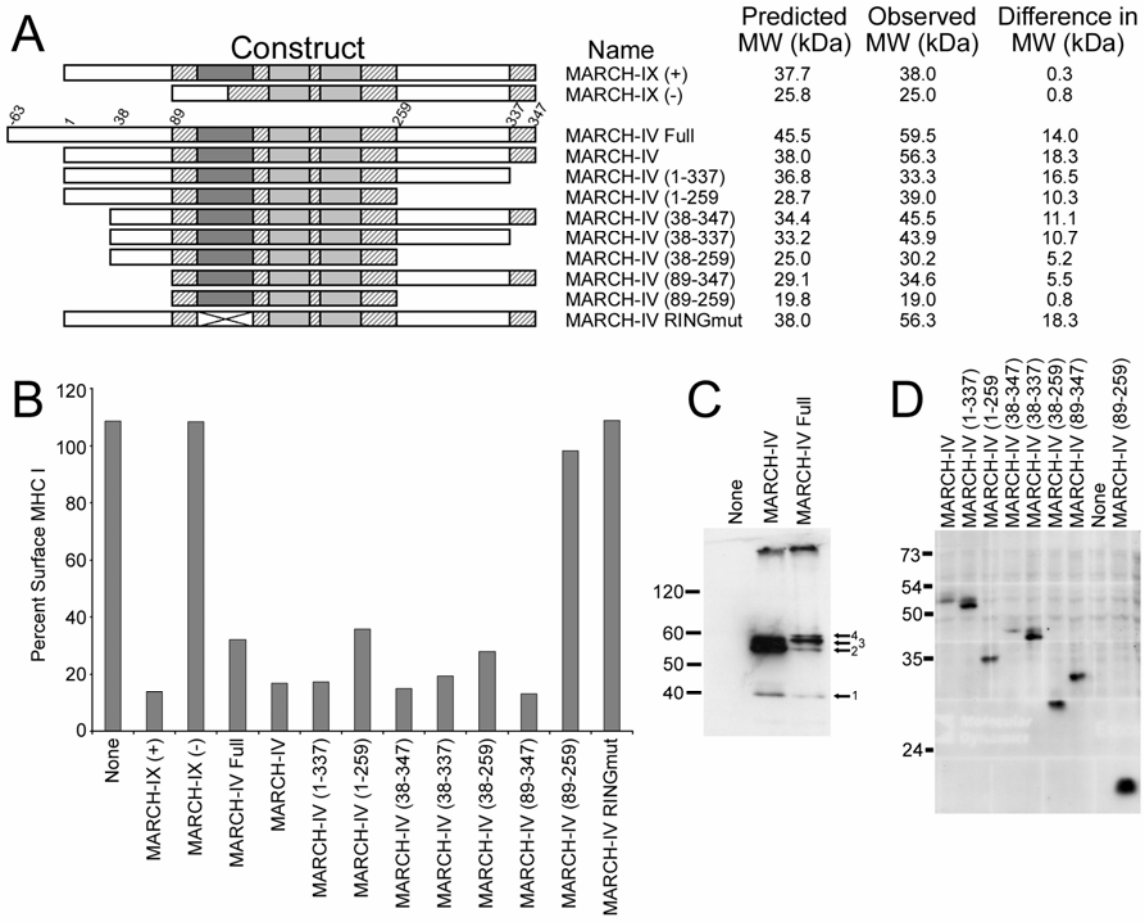

Name	Predicted MW (kDa)	Observed MW (kDa)	Difference in MW (kDa)
MARCH-IX (+)	37.7	38.0	0.3
MARCH-IX (-)	25.8	25.0	0.8
MARCH-IV Full	45.5	59.5	14.0
MARCH-IV	38.0	56.3	18.3
MARCH-IV (1-337)	36.8	33.3	16.5
MARCH-IV (1-259	28.7	39.0	10.3
MARCH-IV (38-347)	34.4	45.5	11.1
MARCH-IV (38-337)	33.2	43.9	10.7
MARCH-IV (38-259)	25.0	30.2	5.2
MARCH-IV (89-347)	29.1	34.6	5.5
MARCH-IV (89-259)	19.8	19.0	0.8
MARCH-IV RINGmut	38.0	56.3	18.3

Figure 6: Functional domains of MARCH-IV and MARCH-IX

(A) A schematic diagram showing the homology between MARCH-IV and MARCH-IX as well as the deletion mutants in MARCH-IV. The RING-CH domain (black), the two TM-domains (gray) and additional regions (hatched) are >90% identical, whereas the remaining parts of the molecules (white) are less than 20% conserved. MARCH-IX (-) represents a splice variant lacking the RING-CH domain. Two conserved cysteines in the RING-CH domain were replaced with serines in the MARCH-IV RING mutant. Amino- and carboxy-terminal deletion constructs of MARCH-IV are indicated, the predicted full-length construct contains a 63 amino acid amino-terminal extension. (B) Ratio (in percent) of the mean fluorescence of surface MHC-I detected by flowcytometry with W6/32 24hours of MARCH-transfected versus non-transfected HeLa cells gated for GFP. Both RING-CH mutants were unable to downregulate MHC surface expression. All MARCH-IV deletion constructs reduced MHC-I surface expression except MARCH-IV (89-259) containing the RING-CH and TM regions only. (C) Immunoprecipitation followed by immunoblot with anti-FLAG reveals the presence of two major protein bands of approximately 55kDa (53,184) in cells transfected with both full-length MARCH-IV and MARCH-IV (1-347) whereas the predicted full-length protein (189) is only a minor species. (D) Immunoblot with anti-FLAG reveals the observed MW of the truncated MARCH-IV proteins. The difference between observed and predicted molecular weight is shown in (A). Only MARCH-IV (89-259) migrated at the predicted position.

Figure 7: Comparative efficacy of MHC-I downregulation by MARCH-IV and viral KSHV-K5

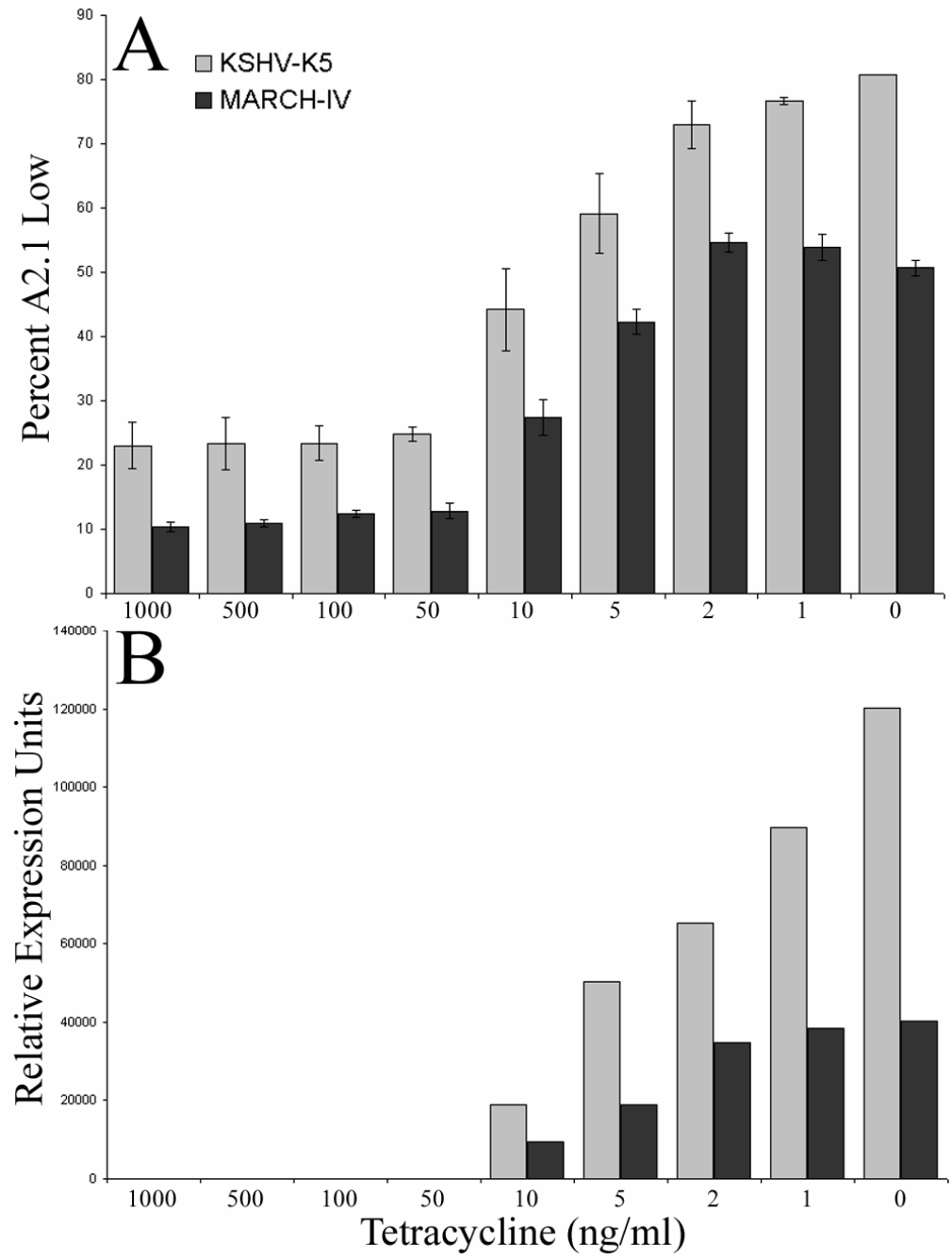

Figure 7: Comparative efficacy of MHC-I downregulation by MARCH-IV and viral KSHV-K5

The efficiency of MARCH-IV downregulation of MHC-I was compared to that of KSHV-K5 using the tetracycline responsive system (A). HeLa cells were transfected in the presence of 1μg/ml tetracycline with constitutively expressed A2.1-331/pUHD10-1 and either MARCH-IV/pUHG10-3 or K5/pBI, both under tet-regulation (45). GFP was used to track transfected cells. Eight hours post-transfection the media was removed and replaced with media containing the given amount of tetracycline. Thirty-six hours later the cells were harvested and A2.1 surface expression was measured by flowcytometry using antibody BB7.2 and a PE conjugated secondary antibody. The graph depicts the average percent of GFP+ cells that exhibited A2.1 downregulation. Error bars depict the range of the results from two separate experiments. Expression of each protein (B) was measured by immunoblotting whole cell lysates with an anti-Flag antibody conjugated to alkaline phosphatase and quantified using a Typhoon 8600 variable mode imager. The graph depicts protein expression as relative units at each tetracycline concentration.

Figure 8: Endocytosis and lysosomal degradation of MHC-I by MARCH-IV and MARCH-IX

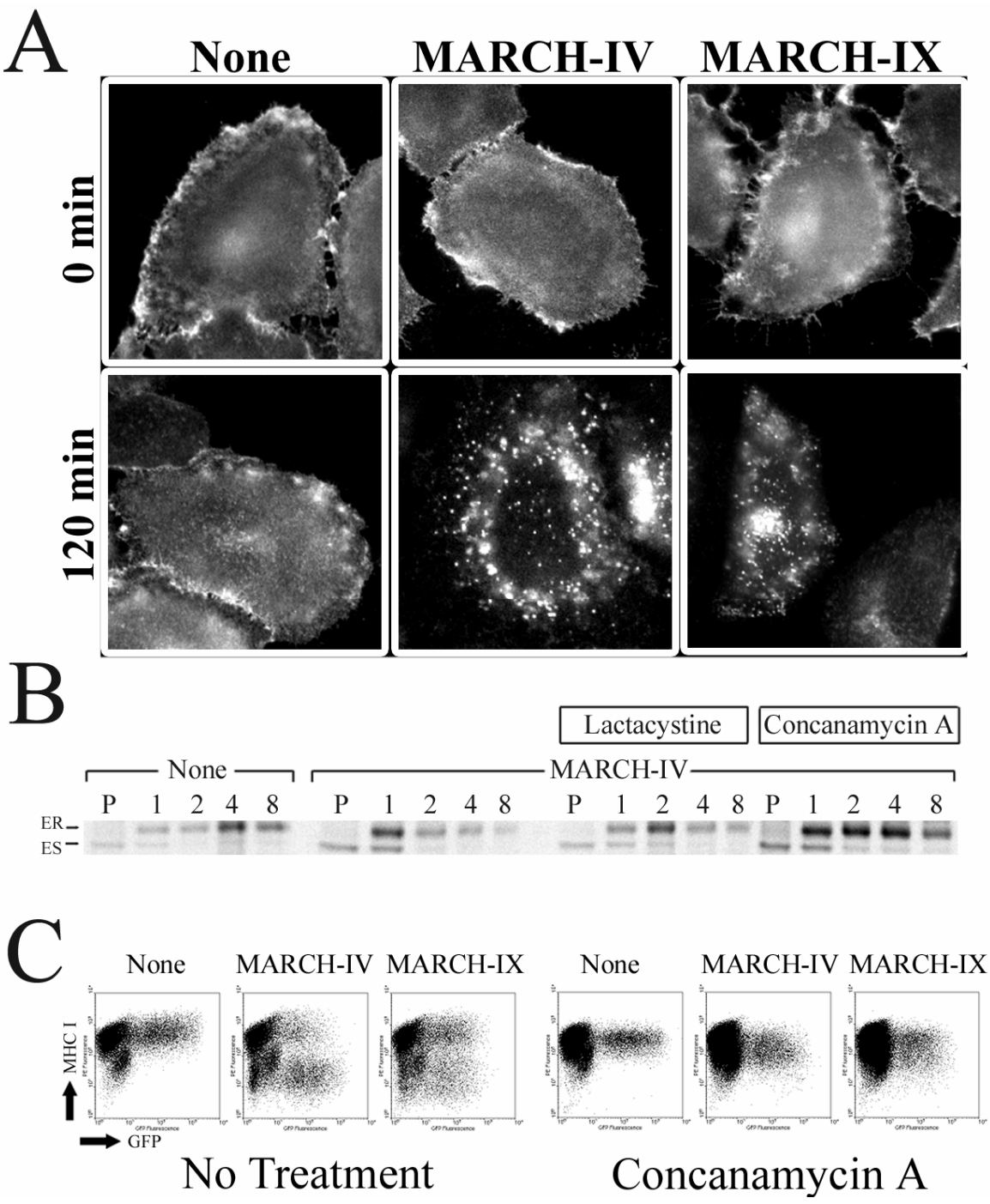

Figure 8: Endocytosis and lysosomal degradation of MHC-I by MARCH-IV and MARCH-IX

(A) Uptake of MHC-I in HeLa cells transfected with vector control, MARCH-IV or MARCH-IX. 24 hours post-transfection MHC-I was stained with antiserum K455 and either fixed after 30 min at 4^{o}C (top panel) or transferred to 37^{o}C for 2 hours (bottom panel) prior to fixation and staining with Alexaflur:594 anti-rabbit secondary antibody. (B) Pulse-chase and immunoprecipitation of HLA-A2.1 transfected alone (none) or together with MARCH-IV. Transfectants were labeled for 30 minutes (P) and chased for 1,2,4 and 8 hours in the presence or absence of the indicated inhibitors. HLA-A2.1 molecules were immunoprecipitated using BB7.2 mAb and treated with Endo H. Endo H resistant (ER) and Endo H sensitive (ES) bands are labeled. (C) Flowcytometry of MHC-I (W6/32 staining) on MARCH-IV or -IX transfected HeLa cells in the presence or absence of concanamycin A.

Figure 9: Vps4 restores MHC-I surface levels and colocalizes with MHC-I in HeLa cells transfected with MARCH-IV and MARCH-IX.

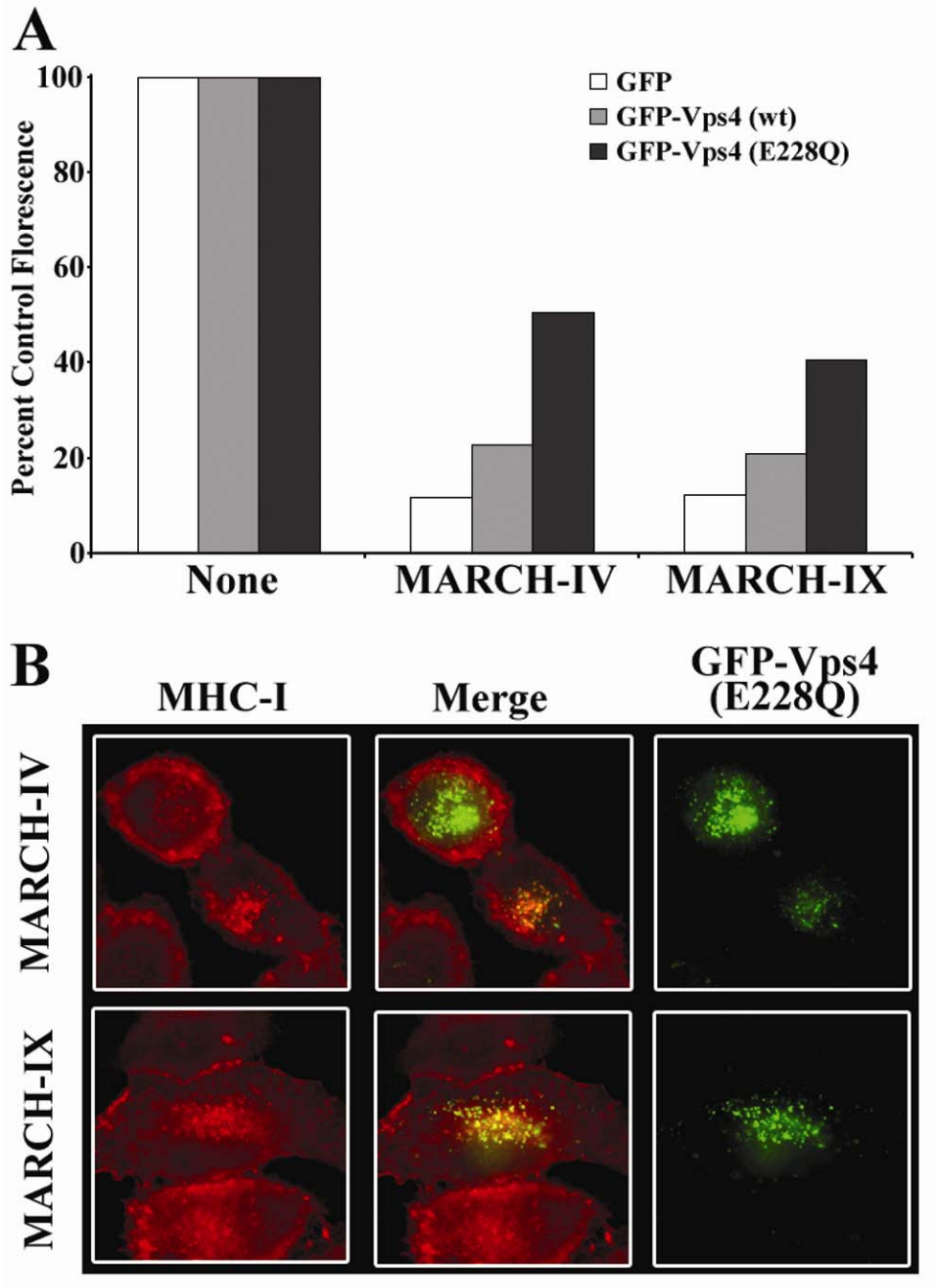

Figure 9: Vps4 restores MHC-I surface levels and colocalizes with MHC-I in HeLa cells transfected with MARCH-IV and MARCH-IX.

(A) HeLa cells were transfected with GFP only or GFP-tagged WTvps4 or the dominant negative, ATP-hydolysis-deficient mutant GFP-vps4(E228Q) (182) together with vector-control, MARCH-IV or -IX. 24 hours after transfection cells stained with W6/32 and the mean fluorescence of GFP-positive cells was determined. The ratio of the mean fluorescence of MARCH-transfected versus the corresponding vector-transfected cells is shown in percent. Co-trasnfection of GFP-vps4(E228Q) partially restored MHC-I surface levels in MARCH-IV and –IX transfected cells compared to cells that were only transfected with GFP-vps4(E228Q) and vector. (B) Uptake and co-localization of MHC-I molecules with GFP-vps4(E228Q). Internalization of MHC-I by MARCH-IV and -IX was monitored as in Fig. 6, except that cells were co-transfected with GFP-vps4(E228Q). Punctuate staining of vps4 (right panel, green) is consistent with its localization to endosomes (182). MHC-I (K455 staining, red, right panel) remained mostly at the cell surface in cells expressing high levels of GFP-vps4(E228Q). (upper left cell in upper panel) whereas MHC-I and vps4 colocalized in cells with lower GPF fluorescence indicating lower vps4 levels (cell in the center of upper and lower panel, merged fluorescence is shown in the middle column). No colocalization of MHC-I and vps4 was observed in the absence of MARCH-IV and -IX and WTvps4 stained the cytoplasm (data not shown).

Figure 10: Ubiquitination of MHC-I and role of carboxy-terminal lysines for MHC-I downregulation by MARCH-IV and MARCH-IX

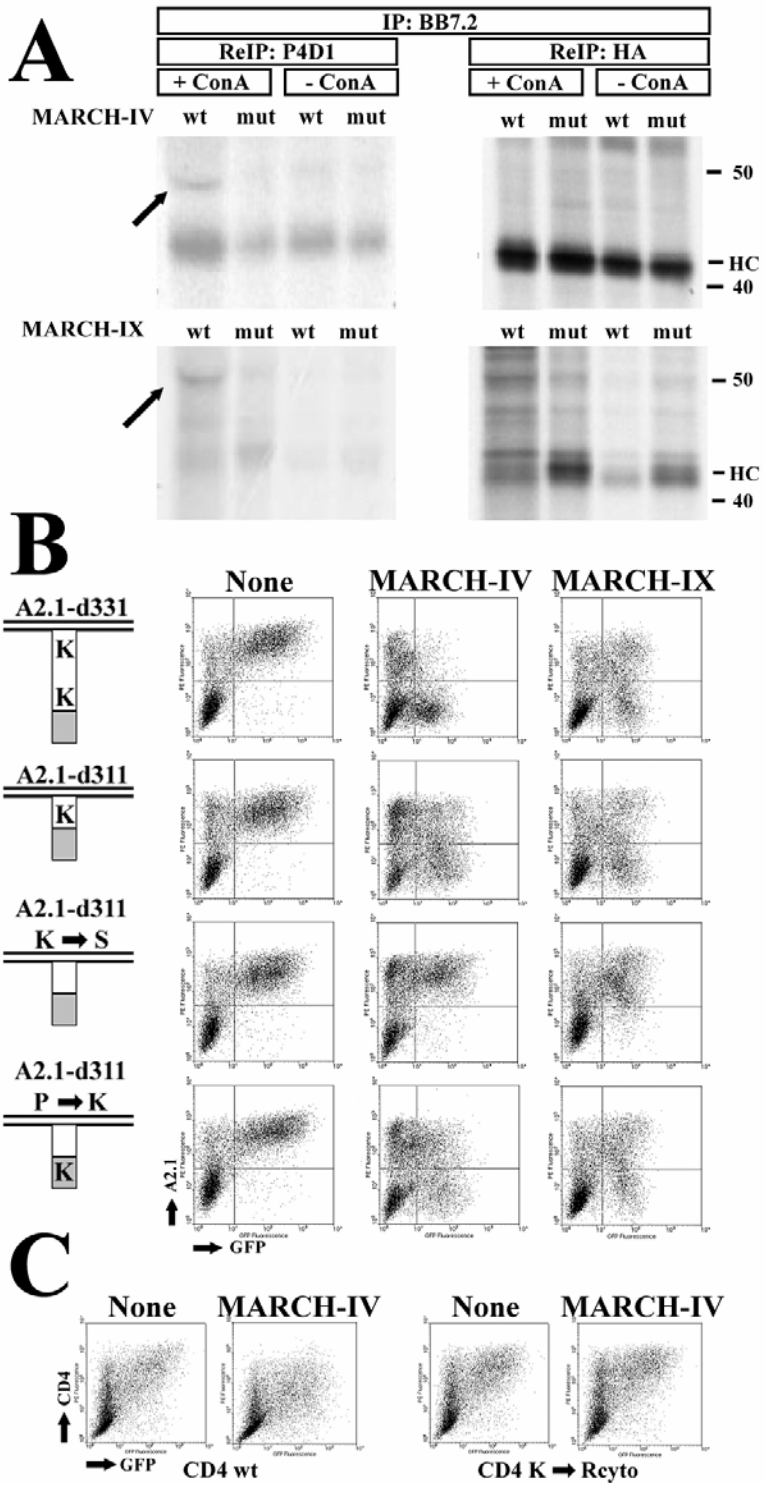

Figure 10: Ubiquitination of MHC-I and role of carboxy-terminal lysines for MHC-I downregulation by MARCH-IV and MARCH-IX

(A) HeLa cells were transiently transfected with HA-tagged HLA-A2.1 d331 (45) and MARCH-IV, -IX or their respective RING-CH mutants. MARCH-IX expression was fully induced by removal of tetracycline whereas MARCH-IV expression was partially repressed with 5ng tetracycline (see also supplemental Figure 2) since high levels of expression were not compatible with the long labeling protocol. Therefore, there is only a slight reduction of MHC-I expression levels in MARCH-IV transfectants compared to MARCH-IX transfectants. Where indicated, cells were treated with ConA prior to and during labeling for 6 hours. HLA-A2.1 was immunoprecipitated with BB7.2 and, after denaturation with SDS, re-immunoprecipitated with ubiquitin-specific antibody P4D1 (90% of the lysate, left panel) or anti-HA (10% of the lysate, right panel). Due to the high amount of MHC heavy chain in the primary immunoprecipitation, some of it was carried over in the P4D1 re-immunoprecipitation. The arrow indicates ubiquitinated heavy chain[2]. (B) Downregulation of HLA-A2.1 lysine mutants by MARCH-IV and -IX. Cytoplasmic tails of HLA-A2.1 are schematically depicted on the left (77). The number of lysines in the A2.1 tail (white) or the HA-tag (gray) is shown. Surface expression of the individual constructs was monitored by flowcytometry with antibody BB7.2. Transfection with vector (left), MARCH-IV (middle) or -IV was tracked by co-transfection of GFP. (C) Surface expression of wildtype CD4 or CD4 lacking lysines in its cytoplasmic tail in the presence of MARCH-IV.

[2] Fig. 10A courtesy of Mandana Mansouri

Chapter 4: 2D-PAGE Analysis of M153R[3]

Introduction

The K3-family of proteins are viral immune evasion proteins found in the herpesviridae and the poxviridae which remove immunologically relevant glycoproteins from the cell surface by acting as ubiquitin ligase (E3) enzymes (108). K3 proteins catalyze the addition of ubiquitin onto lysines in the cytoplasmic tails of their substrates resulting in clathrin dependant endocytosis, targeting down the multivesicular body (MVB) pathway and lysosomal destruction (19,76,77). While all studied K3 proteins downregulate major histocompatibility complex class I (MHC-I), recent evidence demonstrates that these proteins often have additional substrates. For example, the K5 protein encoded by the γ2-herpesvirus Kaposi's Sarcoma associated herpesvirus (KSHV), downregulates: MHC-I, ICAM-1, B7.2, CD1d, CD31, ALCAM, and the interferon-γ receptor (51,55,59,60,191). By removing a select set of cell surface immuno-receptors, K3 proteins render infected cells invisible to immune surveillance. The K3 proteins are likely derived from human homologues termed membrane associated RING-CH (MARCH) proteins. Like K3 proteins, MARCH proteins downregulate specific panels of transmembrane proteins, including MHC-I, MHC-II, ICAM-1, CD4, TfR, B7.2, and Fas (105,192-194). While many substrates are known for both the K3- and MARCH-families, these substrates were identified through antibody based screens which might

[3] This data is not currently published

give a biased view of each family's substrates. To date, attempts have not been made to determine K3- or MARCH-family substrates using a non-biased approach.

M153R is a K3-family member, encoded by the rabbit poxvirus myxoma, which downregulates MHC-I, CD4, Fas, and ALCAM (76,77,191). However, due to the wide variety of proteins targeted by other K3 proteins, additional M153R substrates probably exist. To identify these additional M153R substrates, I used quantitative 2-dimensional polyacrylamide gel electrophoresis (2D-PAGE) to compare the proteomes of cells infected with a recombinant vaccinia virus expressing M153R to that of cells infected with a control vaccinia virus. 2D-PAGE physically separates complex protein samples based on two sequential criteria (126). 2D-PAGE has been used to determine the makeup of protein mixtures (128-131) as well as map cellular responses to various stimuli such as: drug treatment (133), viral infection (134,135), and cancer metastasis (136,137). 2D-PAGE is an excellent technique to determine novel substrates for E3s such as M153R due to the ability to analyze both protein expression and posttranslational modifications.

Our results demonstrate that M153R inhibits a previously undocumented cleavage of the mitochondrial chaperone heat shock protein 60kDa (Hsp60) caused by infection with vaccinia virus. This cleavage is induced late in vaccinia infection and is linked with loss of mitochondrial membrane potential. Since both the mitochondria and Hsp60 play roles in apoptosis(195,196), we hypothesize that M153R plays a previously unidentified role as an early inhibitor of programmed cell death.

Materials and Methods

Reagents

The following antibodies were used: Hsp60 clones LK-1 and H-1 (Santa-Cruz Biotech), cytochrome C and Fas (Pharmingen). Cytosine arabinoside and Staurosporine (Sigma) were used at 40μg/ml and 1μM respectively. Tetramethylrhodamine, ethyl ester, perchlorate (TMRE) was obtained from Molecular Probes and used at .2μM.

Sample Preparation

$2x10^7$ HeLa cells were harvested via trypsinization and washed with PBS. Cells were then resuspended in PBS + 2mM EDTA and lysed mechanically using 30 strokes from a dounce. Lysate was clarified via centrifugation for 5 minutes at 300xg. The clarified supernatant was transferred to a fresh tube and the membrane and soluble proteins separated via centrifugation for 30 minutes at 45,000xg. The soluble proteins were precipitated from the resulting supernatant using 10% Trichloroacedic acid (TCA) (Sigma), while the membrane proteins was resuspended in PBS and centrifuged for 30 minutes at 45,000xg. The resulting pellet was washed in 1ml Acetone:Methanol (9:1) for 2 hours -20°C and then centrifugation for 10 minutes at 16,000xg. The pellet was washed in 50mM sodium bicarbinate (pH 8.5) and the proteins precipitated using 10% TCA. The final pellet was resuspended in 2D-PAGE sample buffer (7.8M Urea, 2.0M Thiourea, 100mM DTT, 4% CHAPS, 1x Biolyte Ampholytes pH 3-10 (BioRad)).

2D-PAGE

300μg of protein were loaded onto a 17cm Ready Strip™ IPG strip (pH 5-8) (BioRad) using passive overnight rehydration. Strips were focused on a Protean IEF Cell (Biorad) using the following conditions: 250V for 20 minutes, 10,000V for 2.5 hours,

10,000V for 40,000 V/hrs. Following focusing strips were reduced and alykylated according to the manufacturers recommendations. Strips were then place on top of a 12% SDS-PAGE gel and separated in the second dimension.

MS and Informatics

Peptide mixtures were analyzed by electrospray ionization tandem MS, which was performed using a modified version of the protocol described by Link and coworkers (197). Briefly, spots were visualized via silver staining (Invitrogen) and recovered from the 2D-PAGE gel by manual extraction. Acrylamide pieces were washed with 50mM sodium bicarbinate in 40% Ethanol followed by acetonitrile. Each wash was repeated 3 times, after which acrylamide spots were dried in a speed vacuum. Spots were rehydrated in 50mM sodium bicarbonate containing 10ng/µl modified trypsin (Promega) and the proteins allowed to trypsinize overnight. The resulting peptide mixture was then loaded onto a reverse phase C-18 capillary column (180 um × 100 mm, BioBasic-18; Thermo Electron, http://www.thermo.com). Peptides were eluted using an acetonitrile gradient (5%, 5 min; 5%–40%, 75 min; 40%–90%, 10 min) into a ProteomeX LCQ Deca XP Plus mass spectrometer (Thermo Electron) equipped with a low-flow (1 µl/min) electrospray source. The instrument was set to trigger data-dependent MS/MS acquisition of the three most intense ions detected during the MS survey scan when total ion current per MS survey scan exceeded 5.0×10^5 counts.

Proteins were identified by analyzing tandem mass spectra with the Sequest algorithm (Thermo Electron) as described by Yates et al. (147) using the human subset of the UniProt/Swiss-Prot protein database (UniProt release 5.1,

http://www.expasy.org/sprot). The search results were further analyzed using PeptideProphet (198). All positive results were manually verified.

Western Blot

SDS-PAGE gels were transferred to PVDF membrane using semi-dry transfer. Membranes were blocked for 1 hour with 10% milk in PBS + 0.1% Tween-20. Membranes were washed three times for 10 minutes with PBS + 1% Tween-20, followed by a single wash with water. Primary antibody was diluted in 1% milk in PBS + 1% Tween-20 and incubated for 30 minutes. Membrane was then washed three times as above. An appropriate HRP conjugated secondary antibody (Santa Cruz) was diluted 1:5000 in 1% milk in PBS + 1% Tween-20 and incubated for 30 minutes. Membrane was then washed three times as above. Membrane was exposed to Supersignal™ west chemiluminescent substrate (Pierce) and analyzed via exposure to light sensitive film.

TMRE Staining

Cells were incubated at 37°C for 30 minutes in DMEM containing .2μM TMRE. Cells were then harvested via trypsinization, washed twice with PBS, and analyzed on a FACScalibur flowcytometer (BD Biosciences).

Results

M153R alters expression of a wide variety of cellular proteins

$2x10^7$ HeLa cells were infected at a multiplicity of infection (MOI) of 10 with recombinant vaccinia virus expressing either CD4 (VV-CD4) or M153R (VV-M153R).

Membrane fractions were prepared as described and 150μg of each sample was labeled with limiting amounts of DIGE fluorophors (Amersham). Combined samples were then focused on a Protean IEF Cell, separated in the second dimension on a 12% SDS-PAGE gel and visualized on a Typhoon 8600 variable mode imager (Molecular Dynamics) (Fig. 11A). Each spot corresponds to a single protein or protein fragment. Spots visualized as red are underrepresented in the VV-M153R infected sample, while spots visualized as green are underrepresented in the VV-CD4 infected sample. Proteins expressed at the same level in both samples are visualized as yellow. 20 spots displaying differential expression were selected for further analysis. These spots were excised from the gel, subjected to tryptic digestion, and analyzed via mass spectroscopy. Only six of the analyzed spots yielded peptides mapping to known cellular proteins. Peptides recovered from four spots, which ran close together as a pair of doublets, mapped to actin (Fig. 11A-Arrow 3), while peptides recovered from the other two spots mapped to the carboxy-terminus of the mitochondrial chaperone Hsp60 (Fig. 11A-Arrow 1 and Fig. 11B).

Analyzed spots correspond to cleavage products of Hsp60

Since the spots containing peptides mapping to Hsp60 were observed at a lower molecular weight (MW) than has been previously reported for full length Hsp60 analyzed using 2D-PAGE (Fig. 11A-Arrow 2 and Swiss 2D-PAGE, http://www.expasy.org/swiss-2dpage/), we hypothesized that our spots might correspond to cleavage products of Hsp60. To test this hypothesis, HeLa cells were infected with VV-CD4, and samples were prepared and separated using 2D-PAGE. The location of Hsp60 was then analyzed via immunoblotting with the anti-Hsp60 antibody LK-1. Importantly, the LK-1 antibody

recognizes an epitope near the carboxy-terminus of Hsp60 within the region of peptides recovered from the initial spot (Fig.11B). In samples from mock infected cells, immunoblot with LK-1 revealed a single spot whose molecular weight and pI corresponded to those predicted for full length Hsp60 was observed (Fig. 12A and Fig. 11A-Arrow 2). In samples infected with VV-CD4, however, multiple spots with lower molecular weights and a wide range of pI's could be seen. Two of these spots displayed the same MW and pI the spots initially selected for analysis (Fig. 12A-Arrow 1). Immunoblot of samples infected with either VV-WT (data not shown) or VV-K5 revealed a similar pattern of spots. To prove that the lower molecular weight spots corresponded to cleavage products of Hsp60, samples were immunoblotted with a second antibody (clone H-1), which recognizes an epitope at the extreme amino-terminus of Hsp60. Samples from VV-WT infected cells, immunoblotted with H-1, failed to display spots with the same MW and pI as those initially analyzed (Fig. 12B). Immunoblot with H-1, however, did reveal spots with lower MW and higher pI than full length Hsp60, thus, while the spots initially selected for analysis corresponded to amino-terminal cleavages of Hsp60, infection with VV-WT results in cleavage of Hsp60 from both the amino- and carboxy-termini. Interestingly, in samples infected with VV-M153R, only spots corresponding to full length Hsp60 were observed following immunoblot with either LK-1 or H-1, suggesting that the reason the initially analyzed spots displayed altered protein expression is the failure of Hsp60 to be cleavage following infection with VV-M153R.

Cleavage of Hsp60 is induced as a late effect of vaccinia infection

To determine the kinetics with which vaccinia infection induces cleavage of Hsp60 analyzed the appearance of cleavage products following infection (Fig. 13A). Spots corresponding to cleavage products of Hsp60 were observed in samples prepared 10 hours post-infection, with additional cleavage products appearing in samples prepared 15 to 25 hours post-infection. In contrast, full length Hsp60 was highly abundant at time points prior to 10 hours post-infection, while at later time points full length Hsp60 steady decreased until it represented a fairly minor fraction at 25 hours. Samples treated with cytosine arabinoside (AraC), which inhibits viral DNA synthesis, showed no evidence of Hsp60 cleavage (Fig. 13B), suggesting that cleavage of Hsp60 requires vaccinia late gene expression.

Expression of M153R actively blocks Cleavage of Hsp60

Both VV-WT and VV-M153R grew to similar titers and caused similar cytopathic effects following infection of HeLa cells (data not shown). This result suggested that the failure of VV-M153R to induce cleavage of Hsp60 was not due to a general viral defect. To rule out this possibility, cells were either infected singlely with VV-WT or coinfected with VV-WT and VV-M153R at various MOI. 15 hours post-infection, cells were harvested and cleavage of Hsp60 was analyzed via immunoblotting with LK-1. Similar levels of Hsp60 cleavage were observed following infection with any MOI of VV-WT (Fig. 14 left side). In contrast, samples coinfected with both VV-WT and VV-M153R displayed significantly reduced cleavage of Hsp60 compared to samples infected with a similar MOI of VV-WT (compare Fig. 14 right to left). These data suggest that expression of M153R actively blocks cleavage of Hsp60.

Cleavage of Hsp60 is not the result of normal Cellular Apoptosis

Since Hsp60 plays a role in the endogenous apoptotic pathway, we hypothesized that cleavage of Hsp60 might be a result of cellular breakdown during apoptosis. To test this, I induced both the endogenous and exogenous apoptotic pathways using the general kinase inhibitor staurosporine (STS) or crosslinking of Fas with anti-Fas antibody. To determine if the endogenous apoptotic pathway played a role in Hsp60 cleavage, Hela cells were treated with 1μM STS for 3 hours. To confirm the induction of apoptosis, cells were fractionated into mitochondrial and soluble fractions and the localization of cytochrome c and Hsp60 were analyzed via immunoblot (Fig. 15). As previously reported, treatment of HeLa cells with STS induced release of cytochrome c from the mitochondria to the cytoplasm (Fig. 15A Top)(199). In samples infected with VV-WT, VV-CD4, or VV-M153R, however, release of cytochrome c was inhibited, probably due to the previously characterized apoptotic inhibitor F1L expressed by vaccinia (199). Consistent with previous results, induction of apoptosis or infection with vaccinia did not alter the mitochondrial localization observed for the majority of Hsp60 (Fig. 15A Bottom). To determine if induction of apoptosis via STS affected cleavage of Hsp60, samples were infected with VV-WT for 12 hours and then treated with STS for an additional 3 hours. In cells infected with either VV-WT or VV-CD4 the addition of STS did not significantly alter the pattern or abundance of Hsp60 cleavage (Fig. 15B). Additionally, mock infected cells treated with STS or cells infected with VV-M153R and treated with STS also failed to display cleavage of Hsp60. These data suggest that, while

treatment with STS induced apoptosis in HeLa cells, that induction does not have an obvious affect on Hsp60.

To determine if the exogenous apoptotic pathway might have a larger impact on Hsp60 cleavage, cells were treated with anti-Fas activating antibody overnight. Cells were then harvested and analyzed as above. Crosslinking of Fas caused release of Hsp60 from the mitochondria to the cytosol (Fig. 15C), however, cleavage was not observed in either soluble or membrane bound Hsp60. This result is consistent with previous findings that induction of apoptosis via crosslinking with Fas antibody had little to no affect on Hsp60 (200). Interestingly, cells treated with anti-Fas antibody and infected with VV-WT also failed to show cleavage of Hsp60, suggesting that while cleavage of Hsp60 is not a direct result of apoptosis, the induction of specific apoptotic pathways might play an important role.

M153R blocks damage to the mitochondria

One of the major steps in apoptosis is the loss of mitochondrial membrane potential (201). To determine if expression of M153R affected the loss of mitochondrial membrane potential, infected cells were stained with TMRE dye for 30 minutes and then analyzed via flowcytometry. Since TMRE incorporates only into mitochondrial membranes with intact membrane potential, it can be used to measure the mitochondrial viability. Cells from mock infected samples stained uniformly TMRE high, demonstrating that their mitochondria were intact (Fig. 16A and B). Following infection with VV-WT or VV-CD4, however, a small percentage of cells displayed a loss of TMRE florescence, corresponding to a loss of mitochondrial membrane potential.

Interestingly, cells infected with VV-M153R displayed far fewer TMRE low cells than cells infected with control viruses, suggesting that expression of M153R inhibited the loss of membrane potential induced by VV-WT infection.

To determine if M153R was able to block the loss of mitochondrial membrane potential induced by other apoptotic stimuli, HeLa cells were infected with vaccinia for 12 hours and then treated with STS for 3 hours. Mock infected cells treated with STS displayed a loss of TMRE florescence, confirming that STS treatment induced loss of mitochondrial membrane potential (Fig. 16C). Similarly, cells infected with VV-WT or VV-CD4 and treated with STS also displayed a similar loss of TMRE florescence, In contrast, cells infected with VV-M153R and treated with STS showed significantly fewer TMRE low cells, suggesting that M153R could inhibit the damage to the mitochondria induced by STS.

Discussion

Our analysis was designed to use 2D-PAGE to identify novel substrates for the K3-family protein M153R. Our data reveal that there are numerous differences in membrane protein expression between cells infected with VV-M153R and cells infected with VV-WT, VV-CD4, or VV-K5 (Fig. 11A and data not shown). This result suggested that M153R affects a global cellular process. Although K3 proteins are not known to directly affect global cellular processes, there is evidence that their downregulation of surface proteins can have significant downstream impacts. For example, in endothelial cells, K5 downregulates the cell surface proteins CD31 (55) and VE-Cadherin (Mansouri, personal communication) resulting in the release of the transcription factor β-catenin

from the cell surface, likely increasing transcriptional activity of β-catenin (our unpublished observations). Similarly, K3 and K5 downregulate the interferon-γ receptor, potentially altering expression of every protein which responds to secreted Interferon-γ (59).

One potential cellular process that could be affected by M153R is apoptosis. M153R has been previously proposed to play a role in apoptosis due to the observed downregulation of Fas (76). Deletion of M153R from myxoma did not increase levels of apoptosis observed during myxoma infection *in vivo*, leading to the conclusion that M153R was not an apoptotic inhibitor. Myxoma-infected cells, however, do not undergo significant apoptosis due to the presence of the apoptotic inhibitor M11L (202). Like F1L, M11L localizes to the mitochondria and inhibits loss of mitochondrial membrane potential and release of cytochrome c (203). It is possible that deletion of M153R did not affect apoptosis *in vivo* due to the expression of M11L. Similarly, the presence of M153R might have played a role in reducing apoptosis in viruses lacking M11L (202). These data leave open the possibility that, in the absence of M11L, M153R might play a key role in regulating apoptosis.

Since F1L is expressed during VV-M153R infection, the observation that samples infected with VV-M153R display significantly fewer TMRE low cells than samples infected with VV-WT, suggests that M153R might have anti-apoptotic effects. Expression of M153R did not alter late markers of apoptosis such as DNA fragmentation; however, since these markers of apoptosis are inhibited by F1L, these data do not indicate that M153R does not inhibit apoptosis. Since F1L inhibits apoptosis at the level of mitochondrial involvement, the observation that M153R protects additional cells from

loss of mitochondrial membrane potential suggests that it functions prior to F1L. However, further studies are needed to determine the exact step at which M153R might inhibit apoptosis.

Our data also reveal that infection with vaccinia results in the amino- and carboxy-terminal cleavage of Hsp60 and that this cleavage is inhibited by expression of M153R. However, while the cleavage of Hsp60 induced by vaccinia was highly reproducibile, Hsp60 cleavage products could only be observed in samples that underwent the purification steps required for 2D-PAGE (outlined in materials and methods). In samples that underwent this purification process, cleavage products of Hsp60 could be observed following either 2D-PAGE or standard SDS-PAGE (data not shown). In contrast, whole cell lysates did not display cleavage of Hsp60 regardless of whether they were separated using standard SDS-PAGE of 2D-PAGE (data not shown). These data suggest that sample preparation plays a role in the observation of Hsp60 cleavage. There are two possible explanations for this observation. First is that cleavage of Hsp60 is the direct result of 2D-PAGE sample preparation. For example, whole cell extracts are generally prepared in the prescence of either SDS or proteosomal inhibitors to prevent protein degradation. However, neither of these compounds is used during my 2D-PAGE sample preparation due to their incompatibility with 2D-PAGE. Thus, certain proteases may be active during 2D-PAGE sample preparation that are inactive during standard whole cell lysate preparation. Since cleavage of Hsp60 is only observed in vaccinia infected samples, however, either the expression or activation of any potential proteases associated with this degradation must be affected by vaccinia infection. A second possibility is that my 2D-PAGE sample preparation enriches a subpopulation of

Hsp60 in which cleavage preferentially occurs. For example, Hsp60 is localized to the mitochondria, cytosol and plasma membrane. If infection with vaccinia induces cleavage of only plasma membrane localized Hsp60, cleaved Hsp60 might represent a small enough percentage of total Hsp60 that it could be missed following immunoblot of a whole cell lysate. In contrast, 2D-PAGE purification might enrich plasma membrane localized Hsp60 to the point that cleavage products of Hsp60 could be easily observed. We are currently unable to distinguish between these two hypotheses and thus, the physiological relevance of Hsp60 cleavage remains very much in doubt.

Since Hsp60 is known to play a role in apoptosis, M153Rs inhibition of Hsp60 cleavage could be either a direct effect or a side effect of M153Rs inhibition of apoptosis. M153Rs localization to the endoplasmic reticulum, late endosomes and plasma membrane(76,77) allows several mechanisms by which it might directly cause cleavage of Hsp60. For example, 20% of ER membranes are in constant contact with the mitochondria (204). Thus, ER localized M153R might cleavage mitochondrial Hsp60 through a direct interaction. A second possibility is that M153R interacts with the small percentage of Hsp60 which traffics to the plasma membrane (205). This hypothesis is supported by the observation that only a small percentage of Hsp60 is cleaved in VV-WT infection.

Alternatively, cleavage of Hsp60 might be a side effect of apoptosis. The observation that Hsp60 cleavage did not occur following treatment with STS or crosslinking with Fas antibody (Fig. 15) suggests that Hsp60 cleavage is not a general feature of apoptosis, however, it is possible that Hsp60 cleavage only results from specific forms of apoptotic stimuli. For example, vaccinia infection induces a specific

form of apoptosis due to the presence of its apoptotic inhibitor F1L (199). Cleavage of Hsp60 might be the result of the incomplete apoptosis induced by vaccinia and blocked by F1L. Interestingly, crosslinking of Fas inhibited cleavage of Hsp60 even in the presence of VV-WT infection (Fig. 15). Normally, apoptosis activates caspases 3 and 8 following release of cytochrome c. Since F1L blocks apoptosis prior to this release, these caspases are not likely to be activated in vaccinia infection. Crosslinking of Fas in HeLa cells, however, activates caspases 3 and 8 without requiring the loss of cytochrome c (206,207). This could lead to differential caspase activation in cells treated with Fas and infected with VV-WT as opposed to cells infected with VV-WT alone.

Whether M153R plays a role as an apoptotic inhibitor during myxoma infection remains to be determined. It has proven difficult to study the potential anti-apoptotic effects of M153R for several reasons. First, M153R is unable to block loss of mitochondrial membrane potential unless it is expressed in the context of a poxviral infection (our unpublished observations). M153R's failure to block loss of mitochondrial membrane potential under these condidtions, however, could be the result of mislocalization of M153R following expression from a plasmid vector (76,77). Unfortunately, all common poxviral vectors contain other apoptotic inhibitors, such as F1L. Since the exact mechanism of M153R's inhibition of Hsp60 cleavage is unknown, the role these other apoptotic inhibitors might play cannot currently be addressed. Second, M153R might block only specific apoptotic pathways, however, the apoptotic pathways induced by infection with VV-WT and myxoma-WT are not currently known. Infection of HeLa cells with myxoma-WT or myxoma-ΔM153R did not result in cleavage of Hsp60 (data not shown), however, HeLa cells are not permissive for full

myxoma infection. Thus, we were unable to determine if the failure of myxoma infection to induce Hsp60 cleavage was the result of an inappropriate apoptotic stimuli or a failure to generate a productive infection. Thus, further investigation is required to determine if the potential anti-apoptotic effects of M153R occur *in vivo*.

Figure 11: 2D-PAGE Analysis of M153R Expressing Cells

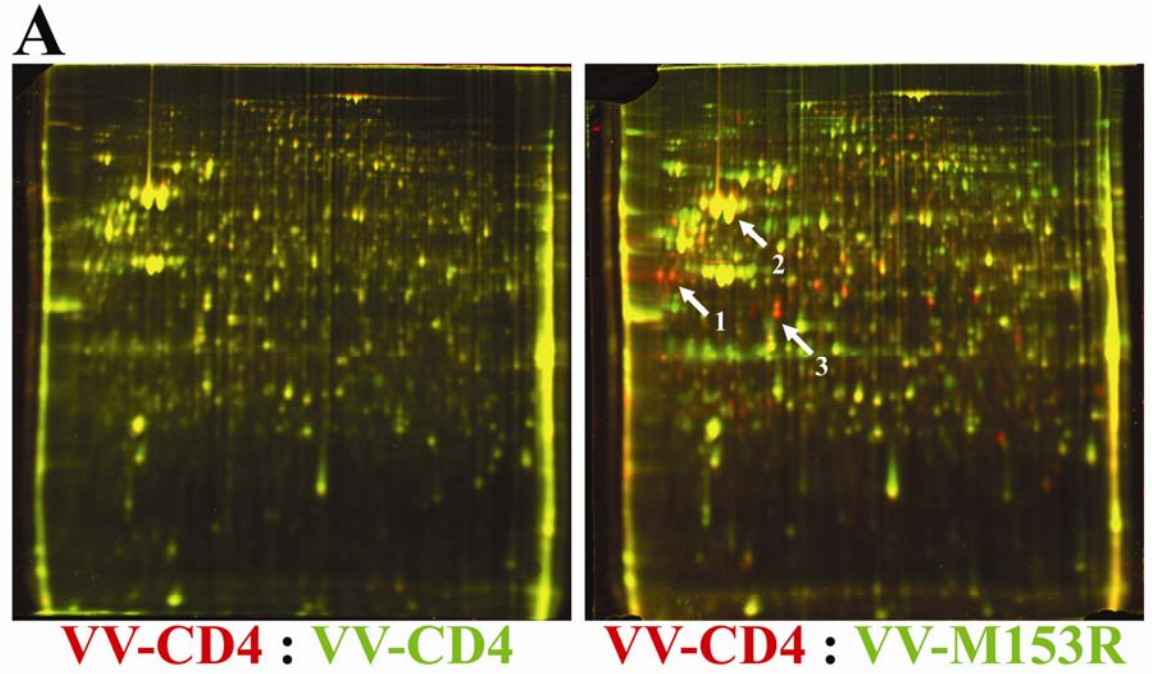

mlrlptvfrqmrpvsrvlaphltrayakdvkfgadaralmlqgvdlladavavtmgpkg
rtviieqswgspkvtkdgvtvaksidlkdkyknigaklvqdvanntneeagdgtttatvla
rsiakegfekiskganpveirrgvmlavdaviaelkkqskpvttpeeiaqvatisangdkei
gniisdamkkvgrkgvitvkdgktlndeleiiegmkfdrgyispyfintskgqkcefqday
vllsekkissiqsivpaleianahrkplviiaedvdgealstlvlnrlkvglqvvavkapgfgd
nrknqlkdmaiatggavfgeegltlnledvqphdlgkvgevivtkddamllkgkgdkaqi
ekriqeiieqldvttseyekeklnerlaklsdgvavlkvggtsdvevnekkdrvtdalnatra
aveegivlgggcallrcipaldsltpanedqkigieiikrtlkipamtiaknagvegsliveki
mqsssevgydamagdfvnmvekgiidptkvvrtalldaagvasllttaevvvteipkeek
dpgmgamggmgggmgggmf

Figure 11: 2D-PAGE Analysis of M153R Expressing Cells

HeLa cells were infected with either VV-CD4 or VV-M153R. 20 hours post-infection cells were harvested and prepared for 2D-PAGE analysis as described. Prior to 2D-PAGE analysis, samples were labeled with either Cy3 (red) or Cy5 (green) DIGE florophors (Amersham). Samples were combined and florescence visualized on a Typhoon 8600 imager (A). The location of full length Hsp60 (arrow 2) and the differentially expressed spot chosen for analysis (arrow 1) are marked. (B) Shows the amino-acid sequence of Hsp60. Peptides regions corresponding to peptides recovered during MS analysis are shown in red. The epitopes of the anti-Hsp60 antibodies LK-1 and H1 are underlined.

Figure 12: Infection with vaccinia results in cleavage of Hsp60

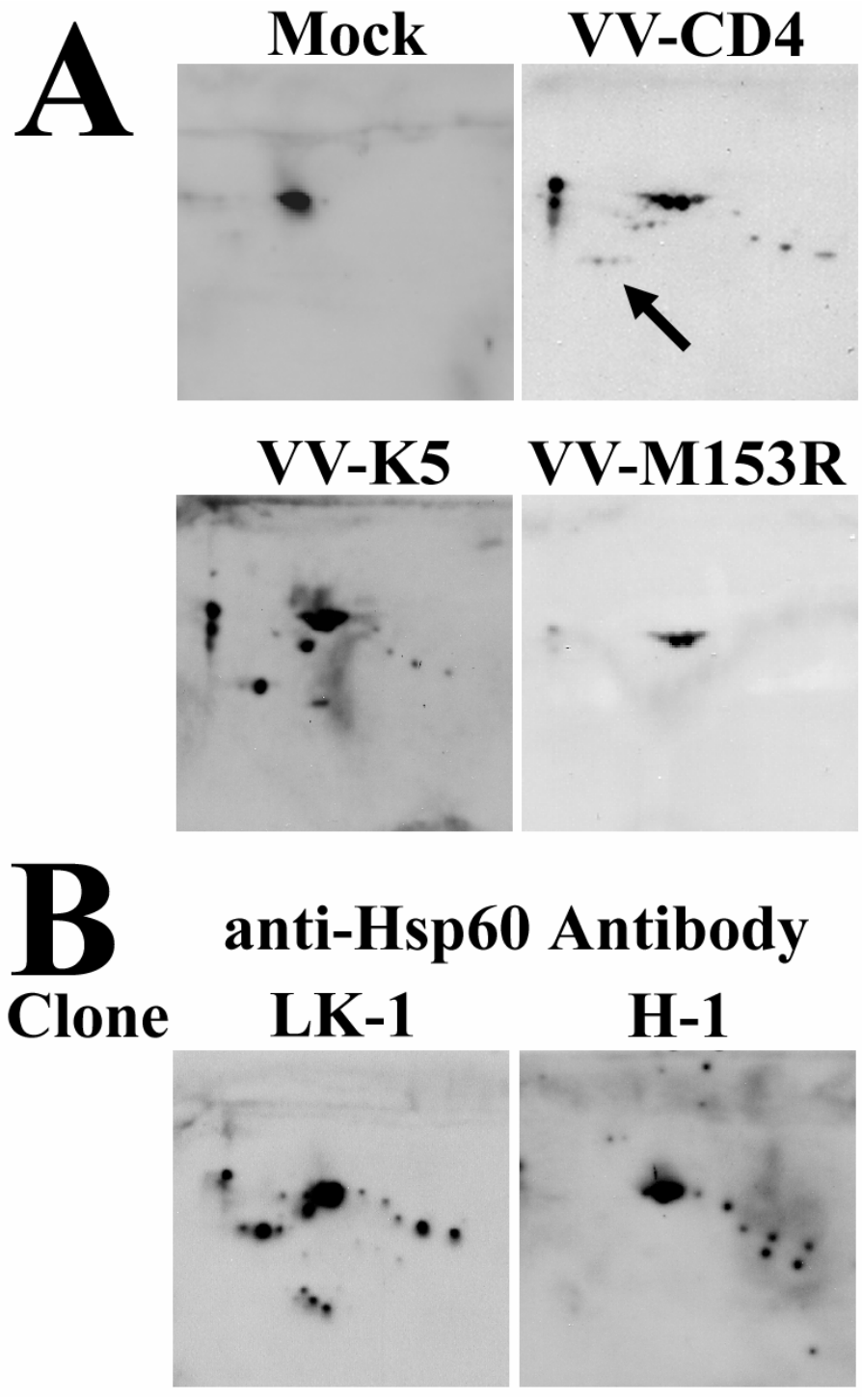

Figure 12: Infection with vaccinia results in cleavage of Hsp60

HeLa cells were infected with VV-CD4, VV-K5 or VV-M153R. Samples were prepared as described in materials and methods. Following 2D-PAGE analysis, gels were transferred to PVDF membranes and the localization of Hsp60 was analyzed via immunoblot with LK-1 (A). An arrow indicates the location of the spots which correspond to the spots initially selected for MS analysis. To determine if these spots represented cleavage products of Hsp60, cells were infected and samples prepared as above. Samples were then analyzed via immunoblotting with either the LK-1 or H-1 antibodies (B).

Figure 13: Cleavage of Hsp60 is a late effect following vaccinia infection

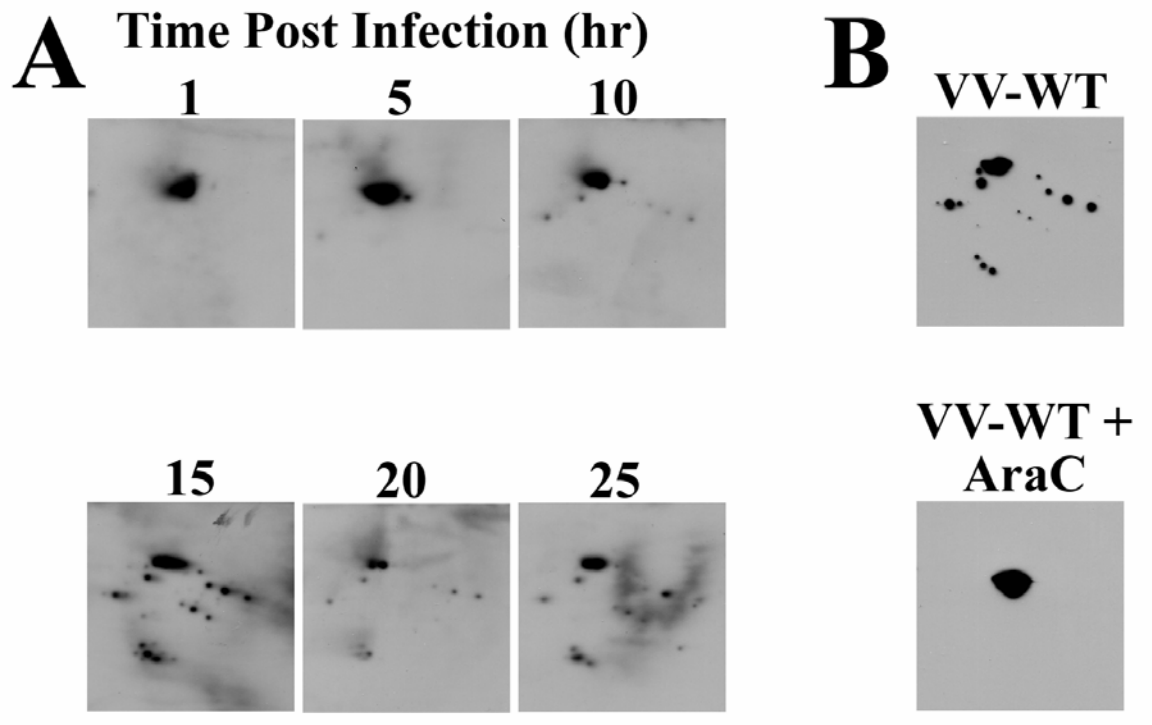

Figure 13: Cleavage of Hsp60 is a late effect following vaccinia infection

HeLa cells were infected with VV-WT. At the indicated time points post-infection, cells were harvested, samples separated using 2D-PAGE and the presence of cleaved Hsp60 was determined via immunoblot with LK-1 (A). To determine if vaccinia gene expression was required for Hsp60 cleavage, HeLa cells were infected in the presence of the viral replication inhibitor AraC. 16 hours post-infection cells were harvested and analyzed as above.

Figure 14: M153R actively blocks cleavage of Hsp60

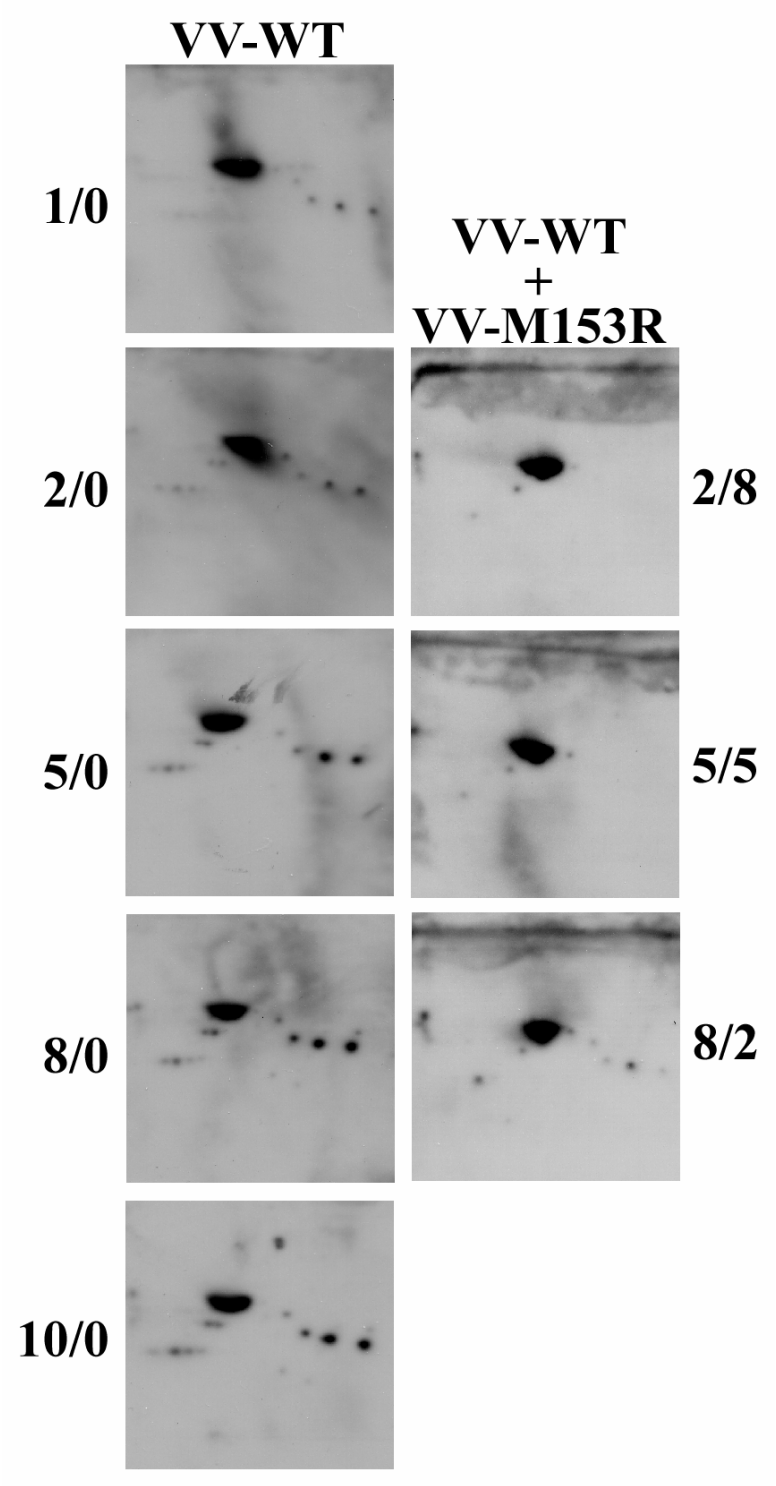

Figure 14: M153R actively blocks cleavage of Hsp60

Cells were infected with varying MOI's of either VV-WT alone (Left) or VV-WT + VV-M153R (Right). 16 hours post-infection cells were harvested and analyzed as previous described. The numbers to the left and right of the immunoblots show the final MOI's of each virus used to infect that sample (VV-WT/VV-M153R).

Figure 15: Cleavage of Hsp60 is not induced by other forms of apoptosis

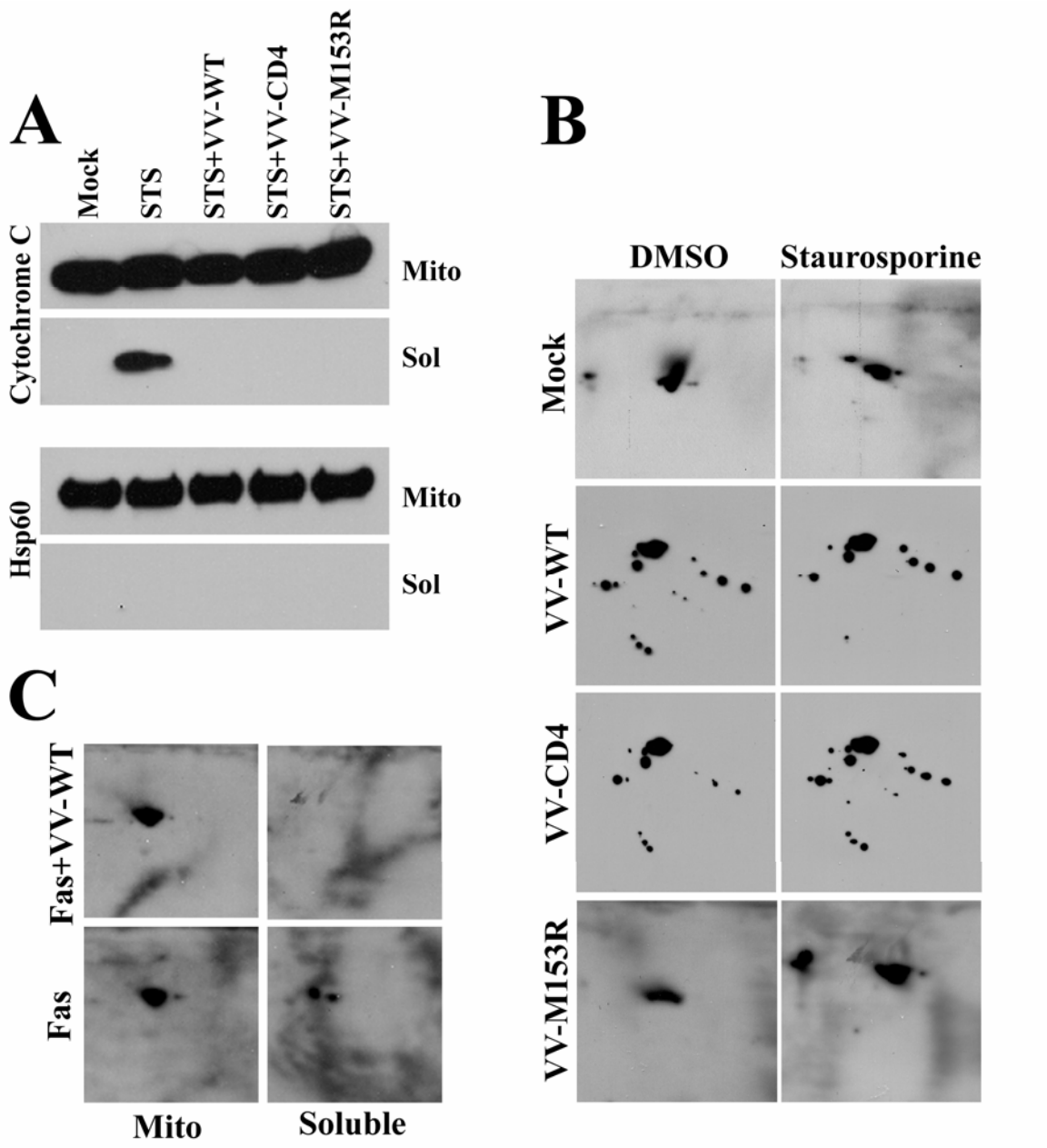

Figure 15: Cleavage of Hsp60 is not induced by other forms of apoptosis

HeLa cells were infected with VV-WT, VV-CD4, or VV-M153R for 12 hours and then treated with STS for an additional three hours. Cells were then harvested and mitochondrial and soluble fractions prepared as previously described (199). The presence of cytochrome C and Hsp60 in each fraction was then analyzed via immunoblot (A). Cells were infected with various VV and treated with STS as above. Cells were then harvested, samples separated using 2D-PAGE and the cleavage of Hsp60 analyzed via immunoblot with LK-1 (B). Cells were treated with an activation Fas antibody for 16 hours either in the presence of absence of VV-WT infection. Cells were then harvested and prepared for 2D-PAGE as described in the materials and methods. Both the membrane fraction and the soluble fraction were analyzed for the localization and cleavage of Hsp60 via immunoblot using LK-1 (C).

Figure 16: M153R blocks loss of mitochondrial membrane potential

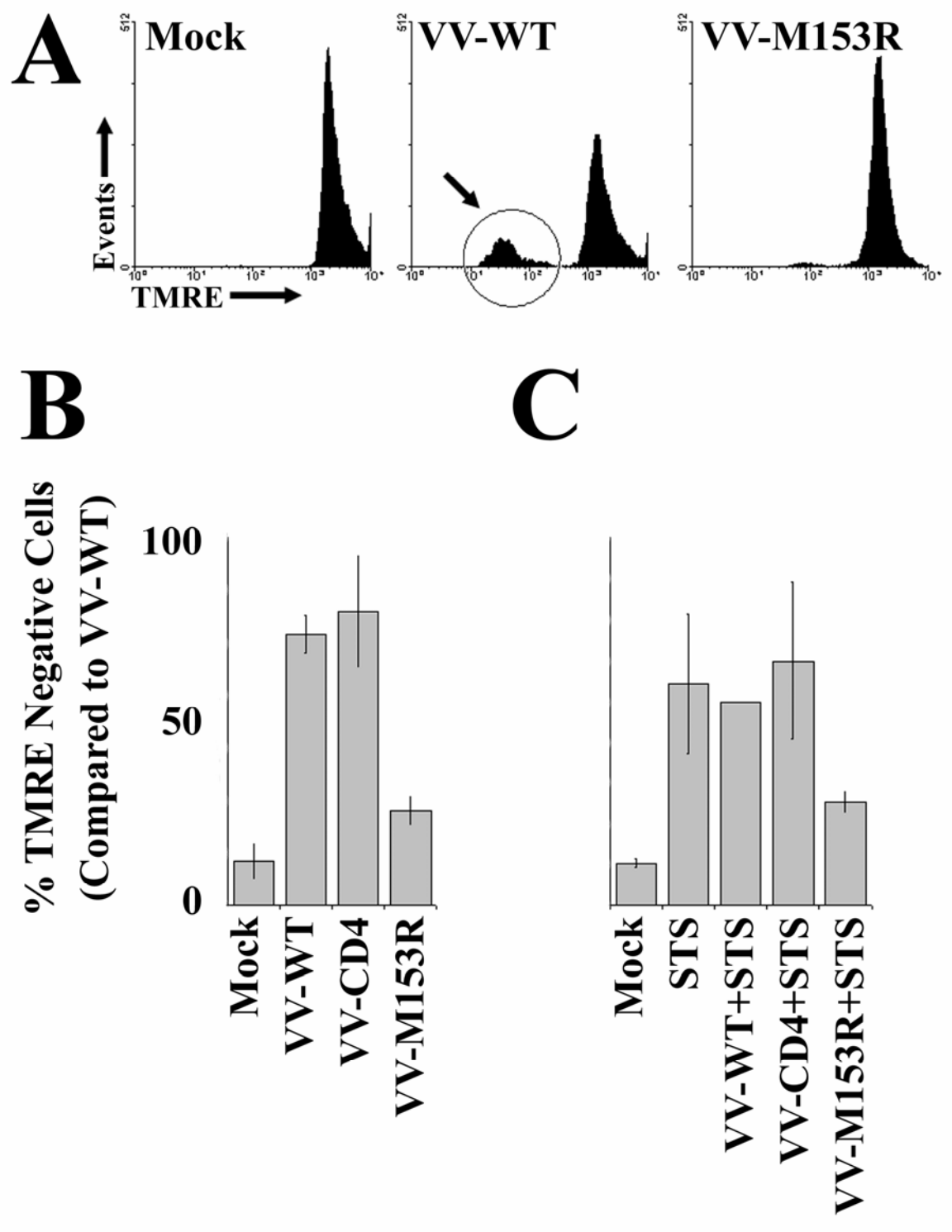

Figure 16: M153R blocks loss of mitochondrial membrane potential

Cells were infected with VV-WT, VV-CD4, or VV-M153R. 16 hours post-infection media was removed and cells were incubated in DMEM containing 0.2μM TMRE dye for 30 minutes. Cells were then trypsinized and the intensity of TMRE florescence was measured using flowcytometry. Cells in which some mitochondria have lost their membrane potential stain TMRE low as indicated by the circle and arrow (A). The percent of cells which are TMRE low was quantitated. The results of three separate experiments were combined and the average percent TMRE low cells and standard deviation are shown (B). To determine if M153R blocked the loss of mitochondrial membrane potential induced by other stimuli, cells were infected with VV-WT, VV-CD4, or VV-M153R for 12 hours followed by treatment with STS for three hours. Cells were then labeled with TMRE and analyzed as above. The results and standard deviation of three separate experiments is shown (C).

Chapter 5: SILAC Analysis of K5[4]

Introduction

Viral and bacterial virulence often correlates with the pathogen's ability to modulate the host's immune response. One pathway that is frequently targeted by intracellular pathogens, particularly viruses, is antigen presentation by major histocompatibility complex class I (MHC-I) molecules. By interfering with MHC-I expression, transport, or peptide loading, viruses become invisible to cytotoxic T cells. Interestingly, many viral gene products that interfere with MHC-I also target other immunologically relevant host cell proteins. For instance, US3 and US11 of human cytomegalovirus affect surface expression of both MHC-I and MHC-II (12,208). The murine cytomegalovirus protein m152 causes mislocalization of both MHC-I and Rae-1, an unrelated molecule that is a ligand for the activating receptor NKG2D found on natural killer cells and T cells (209,210). Finally, the HIV-1 proteins nef and vpu both downregulate MHC-I and the T cell co-receptor CD4 (211-214).

This multi-functionality is likely advantageous for the virus since it interferes with recognition by different immune cells and might counteract negative side effects of MHC-I downregulation such as activation of natural killer cells. These observations, however, also raise the question of whether the currently known host cell proteins are the only targets of a given viral immune regulator or whether additional targets exist. To

[4] This chapter has been previously published under the following reference:
Bartee E, McCormack AL, Früh K. Quantitative membrane proteomics reveals new cellular targets of viral immune modulators. PLoS Pathogens. 2006 Oct;2(10).
All data included in this thesis is my work except where noted by footnote.

address this question experimentally, we selected the K5 protein of Kaposi Sarcoma associated herpesvirus (KSHV), a particularly promiscuous member of a family of viral immune modulators. KSHV encodes two homologous members of the K3-family of viral immune modulators, K5 and K3 (19,20). These proteins display an amino-terminal RING-CH domain facing the cytoplasm which is followed by two membrane-traversing domains, resulting in a type III transmembrane topology (48). K3-family immune modulators are also found in several poxviral genomes (76,77) and are most likely derived from host genes since many eukaryotic organisms, including humans, contain similar proteins, termed membrane-associated RING-CH (MARCH) proteins, or c-MIR (105,181). Both viral and mammalian members of this family act as RING-type ubiquitin ligases (RING-E3s) and mediate the ubiquitination of lysines or cysteines in the cytoplasmic tail of transmembrane proteins (49,63). In most cases, ubiquitination occurs post–endoplasmic reticulum (ER), and ubiquitinated transmembrane proteins are endocytosed, sorted to multivesicular bodies (MVBs), and degraded in lysosomes (19,20,47,77,105). ER-associated proteosomal degradation (ERAD) has also been observed for the K3 protein of murine γ2-herpesvirus 68 (63) and for some substrates of K5 (55).

All viral K3-family proteins studied so far, and two of the human MARCH proteins, target MHC-I for degradation. Several K3-family proteins target other immunoreceptors in addition to MHC-I. For example, K5 also downregulates CD1d, ICAM-1, PECAM (CD31), and B7.2 (51,54,55,60), and M153R also targets CD4 (77). While the rules for substrate selection have yet to be established, this protein family has likely evolved to target subsets of transmembrane proteins. These proteins are thus an

excellent model for viral immune modulators that have more than one cellular target. In addition, these proteins are representative for other ubiquitin ligases that target certain groups of proteins, not all of which might be known (175).

K5 was initially identified by screening the KSHV genome for gene products inhibiting MHC-I expression (19). Further targets for K5 were then revealed by monitoring the expression of a small set of cell surface proteins, particularly those involved in T cell recognition of infected cells (51,55,60). These experiments, however, did not rule out that expression of other cellular proteins is inhibited by K5. Ideally, to determine whether additional targets exist, the entire cellular proteome would be studied in the presence or absence of K5. A method to absolutely quantify the entire protein complement of a cell has yet to be developed; however, recent advances in quantitative proteomics using stable isotope labeling allow the *relative* quantification of proteins in different samples by mass spectrometry (MS) (158).

In cell culture, the preferred method of comparative quantitative proteomics is to metabolically incorporate heavy or light forms of specific amino acids. This technique is known as stable isotope labeling with amino acids in cell culture (SILAC) (155,215). SILAC incorporates naturally occurring amino acids (C^{12} and N^{14}) into one sample and isotopically labeled amino acids (C^{13} and N^{15}) into another sample. The ratio of the "light" to "heavy" peptide can then be determined upon MS analysis of the combined samples. SILAC has been successfully used in yeast, plant, and mammalian cells to measure relative protein abundance (166-168).

K5 localizes to the ER, Golgi, and plasma membranes (48,55). Since K5 is known to degrade other transmembrane proteins, I focused on identifying proteins that were

reduced upon K5 expression in ER, Golgi, and plasma membrane fractions. In three independent repeat experiments I observed that MHC-I, activated leukocyte cell adhesion molecule (ALCAM), bone marrow stromal antigen 2 (BST2), and syntaxin-4 (STX4) were consistently reduced in plasma membranes of K5-expressing cells, whereas only K5 itself was increased in any fraction. While reduced MHC-I expression was expected, none of the other proteins were previously known to be affected by K5. Importantly, downregulation of each of these proteins by K5 was confirmed in independent experiments and by independent methods, thus validating the quantitative proteomics approach as a new method for identifying cellular proteins affected by viral immunomodulators.

Materials and Methods

Reagents and antibodies.

Concanamycin A (Sigma, http://www.sigmaaldrich.com) and MG132 (Sigma) were used at 50 nM and 50 μmol, respectively. The following reagents were obtained as indicated: protein A/G beads (Santa Cruz Biotechnology, http://www.scbt.com), ammonium bicarbonate (Sigma), sodium carbonate (Fisher Scientific, https://www1.fishersci.com), sucrose (Fisher Scientific), and urea (Fisher Scientific). The following antibodies were used: W6/32 (made in-house); anti-BST2 (Genetex, http://www.genetex.com); anti-Bap31 (Affinity Bioreagents, http://www.bioreagents.com); anti-STX4, anti-CD9, and anti-ALCAM (BD Biosciences, http://www.bdbiosciences.com); anti-Flag:FitC and anti-HA (Sigma); anti-ubiquitin (clone P4D1 from Invitrogen, http://www.invitrogen.com); anti-CD29 (University of

Iowa Developmental Studies Hybridoma Bank, http://www.uiowa.edu/~dshbwww); and goat anti-mouse Alexa Fluor 594 (Molecular Probes, http://probes.invitrogen.com).

Plasmids and cloning.

The following plasmids have been described previously: K5 C-Flag/pUHD10-1, K5 RING C-Flag/pUDH10-1, K3/pUDH10-1, M153R C-Flag/pUHD10-1, K5DE12 C-Flag/pUHD10-1, plasmids expressing both Vps4 and Vps4mut, and all full-length MARCH constructs in pUHD10-1 (45,77,105,182). An adenoviral vector expressing K5 C-Flag (Ad-K5) has been described previously (55). Adenovirus-expressing vpu was a generous gift from A. Moses (Vaccine and Gene Therapy Institute, USA).

A plasmid containing the ALCAM cDNA was a gift from G. Swart (Radboud University, Netherlands). ALCAM-HA was generated from this plasmid by PCR amplification of the ALCAM open reading frame. A carboxy-terminal HA tag was added during the amplification. The PCR product was then digested using suitable enzymes and ligated into the pUHD10-1 vector. MARCH-VIII truncation mutants (Δ46, Δ62, and Δ74) were generated by PCR amplification of the given region. An amino-terminal FLAG tag was added to each construct during amplification. Each PCR was then digested using suitable enzymes and ligated into the mammalian-expressing vector pUHD10-1. An adenoviral vector expressing MARCH-VIII was generated by cloning the full-length open reading frame from MARCH-VIII into the pShuttle vector (Stratagene, http://www.stratagene.com). Ad-MARCH-VIII virus was generated by linearization, transfection, and amplification according to the manufacturer's directions.

Culture conditions.

Prior to labeling, HeLa-Tet Off cells were grown in DMEM (Invitrogen) supplemented with 10% fetal calf serum (Hyclone, http://www.hyclone.com) and 1× Pen/Strep (Invitrogen). KSHV-infected DMVECs were established and maintained as previously described. KSHV-infected DMVECs were used in experiments when >90% of the cells expressed LANA-1.

Stable isotope labeling of HeLa cells.

Cells were labeled with stable isotopes using labeling medium (DMEM, Invitrogen) lacking the amino acids L-lysine and L-leucine (prepared according to the manufacturer's protocol). Medium was supplemented with 10% dialyzed fetal calf serum (Hyclone), 1× Pen/Strep (Invitrogen), and either isotopically light L-lysine and L-leucine (Sigma) or isotopically heavy L-lysine (U-13C6, 98%; U-15N2, 98%) and L-leucine (U-13C6, 98%; 15N, 98%) (Cambridge Isotope, http://www.isotope.com). Cells were maintained in labeling medium for 6 days prior to initiation of the experiment to insure complete labeling.

Preparation of samples for MS/MS analysis.

Cells grown in labeling medium were infected with either Ad-K5 (heavy-labeled cells) or Ad-WT (light-labeled cells) at an MOI of 25. Then 24 h post-infection, cells were harvested by scraping, washed twice in PBS, resuspended in PBS containing 5 mM

EDTA, and lysed by douncing. Unlysed cells and debris were cleared from the lysate by centrifugation for 5 min at 3,000 × *g*. The cleared lysates were separated into membrane and soluble fractions by centrifugation for 30 min at 45,000 × *g*. The membrane fraction was resuspended in PBS by sonication and separated over a discontinous sucrose gradient (2 M, 1.6 M, 1.25 M, 1.2 M, and 0.8 M) by centrifugation for 2.5 h at 25,000 rpm (Sorvall SW-28 rotor, http://www.sorvall.com). The bands corresponding to the plasma membrane (0.8–1.2 M interphase), Golgi (1.25–1.2 M interphase), and ER (1.6–1.25 M interphase) fractions were removed, diluted 5× in Tris-EDTA (pH 8.0), and centrifuged for 30 min at 45,000 × *g* to pellet the proteins contained in each fraction. Pellets were washed for 30 min in 50 mM sodium bicarbonate (pH 11.5) and centrifuged for 30 min at 45,000 × *g*, followed by a second wash in 50 mM ammonium bicarbonate (pH 8.5) and further centrifugation for 30 min at 45,000 × *g*. Final pellets were resuspended in 8.0 M deionized urea and 50 mM ammonium bicarbonate (pH 8.5) and protein levels quantitated using the Bio-Rad Protein Assay (Bio-Rad, http://www.biorad.com). Samples were reduced with DTT (Sigma) and alkylated with iodoacetamide (Sigma) prior to overnight digestion with trypsin (Promega, http://www.promega.com).

Chromatography, MS, and informatics.

Peptide mixtures were analyzed by electrospray ionization tandem MS, coupled to two-dimensional liquid chromatography, which was performed using a modified version of the protocol described by Link and coworkers (197). Briefly, 22 µg of sample was loaded onto an Opti-Pak capillary SCX trap cartridge (Optimize Technologies, http://www.optimizetech.com) and eluted stepwise (12.5, 25, 37.5, 50, 62.5, 75, 87.5,

100, 112.5, 125, 200, 300, or 450 mM ammonium acetate in 0.1% formic acid) onto a reverse phase C-18 capillary column (180 um × 100 mm, BioBasic-18; Thermo Electron, http://www.thermo.com). Peptides were then eluted using an acetonitrile gradient (5%, 5 min; 5%–40%, 75 min; 40%–90%, 10 min) into a ProteomeX LCQ Deca XP Plus mass spectrometer (Thermo Electron) equipped with a low-flow (1 μl/min) electrospray source. The instrument was set to trigger data-dependent MS/MS acquisition of the three most intense ions detected during the MS survey scan when total ion current per MS survey scan exceeded 5.0×10^5 counts.

Proteins were identified by analyzing tandem mass spectra with the Sequest algorithm (Thermo Electron) as described by Yates et al. (147) using the human subset of the UniProt/Swiss-Prot protein database (UniProt release 5.1, http://www.expasy.org/sprot). The search results were further analyzed using PeptideProphet (198). SILAC ratios were determined using the ASAPRatio algorithm (160). Multiple peptides derived from a single protein were included if PeptideProphet probability was greater than or equal to 0.85. All positive results were manually verified. The putative subcellular localization of proteins was determined using the Swiss-Prot database.

Immune fluorescence and flowcytometry.

Cells (1.5×10^4) were plated on 15-mm coverslips (Fisher Scientific) and allowed to adhere overnight prior to transfection. Following transfection, cells were washed with PBS, fixed with 2% paraformaldehyde for 20 min at room temperature, and permeabilized with 0.2% Triton X-100 for 3 min at room temperature. Nonspecific

binding sites were blocked with 3% BSA and 0.5% fish gelatin in PBS for 30 min at 37°C. The fixed cells were incubated overnight at 37°C with primary antibody diluted in blocking solution. Secondary and conjugated antibodies were diluted in blocking solution and incubated with the cells for at least 30 min at 37°C. Cells were washed six times with PBS between all antibody treatments. Slides were fixed a second time in 2% paraformaldehyde after the final antibody treatment and washed twice with PBS. Coverslips were then mounted on slides and covered with Vectashield H-1200 + DAPI (Vector Laboratories, http://www.vectorlabs.com).

For flowcytometry, cells were removed from tissue culture dishes with 0.05% trypsin-EDTA (Invitrogen), washed with ice-cold PBS, and incubated with appropriate antibody for 30 min at 4°C. The cells were washed with ice-cold PBS and either resuspended in ice-cold PBS or incubated with PE-conjugated anti-mouse secondary antibody (Dako, http://www.dako.com) and washed again before analysis with a BD Biosciences FACSCalibur flowcytometer.

Metabolic labeling, immunoprecipitation, and Western blotting.

HeLa cells were grown to 80% confluency in 100-mm tissue culture dishes and were transfected as above. At 24 h post-infection, cells were incubated in serum-free and methionine-free medium for 30 min, and metabolically labeled with ^{35}S-cysteine/^{35}S-methionine (300 μCi/plate; Amersham, http://www.amersham.com) for 20 min. After labeling, cells were washed twice with PBS and the label was chased for the indicated time in DMEM containing excess cold methionine/cysteine. Following chase, cells were lysed in PBS containing 1% NP-40 and protease inhibitors (Roche,

http://www.roche.com). The cell lysate was pre-cleared with protein A/G agarose beads overnight and incubated with 3 μg of antibody for 1 hours, followed by 1 hours with protein A/G beads. Immunoprecipated proteins were washed five times with 1% NP-40 in PBS. All samples were boiled in Laemmli buffer and analyzed by SDS-PAGE gel electrophoresis. Gels were fixed, dried, and exposed to Kodak (http://www.kodak.com) BioMax MR film. Western blotting was accomplished using the WesternBreeze Chemiluminescent Detection System (Invitrogen) following semi-dry transfer to PVDF membranes (Millipore, http:// www.millipore.com).

Results

Membrane Preparation and Mass Spectrometric Analysis

Since all previously described targets of K5 were type I transmembrane glycoproteins, we hypothesized that novel targets of K5 were most likely to be found in the membrane fraction. Most targets of K5 are ubiquitinated in a post-ER compartment and then sorted to endosomes in a clathrin-dependent process (108). We recently showed, however, that newly synthesized CD31/PECAM is degraded by K5 prior to ER exit by ERAD (55). Thus, novel targets could be eliminated from either the plasma membrane or from intracellular membranes, particularly within the exocytic pathway. For these reasons, we wanted to measure changes in the proteome of the plasma membrane, the Golgi membrane, and the ER membrane.

To measure changes in the membrane proteome I used SILAC coupled with MS analysis. Since SILAC incorporates differentially weighted tags directly into proteins,

this method allows the fractionation of membranes after combination of samples, thus minimizing variation due to sample preparation. The weight differential is then used to discriminate between peptides derived from each sample and to determine relative protein abundance by mass spectrometric analysis. Previous work has demonstrated that isotopically labeled amino acid analogs are indistinguishable from the natural product with respect to supporting cell growth in tissue culture (155). For our experiments, I added both $N^{15}/_{6}C^{13}$-labeled leucine and $_{2}N^{15}/_{6}C^{13}$-labeled lysine to HeLa cells. Since trypsin cleaves after lysines, and almost 70% of predicted tryptic peptides in the human genome contain at least one leucine, this double labeling procedure ensures that most tryptic peptides will contain at least one isotopic amino acid (215). HeLa cells were grown in labeling medium for 5 days prior to expression of K5 via adenovirus transduction. Due to rapid doubling of HeLa cells, this time frame allowed for the complete incorporation of isotopic amino acids (unpublished data). Control cells were grown in medium containing natural amino acids and transduced with the same multiplicity of infection of control adenovirus. K5-mediated downregulation of MHC-I was confirmed by flowcytometry 24 hours post-infection (unpublished data). To minimize variation due to biochemical procedures, plasma membrane, ER, and Golgi fractions were generated by sucrose gradient separation after lysis of the combined labeled and unlabeled cells (Figure 17). To further control for technical and biological variation, I repeated each experiment three times. Tryptic peptides from the resulting fractions were separated by two sequential chromatography steps (strong cation and reverse phase) prior to analysis by MS using an LCQ ion-trap instrument in data-dependent MS/MS mode. Tandem mass spectra of dissociated peptides were used to

search the human subset of the UniProt database, which was spiked with the viral K5 sequence using SEQUEST (216). To discriminate true assignments of MS/MS spectra to peptide sequences from false assignments, I applied PeptideProphet software using a score of 0.85 as the cutoff value for each identified peptide (198).

For each fraction I identified 500–700 unique proteins by at least one peptide in at least one experiment (Figure 18A). Of these, 100–150 proteins were identified in all three experiments, a finding that is consistent with previous reports (217). To validate the membrane preparations, I analyzed proteins that were identified in all three replicate experiments of each fraction with respect to their subcellular localization (Figure 18B). The plasma membrane fraction contained a large percentage of predicted cell surface proteins. The ER and the Golgi fraction contained both bona fide ER- and Golgi-resident proteins and many plasma membrane or transmembrane proteins, presumably on route to the cell surface. In addition, all fractions contained significant numbers of proteins predicted to localize to other intracellular organelles such as the nucleus, cytoplasm, or mitochondria. These proteins are likely derived from contaminating protein fractions. Since K5 is not expected to affect proteins in these compartments, these proteins serve as internal controls.

Differentially Expressed Proteins

To identify proteins whose expression was altered by K5, I analyzed proteins identified in all three experiments using the program ASAPRatio (160). ASAPRatio calculates protein expression ratios based on peak intensities (Fig. 18C). Since a 1.5-fold cutoff was previously shown to reflect a significantly different protein level (215),

proteins displaying a 1.5-fold change in either direction were considered differentially expressed. However, instead of limiting our analysis to proteins identified by multiple peptides in a single experiment as done previously (215), I accounted for biological variation by focusing on proteins that changed in the same direction in all three experiments, regardless of the number of peptides identified in either experiment. Using these criteria, only one protein changed in the ER and Golgi fractions. This protein was K5 itself, which was scored as "upregulated" due to being present in only the transduced samples. K5 was also scored as upregulated in the plasma membrane fraction of K5-expressing cells. Additionally, four proteins were downregulated in all three plasma membrane samples (Figure 18A; Table 1). Within this list were peptides mapping to the *HLA-A01* allele, which were present in significantly lower amounts in the plasma membrane fraction, but not in the ER or Golgi fractions. The lack of statistically significant MHC-I downregulation in the ER fraction is consistent with the observation that MHC-I assembly in the ER is not affected by K5 (19,20). Since both internal controls (transduced K5 as well as the K5 target protein MHC-I) were successfully identified as displaying altered ratios, I anticipated that the three remaining proteins in the plasma membrane fraction had a high chance of being true positive results.

Each of these three proteins was not previously identified as downregulated by K5: BST2 (also known as HM1.24 and CD316), STX4, and ALCAM (CD166). To independently confirm the downregulation of these proteins, I obtained specific antibodies for each and analyzed their expression in the presence or absence of K5.

BST2

BST2 (Hs.118110) is a protein of largely unknown function that has been implicated in normal as well as malignant B cell differentiation (218,219). BST2 contains both an amino-terminal transmembrane domain and a carboxy-terminal GPI linker resulting in an unusual topology (220). Despite this topological difference and lack of relationship to other K5 targets, BST2 was consistently scored as the most strongly underrepresented protein in K5-expressing cells (Table 1). A dramatic reduction of BST2 expression was confirmed in immunoblot of Ad-K5 infected HeLa cells, whereas BST2 was unaffected in Mock- or Ad-WT infected cells (Figure 19A). BST2 expression was also strongly reduced upon adenovirus-mediated expression of the human K5 homologue MARCH-VIII, but was less affected by the HIV protein vpu, which recruits a cellular ubiquitin ligase. To determine whether downregulation of BST2 required the ubiquitin ligase activity of K5, I transfected a catalytically inactive mutant of K5 (K5-RING) that lacks two critical cysteines in the K5-RING domain (45), and monitored BST2 expression by immunoblot. While transiently transfected K5 was still able to downregulate BST2, the K5-RING construct did not show an effect despite significantly higher levels of expression (Figure 19B). Whether this reduction of BST2 levels is a direct consequence of K5 ubiquitinating BST2, or an indirect consequence of the downregulation of other proteins by K5, has not yet been established. However, these experiments clearly confirm that BST2 protein levels are reduced in K5-expressing cells and demonstrate that this reduction requires catalytically active K5.

Syntaxin-4

The second protein identified as downregulated by K5 was STX4 (Hs.83734). Syntaxins belong to the t-SNARE (target-membrane-associated soluble N-ethylmaleimide fusion protein attachment protein receptor) family and are responsible for correctly targeting and fusing intracellular vesicles during transport (221). STX4 is a plasma membrane localized t-SNARE and mediates docking of transport vesicles at the cell surface. Interestingly, Syntaxin-6, a Golgi-localized t-SNARE, was previously observed to associate with MARCH-II and -III, human homologues of K5 (192,222). To confirm the reduction of STX4 protein in K5-expressing cells and to determine whether K5 or any of the MARCH proteins associate with STX4, I performed immunoblots and immunofluorescence experiments. Reduced levels of STX4 were observed in K5-expressing HeLa cells, thus confirming the mass spectrometric results (Figure 20A). Interestingly, STX4 levels were also reduced upon expression of MARCH-VIII, but not upon expression of vpu, suggesting that STX4 is specifically targeted by transmembrane RING-CH proteins. In immune fluorescence analysis of control cells, STX4 was observed at the plasma membrane. Expression of K5 led to a decrease in the overall intensity of STX4, but co-localization was not observed in these studies (Figure 20B). In contrast, significant co-localization was observed upon transfection of all MARCH proteins, except for MARCH-III and a naturally occurring truncated splicing product to MARCH-IX ("−RING" in Figure 20B). Moreover, STX4 was enriched in the subcellular compartments corresponding to the subcellular localization previously shown for the MARCH proteins (105). Thus, MARCH-IV and -VIII relocated STX4 to the Golgi and endosomes, respectively. Since these results are similar to the previously reported

binding of Syntaxin-6 to MARCH-II and -III (192,222), STX4 probably also interacts with the MARCH proteins which are able to induced STX4 relocalization.

The lack of co-localization of STX4 with K5 could be due to K5 degrading STX4. However, STX4 levels are also reduced in MARCH-VIII expressing cells, yet MARCH-VIII clearly associates with STX4. Alternatively, only the minor fraction of K5 that traffics to the plasma membrane (55) might interact with STX4, whereas the major, ER-localized population of K5 molecules cannot. To determine whether ER exit was the determining factor for co-localization with STX4, I generated truncated versions of MARCH proteins that were unable to leave the ER. Previous work has demonstrated that a carboxy-terminal PDZ motif in MARCH proteins is required for their forward transport since deletion of the final four amino acids resulted in ER retention of MARCH-II and -III (192,222). While I could not confirm such a role for the carboxy-terminal 45 amino acids in MARCH-VIII, I did observe that MARCH-VIII truncated by 62 or 74 amino acids was unable to exit the ER (Figure 20C). Importantly, ER-resident MARCH-VIII mutants did not interact with STX4. This observation raised the possibility that STX4 regulates ER exit of MARCH-VIII by binding within the 16 residues that differ between the Δ46 and Δ62 mutants. Small interfering RNA knockdown of STX4, however, had no effect on MARCH-VIII localization (unpublished data), so we consider this hypothesis unlikely. Therefore, we conclude that STX4 associates only with MARCH proteins that have left the ER. These data also suggest that STX4 associates, at least transiently, with the minor fraction of surface-expressed K5. This K5 fraction is not visible by immune fluorescence analysis, but can be detected by cell surface biotinylation (55). Our data further suggest that K5 and MARCH proteins not only interact with, but also degrade

syntaxins. Since syntaxins play a major role in vesicular traffic, the reduction of syntaxin levels could mislocalize transmembrane proteins, which might facilitate their targeting for ubiquitination. Further work will be required to address the role of syntaxins in the function of this protein family.

ALCAM (CD166)

ALCAM (CD166, Hs.591293) is a type I transmembrane glycoprotein of the Ig superfamily that is the ligand for the scavenger receptor CD6 on T cells (223). The ALCAM:CD6 interaction is part of the immunological synapse and is considered a co-stimulatory signal involved in lymphocyte activation and thymocyte development (224-226). Using transfection of a hemagglutinin epitope (HA)–tagged construct, I confirmed that co-transfection of K5 very efficiently eliminated ALCAM-HA (Figure 21A). Additionally, downregulation of ALCAM from the cell surface was confirmed by flowcytometry of HeLa cells transduced with Ad-K5. In contrast to ALCAM, K5 did not alter surface expression of CD9 or CD29 (Figure 21B). The co-stimulatory function of ALCAM renders this molecule an attractive target for viral immune modulators. To determine whether other viral K3 family proteins target ALCAM, I transfected K3 and the myxomavirus homologue M153R and monitored ALCAM expression by flowcytometry. Interestingly, M153R clearly reduced ALCAM surface levels, whereas the K3 protein, the most closely related K5 homologue, did not affect ALCAM (Figure 21C). This result is consistent with previous observations that K3 targets are limited to classical and nonclassical MHC-I–like molecules (19,20,60), whereas both K5 and M153R display broader substrate specificity (51,54,55). Within the MARCH family,

MARCH-IV and -IX downregulated ALCAM to a significant degree, while a modest effect was observed with MARCH-VIII (Figure 21C). The RING and transmembrane domains of MARCH-IV and -IX are highly homologous to each other, and this result is consistent with previous observations showing that the range of substrates for these two MARCH proteins overlaps with that of K5 (105).

The catalytically inactive K5-RING construct (45), as well as a K5 construct lacking acidic clusters in its carboxy-terminal domain (K5DE12) (52,55), did not affect surface expression of ALCAM (Figure 21C). These data suggest that downregulation of ALCAM requires the ubiquitin ligase activity and proper subcellular targeting of K5.

To investigate whether ALCAM downregulation occurs in KSHV-infected endothelial cells, I took advantage of the fact that K5 is not expressed in latently infected dermal microvascular endothelial cells (DMVECs), but can be induced upon addition of phorbol 12-myristate 13-acetate (PMA), which activates the lytic cycle (55). As shown previously, PMA treatment reduced expression of MHC-I on the cell surface of KSHV-infected DMVECs, but not uninfected DMVECs (Figure 21D). The mean florescence of ALCAM was unchanged in latently infected DMVECs, but was reduced approximately two-fold upon PMA treatment. In contrast, levels of CD81, a multiple transmembrane-spanning plasma membrane protein that is elevated in latently infected cells, did not change upon PMA treatment. Since PMA treatment does not induce lytic gene expression, and hence K5 expression, in all of the KSHV-infected cells (227), the actual levels of downregulation of both MHC-I and ALCAM might be considerably higher in individual cells. The correlation of ALCAM downregulation and K5 expression, however, renders it highly likely that virally expressed K5 is causing this effect.

Taken together, these data suggested that ALCAM is a bona fide substrate for the viral ubiquitin ligase K5. To confirm that ALCAM downregulation involved K5-dependent conjugation of ubiquitin, I transfected HeLa cells with ALCAM-HA either in the presence or absence of Ad-K5. Ad-vpu, Ad-K5DE12, and Ad-MARCH-VIII were used as controls to show that ALCAM was not downregulated by any ubiquitin ligases expressed from an adenovirus. Then, 24 hours post-transfection, cells were lysed and ALCAM precipitated using an antibody against the HA epitope. Samples were resolved on a SDS-PAGE gel, and the presence of ubiquitinated ALCAM-HA was analyzed by immunoblotting with the anti-ubiquitin antibody P4D1. In cells transfected with ALCAM-HA alone, ubiquitinated ALCAM-HA was undetectable (Figure 22A). In the presence of K5, however, substantially increased levels of ubiquitinated ALCAM-HA were observed, consistent with K5-mediated ubiquitination of ALCAM. Acidic cluster–deleted K5 and HIV-vpu did not affect the process, whereas MARCH-VIII slightly increased ALCAM-HA ubiquitination, consistent with the slight downregulation of endogenous ALCAM observed by flowcytometry.

Depending on the subcellular localization of the ubiquitination reaction, K5 targets are degraded in lysosomes or by the proteosome (55). To determine which degradation system was responsible for ALCAM degradation, I followed the maturation and degradation of ALCAM-HA using pulse-chase analysis in the presence of proteosomal inhibitors or inhibitors of endosomal acidification. In the absence of K5, ALCAM-HA acquired complete resistance to endoglycosidase H within two hours post-labeling, indicating intracellular transport of ALCAM through the Golgi complex (Figure 22B). After chasing for eight hours, ALCAM-HA levels remained high in control cells,

showing only a minor reduction due to endogenous turnover. Expression of K5 did not alter ALCAM biosynthesis or trafficking through the Golgi; however, amounts of endoglycosidase H–resistant ALCAM were significantly reduced, consistent with a post-Golgi degradation mechanism. K5-dependent degradation of ALCAM was inhibited by inhibiting lysosomal acidification with concanamycin A but not by the proteosomal inhibitor MG132. A similar effect was observed with fluorescent microscopy analysis (unpublished data). To determine whether ALCAM is targeted to lysosomes via the MVB pathway, I co-transfected K5 with a dominant negative version of the AAA-ATPase Vps4 (DNvps4), which prevents MVB formation (228). Expression of DNvps4 partially restored surface expression of both MHC-I and ALCAM measured using flowcytometry, whereas WTvps4 had only a minor effect (Figure 22C). Taken together, these data indicate that K5 ubiquitinates ALCAM in a post-ER compartment, thus triggering ubiquitin-mediated endocytosis and targeting of ALCAM for lysosomal destruction via the MVB pathway. Since this mechanism is similar to that of other K5 targets, we conclude that ALCAM is a novel substrate for K5 as well as a target for M153R. Thus, we present a novel approach for the systematic identification of substrates for transmembrane ubiquitin ligases as well as viral immune modulators targeting membrane proteins.

Discussion

The goal of this work was to systematically search for novel targets of viral immune modulators. To this end, I applied SILAC, a quantitative proteomics method based on metabolic isotope labeling. Until now, the SILAC method was mainly used for

global comparative proteomics experiments expected to yield a relatively large number of changes, such as the comparison of cell surface proteins from Th1 versus Th2 cells (229), differential protein secretion from cancer versus normal cells (230), proteins associated with stimulation of a given receptor (231), or changes in substrates trapped by a mutant protease complex upon stress activation (232). To our knowledge, however, our data represents the first time SILAC has been used in an experiment where only a few protein changes were expected. A major challenge for this approach was to identify true changes among the high rate of false positives that are caused by false peptide identification, inaccurate measurements of peptide intensity by, or biological variation arising during the labeling procedure. For these reasons, protein quantitation in SILAC experiments is usually limited to proteins that are identified by two or more peptides (e.g., (232)). Limiting quantiation to proteins identified by two or more peptides allows confirmation of each peptide by a second peptide from the same protein, thus raising confidence that calculated protein ratios are accurate. This approach, however, severely limits proteome coverage, particularly for low abundance proteins that are often identified by only one peptide. For this reason I sought to include all identified proteins in my analysis regardless of how many peptides were used in their identification. Inclusion of single peptide identifications raised the background for individual experiments to the point that it was impossible to discriminate between true positives and false positives purely by a fold-change cutoff (unpublished data). By analyzing three biological replicate experiments, I were able to identify true positives. The use of three replicates sets a high threshold and might exclude potential substrates. However, upon lowering the stringency (either two out of three experiments or several peptides in one experiment), I was unable

to confirm additional targets from a few selected candidates, suggesting a dramatic increase in the false positive rate (unpublished data). In contrast, using three replicates resulted in 100% specificity.

The rate of false negatives—the proteins that were affected by K5 but were eliminated by these selection criteria—is difficult to gauge since only a few of the known K5 targets (MHC-I and ICAM-1) are present in HeLa cells. No peptides derived from ICAM-1 were identified, probably since ICAM-1 is expressed at low levels in this cell type unless induced by pro-inflammatory stimuli. A better estimate of the false negative rate could potentially be obtained by analyzing other cell types, such as B cells and endothelial cells that express high levels of multiple K5 targets. The sensitivity of the method is therefore presently unknown. However, since only a fraction of the membrane proteome was identified here, it is likely that additional targets for K5 will be revealed by improved protein identification, improved analysis methods, or improved enrichment of the target proteome.

Using specific antibodies as well as epitope tagging, I confirmed the K5-dependent reduction in protein abundance for BST2, STX4, and ALCAM in independent experiments. Of these proteins, only BST2 was unrelated to protein families previously shown to interact with or be targeted by the MARCH family or K3 family proteins. Downregulation of BST2 required the ubiquitin ligase function of K5, suggesting that the reduced expression of BST2 is linked to the enzymatic function of K5. However, I have not ruled out the possibility that BST2 levels are indirectly affected by another protein that is targeted by K5. Thus, one of the limitations of the SILAC approach is that this technique does not discriminate between proteins that are targeted directly and proteins

that are targeted indirectly by the transmembrane ubiquitin ligases. This limitation could possibly be overcome by combining the SILAC analysis with proteomic analysis of ubiquitinated proteins (233,234). Further experiments will be needed to determine whether BST2 is a bona fide target of K5 or related molecules. If so, BST2 could play an as yet unknown role in immune defense.

The identification of STX4 by the SILAC method was surprising for several reasons. First, the K5-induced changes in STX4 levels were relatively modest compared to those for MHC-I, ALCAM, or BST2. This observation demonstrates that even moderately changing proteins can be identified by SILAC, provided these changes can be measured reproducibly. Second, previous observations suggested that MARCH proteins interact with but do not degraded syntaxins. Third, STX4 is quite different from the typical K5 substrates, which mostly represent type I glycoproteins of the Ig superfamily. In contrast, STX4 is a type II transmembrane protein with a carboxy-terminal tail-anchor and multiple coiled-coil domains. As discussed above for BST2, K5 might therefore mediate degradation of STX4 through an indirect mechanism. However, the co-localization of STX4 with all MARCH proteins that locate to post-ER compartments suggests that STX4 interaction is a general feature of the entire protein family, including K5. STX4 thus joins a growing list of vesicular trafficking regulators interacting with MARCH-family or K3-family proteins. In addition to the above-mentioned Golgi t-SNARE syntaxin-6 that interacts with MARCH-II and -III, this list includes the COP-I adaptor protein PACS-2 (55) and the ER/*cis*-Golgi-located adaptor protein Vap-A (R. Means and S. Lang, personal communication). Either such interactions could locate the RING-CH proteins to specific vesicular compartments, or the RING-CH protein could

interfere with the function of the vesicular regulators. In the case of STX4, downregulation of STX4 might reduce the exocytosis of certain proteins. For instance, STX4 is required for the secretion of insulin in pancreatic beta cells (235). One could therefore speculate that, by degrading STX4, KSHV prevents the secretion of immune stimulatory chemokines or cytokines. Interestingly, another membrane-associated RING ubiquitin ligase, termed Staring, was previously shown to interact with, ubiquitinate, and degrade syntaxin-1 (236). Therefore, degradation of STX4 by endogenous MARCH proteins could play a role in the turnover of STX4, thus regulating exocytosis.

The final novel protein identified by our SILAC screen was ALCAM (CD166). Similar to other proteins downregulated by K5, ALCAM is a type I glycoprotein of the Ig superfamily. Several lines of evidence suggest that ALCAM is a bona fide target of K5. ALCAM downregulation required a functional RING-CH domain and acidic motif in K5. Similar to other K5 target molecules, ALCAM was ubiquitinated and targeted to lysosomes via the MVB pathway. K5 most likely ubiquitinates ALCAM at the plasma membrane, resulting in ubiquitin-mediated endocytosis and lysosomal destruction.

In addition, I observed that the myxomavirus protein M153R downregulated ALCAM, likely by a similar mechanism. M153R has previously been shown to prevent T cell recognition of myxomavirus-infected cells (76). In addition, Coscoy et al. demonstrated that K5-transfected B cells do not stimulate T cells (51). While the predominant reason for this lack of T cell recognition is likely the downregulation of MHC-I from the cell surface, Coscoy et al. showed that the elimination of B7.2 and ICAM-1 further reduces T cell receptor (TCR) signaling (51). These observations led to the conclusion that the combined effect of preventing both the primary signal via the

TCR and the co-stimulatory signals via LFA-1 and CD28, the respective ligands of ICAM-1 and B7.2, minimizes T cell activation by KSHV-infected B cells. Similar to LFA-1 and CD28, ALCAM's ligand, CD6, becomes an integral part of the immunological synapse. Specifically, ICAM-1 forms a ring around the synapse, whereas CD28 and CD6 co-localize with the TCR in the center of the synapse (224). This supramolecular structure is required for the sustained TCR engagement needed to generate the full repertoire of T cell responses, including signal transduction, cytokine generation, and cell proliferation (237). Although the function of CD6 has not been studied as extensively as that of LFA-1 and CD28, there is accumulating evidence that the CD6:ALCAM interaction contributes to formation and function of the immunological synapse. Antibodies to CD6 activate T cells (238) and CD6-blocking antibodies or recombinant ALCAM-Fc proteins inhibit T cell proliferation induced by dendritic cells (226). Taken together, these observations strongly support the notion that, by downregulating ALCAM, K5 and M153R further optimize the ability of their respective viruses to prevent T cell activation. Moreover, the finding that ALCAM is eliminated by immune modulators from both herpesviruses and poxviruses suggests that the ALCAM:CD6 ligand receptor pair plays a previously unappreciated role in anti-viral immunity.

In summary, our results validate the use of quantitative proteomics to identify new substrates of viral and cellular immune modulators. In addition to identifying this specific class of transmembrane ubiquitin ligases, it is conceivable that this approach can be used to identify additional targets for any viral proteins that are known to reduce the abundance of their host cell target molecules. Since many viral proteins are considered to

be multi-functional, such a systematic, unbiased search for novel host cell targets could help to reveal new functions of viral proteins. This proteomics approach can also be used to find novel targets for cellular proteins that degrade a specific set of targets, such as novel substrates for cellular ubiquitin ligases. Since ubiquitin ligases are one of the most abundant gene families in the human genome, almost every protein in the human genome might be regulated by one or more ubiquitin ligases. Identifying the ligase:substrate relationship will be a daunting but important task in unraveling the regulatory networks that govern cellular functions.

Figure 17. Schematic Representation of the SILAC Labeling and Purification Protocol

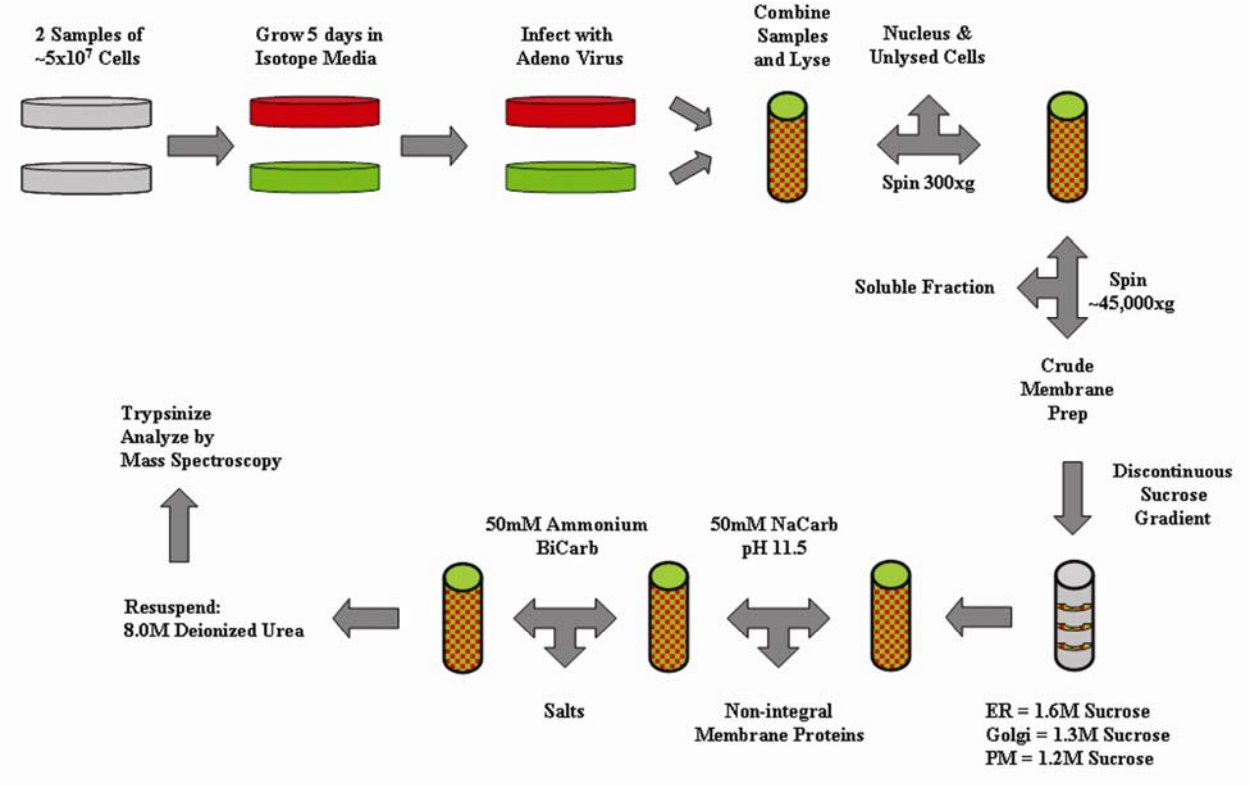

Figure 17. Schematic Representation of the SILAC Labeling and Purification Protocol

HeLa cells were grown for five days in labeling medium to ensure complete labeling. They were then infected with either adenovirus vector (light sample) or adenovirus-expressing K5 (heavy sample). Then 24 hours post-infection cells were harvested and counted, and equal numbers of cells combined. Samples were lysed in a Dounce homogenizer and unlysed cells removed by centrifugation. Membrane and soluble proteins were separated by centrifugation. The membrane pellet was resuspended, and different membrane fractions were separated over a discontinuous sucrose gradient. The bands corresponding to the plasma membrane (PM), Golgi, and ER fractions were removed and the proteins pelleted. The resulting pellet was then washed with sodium carbonate to remove non-integral membrane proteins, followed by ammonium bicarbonate to remove salts and other impurities. The final pellet was resuspended in 8M urea and digested with trypsin for MS/MS analysis.

Figure 18. Protein Identification and Differential Peptide Quantification

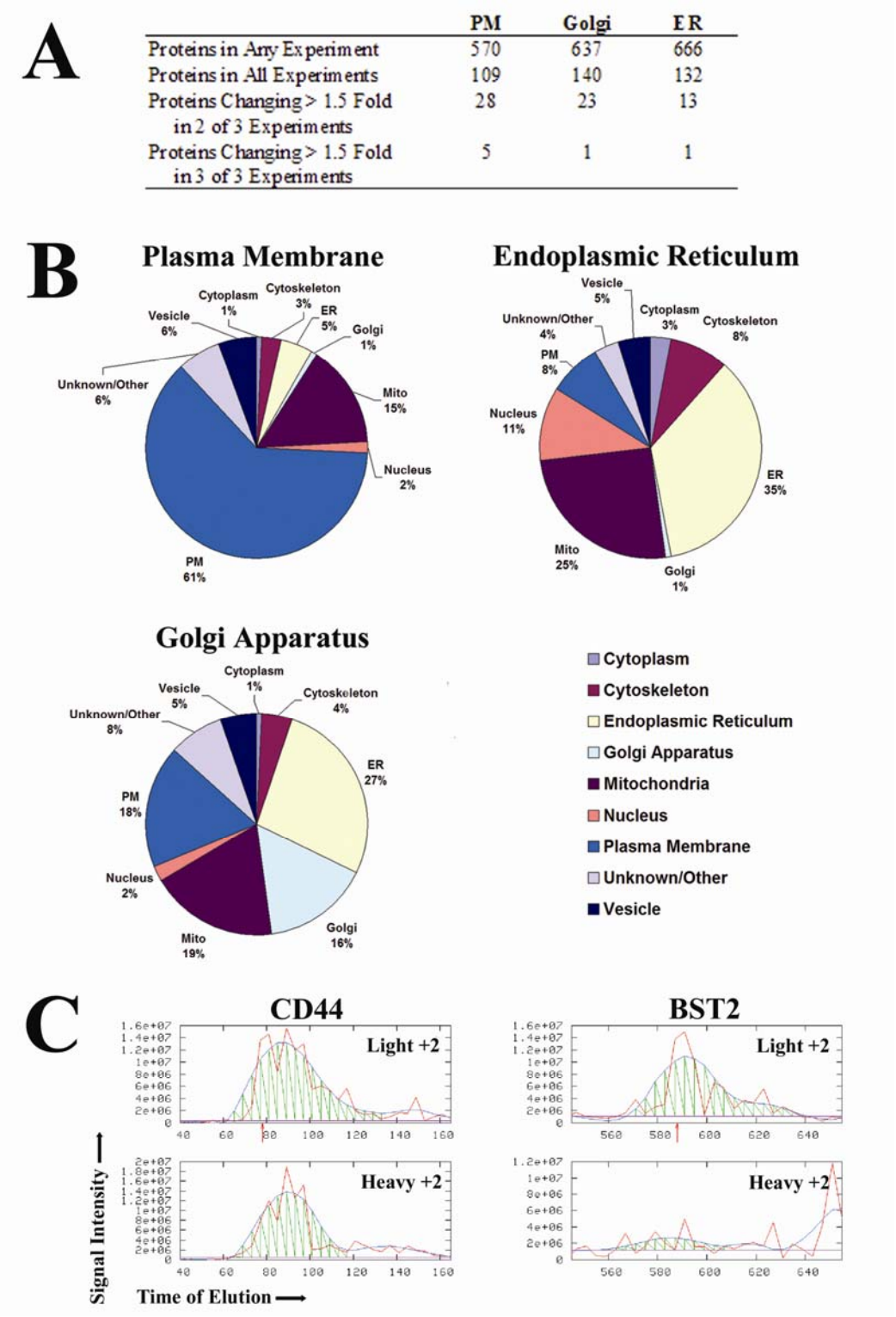

Figure 18. Protein Identification and Differential Peptide Quantification

(A) Approximately 500–700 proteins were identified by at least one peptide in each fraction; however, fewer than 150 proteins per fraction were identified in all three replicates. Of these, only five proteins changed more than 1.5-fold in the plasma membrane (PM) fraction, while only one protein changed more than 1.5-fold in all three replicates of either the golgi or ER fractions. (B) Proteins present in all three replicates of each fraction were analyzed for their predicted subcellular distribution using annotations in the Swiss-Prot proteomics database. (C) Comparison of signal intensities obtained for selected peptides from the indicated proteins. The red line indicates the actual raw data recovered from the mass spectrometer; the blue line is a hypothetical best fit line drawn to help analyze elution time of the light and heavy peptides. The orange arrows indicate the time at which the initial MS/MS scan was initiated. Peptides derived from unaltered proteins, such as CD44, display a similar intensity for both the light and heavy isotopes. Peptides derived from differentially expressed proteins, such as BST2, show clearly different intensity peaks for the light and heavy peptides. Note the slightly different scale for intensity of each peptide.

Table 1: Differentially expressed Proteins

Protein	Ratio			Unique Peptides
	Exp 1	Exp 2	Exp 3	
PM Fraction				
CD166 (ALCAM)	2.04 +/- 0.24 (1, 2)	2.59 +/- 0.96 (1, 3, 4)	1.68 +/- 0.19 (1)	(1) WKYEKPDGSPVFIAFR (2) ALFLETEQLKK (3) DLGNMEENKK (4) WSLTLIVEGKPQIK (5) SMIASTAITVHYLDLSLNPSGEVTR
BST2	3.14 +/- 0.36 (1, 2, 3)	3.19 +/- 2.39 (2, 3)	1.83 +/- 0.59 (2)	(1) ENQVLSVR (2) KVEELEGEITTLNHK (3) LQDASAEVER
Syntaxin 4	1.55 +/- 2.9 (1, 2)	2.20 +/- 0.87 (3, 4)	1.67 +/- 0.31 (4)	(1) AIEPQKEEADENYNSVNTR (2) VALVVHPGTAR (3) KTQHGVLSQQFVELINK (4) TQHGVLSQQFVELINK
MHC-I	2.69 +/- 0.89 (1, 2, 3, 4, 5)	2.60 +/- 2.52 (1, 2, 3, 4 7, 8, 9, 10 11, 12)	1.68 +/- .22 (1, 3, 5, 8)	(1) DGEDQTELVETRPAGDGTHQK (2) RYLENGKETLQR (3) YLENGKETLQR (4) AQSQTDRVDLGTLR (5) YTCHVQHEGLPEPLTLR (6) YTCHVQHEGLPK (7) GYHQYAYDGK (8) GYHQYAYDGKDYIALK (9) KGGSYSQAASSDSAQGSDVSLTACK (10) THMTHHAVSDHEATLR (11) HKWEAAHVAEQWR (12) THVTHHPVSDHEATLR
KSHV-K5	0.00 +/- 0.00 (1)	0.26 +/- 0.05 (1, 2, 3, 4)	0.30 +/- 0.19 (3)	(1) ALYAANNTR (2) EEVGNEGIHPCACTGELDNNHPQCLSTWLTVSR (3) TDLCAPTKKPVR (4) VTVLPYR
ER Fraction				
KSHV-K5	0.29 +/- 0.02 (1, 2)	0.04 +/- 0.01 (1, 2)	0.06 +/- 0.06 (2, 3, 4)	(1) ALYAANNTR (2) EEVGNEGIHPCACTGELDNNHPQCLSTWLTVSR (3) TDLCAPTKKPVR (4) VTVLPYR
Golgi Fraction				
KSHV-K5	0.20 +/- 0.10 (1, 4)	0.02 +/- 0.01 (1, 2)	0.10 +/- 0.11 (1, 2, 3, 4)	(1) ALYAANNTR (2) EEVGNEGIHPCACTGELDNNHPQCLSTWLTVSR (3) TDLCAPTKKPVR (4) VTVLPYR

Table 1: Differentially expressed Proteins

The Uniprot designation of each protein displaying a skewed ratio in all three experiments is given as well as the ratio reported in each experiment, the unique peptides used to identify that protein, and the experiment in which each peptide was recovered.

Figure 19. BST2 Is Differentially Expressed in K5-Expressing Cells

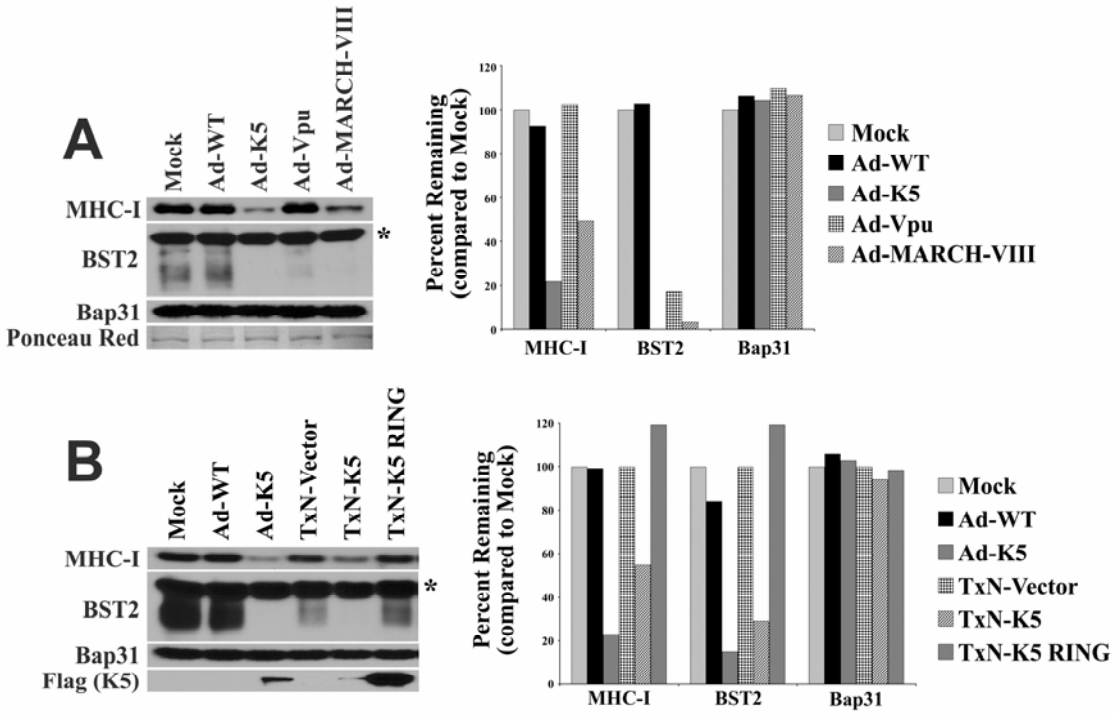

Figure 19. BST2 Is Differentially Expressed in K5-Expressing Cells

HeLa cells were transduced with Ad-WT, Ad-K5, Ad-vpu, or Ad-MARCH-VIII. Then 24 hours post-infection, cells were harvested and whole cell lysates were analyzed for the abundance of BST2 and MHC-I by Western blotting. Note that BST2 is highly glycosylated and runs as multiple bands. The high molecular weight band marked with an asterisk is non-specific. Equal protein loading was confirmed by visualizing the ER resident chaperone Bap31 as well as general protein staining with Ponceau red ((A), left). The intensity of each band was quantified using densitometry ((A), right). The specificity of BST2 downregulation was confirmed by transfecting K5 or a catalytically inactive K5-RING mutant, which showed no effect on either MHC-I or BST2 (B). The protein bands corresponding to BST2 are more intense in (B) than in (A) because of longer exposure of the autoradiograph as well as variation in electrophoretic separation. Note that the same lysates were analyzed in lanes 1–3 of the blots in both (A) and (B).

Figure 20. K5 Causes Downregulation but Not Relocalization of STX4

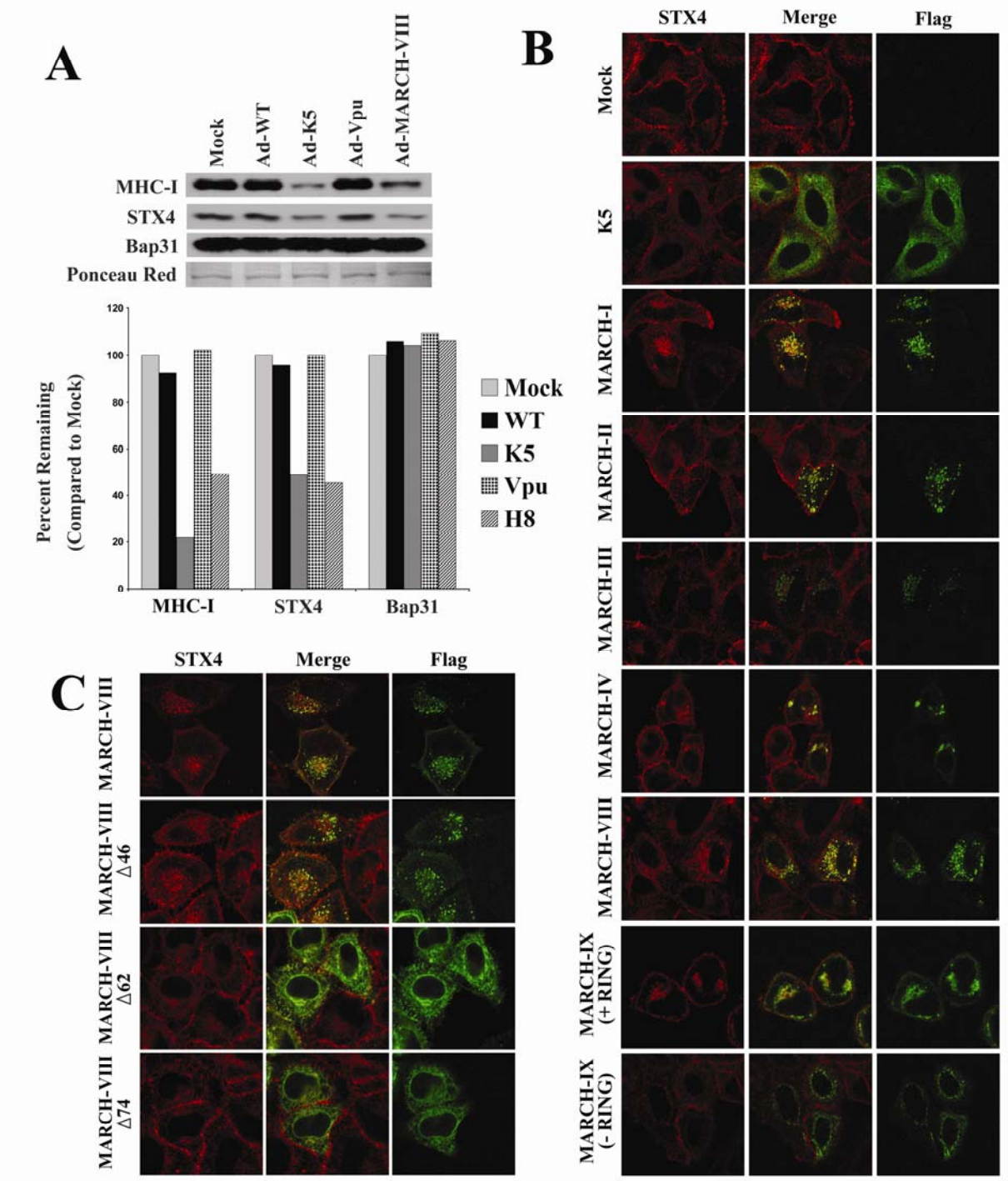

Figure 20. K5 Causes Downregulation but Not Relocalization of STX4

(A) HeLa cells were transduced with Ad-WT, Ad-K5, Ad-vpu, or Ad-MARCH-VIII. Then 24 hours post-infection cells were harvested and whole cell lysates were analyzed as in Figure 19, except that antibodies specific for STX4 were used. Expression of K5 resulted in a moderate but reproducible reduction of STX4 levels. (B) To determine if K5 or MARCH proteins caused a relocalization of STX4, HeLa cells were transfected with carboxy-terminally FLAG-tagged versions of the E3s shown. Cells were then analyzed for the location of STX4 (using an Alexa Fluor 594–conjugated secondary antibody, shown as red) as well as the overexpressed E3 (using a FITC-conjugated anti-FLAG antibody, shown as green). Co-localization of STX4 and the ubiquitin ligases is revealed as yellow co-staining. While K5 did not co-localize with STX4, several MARCH family proteins relocalized STX4 to a MARCH-containing compartment. A naturally occurring splice variant of MARCH-IX that lacks a complete RING domain and fails to exit the ER was unable to relocalize STX4. (C) carboxy-terminal truncation mutants of MARCH-VIII that failed to exit the ER do not co-localize with STX4.

Figure 21. K5 Downregulates ALCAM

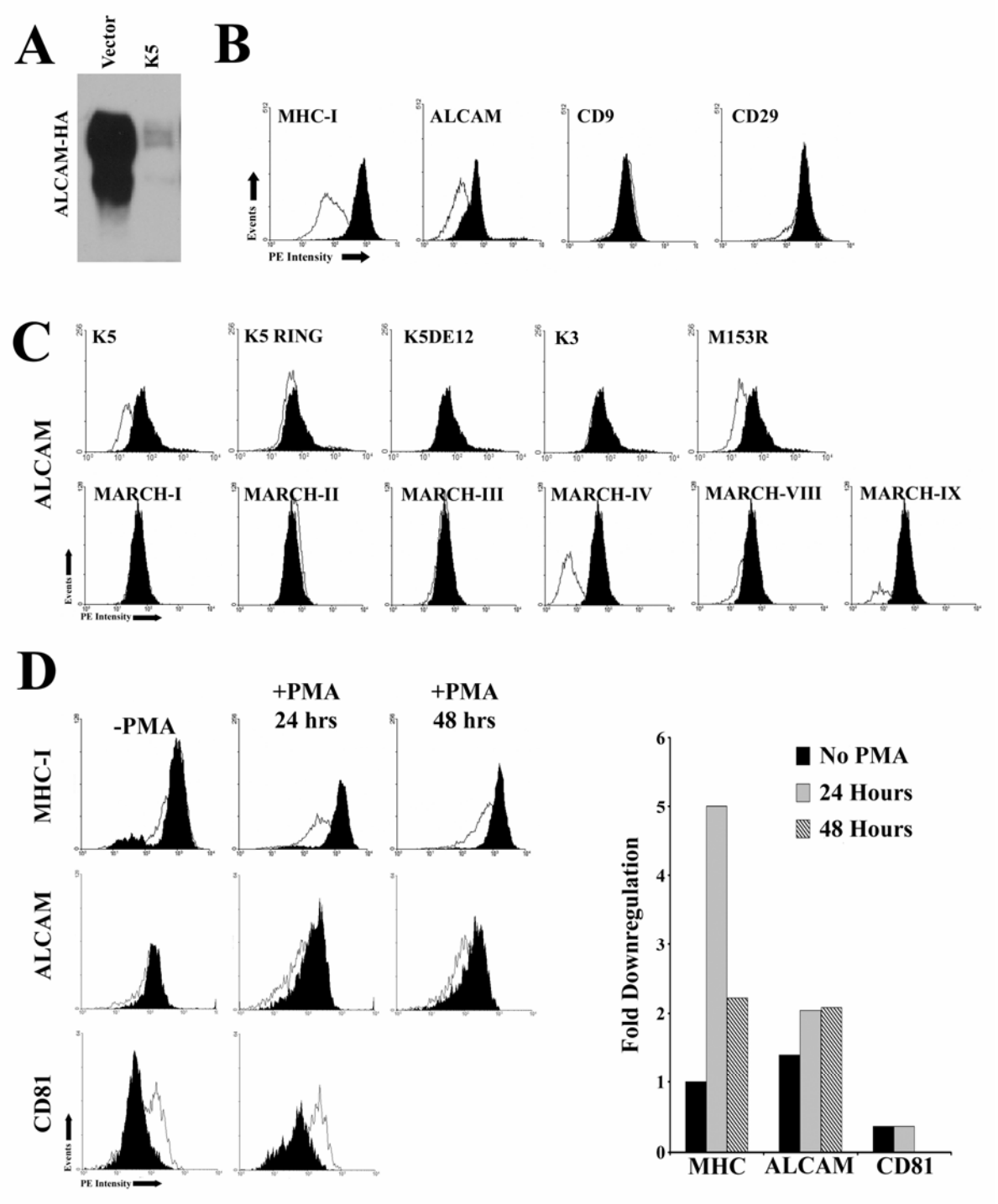

Figure 21. K5 Downregulates ALCAM

(A) carboxy-terminally HA-tagged ALCAM was co-transfected with K5 or control plasmid. Then 24 hours post-transfection cells were harvested and the abundance of ALCAM-HA in each lysate was measured by Western blotting with anti-HA antibody. (B) Cell surface expression of endogenous ALCAM in the presence or absence of K5 was determined by flowcytometry. HeLa cells were co-transfected with K5 and a green fluorescent protein (GFP)–expressing plasmid to identify transfectants. Then 24 hours post-transfection cells were harvested and stained with antibodies against MHC-I, ALCAM, CD9, and CD29. Both vector (solid black) and K5-transfected (white) cells were gated for GFP-expressing cells. (C) ALCAM downregulation by K5-related proteins was determined by transfecting HeLa cells with viral K3 family members (K3 and M153R) and the indicated human MARCH proteins. Also examined were mutant K5 proteins with enzymatically inactive RING-CH domains (K5-RING) or lacking acidic residues implicated in subcellular targeting (K5DE12). Neither K5 mutant reduced ALCAM levels. KSHV K3 was unable to downregulate ALCAM, whereas the myxomavirus M153R protein significantly reduced ALCAM surface expression. Two of the MARCH proteins, MARCH-IV and MARCH-IX, strongly downregulated ALCAM, while MARCH-VIII showed a minimal effect. (D) To determine whether ALCAM expression was affected by KSHV, latently infected immortalized DMVECs were treated with PMA to induce expression of lytic genes including K5. Surface levels of either MHC-I or ALCAM were measured by flowcytometry 24 and 48 hours post-induction. CD81, measured at 24 hours, was used as a control. The ratio between the mean

fluorescence intensity of infected and uninfected samples from these experiments is shown as fold change on the right.

Figure 22. Ubiquitination and Lysosomal Degradation of ALCAM in the Presence of K5

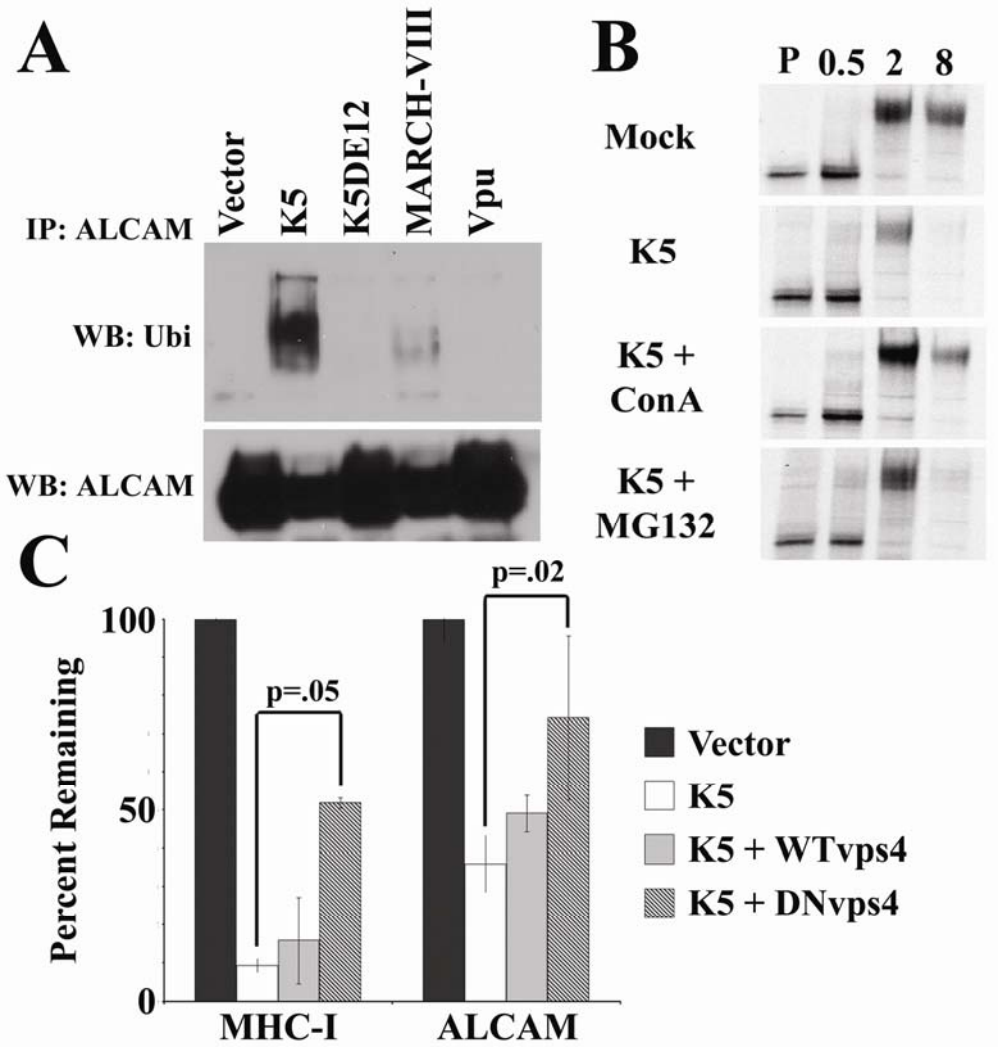

Figure 22. Ubiquitination and Lysosomal Degradation of ALCAM in the Presence of K5

(A) Ubiquitination of ALCAM was examined by co-transfection of HeLa cells with ALCAM-HA as well as the indicated E3s. Then 24 hours post-transfection, cells were lysed in 1% CHAPS, and ALCAM-HA was immunoprecipitated using anti-HA antibody. Samples were resolved on an 8% SDS-PAGE gel, transferred to PVDF, and immunoblotted (WB) with the anti-ubiquitin (Ubi) antibody P4D1 (top) or anti-HA (bottom). Ubiquitinated ALCAM was visible upon co-transfection of K5 and MARCH-VIII, but not with the inactive K5DE12 mutant and the unrelated HIV immune modulator vpu. (B) To determine whether ubiquitinated ALCAM was degraded by proteosomes or in lysosomes, the fate of newly synthesized ALCAM-HA was determined by metabolic labeling for 10 min with S^{35} Met/Cys and chasing the label for the indicated times (hours) in the presence of the indicated inhibitors. Following lysis, ALCAM-HA was immunoprecipitated using the HA antibody and samples were treated overnight with endoglycosidase H followed by electrophoretic separation. Note the increased recovery of ALCAM at eight hours in the presence of the endosomal/lysosomal proton pump inhibitor concanamycin A (ConA), but not in the presence of the proteosomal inhibitor MG132 (50 μmol). (C) Surface expression of ALCAM can be restored by overexpressing a dominant negative version of the AAA-ATPase Vps4 (DNvps4), which is essential for targeting proteins to MVBs. HeLa cells were transfected as indicated together with GFP to identify transfected cells. Then 24 hours post-transfection cells were harvested and the surface expression of either MHC-I or ALCAM was analyzed using flowcytometry. The graph shows the ratio of mean fluorescence intensity from K5-

transfected cells to that of control cells after gating for GFP. Data are averaged from three separate experiments.

Chapter 6: SILAC Analysis of MARCH-VIII[5]

Introduction

Ubiquitination plays a key role in regulating many diverse cellular functions, including cell cycle control (85), DNA repair (86), signaling (87), and protein destruction via the lysosome (88-90). The ubiquitin pathway consists of ubiquitin, a single ubiquitin activating enzyme (E1), a small number of ubiquitin conjugating (E2) enzymes, and a wide variety of ubiquitin ligases (E3) enzymes. Due to the limited variability in E1 and E2s, much of the regulation of the ubiquitin pathway is carried out by E3s (93). E3s provide specificity to the ubiquitin pathway by linking E2s with their substrates.

Membrane associated RING-CH (MARCH) proteins, are a recently discovered family of human transmembrane E3s (105,181). Six MARCH proteins are homologues of the K3-family of viral immune evasion proteins (19,20,76). Both the MARCH proteins, and their viral homologues, catalyze the ubiquitination of lysines in the cytoplasmic tails of their transmembrane substrates (105,193,194,239). Ubiquitination usually occurs post-ER, possibly at the plasma membrane, and results in the endocytosis of the substrate and subsequent targeting to multivesicular bodies (MVB) followed by lysosomal degradation (105,240).

A wide variety of substrates have been suggested for MARCH proteins. MARCH-I and -VIII (alias cMIR) mediate the destruction of Major histocompatibility complex class I and class II (MHC-I and MHC-II), CD86 (B7.2), CD166 (ALCAM),

[5] This data is not currently published

CD95 (Fas), and transferrin receptor (TfR) (105,181,191,194). In contrast, MARCH-IV and –IX mediate the destruction of MHC-I, CD4, and CD54 (ICAM-1) (105,193). Each of these MARCH targets was identified using techniques that screened each MARCH protein for downregulation of a single substrate. A clear understanding of MARCH protein substrate selection is unknown. However, those proteins tested as potential substrates, represent only a limited and biased portion of the proteome. Thus, additional MARCH substrates probably exist.

We have recently used a quantitative proteomics-based method to elucidate novel membrane-associated substrates for the viral MARCH homologue K5 (alias MIR2) (191). I used stable isotope labeling with amino acids in cell culture (SILAC) to differentially label HeLa cells prior to expression of K5 or a control vector (155,215). SILAC incorporates either 'light' (C^{12}/N^{14}) or 'heavy' amino acids (C^{13}/N^{15}) into cellular proteins through metabolic labeling. SILAC labeling allows the relative quantitation of protein abundance by determining the ratio of tryptic peptides identified in each sample using mass spectroscopy. By analyzing at least three replicate experiments I was able to identify and independently confirm several novel substrates for K5 (191).

Using this proteomics approach in human fibroblasts, I now present evidence that MARCH-VIII and -IV downregulate the cell surface proteins CD44 and CD81, and that siRNA treatment against MARCH-IV increased CD81 surface levels. In addition, I show that MARCH proteins interact with the ER resident chaperone Bap31. These data expand the function of the MARCH-family as well as confirming the ability of our SILAC based technique to elucidate novel targets for E3s.

Materials and Methods

Reagents

The following antibodies were used: anti-CD44 (clones F-4 and DF1485) and anti-CD81 (clone 5A6) (Santacruz Biotechnology (Http://www.scbt.com), anti-Bap31 (Affinity Bioreagents, http://www.bioreagents.com), anti-TfR (US Biologicals, http://www.usbio.net), anti-Flag (Sigma, http://www.sigmaaldrich.com). Plasmids expressing MARCH cDNA's have been described previous (105). Ad-MARCH-VIII and Ad-K5 have been described previously (55,191). Ad-Vpu was a generous gift from A. Moses (Vaccine and Gene Therapy Institute, USA).

Cells

Human foreskin fibroblasts were obtained from ATCC (http://www.atcc.org) and maintained in DMEM (Invitrogen, http://www.invitrogen.ciom) supplemented with 10% fetal calf serum (Hyclone, http://www.hycone.com) and 1x pen/strep.

Stable isotope labeling of HFF cells.

Cells were labeled with stable isotopes using labeling media (DMEM, Invitrogen) lacking the amino acids L-lysine and L-leucine (prepared according to the manufacturer's protocol). Labeling media was supplemented with 10% dialyzed fetal calf serum (Hyclone), 1× Pen/Strep (Invitrogen), and either isotopically 'light' L-lysine (U-12C6, 98%; U-14N2, 98%) and L-leucine (U-12C6, 98%; 14N, 98%) (Sigma) or isotopically

'heavy' L-lysine (U-13C6, 98%; U-15N2, 98%) and L-leucine (U-13C6, 98%; 15N, 98%) (Cambridge Isotope, http://www.isotope.com). Cells were maintained in labeling media long enough to allow for six doublings prior to initiation of the experiment to insure complete labeling.

Preparation of samples for MS/MS analysis.

Cells grown in labeling media were infected with, Ad-Tet + Ad-MARCH-VIII (heavy-labeled cells) or Ad-Tet alone (light-labeled cells) at an MOI of 200. 24 hours post-infection, cells were harvested by scraping, washed twice in PBS, resuspended in PBS containing 5 mM EDTA, and lysed by douncing. Unlysed cells and debris were cleared from the lysate by centrifugation for 5 min at 3,000 × *g*. The cleared lysates were separated into membrane and soluble fractions by centrifugation for 30 min at 45,000 × *g*. The membrane fraction was resuspended in PBS by sonication and separated over a discontinuous sucrose gradient (2 M, 1.6 M, 1.25 M, 1.2 M, and 0.8 M) by centrifugation for 2.5 h at 25,000 rpm (Sorvall SW-28 rotor, http://www.sorvall.com). The bands corresponding to the plasma membrane (0.8–1.2 M interphase), Golgi (1.25–1.2 M interphase), and ER (1.6–1.25 M interphase) fractions were removed, diluted 5× in Tris-EDTA (pH 8.0), and centrifuged for 30 min at 45,000 × *g* to pellet the proteins contained in each fraction. Pellets were washed for 30 min in 50 mM sodium bicarbonate (pH 11.5) and centrifuged for 30 min at 45,000 × *g*, followed by a second wash in 50 mM ammonium bicarbonate (pH 8.5) and further centrifugation for 30 min at 45,000 × *g*. Final pellets were resuspended in 8.0 M deionized urea and 50 mM ammonium

bicarbonate (pH 8.5) and protein levels quantitated using the Bio-Rad Protein Assay (Bio-Rad, http://www.biorad.com). Samples were reduced with DTT (Sigma) and alkylated with iodoacetamide (Sigma) prior to overnight digestion with trypsin (Promega, http://www.promega.com).

Chromatography, MS, and informatics.

Peptide mixtures were analyzed by electrospray ionization tandem MS, coupled to two-dimensional liquid chromatography, which was performed using a modified version of the protocol described by Link and coworkers (197). Briefly, 22 μg of sample was loaded onto an Opti-Pak capillary SCX trap cartridge (Optimize Technologies, http://www.optimizetech.com) and eluted stepwise (12.5, 25, 37.5, 50, 62.5, 75, 87.5, 100, 112.5, 125, 200, 300, or 450 mM ammonium acetate in 0.1% formic acid) onto a reverse phase C-18 capillary column (180 um × 100 mm, BioBasic-18; Thermo Electron, http://www.thermo.com). Peptides were then eluted using an acetonitrile gradient (5%, 5 min; 5%–40%, 75 min; 40%–90%, 10 min) into a ProteomeX LCQ Deca XP Plus mass spectrometer (Thermo Electron) equipped with a low-flow (1 μl/min) electrospray source. The instrument was set to trigger data-dependent MS/MS acquisition of the three most intense ions detected during the MS survey scan when total ion current per MS survey scan exceeded 5.0×10^5 counts.

Proteins were identified by analyzing tandem mass spectra with the Sequest algorithm (Thermo Electron) as described by Yates et al. (147) using the human subset of the UniProt/Swiss-Prot protein database (UniProt release 5.1,

http://www.expasy.org/sprot). The search results were further analyzed using PeptideProphet (198). SILAC ratios were determined using the ASAPRatio algorithm (160). Multiple peptides derived from a single protein were included if PeptideProphet probability was greater than or equal to 0.85. All positive results were manually verified.

Real-Time PCR

Short (50-100bp) fragments from MARCH-I, -II, -IV, -VIII and -IX cDNA were amplified via PCR using appropriate primers. The PCR reaction was carried out in the following buffer: 1x SYBR Green PCR Buffer (PE Biosystems), 3mM $MgCl_2$, 0.8mM dNTP's, 0.625U Amplitaq Gold (PE Biosystems), 0.01µl Amperase (PE Biosystems), and 50nM primers. 20µl buffer was added to 5µl template cDNA and run under the following conditions: 95^0C for 10min, followed by 40 cycles of 95^0C for 15 seconds, 60^0C for 1 minute. Amplification was tracked via SYBR-Green (PE Biosystems) incorporation using an ABI-PRISM 7700 Sequence Detection System (Applied Biosystems, Foster City, CA).

Co-immunoprecipitation, Immunoblot, and Surface Labeling

Cells were washed twice with PBS and lysed in PBS containing 1% CHAPS (Sigma). Lysates were precleared with protein A/G agarose beads and incubated with 1µg of antibody for 1 hr and followed by 1 hr incubation with protein A/G beads. Immunoprecipated proteins were washed four times with PBS containing 1% CHAPS. Samples were boiled in SDS buffer and analyzed by SDS-PAGE gel electrophoresis. For Western blot analysis, SDS-PAGE gels were transferred to Immobilon-P PVDF

membrane (Millipore) using semidry transfer. Following transfer, membranes were blocked in 10% milk in PBS + 1% tween-20. Membranes were incubated with primary and secondary antibodies in 5% milk for 30 minutes. Following each antibody incubation, membranes were washed 3 times with PBS + 1% tween-20, and once with dH_2O.

Surface biotinylation studies were carried out using the Cell Surface Protein Biotinylation and Purificaiton Kit (Pierce) according to the manufacturer's recommendations.

Flowcytometry

Cells were removed from tissue culture dishes with 0.05% trypsin-EDTA (Invitrogen), washed with ice-cold PBS, and incubated with appropriate antibody for 30 min at 4 °C. The cells were washed with ice-cold PBS and either resuspended in ice-cold PBS or incubated with PE-conjugated anti-mouse secondary antibody (Dako, http://www.dako.com) and washed again before analysis with a BD Biosciences FACSCalibur flowcytometer.

siRNA Treatment

Knockdown of Bap31 was accomplished using anti-BCAP-31 (Bap31) siGENOME siRNA (Dharmacon, http://www.dharmacon.com). siRNA transfection was accomplished using Oligofectamine (Invitrogen, http://www.invitrogen.com) according to manufacturers recommendations. 25% confluent 35mm dishes of HFF's were treated twice with 5µl siRNA (20µM). Treatments were 6 hours apart. Three days post

treatment, cells were treated again with siRNA as described. Cells were analyzed 4 days after the second siRNA treatment.

Results

Proteomic Analysis of MARCH-VIII-expressing human fibroblasts

MARCH proteins introduce specific lesions in the plasma membrane proteome by ubiquitinating subsets of transmembrane proteins. Previously, I analyzed whether MARCH proteins target a panel of cell surface proteins which were selected because they were known substrates of viral MARCH homologues (19,20,51,54). In order to determine novel substrates for MARCH proteins by an unbiased approach, I applied a recently developed quantitative proteomics-based method which allowed us to screen for changes induced in the plasma membrane proteome following expression of the viral MARCH-homologue K5 (191). To identify novel substrates for MARCH proteins in human cells, I used primary foreskin fibroblasts (HFF) expressing low levels of endogenous MARCH proteins (Fig. 23). MARCH expression in these cells is representative for many human cells and tissues (our unpublished observations) (105).

To detect changes in the membrane proteomes of HFFs upon forced-expression of MARCH-VIII I compared the abundance of metabolically labeled proteins identified by tandem MS/MS. HFFs were grown in either 'light' media containing normal leucine $N^{14}/_{6}C^{12}$ and lysine $_{2}N^{14}/_{6}C^{12}$, or 'heavy' media containing $N^{15}/_{6}C^{13}$ leucine and $_{2}N^{15}/_{6}C^{13}$ lysine. To ensure complete labeling, cells were grown in labeling media for six doublings (~2 weeks). Following metabolic labeling, 'light' labeled samples were infected with Adenovirus expressing the Tetracycline regulatable-transactivator (Ad-Tet)

alone, while 'heavy' labeled samples were infected with Ad-Tet together with adenovirus expressing Tet-induced MARCH-VIII (Ad-MARCH-VIII). 24 hours post-infection, cells were harvested via mechanical scraping and cellular fractions were separated as described (191). Due to low yields of ER and Golgi membranes, however, only the plasma membrane (PM) fraction was analyzed in these experiments. Following trypsinization, PM fractions were separated with two-dimensional liquid chromatography (strong cation exchange followed by reverse phase chromatography) and then analyzed by MS using a LCQ ion-trap instrument in data-dependent MS/MS mode. Ion spectra were identified using SEQUEST software (147) and statistically analyzed using PeptideProphet (198). To limit false positive peptide identifications a PeptideProphet cutoff of 0.85 was applied to each peptide identified. To further minimize experimental error and limit false positive results, three biological replicates were prepared and independently analyzed. Each experiment resulted in the identification of between 300-500 unique proteins.

To determine proteins whose expression was altered by MARCH-VIII, ratios between 'heavy' and 'light' peptide peaks were determined using the ASAPRatio algorithm (160). Ratios of individual peptides belonging to the same protein were grouped together using ProteinProphet to obtain a ratio for the expression of each identified protein (160). HFFs express three known substrates of MARCH-VIII: TfR, MHC-I, and ALCAM (105,191). However, I failed to recover peptides corresponding to TfR or the MHC-I heavy chain in any of the experiments. This is likely due to the low expression levels of both TfR and MHC-I in HFFs. In contrast, the MHC-I light chain, β2-microglobulin (β_2M), was recovered in all three experiments (Table 2). The recovery

of β_2M but not MHC-I heavy chain might be due to the fact that β_2M is non-polymorphic in contrast to the multiple MHC-I alleles present in the mixed population of primary fibroblasts. Since peptides derived from ALCAM were recovered in only two of the three experiments, I considered proteins identified in the top or bottom 25% of two out of three experiments as possible targets if they were absent from the third experiment due to a failure to recover any peptides. Using this initial filter resulted in the identification of 13 proteins which might be regulated by expression of MARCH-VIII (Table 2).

Of these 13 proteins, only two displayed increased abundance upon expression of MARCH-VIII: MARCH-VIII itself and Grp78/Bip. Grp78/Bip is an ER resident chaperone that is transcriptionally upregulated as part of the unfolded protein response, which is triggered by elevated levels of viral or cellular proteins in the ER. Grp78/Bip has been shown previously to be upregulated upon expression of the viral protein US11 (241). Therefore, it is likely that upregulation of Grp78 is due to the forced expression of MARCH-VIII. However, this has yet to be confirmed experimentally.

The remaining 11 all proteins displayed lower levels in Ad-MARCH-VIII-transduced cells compared to control cells. Of these proteins, three were downregulated in all three experiments: β_2M, CD44, and CD81. Since MHC-I is known to be moderately downregulated by MARCH-VIII (105), the observed reduction of β_2M is likely caused by the removal of MHC-I from the cell surface. Alternatively, MARCH-VIII might also downregulate some of the non-classical HLA-like molecules that associate with β_2M. However, I did not recover any peptides mapping to these non-classical MHC molecules in any of our experiments. Since expression of both CD44 and CD81 were consistently lower in the presence of MARCH-VIII in all three experiments, these molecules

represented the most likely candidates for novel MARCH-VIII substrates. CD44 is a type I transmembrane glycoprotein that connects a variety of extracellular matrix proteins, most notably hyaluronic acid, to the cell surface (242). CD81 is a member of the tetraspannin family which regulates the special and temporal localization of other surface proteins, CD81 is also a coreceptor for Hepatitis C virus (243,244).

Proteins downregulated in two of three experiments were considered less likely to be true substrates for MARCH-VIII. In fact, most of the proteins found in this class seemed unlikely targets for MARCH-VIII since they localized to fractions contaminating our membrane preparation, such as cytosolic, nuclear or mitochondrial (not shown). However two proteins, CD9 and Bap31, represented potentially true positives due to their transmembrane structure and location at the plasma membrane or intracellular vesicular compartments. Like CD81, CD9 is a surface glycoprotein of the tetraspannin family. CD9 and CD81 interact with each other and regulate many of the same cellular processes (243,245,246). Bap31 is a molecular chaperone that regulates intracellular trafficking of a number of cell surface proteins, including MHC-I (7,247-250). Therefore, we included CD9 and Bap31 for further validation studies.

Bap31, but not CD9 is removed from the cell surface by MARCH-VIII

To validate our proteomics results, I examined CD9 expression by flowcytometry in both HeLa cells and HFFs. However, expression of MARCH-VIII in either cell type did not result in the downregulation of CD9 from the cell surface (data not shown). Thus, the lower levels of CD9-derived peptides seemed to be a false-positive result caused by experimental variation.

Unlike CD9, Bap31 is an ER resident chaperone associated with the forward transport of a wide variety of cell surface proteins, including MHC-I, cellubrevin, cystic fibrosis transmembrane conductance regulator (CFTR), membrane bound IgD, CD18, and CD11b (7,247-250). This trafficking is mediated by a direct interaction between Bap31 and its cargo (7,250). To determine whether MARCH-VIII reduces Bap31 levels, I initially measured total Bap31 in Ad-MARCH-VIII transduced HFFs by immunoblot. However, no change in total Bap31 levels were observed in MARCH-VIII transduced cells (Fig. 24).

While most Bap31 localizes to the ER, a small portion of Bap31 is present in the Golgi and at the plasma membrane (250,251). Since our initial proteomic screen showed a reduction of Bap31 levels in a fraction highly enriched for the plasma membrane, we hypothesized that expression of MARCH-VIII might affect the small portion of Bap31 localized to the cell surface. To test this hypothesis, HFFs were infected with Ad-Tet or Ad-MARCH-VIII and, 24 hours post-infection, proteins at the cell surface were labeled with biotin using the Cell Surface Biotinylation and Purificaiton Kit (Pierce). The biotinylated fraction was then purified according to the manufacturer's recommendations. A small portion of each whole cell lysate (WCL) was removed prior to biotin purification to confirm total Bap31 levels. Both biotinylated and WCL fractions were separated using SDS-PAGE and the levels of MARCH-VIII, Bap31, and TfR were analyzed by immunoblot (Fig. 24). While the majority of MARCH-VIII was seen in the WCL fraction, MARCH-VIII was also present in the biotin fraction suggesting that a small portion of MARCH-VIII traffics to the cell surface. As previously described, a small portion of Bap31 was seen in the biotin fraction, suggesting a cell surface localization

(250). Interestingly, the levels of biotinylated Bap31 were significantly reduced following expression of MARCH-VIII. In contrast, total Bap31 levels in the WCL fraction remained unchanged. These data suggested that MARCH-VIII does not degrade ER localized Bap31, but either inhibits Bap31 trafficking to the cell surface or degrades surface expressed Bap31.

Bap31 interacts with MARCH proteins

Since Bap31 interacts with a wide variety of proteins it possible that the reduction of Bap31 surface levels was due to MARCH-VIII binding to Bap31 in intracellular membrane compartments. To examine this hypothesis I transfected a MARCH-VIII expression plasmid into both HeLa cells and HFFs. 24 hours post-transfection, cells were lysed in the mild detergent CHAPS to preserve protein:protein interactions. MARCH-VIII was immunoprecipitated using an anti-Flag antibody and samples were separated using SDS-PAGE. Following transfer to PVDF membrane, the presence of Bap31 in each sample was analyzed by immunoblot. A strong signal for Bap31 was observed following MARCH-VIII immunoprecipitation in HeLa cells transfected with MARCH-VIII (Fig. 25A). This suggests that Bap31 interacted directly with transfected MARCH-VIII. 5% of each sample was blotted using anti-Flag antibody to confirm expression of MARCH-VIII. Since no MARCH-VIII was detected in the WCL, the failure to observe Bap31 in samples from transfected HFFs is likely due to low transfection efficiency. In contrast, when MARCH-VIII was expressed by adenovirus transduction, Bap31 was also clearly present following MARCH-VIII immunoprecipitation from HFF (Fig. 25B). This

strongly suggests that MARCH-VIII interacts directly with Bap31 independent of the cell type.

Since Bap31 interacted with MARCH-VIII, I tested whether Bap31 would interact with other MARCH proteins or viral immune evasins. Expression plasmids for each construct were transfected into HeLa cells and then analyzed as above. Bap31 was observed in samples transfected with virtually all MARCH proteins with the notable exception of MARCH-II despite clearly detectable MARCH-II expression. Similarly, very little Bap31 was observed in samples transfected with Vpu, a viral E3 not related to the MARCH-family. K5 and MARCH-IX form SDS-stable high molecular weight complexes so that very little protein corresponding to the predicted molecular weight is recovered (see also Fig. 25E). Nevertheless, Bap31 was recovered with each of these proteins. We conclude that Bap31 interacts with most members of the MARCH-family.

Previous interactions with Bap31 have been shown to be mediated through the transmembrane domains (7,250). To determine if this was true for Bap31's interactions with the MARCH proteins I used a series of amino- and carboxy-terminal truncations. Expression plasmids for each truncation were transfected into HeLa cells. Following immunoprecipitation of each truncation using an anti-Flag antibody, each sample was analyzed for the presence of Bap31 by immunoblot. Deletion of the entire carboxy-terminus of either MARCH-VIII (MARCH-VIII 1-220) or MARCH-VI (MARCH-IV 1-259) had no effect on Bap31 binding (Fig. 25D and 25E). These data suggest that the interaction between Bap31 and MARCH proteins is not mediated through the carboxy-terminus. Similarly, deletion of the entire amino-terminus of MARCH-IV (MARCH-IV 89-347) or disruption of the RING-CH domain through mutational analysis (MARCH-IV

C to S) or addition of the metal chelator EDTA (MARCH-IV + EDTA) did not prevent the interaction with Bap31. These results suggested that the amino-terminus and RING-CH domain of MARCH proteins do not mediate the interaction with Bap31. Finally, Bap31 was also recovered following expression of a construct encoding just the transmembrane domains of MARCH-IV (MARCH-IV 89-259). Despite significantly different levels of expression, similar levels of Bap31 were recovered from cells expressing just the transmembrane domains of MARCH-IV and from wild-type MARCH-IV. This strongly argues that Bap31 interacts with the MARCH proteins through their transmembrane domains.

Bap31 targets MARCH-VIII to the cell surface

Since Bap31 serves as a forward cargo transporter, it might play a role in the correct folding and ER exit of MARCH-VIII. To test this hypothesis I depleted HeLa cells of Bap31 using siRNA. Following Bap31 depletion, cells were transfected with MARCH-VIII. 24 hours post-transfection, the cell surface was labeled with biotin and both biotin and WCL fractions were prepared as above. Following separation using SDS-PAGE, the levels of MARCH-VIII and Bap31 in each fraction was analyzed via immunoblot (Fig. 26A). Although only a partial knockdown of Bap31 was achieved (Fig. 26A and 26B Bottom), the levels of Bap31 present in the biotinylated fraction were significantly reduced (Fig. 26A Top). In cells depleted of Bap31, a significantly reduced amount of MARCH-VIII was observed in the biotinylated fraction. This observation was not due to lower overall expression, since similar levels of MARCH-VIII were observed in the WCL fraction. Despite knockdown of Bap31, some MARCH-VIII was still

present in the biotinylated fraction. This result might be due to incomplete knockdown of Bap31, since Bap31 was still co-immunoprecipitated with MARCH-VIII even following siRNA treatment (Fig. 25B). Presumably due to the remaining MARCH-VIII, I did not observe an effect of Bap31 knockdown on the downregulation of MARCH-VIII target proteins, such as B7.2 (data not shown). Taken together these data suggest that Bap31 supports the intracellular transport of MARCH proteins by intra-membrane interactions. Due to this interaction, Bap31 remains intracellular upon forced expression of MARCH proteins, which explains its reduced presence in the plasma-membrane fraction of MARCH-VIII transduced cells. We conclude that Bap31 plays an important role in the folding, assembly and intracellular transport of MARCH proteins.

Confirmation of CD44 and CD81 downregulation

The most likely candidates for novel MARCH-VIII substrates were CD44 and CD81 since both proteins were present at reduced amounts in all three biological replicates. To independently confirm that CD44 and CD81 were downregulated by MARCH-VIII, HFFs were transduced with either Ad-Tet or Ad-MARCH-VIII together with Ad-Tet and expression of CD44 and CD81 was examined by flowcytometry at 24 hours post-infection (Fig. 27). Samples transduced with Ad-MARCH-VIII (white line) displayed a reduction of both CD44 and CD81 at the cell surface compared to cells infected with Ad-WT (black line).

To compare the steady state levels of CD44 and CD81 in the presence or absence of MARCH-VIII I used immunoblotting. HFFs were transduced as above and whole cell lysates were analyzed via immunoblot using specific antibodies (Fig. 27). In samples

transduced with Ad-MARCH-VIII, a significant reduction of both CD44 and CD81 was seen. In contrast, transduction with adenovirus expressing either K5 or Vpu did not affect either CD44 or CD81 levels. Equal protein loading was confirmed by immunoblotting for Bap31 since total levels of Bap31 do not change upon MARCH expression as discussed above. Thus, both CD44 and CD81 are specifically affected by MARCH-VIII but not by viral E3s.

Specificity of CD44 and CD81 downregulation by the MARCH-Family

MARCH proteins display specific, but overlapping substrate specificity (105). Therefore, I tested whether expression of any other MARCH protein downregulated CD44 or CD81. For these experiments I used HeLa cells since these cells can be easily transfected with expression plasmids for each MARCH protein. A plasmid expressing GFP was co-transfected to track transfected cells. 24 hours post-transfection, cells were harvested and surface expression of CD44 and CD81 was analyzed using flowcytometry (Fig. 28). Each histogram shows the mean florescence intensities of the GFP+ cells (white line) and GFP- cells (black line) from the same sample. In addition to MARCH-VIII, a significant downregulation of both CD44 and CD81 was observed in cells expressing MARCH-IV. This result is surprising since the closest homologue of MARCH-VIII is MARCH-I. These two MARCH proteins have demonstrated similar substrate specificity in all previous experiments (105,194,239).

Knockdown of MARCH-IV results in upregulation of CD81

Since HHFs express endogenous MARCH-IV and -VIII (Fig. 29), I tested whether the steady state level of CD44 or CD81 was affected by these E3s. HFFs were treated with siRNA against both MARCH proteins either separately or in combination. Knockdown of each MARCH protein was confirmed on the RNA level using real time PCR (Fig. 29A). Treatment with either MARCH-IV or -VIII siRNA reduced corresponding MARCH RNA by around 90%. RNA levels for MARCH-IV or –VIII were unchanged by treatment with the mis-matched siRNA, showing that depletion was sequence specific. Additionally, treatment with a siRNA against MARCH-I, which is not expressed in HFFs, had no effect on the RNA levels of either MARCH-IV or –VIII. Following depletion of MARCH-IV or MARCH-VIII, cells were harvested and the surface levels of CD44 and CD81 were measured using flowcytometry. Treatment with siRNA against either MARCH-IV or –VIII did not alter surface levels of CD44 (Fig. 29B). Similarly, CD81 levels did not change upon MARCH-VIII knockdown. In contrast, treatment with siRNA against MARCH-IV resulted in a 50% increase in the surface levels of CD81 compared to either untreated cells or cells treated with other siRNA (Fig. 29B). While modest, this increase was reproducible over five separate experiments and statistically significant with a p value < 0.01 compared to treatment with siRNA against MARCH-I. This increase was not due to increased transcription of CD81 since treatment with MARCH-IV siRNA did not increase levels of CD81 mRNA (Fig. 29A). Co-transfection of siRNA against MARCH-IV and MARCH-VIII did not further increase CD81 levels. The failure of MARCH-VIII to affect endogenous CD81 might be the result of MARCH-VIII being expressed at levels that are too low to influence CD81

expression (Fig. 23). These data clearly show that depletion of endogenous MARCH-IV affects surface expression of CD81.

Discussion

The goal of this study was to use an unbiased proteomics approach to identify cell surface proteins regulated by transmembrane ubiquitin ligases of the MARCH protein family. Using the viral MARCH homologue K5, I had previously demonstrated that it is possible to identify novel targets for both the protein used in the proteomics screen as well as other family members (191). For instance, ALCAM was identified as a novel substrate for K5; however, follow up experiments demonstrated that ALCAM was also downregulated by MARCH-VIII and Myxomavirus M153R. Similarly, I now show that CD44 and CD81 are downregulated by MARCH-VIII which was used in the proteomic screen, and by MARCH-IV. Interestingly, expression of CD44 or CD81 was not affected by any viral protein tested, suggesting that these endogenous substrates of MARCH-IV and –VIII specific. Also surprising, was the observation that MARCH-I and -IX, which are closely related to MARCH-IV and -VIII, did not affect CD81 and CD44. This result is in contrast to our previous observations which showed that sequence homology, particularly in the transmembrane domains, strongly correlated with substrate specificity. Why a similar correlation is not observed for CD81 and CD44 is presently unknown.

While both CD44 and CD81 are widely expressed on different cell types, their regulation has been shown to play a particularly important role in the developing immune system. Like most MARCH targets, CD44 is a type I transmembrane glycoprotein. CD44

occurs in many splice variants and connects a variety of extracellular matrix proteins, most notably hyaluronic acid, to the cell surface (242). CD44 is regulated during T cell development (252), leukemia (253), and following treatment with various cytokines (254). Although elimination of MARCH-IV, -VIII, or both from fibroblasts did not change the steady state levels of CD44, this could be the result of endogenous expression levels of MARCH-IV and –VIII simply being too low in HFFs to influence CD44 turnover. Whether CD44 is regulated in more dynamic situations where MARCH proteins are regulated, such as during dendritic cell maturation (194,255,256) has not yet been determined. For example, in addition to the reported transcriptional induction of CD44, it is conceivable that the downregulation of MARCH-VIII further increases CD44 steady state levels, contributing to the adhesive properties of DCs. MARCH-IV and -VIII could also play a role for the hyaluronic acid-induced endocytosis of CD44 and its subsequent targeting to the multivesicular bodies (MVB) (257) since MARCH-IV- and -VIII targets reach the MVB (105,181,194).

In contrast to CD44, CD81 surface levels were increased upon depletion of MARCH-IV, suggesting that, in fibroblasts, MARCH-IV is involved in the natural turnover of CD81. While depletion of MARCH-VIII had no effect on CD81 levels in fibroblasts, the higher MARCH-VIII levels in other cell types or tissues might affect CD81. Unlike most MARCH-targets, which are single-span transmembrane proteins, CD81 belongs to the tetraspanin family, four-transmembrane proteins that are part of membrane microdomains and bind to a large number of other proteins, including CD4, CD8, CD19, CD9, CD63, MHC-I, and MHC-II (243,246,258-261). Several of the CD81-interacting proteins have been shown to be downregulated by MARCH-IV or –VIII,

leading to two possible models for CD81 downregulation. First it is possible that CD81 surface expression is indirectly affected via downregulation of these bona-fide targets. Alternatively, some of these proteins might be affected as a consequence of the direct downregulation of CD81. In fact, targeting a protein with widespread protein:protein interactions, such as CD81, might explain how MARCH proteins downregulate such a variety of substrates with no sequence similarity. Unfortunately, our observations that MARCH-IV constructs lacking a functional RING-CH domain and mutants of MARCH-VIII unable to downregulate B7.2 both fail to downregulate CD81 are consistent with either model. Thus, further work is required to distinguish between these two models.

CD81 is also a coreceptor for hepatitis C virus (HCV) (244,262). Cells that are depleted of surface CD81 are no longer permissive for HCV infection (263). CD81 activation also plays a role in HIV mediated syncytia formation (264) and HIV transcription (265). Removal of CD81 from the cell surface by overexpression or pharmacological induction of either MARCH-IV or –VIII therefore might represent a novel therapeutic treatment to inhibit HCV or HIV infection.

The validation of both CD81 and CD44 by independent methods confirms our previous conclusion that three biological replicates give a high level of confidence for the specificity of the results (191). Since ALCAM, a known substrate of MARCH-VIII; was identified in only two of the three experiments, however, I selected two additional potential candidate proteins, CD9 and Bap31, for validation based on their subcellular localization as well as their known interaction with MARCH-VIII substrates. Only Bap31, however, confirmed using independent methods, indicating that the false-positive rate is high in these types of experiments when biological replicates are limited. This

false-positive rate is primarily due to the inaccuracy of quantitation using the mass spectrometer.

Unlike CD44 and CD81, steady state levels of Bap31 were not diminished following expression of MARCH-VIII (Fig. 28). Instead, I found that MARCH-VIII bound to Bap31 and prevented Bap31 from trafficking to the cell surface. Interestingly, depletion of Bap31 resulted in lower surface expression of MARCH-VIII. Since Bap31 is known to function as a forward cargo molecule for several other proteins (7,247-250) we conclude that that Bap31 chaperones the folding, assembly or intracellular transport of the MARCH-family. While depletion of Bap31 affected intracellular transport of MARCH-VIII, this depletion did not prevent MARCH-VIII-mediated downregulation of transfected B7.2 (data not shown). This result, however, is likely due to insufficient knockdown of Bap31, resulting in adequate amounts of MARCH-VIII available at the cell surface to ubiquitinate B7.2.

Interestingly, the MARCH-family and their viral homologues have been shown to interact with several other intracellular trafficking molecules. Depletion of PACS2 inhibited K5 mediated degradation of newly synthesized CD31, suggesting that it played a key role in K5 function (55). Several members of the MARCH-family have been shown to interact directly with members of the syntaxin family of SNARE proteins (191,192,222), however, the functional consequences of these interactions are not currently understood. Truncated versions of MARCH-VIII, which are unable to interact with syntaxins, are still able to interact with Bap31 (191). These data suggest that the interaction with Bap31 occurs in the transmembrane domains. This observation is consistent with previous findings that Bap31's interaction with MHC-I, IgD, cellubrevin,

and p450 localizes to the transmembrane domains (247,249,266,267). Interestingly, expression of Bap31 is required for surface expression of CD81 (268). Thus, inhibition of Bap31 might play some role in MARCH-IV and –VIII downregulation of CD81.

In summary, I present the first systematic identification of endogenous substrates for the MARCH-family. By using this non-biased approach, I demonstrated that the tetraspanin CD81 is downregulated by both MARCH-IV and –VIII thus expanding the structural range of possible MARCH substrates. I were also able to show that depletion of endogenous MARCH-IV increased the surface expression of CD81. This is the first time that a substrate of MARCH-IV has been affected by depletion of endogenous protein. Together, with recent progress in generating *ko* mice and observing regulation of MARCH protein expression, these approaches will be useful in unraveling the function of this class of proteins

Figure 23: MARCH expression in HFF

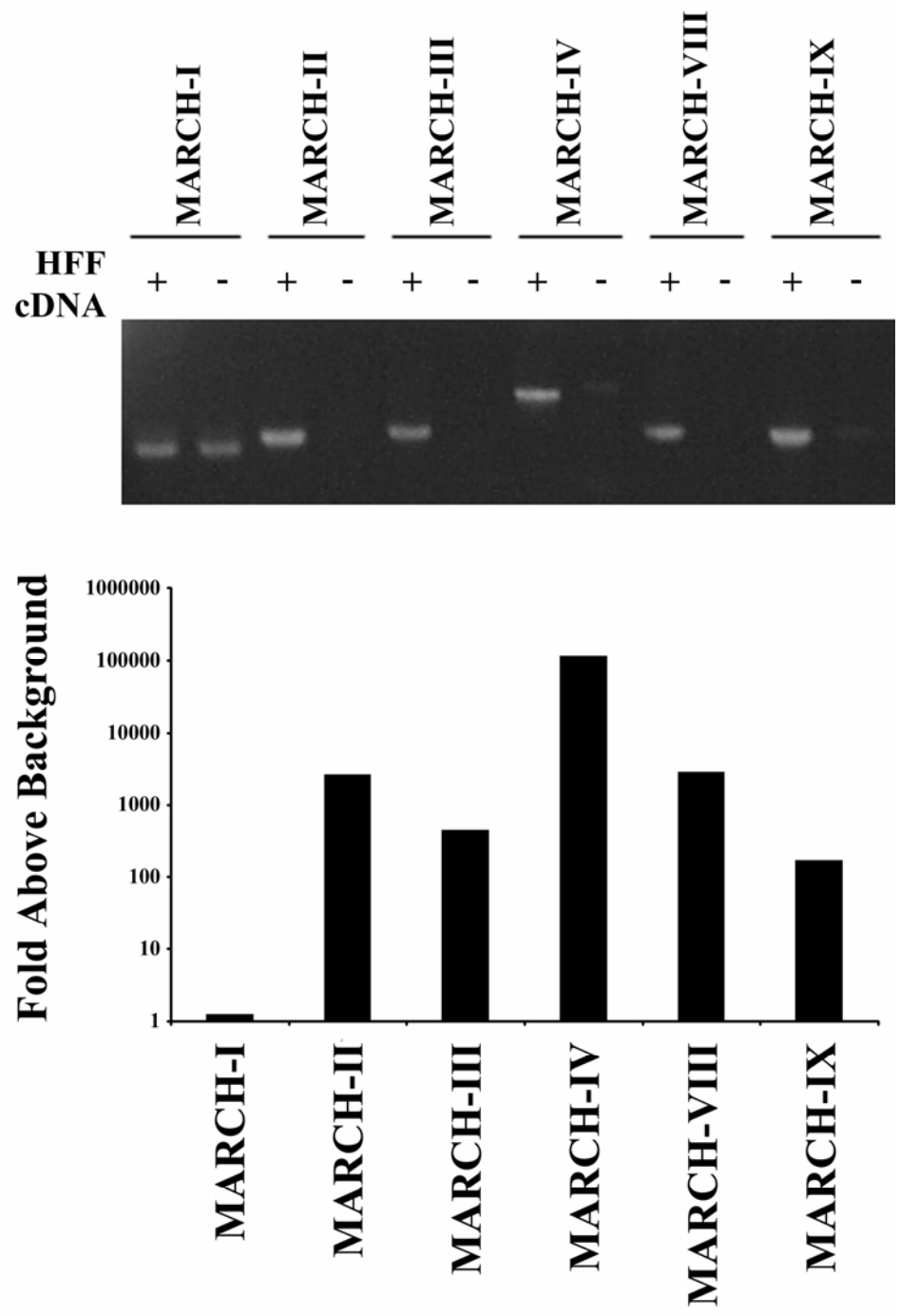

Figure 23: MARCH expression in HFF

RNA was extracted from HFF cells using RNeasy kit (Qiagen). 2µg of RNA was used to synthesize random primed cDNA. Expression of each MARCH protein was then analyzed using real-time PCR. MARCH expression in shown as the fold change between samples containing HFF cDNA and no template control samples (Bottom). The products from this PCR were run on a 1% agarose gel and visualized using sybr green (Top).

Table 2: Proteins displaying a skewed ratio following overexpression of MARCH-VIII

Protein	Average Ratio	Identified in	Unique Peptide
Downregulated			
β2MG	2.41	3/3	2
CD44	1.70	3/3	6
CD81	3.10	3/3	2
Bap31	2.35	2/3	1
CD166	2.93	2/3	4
CD9	2.43	2/3	3
DAG1	2.81	2/3	1
ECHA	2.51	2/3	1
EGLN	2.29	2/3	2
RALA	3.06	2/3	1
RL15	3.02	2/3	1
Upregulated			
MARCH-VIII	0.10	3/3	3
Grp78	0.85	3/3	11

Table 2: Proteins displaying a skewed ratio following overexpression of MARCH-VIII

13 proteins displayed a skewed ratio following overexpression of MARCH-VIII in two of three replicate experiments. Listed are the Uniprot (http://www.expasy.org/sprot) designation for each protein, as well as the average ratio observed. Ratios given are Ad-Tet:Ad-MARCH-VIII. Ratios above one correspond to proteins that are downregulated by expression of MARCH-VIII while ratios below one correspond to proteins that are upregulated by expression of MARCH-VIII. Also given is the number of unique peptides used to identify each protein and whether that protein was scored as skewed in 2/3 or 3/3 experiments.

Figure 24: MARCH-VIII affects surface expression of Bap31

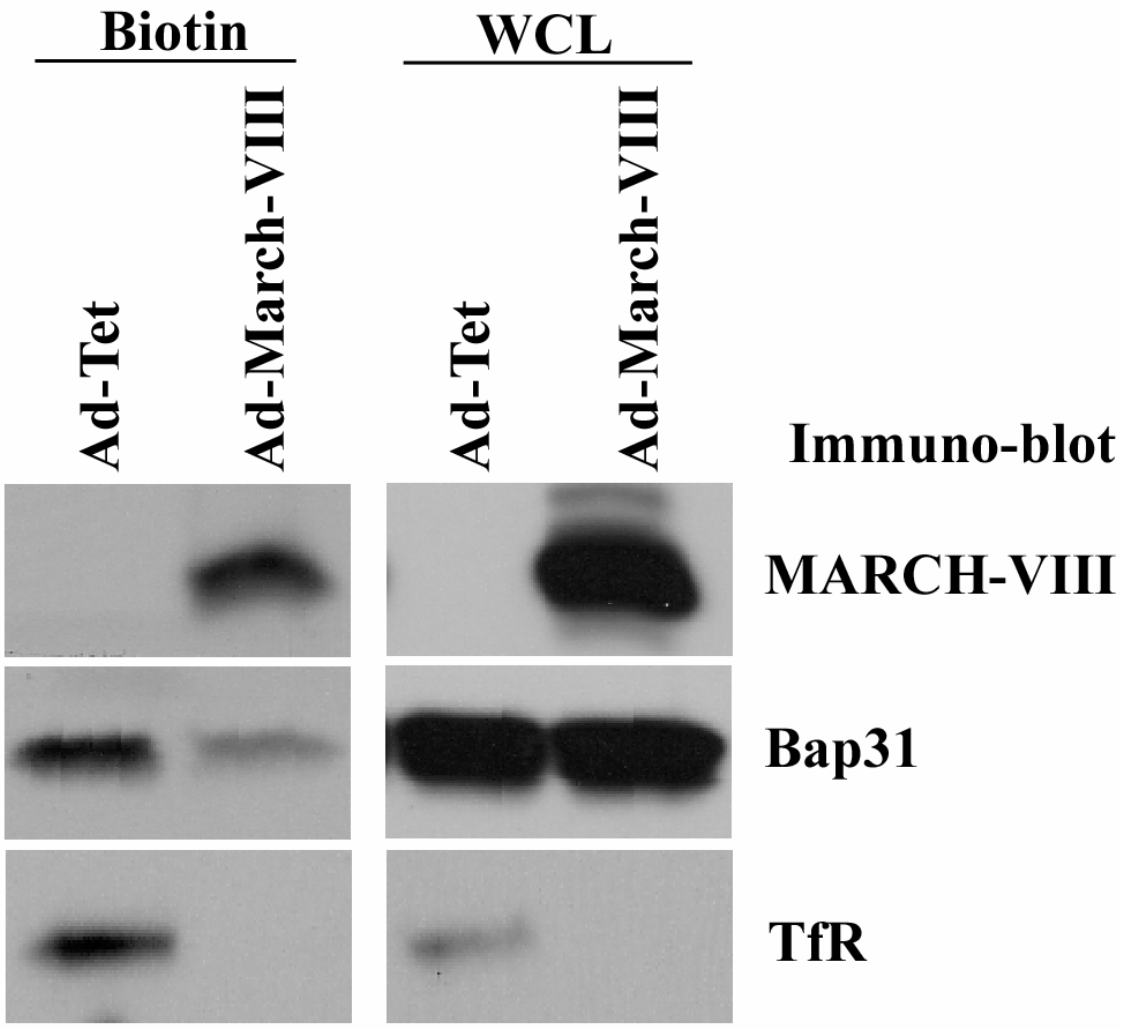

Figure 24: MARCH-VIII affects surface expression of Bap31

HFF's were infected with Ad-MARCH-VIII or Ad-Tet. 24 hours post-infection cells were biotinylated using the Cell surface Biotinylation and purification kit (Pierce). Prior to purification of biotinylated proteins, 100µl of each sample was removed for analysis of protein expression in each whole cell lysate (WCL). Expression of Bap31 was analyzed in both the biotinylated fraction and the whole cell lysate using immunoblot. Expression of MARCH-VIII and the known MARCH-VIII substrate TfR were included as controls.

Figure 25: MARCH-VIII interacts with Bap31 through the transmembrane domains

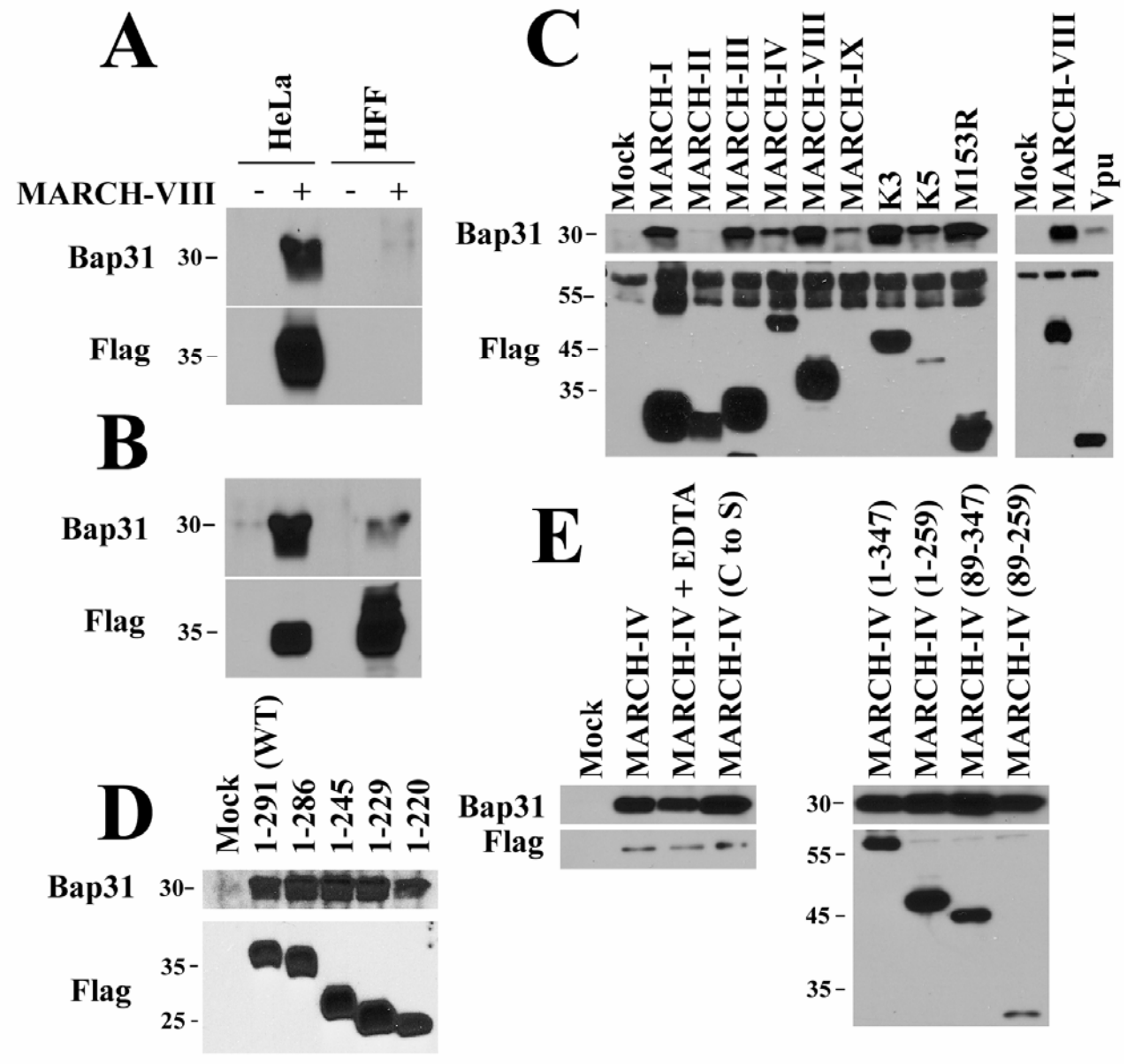

Figure 25: MARCH-VIII interacts with Bap31 through the transmembrane domains

MARCH-VIII carboxy-Flag was expressed in HeLa cells and HFF's using either transfection (A) or adenoviral transduction (B). Cells were lysed in 1% CHAPS and MARCH-VIII was immunoprecipitated using the anti-Flag antibody. Following immunoprecipitation, samples were separated on an SDS-PAGE gel and the presence of Bap31 was analyzed via immunoblot. 5% of each sample was blotted with anti-Flag antibody to confirm MARCH-VIII expression. Note that in transfected HFF's virtually no MARCH-VIII is present due to the extremely low transfectability of these cells. HeLa cells were transfected with carboxy-terminally flag tagged versions of each MARCH protein as well as the K3-family proteins K3, K5, M153 and the HIV protein Vpu. 24 hours post-transfection each sample was lysed and analyzed as above (C). Expression of each transfected protein was confirmed by blotting 5% of each immunoprecipitation with the anti-Flag antibody. To determine which region of MARCH proteins were required for interaction with Bap31 I used a series of previously constructed MARCH-IV and -VIII truncations. HeLa cells were transfected with carboxy-terminally flag-tagged versions of either MARCH-VIII truncation (D) or MARCH-IV truncations (E Right). 24 hours post-transfection samples were lysed and analyzed as above. No effect on Bap31 coimmunoprecipitation was observed following the removal of the entire carboxy-terminus of MARCH-VIII (1-220) or MARCH-IV (1-259), removal of the entire amino-terminus of MARCH-IV (89-347) or disruption of the MARCH-IV RING-CH domain by either mutation (MARCH-IV C to S) or addition of EDTA.

Figure 26: Depletion of Bap31 reduces surface expression of MARCH-VIII

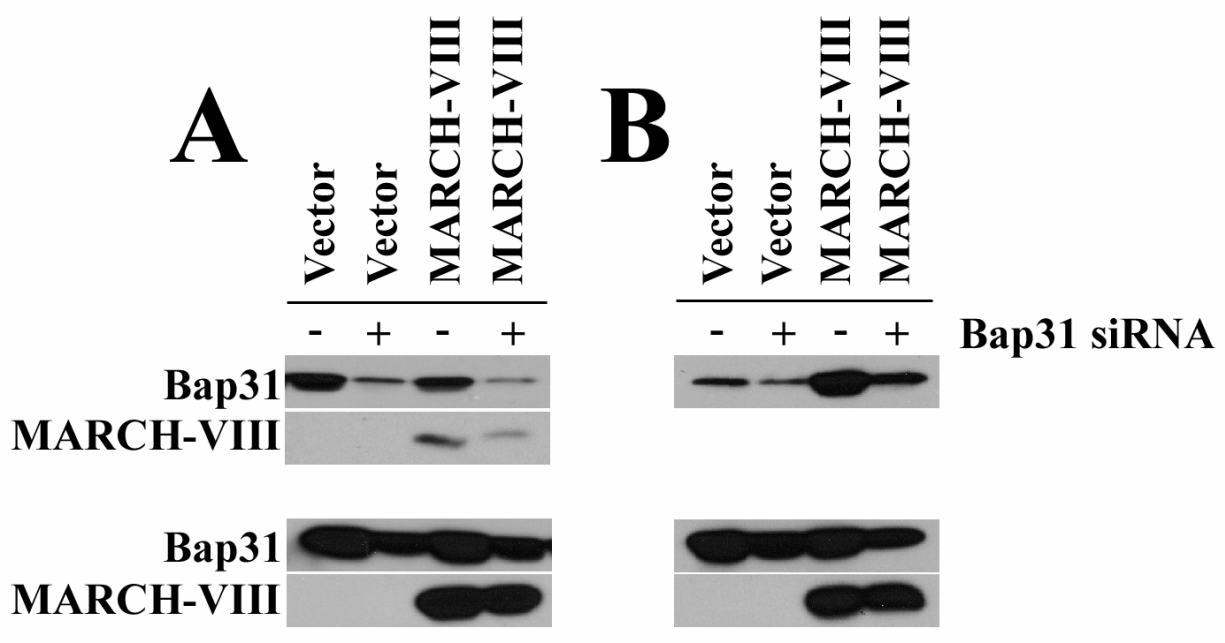

Figure 26: Depletion of Bap31 reduces surface expression of MARCH-VIII

HeLa cells were depleted of Bap31 using siRNA as described in the materials and methods section. Following Bap31 depletion, HeLa cells were transfected with a plasmid expressing MARCH-VIII. 24 hours post-transfection cells were biotinylated. Following separation via SDS-PAGE gels, surface expression (Top) or total expression (Bottom) of both Bap31 and MARCH-VIII were analyzed via immunoblot (A). Cells depleted of Bap31 show reduced surface expression of both Bap31 and MARCH-VIII. Depletion of Bap31 also reduced the levels of Bap31 associated with MARCH-VIII. HeLa cells were depleted of Bap31 as described. Following Bap31 depletion, cells were transfected with a plasmid expressing MARCH-VIII. 24 hours post-transfection cells were lysed in 1% CHAPS and MARCH-VIII was immunoprecipitated using an anti-Flag antibody. Samples were separated via SDS-PAGE and the presence of Bap31 determined by immunoblot (B Top). Expression of Bap31 and MARCH-VIII were confirmed in whole cell lysates (B Bottom).

Figure 27: CD44 and CD81 are differentially expressed following MARCH-VIII expression

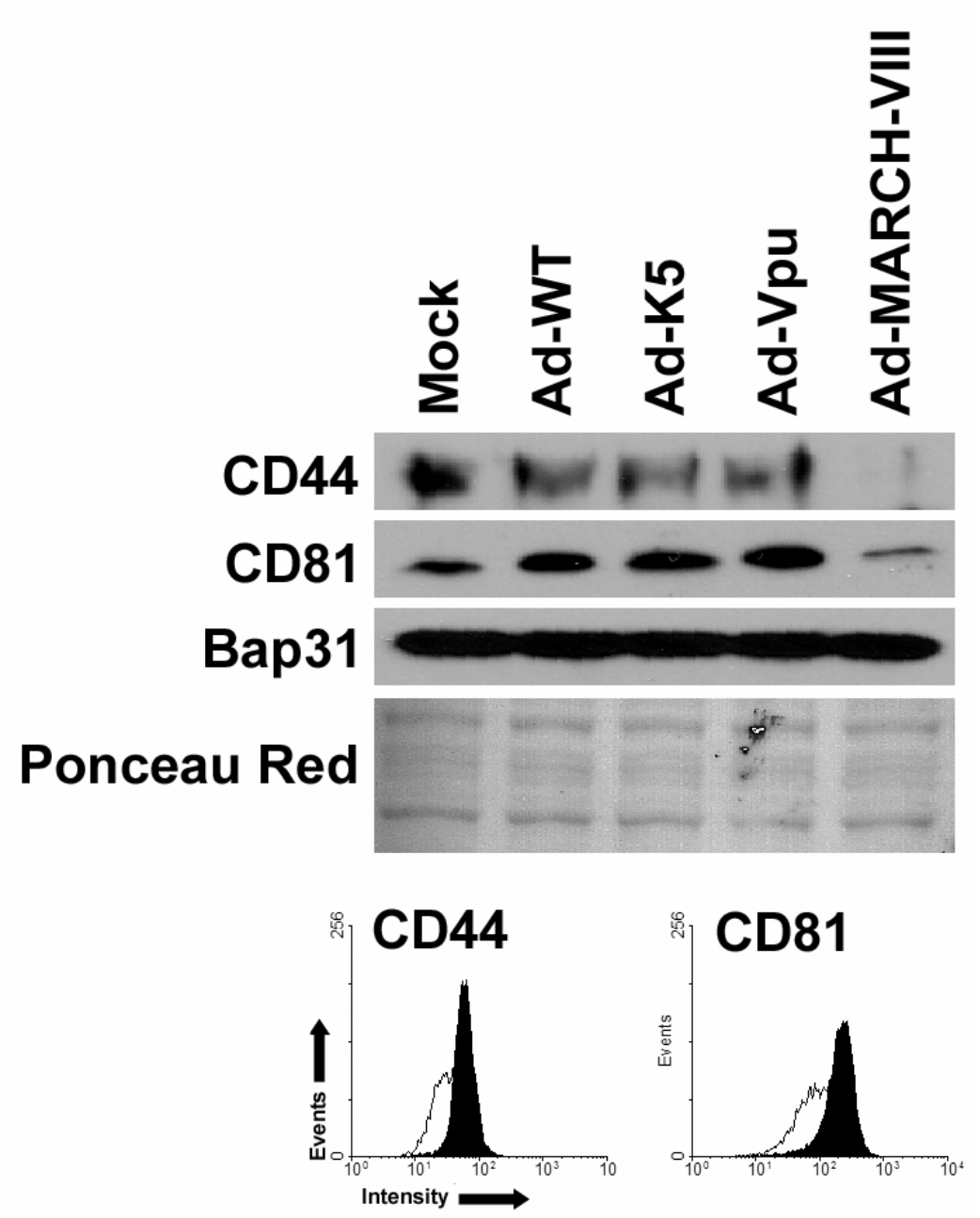

Figure 27: CD44 and CD81 are differentially expressed following MARCH-VIII expression

HFF's were infected with Ad-WT, Ad-K5, Ad-Vpu, or Ad-MARCH-VIII. 24 hours post-infection cells were harvested and whole cell lysates were analyzed for the abundance of CD44 and CD81 using immunoblot. Samples infected with Ad-MARCH-VIII display significantly reduced levels of both CD44 and CD81 compared to either Mock infected samples or samples infected with other control adenoviruses (Top). Equal protein loading was confirmed by immunoblotting for the ER resident chaperone Bap31 as well as ponceau red staining. To confirm that CD44 and CD81 were removed from the cell surface, HFF's were infected as above. 24 hours post-infection cells were harvested and processed for flowcytometry (Bottom). Samples infected with Ad-MARCH-VIII (white line) display reduced surface expression of CD44 and CD81 compared to samples infected with Ad-Tet (Black line).

Figure 28: Downregulation of CD44 and CD81 by other members of the MARCH-family

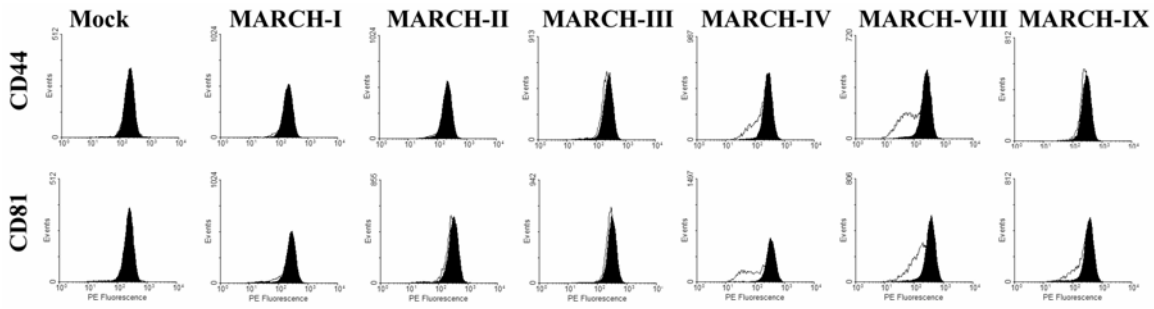

Figure 28: Downregulation of CD44 and CD81 by other members of the MARCH-family

HeLa cells were transfected with plasmids expressing cDNA's for each MARCH protein as well as GFP to track transfected cells. 24 hours post-transfection cells were harvested and analyzed for flowcytometry. Each histogram displays the GFP+ cells (White line) and the GFP- cells (Black line) from the same sample. GFP+ cells from samples transfected with either MARCH-IV or MARCH-VIII displayed reduced surface expression of both CD44 and CD81. Expression of the remaining MARCH proteins had minimal to no effect of surface levels of either CD44 or CD81.

Figure 29: Depletion of MARCH-IV affects surface expression of CD81

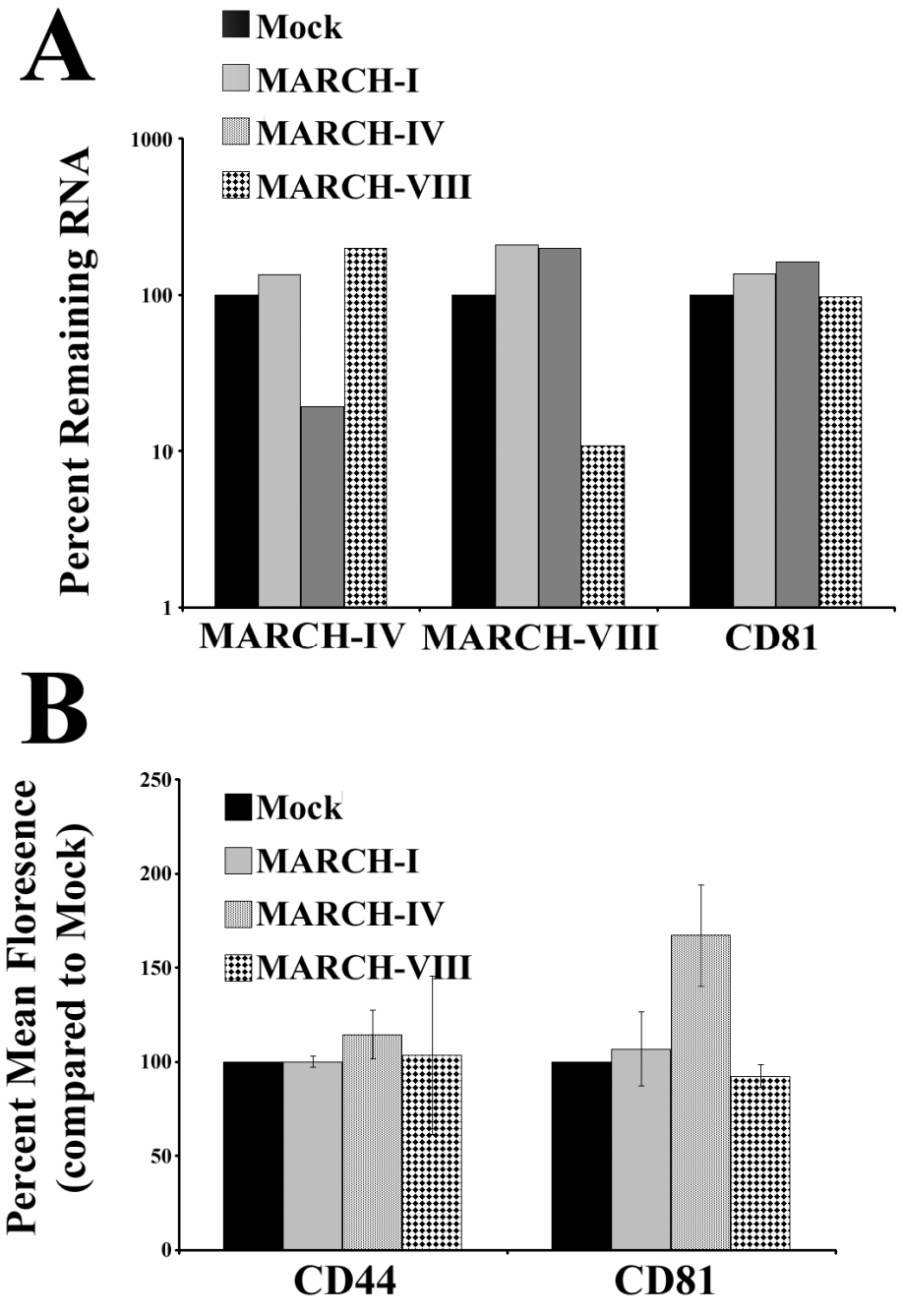

Figure 29: Depletion of MARCH-IV affects surface expression of CD81

HFF's were treated with siRNA against MARCH-I, -IV, or –VIII as indicated. Cells were treated with siRNA four times over the course of 7 days as outlined in materials and methods. The success of each siRNA treatment was determined by knockdown of the MARCH mRNA using real time quantitative PCR (A). In parallel, cells were harvested via trypsinization and the surface levels of CD44 and CD81 were measured using flowcytometry (B). Graphs are displayed as percent mean florescence intensity compared to untreated cells. The average and standard deviation from five separate experiments are shown.

Chapter 7: Discussion

Discovery of MARCH proteins

The completion of the human genome project deposited a large number of hypothetical proteins into the public databases. Frequently, however, these proteins are uncharacterized, making them largely inaccessible to further investigation. This lack of characterization is particularly problematic for proteomic and genomic studies, where the large volumes of data generated often make complete analysis of a data set unfeasible. Proteins annotated in the public databases as hypothetical or uncharacterized are often overlooked in these analyses since the lack of reagents makes follow up experiments are extremely difficult. Our results characterize a novel family of human proteins termed Membrane Associated RING-CH (MARCH) proteins, which are homologous to the viral K3-family of immune evasion proteins. Annotation of the MARCH proteins in public databases, as well as the general characterization of their function, allows other investigators access to this new protein family.

To date nine human MARCH proteins have been identified (105). Three of these proteins, however, MARCH-V, -VI, and –VII, are divergent enough from the other six that they might not be true members of the MARCH family. For example, MARCH-V contains four transmembrane domains and localizes to the mitochondria (269) while MARCH-VII's RING-CH domain is highly divergent and is preceded by a 500 amino acid extension not found in any other MARCH protein. MARCH-VI, meanwhile, contains 12 transmembrane domains and is likely the human homologue of yeast Doa10.

Since Doa10 is the only MARCH homologue found in yeast, this gene likely represents an ancestral gene that the other MARCH genes evolved from, however, unlike human members of the MARCH-family, which primarily degrade proteins via the lysosome, Doa10 functions by degrading misfolded proteins via the ERAD pathway. This suggests that the expansion of the MARCH proteins in humans represents the evolution of additional MARCH functions. MARCH homologues, however, are fairly common in many lower organisms and plants (our unpublished observations), so expansion of the MARCH-family is not specific to mammals. The function of these non-human MARCH proteins, however, is currently unknown.

Initial studies on the K3-family hypothesized that both the herpesviridae and poxviridae had acquired MARCH homologues from their hosts in separate events (74,76). The observation that K3-family proteins are functional MARCH homologues, explains the presence of these proteins in two highly divergent viral families. Presumably, both viral families acquired the K3 genes to downregulate surface proteins which were already targeted by one or more MARCH proteins. Since K3 proteins and MARCH proteins display slightly different substrate specificity, however, the viral genes probably evolved after each virus acquired them from their host. Since evolution tends to conserve regions of genes which are required for function, the divergence of the K3 genes from the MARCH genes can help identify these regions. For example, all K3 and MARCH proteins contain acidic clusters at various locations. Without any further analysis, these data suggest that acidic clusters serve an important function for both families.

Physiological Substrates of MARCH Proteins

Multiple substrates have been proposed for each MARCH protein (105,192-194,222). Downregulation of most of these substrates, however, has only been observed in forced-expression systems which might not accurately reflect MARCH proteins physiological function. For example, upon forced-expression MARCH-I and –VIII downregulate MHC-II, TfR, Fas, ALCAM, and CD86(B7.2), while MARCH-VIII alone also downregulates MHC-I, CD44, and CD81 (105,181,191,194)(our unpublished observations). Determining which of these substrates are physiologically relevant, however, has proven difficult. For example, MHC-I, TfR, Fas, ALCAM, CD44, and CD81, were downregulated only following expression of high levels of MARCH-I and/or –VIII (our unpublished observations). Since physiological MARCH expression is relatively low, this suggests that MARCH-I and -VIII will not affect these substrates *in vivo*. Additionally, depletion of MARCH-VIII from HFF's did not affect surface expression of CD44, CD81 or TfR (our unpublished observations); while depletion of MARCH-II, which also downregulates TfR only at high levels of expression, did not affect the localization of TfR or the uptake of labeled transferrin (192). While these experiments do not conclusively demonstrate that these proteins are not MARCH substrates, they suggest that regulation would only occur in cells with extremely high endogenous MARCH expression.

The only known physiological substrate for MARCH-I and –VIII is MHC-II. B cells from MARCH-I knockout mice display increased surface expression of MHC-II and increased ability to present antigen, proving that MARCH-I regulates MHC-II *in vivo* (239). MHC-II is also likely to be a MARCH substrate in dendritic cells. MHC-II is

differentially expressed in immature (iDC) and mature (mDC) dendritic cells. In iDC's lysines in the cytoplasmic tail of HLA-DRβ are ubiquitinated, resulting in retention of MHC-II in intracellular MVBs (270-272). Upon DC maturation, intracellular MHC-II is released, resulting in increased surface expression. Since the mechanism of MHC-II retention in iDCs is similar to that shown for MARCH-I and -VIII, several groups hypothesized that MHC-II was a target of MARCH-I and -VIII in iDC's (194,270). This hypothesis is supported by the observation that MARCH-VIII is downregulated during DC maturation (unpublished communications with Dr. Viktor Steimle). Since B7.2 is also upregulated during DC maturation, it seems likely that B7.2 is also a physiological substrate of MARCH-I and/or –VIII.

Multiple substrates have also been proposed for MARCH-IV and –IX, including MHC-I, CD4, CD44, CD81, and ICAM-1 (105,193). While high levels of MARCH-IV expression were required to downregulate CD81, I were able to demonstrate that depletion of endogenous MARCH-IV resulted in increased CD81 surface expression (our unpublished observations). This result makes CD81 the only confirmed substrate of any human MARCH protein. However, a second likely physiological substrate for MARCH-IV and –IX is MHC-I. This hypothesis is supported by several lines of evidence. First, only low levels of MARCH-IV and –IX were required to downregulate MHC-I, suggesting that this downregulation could occur at physiological levels of MARCH expression (105). Second, both herpesviruses and poxviruses downregulate MHC-I using acquired MARCH homologues. The observation that two highly divergent viral families acquired a MARCH homologue for the same function argues that one of the MARCH proteins affects MHC-I *in vivo*. The most likely candidate for this regulation is MARCH-

IV and/or –IX. Despite this evidence, depletion of endogenous MARCH-IX from HeLa cells did not alter surface expression, steady state levels, intracellular trafficking, endocytosis, or peptide stability of MHC-I (Appendix 1A). This negative result, however, can be explained in several ways. First, peptide bound MHC-I is an extremely stable molecule, with a half life significantly longer than eight hours (105). Due to this long half life, the techniques utilized might not have been sensitive enough to detect a subtle stabilization of MHC-I following depletion of MARCH-IX. A similar problem has been observed with MHC-I phosphorylation. The carboxy-terminal tail of MHC-I was long known to be phosphorylated (273). The function of this phosphorylation, however, could not be determined until the phosphorylation site was knockedout out *in vivo*. Thus, the effect of MARCH–IX on MHC-I might be too subtle to be easily detected. Since MHC-I is misregulated in many cancer cells, a second possibility is that HeLa cells are not an accurate model for the study of MARCH-IX. MARCH-IX might only affects MHC-I in certain cell types or under certain conditions. A third possibility is that the function of MARCH proteins is more redundant than currently appreciated. While MARCH-IV and –IX have the largest effect on MHC-I, MARCH-VIII also downregulates MHC-I in certain cell-types (105) (our unpublished observations). Thus, MARCH-VIII might be able to regulate MHC-I following depletion of MARCH-IX. Additionally, while overexpression of MARCH-I did not downregulate MHC-I in HeLa cells, MARCH-I and –VIII share significant substrate specificity (105). Since MARCH-VIII's downregulation of MHC-I is cells type specific, MARCH-I could also target MHC-I under the appropriate conditions.

Physiological Impact of MARCH Proteins

Since physiological substrates for most MARCH proteins are not currently known, the exact function of MARCH proteins *in vivo* is difficult to determine. Several lines of evidence, however, suggest that these genes play a role in modulating the immune response. First, MARCH proteins are highly expressed in many immune cells and tissues suggesting that these genes have an immunological function (105,194,239,240). Second virtually all suspected MARCH substrates are immunologically relevant. For example, between then MARCH-IV and -IX downregulate MHC-I and CD4, both of which play major roles in antigen presentation and T cell activation (105), CD44, which regulates T cell development, homing, and activation (252,274,275), CD81, which spatially organizes multiple immunologically relevant proteins, including CD4, CD8, MHC-I and MHC-II (258,259), and ICAM-1, a co-receptor for T cell activation (193). These data suggest that MARCH-IV and –IX could regulate T cell activation by downregulating costimulatory molecules on both T cells and antigen presenting cells.

Alternatively, MARCH-I and –VIII are likely to downregulate MHC-II and B7.2 *in vivo* (105,194,239). This downregulation has been shown to be important in B cells and is also likely to play a role in monocytes and dendritic cells (194,239,276,277)(our unpublished observations). Forced-expression of MARCH-VIII meanwhile downregulates CD44 and CD81, which are also expressed on the surface of DC's. CD44 is upregulated in DC's following CD40 activation through CD154 as well as treatment with osteopontin (278-280). Following osteopontin treatment, CD44 protein levels increased while expression of CD44 mRNA was unchanged, suggesting that upregulation

of CD44 was post-translational. Thus, upregulation of CD44 following treatment with osteopontin might be the result MARCH-VIII being downregulated. In contrast, CD81 is not known to be regulated during DC maturation; however, DC's can phagocytose CD81+ exosomes which also carry the MARCH-VIII substrates TfR and MHC-II (245,281,282). Following phagocytosis, these exosomes are targeted down the MVB pathway (282). Since MARCH-VIII targets its substrates down the MVB pathway, it could play a role in the targeting of phagocytosed CD81+ exosomes. As previously noted, CD44 and CD81 play roles in T cell regulation. Interestingly, MARCH-VIII is highly expressed in the human Jurkat T cell line (our unpublished observations). Thus, like MARCH-IV and –IX, MARCH-VIII might also regulate development and activation of T cells.

While all these data suggest that MARCH proteins play a significant role in modulating several arms of the immune response, the mechanism each MARCH protein uses to accomplish this might be very different. For example, MARCH-I and –VIII appear to play direct roles in the immune response by altering surface expression of their substrates following immunological stimuli. In contrast, the expression of MARCH-IX in virtually all tissues suggests that it might play a house keeping function, possibly by regulating the steady state turnover MHC-I (105). For peptide bound MHC-I to accurately reflect the current cellular milieu, preexisting MHC-I must be slowly degraded and replaced with newly synthesized peptide:MHC-I complexes. While overexpression of MARCH-IX removes most MHC-I from the cell surface, low levels of MARCH-IX only slightly increase the MHC-I turnover (our unpublished observations). Thus, low

level expression of MARCH-IX might degraded preexisting MHC-I slowly, maintaining space for newly synthesized peptide:MHC-I complexes.

Unlike MARCH-IX, MARCH-IV is expressed almost exclusively in the brain and placenta (105), tissues which display highly restricted immune responses. This expression pattern suggests that MARCH-IV regulates the immune response in these privileged tissues. One possible target for this regulation is HLA-G, a variant of classical MHC-I which is expressed only in brain microglial cells and extravillous trophoblasts at the fetal–maternal interface (283,284). Since HLA-G is highly homologous to classical MHC-I (285), and MARCH-IV expression matches HLA-G expression, it seems likely that MARCH-IV could target HLA-G. Since the brain and placenta are both highly transcriptionally active during fetal development, a second possibility is that MARCH-IV plays a role only during this stage. MARCH-IV could regulate MHC-I, or another target, in the fetus, while MARCH-IX plays a similar role in adults.

MARCH proteins' ability to modulate the immune response, both positively and negatively, makes them attractive targets for viruses. The wide range of MARCH substrates means that, by regulating MARCH expression, viruses could inhibit antigen presentation, T cell costimulation, DC maturation, B cell, and T cell activation. For example, viruses could downregulate MHC-I by artificially upregulating expression of MARCH-IV or –IX. While viral regulation of MARCH proteins has not been extensively studied, HIV infection does upregulate expression of MARCH-II in Jurkat T cells (our unpublished observations). Since physiological substrates of MARCH-II are unknown, however, it is impossible to address the role of this regulation in viral infection.

Mechanism of MARCH Function

Early experiments suggested that both the K3-family and MARCH-family functioned via a fairly simple mechanism (49,105). Proteins from both families interacted with substrates through their transmembrane domains, catalyzing the ubiquitination of lysines in their substrates cytoplasmic tail. This targeted the substrate down the MVB pathway, resulting in lysosomal degradation (reviewed in (74)). Recent evidence, however, suggests that both families might have a more complex mechanism. K5 downregulation of CD31, for instance, occurrs via two distinct mechanisms (55). Preexisting CD31 is downregulated via lysosomal degradation; while newly synthesized CD31 is degraded in the proteosome. Evidence suggests that MARCH proteins might also use a similar two-pronged approach. MARCH-VIII degrades preexisting B7.2 via enhanced endocytosis and lysosomal targeting (181)(our unpublished observations); however, newly synthesized B7.2 is degraded with rapid kinetics reminiscent of proteosomal degradation (our unpublished observations). The importance of this two-pronged approach is not yet understood. Each mechanism might be differentially regulated to yield distinct results. For example, prolonged stimulation through B7.2 is required for activation of naïve T cells (286). By degrading only newly synthesized protein, MARCH-VIII might increase the duration of T cell costimulation, while still maintaining stable levels of total B7.2. In contrast, degradation of preexisting B7.2 might reduce the duration of costimulation without depleting total B7.2 levels. Similarly, selective degradation of preexisting or newly synthesized MHC-I or MHC-II could regulate the peptide repertoire displayed by these proteins at various times.

A second poorly understood element of MARCH function is the mechanism of substrate recognition. A direct interaction between MARCH proteins and their substrates is known to occur within the transmembrane domains of both proteins (105). This observation explains the observation that MARCH proteins with highly homologous transmembrane domains have virtually identical substrate specificity (105). However, although all studied K3 proteins, as well as MARCH-IV and -IX downregulate MHC-I, there is no obvious conservation within the transmembrane domains of these proteins that could account for this specificity. Additionally, although the transmembrane domains of MARCH-I and –VIII are 95% identical; MARCH-VIII downregulates CD44 and CD81, while MARCH-I does not. Substrate specificity is therefore unlikely to be determined simply by a recognition motif found within each MARCH protein.

Several other factors might also play roles in mediating substrate selection. First is subcellular localization. MARCH-VIII constructs lacking a 16 amino acid region in the carboxy-terminus or MARCH-IV constructs lacking the entire amino- and carboxy-termini localize almost exclusively in the ER (191) (our unpublished observations). In both cases, the mislocalized MARCH protein iss unable to downregulate its suspected substrate (105)(Appendix 1B). Other groups have shown that localization of MARCH-II and –III depends on a four amino acid PDZ binding motif at the extreme carboxy-terminus (192,222). Deletion of this region results in retention of both MARCH-II and –III in the ER, however, the functionality of these constructs was not determined. Interestingly, the consensus PDZ binding motif is found in all six major MARCH proteins (105). Mutation of this region in MARCH-IV or –VIII, however, has no effect on the localization of either protein (105)(Appendix 1B). The PDZ motif might serve as

the major localization signal for certain MARCH proteins, while for others this motif is either a secondary signal or serves a different function entirely.

Another example of how subcellular localization can affect substrate selection is the acidic cluster mutants of K5. These mutants, which are unable to interact with PACS2, still downregulate MHC-I but are unable to degrade newly synthesized CD31 (55). Since PACS2 functions to retrotranslocate proteins from the TGN to the ER, this suggests that a specific ER localization is required for K5 to differentiate between MHC-I and CD31. Interestingly, PACS2 interacts with acidic clusters which are found in K3, K5, and all known MARCH proteins. While a functional analysis of the acidic clusters found in MARCH proteins has not been attempted, these regions likely mediate an interaction with PACS2, and that this interaction will prove important to MARCH function. One possible function for the acidic clusters is in recruitment of E2s. K3 needs to interact with two E2s to degrade MHC-I (50). Interestingly, the phenotype observed for depletion of one of these E2s, UbcH5, parallels that seen for deletion of K5's acidic clusters (50,52). While the acidic clusters in the K3-family all localize to the carboxy-terminus, the acidic clusters found in MARCH proteins localize to both the amino- and carboxy-termini. If the acidic clusters play a role in E2 recognition, this differential localization could correspond to unique E2 requirements for each MARCH protein.

A second factor which might influence substrate specificity is protein:protein interactions. For example, MARCH proteins are known to interact with members of the syntaxin family of SNARE proteins. Syntaxins are trafficking molecules which localize other proteins to subsets of intracellular vesicles. Overexpression of any MARCH protein, except MARCH-III, results in the relocalization of STX4 to a MARCH

containing compartment, and previous studies have demonstrated that MARCH-II and –III interact with STX6 (192,222). Thus, syntaxins likely interact directly with all members of the MARCH-family. Interacting with syntaxins could localize MARCH proteins to unique intracellular vesicles, allowing them to target only proteins found within this specific vesicle. Failure to interact with syntaxins, meanwhile, could mislocalize MARCH proteins rendering them unable to interact with their substrates. Interestingly, the only MARCH protein which failed to relocalize STX4 was MARCH-III since no substrate has been observed for MARCH-III even upon overexpression. This MARCH protein might fail to downregulate any substrates due to the inability to interact with syntaxins in the systems tested. While this hypothesis is supported by the observation that mutants of MARCH-VIII, which failed to relocalize STX4, also mislocalized and failed to downregulate B7.2 (191); STX4 interacts with virtually all MARCH proteins (191). This widespread interaction argues against syntaxins playing a role in MARCH substrate selection. Other MARCH proteins, however, are known to interact with other syntaxins. For example, MARCH-II interacts with syntaxin-6, 8 and 13, but not with syntaxin-16 (192). Thus, interaction with a specific set of syntaxins might mediate MARCH substrate selection.

MARCH binding to Bap31 and CD81 might also play a role in substrate selection. Bap31 functions both as an ER resident chaperone and a forward cargo receptor (7,247-250,287). Depletion of Bap31 results in reduced expression of MARCH-VIII at the cell surface, demonstrating that Bap31 represents a key forward trafficking protein for MARCH-VIII (our unpublished observations). Interestingly, Bap31 is also a known cargo receptor for MHC-I (6,7), raising the possibility that Bap31 mediates an interaction

between MARCH-VIII and MHC-I. Similarly, CD81, which is targeted by MARCH-IV and –VIII, is involved in the special and temporal organization of MHC-I, MHC-II, CD4, and TfR (258,264,281). Interestingly, all of these proteins are targets of either MARCH-IV or –VIII, suggesting that the MARCH:CD81 interaction might play a role in substrates selection.

A final example of how protein:protein interactions could influence MARCH substrate selection is the potential requirements of each MARCH protein for a distinct set of E2s. MARCH:E2 interactions could play a role in MARCH protein substrate selection by restricting the subcellular compartment in which each MARCH protein could ubiquitinate its substrate. For example, Ubc6 localizes primarily to the ER (288). MARCH proteins which interact with Ubc6 would therefore be unable to ubiquitinate their substrates unless they interacted with them in the ER.

A third factor which might influence MARCH substrate selection is oligomerization. Several groups have observed that MARCH proteins both homo- and hetero-oligomerize. For example, a naturally occurring splice variant of MARCH-IX, which lacks a complete RING-CH domain, forms a hetero-oligomer with full length MARCH-IX (193). This interaction stabilized full length MARCH-IX leading to increased downregulation of ICAM-1. Similarly, MARCH-II forms a hetero-oligomer with MARCH-III (222); however, further experiments were not performed to determine the functional consequences of this interaction. Similar to what has been observed for the toll like receptors (TLRs), oligomerization might affect MARCH substrate selection by altering the specificity of each MARCH protein. For example, homo-oligomers of TLR2 bind several ligands, including tri-actylated lipoproteins, which are observed in many

bacteria. Following hetero-dimerization with TLR1 or TLR6, however, TLR2 recognizes di-actylated lipoproteins or peptidoglycan (289-292). Alternatively, oligomerization might serve as a post-translation mechanism to regulate MARCH protein activity. While oligomerization enhances the function of MARCH-IX, mutants of K5 lacking a functional RING-CH domain act as dominant negatives (48). This observation confirms the importance of oligomerization for the MARCH-family, but suggests that it might play a distinct role for each protein. Despite the apparent widespread occurrence of oligomerization in the MARCH-family, oligomerization is not a general characteristic of all MARCH proteins, since MARCH-VIII is unable to homo- or hetero-oligomerize with any naturally occurring MARCH protein (Appendix 1B and our unpublished observations).

The domain mediating MARCH oligomerization is currently unknown. RING domains have previously been shown to form large scale oligomers (293,294), suggesting that the observed oligomerization of MARCH proteins could occur through their RING-CH domains. Since both K5 and MARCH-IX can oligomerize with variants lacking a RING-CH domain, however, another region might be involved. One possibility for this region is the transmembrane domains. This hypothesis is supported by the observation that only the transmembrane domains and a small portion of the carboxy-terminus are required for K5 oligomerization (48).

A final factor which might influence MARCH substrate selection is RNA splicing. Most MARCH mRNAs display some level of differential splicing, most notably the variant of MARCH-IX lacking a functional RING-CH domain. This splicing event has not been shown to affect MARCH-IX substrate specificity, but does regulate

MARCH-IX function by stabilizing full length MARCH-IX. The public databases contain at least four amino-terminal splice variants of MARCH-I, each of which produces a unique protein product (our unpublished observations). Each of these variants might have a slightly different specificity, for instance, each variant might downregulate distinct alleles of MHC-II. However, since the RING-CH domain, both transmembrane domains, and carboxy-terminus of all these variants are identical, it is unlikely that these variants will display vastly different substrate specificity. Their exact role *in vivo*, however, might be very different. For instance, different splice variants might have different half-lives or recruit distinct E2 enzymes. Since different E2s mediate different forms of ubiquitination, which can have very different results (50), similar splice variants of MARCH-I might have very different functions, such as destruction of MHC-II versus retention in intracellular vesicles. Alternatively, differential splice variants might be expressed in different cell types or tissues, where unique E2 expression could require different interacting motifs. MARCH-VIII also displays significant alternative splicing, however, in contrast to MARCH-I, MARCH-VIII splice variants occur strictly within the 3' UTR and all encode the same protein product. A likely role for this splicing is regulation of mRNA expression or turnover. For example, these splicing events might play a role in removal of MARCH-VIII mRNA following a DC maturation stimulus.

Therapeutic Uses for MARCH Proteins

Primarily due to the known effects of overexpressing each MARCH protein, there are several potential therapeutic uses for the MARCH-family. For example, T cells play a key role in advancement of rheumatoid arthritis (295). Recently, the FDA approved a

drug called Abatacept (Orencia) for the treatment of severe rheumatoid arthritis patients. Abatacept works by binding to CD80(B7.1) and B7.2, thereby inhibiting their activation of CD28 and depriving T cells of their costimulation (295). Since MARCH-I and –VIII both downregulate B7.2, overexpression of either MARCH protein in APCs might function similar to treatment with Abatacept, making these genes possible treatments for T cell over activation diseases. A second possible therapeutic use for MARCH proteins is the autoimmune disorder Behcet's disease. While the cause of Behcet's disease is not known, it shares a strong association with the MHC-I alleles HLA-B27 and HLA-B54 (296). Due to this association, removal of these alleles by overexpression of MARCH-IV or –IX might prove therapeutic for this disease. Conversely, knockout of MARCH-I stimulates antigen presentation by B cells *in vivo* (239). Thus, inhibition of MARCH-I, through either depletion of forced-expression of a dominant negative, could be used to stimulate B cell mediated antigen presentation. Similarly, inhibition of MARCH-VIII from iDCs is likely to be a key step in DC maturation (194,239,270). Forced-depletion of endogenous MARCH-VIII might therefore simulate the maturation of DCs.

MARCH proteins might also be useful in regulating viral infection. CD81 has been shown to be a coreceptor for HCV infection (244). Inhibition of HCV binding to CD81 efficiently blocked viral infection (262,297), while normally permissive cells, depleted of CD81, no longer supported HCV infection (263). Since expression of MARCH-IV or –VIII removes CD81 from the cell surface, overexpression of either protein might be able to inhibit HCV infection. CD81 activation also increases HIV mediated syncytia formation (264) and HIV transcription (265). Thus, overexpression of

MARCH-IV or –VIII could inhibit some of the cytopathic effects associated with HIV infection.

Finally, due to the overlapping specificity of MARCH proteins with K5, one of the MARCH proteins probably downregulates CD31 (55). CD31 stimulates angiogenesis, which is clinically important for the metastasis of many cancers (298-301). Removal of CD31 from the surface of cells within these cancers may block new blood vessel formation, inhibiting tumor growth by depriving the tumor of blood born nutrients and inhibiting metastasis. CD31 is also a factor in transplant biology (302,303). Mismatch of CD31 alleles in bone marrow and hematopoeitic stem cell transplants correlates with graft versus host disease (302). Removal of CD31 from the cell surface might therefore be useful in a large number of therapeutic applications, from cancer treatment to transplant biology.

Due to several factors, a better understanding of MARCH substrate selection is important to any therapeutic use of these proteins. The first factor is the broad substrate specificity of many MARCH proteins. The ability to downregulate an individual surface protein is unlikely to be of significant use if it is always coupled to the removal of 4-5 other proteins. The observation that downregulation of specific K5 substrates is genetically separable(48), however, suggests that creation of MARCH constructs specific to a single substrate might be possible. Second, a better understanding of MARCH substrate selection could lead to the ability to selectively remove virtually any protein from the cell surface. The potential uses for this ability, both scientifically and therapeutically, are virtually endless.

2-Dimensional-PAGE

Previous studies on the MARCH- and K3-families used antibody based methods to identify substrates. The use of these techniques created a potentially biased view of each families targets since only a small number of potential substrates were tested. For instance, prior to our proteomic analysis, all known substrates of K5 were type 1 membrane glycoproteins, leading to the hypothesis that K5 only downregulated proteins which belonged to this group. One reason all K5 substrates were related, however, was that these proteins constituted the majority of potential substrates which had been tested. Thus, a non-biased approach to discovering MARCH- and K3-family substrates was needed.

Our 2D-PAGE approach to determining novel substrates for M153R revealed two significant findings. Our first major finding was that expression of M153R alters significantly more cellular proteins than expression of K5. Since K3 proteins are fairly substrate specific, the number of proteins affected suggests that M153R regulates a major cellular process. Since expression of M153R downregulates Fas and blocks the loss of mitochondrial membrane potential induced by STS, one possibility for this process is apoptosis. While previous studies demonstrated that deletion of M153R did not affect apoptosis induced via myxoma infection *in vivo* (76), these studies failed to address the presence of M11L, an apoptotic inhibitor encoded by myxoma. In the presence of M11L, myxoma infected cells do not undergo significant apoptosis (202,203). Thus, deletion of M153R might not have altered apoptosis *in vivo* since apoptosis was still blocked by M11L. Similarly, while the deletion of M11L enhanced apoptosis induced by myxoma infection (202), this result does not rule out the possibility that myxoma encodes other

apoptotic inhibitors, such as M153R. Thus, current data does not rule out the possibility that M153R is an apoptotic inhibitor.

M153R could regulate apoptosis through several possible mechanisms. The first is M153R's downregulation of Fas (76). Crosslinking of Fas is one of the major mechanisms of inducing apoptosis. By downregulating Fas, M153R could inhibit the ability of cells to activate this apoptotic pathway. While the absence of FasL during vaccinia infection, argues that M153R mediated downregulation of Fas might not affect apoptosis in this context, the variety of cellular apoptotic pathways makes it impossible to rule out this possibility entirely. However, a more likely mechanism is that M153R inhibits apoptosis through its interaction with Bap31 (our unpublished observations). The caspase mediated cleavage of cell surface Bap31 results in the generation of a proapoptotic Bap31 derived peptide known as p20. This peptide causes Ca^{++} flux in the ER resulting in release of cytochrome C and loss of mitochondrial membrane potential (304,305). Since expression of MARCH-VIII inhibits the surface localization of Bap31, it is likely that expression of M153R does as well. Thus, M153R could hinder apoptosis by inhibiting the generation of p20. In contrast, M153R could enhance apoptosis through an interaction with PACS2. Overexpression of K5, and likely M153R, mislocalizes PACS2, effectively depleting cellular stores of this protein (55). Depletion of PACS2, in turn, induces apoptosis in a Bap31 dependant manner (57).

M153R could also alter expression of a wide variety of proteins by directly regulating the course of vaccinia infection. While obvious differences were not observed in titer or cytopathic effect following infection with VV-WT or VV-M153R *in vitro*, deletion of M153R reduced myxoma virulence *in vivo* (76), demonstrating that M153R

can play a major role in poxviral infection. This phenotype was attributed to M153R's downregulation of MHC-I; however, inflammatory infiltrates were identical following infection with wild-type or ΔM153R myxoma, suggesting that the immune response to both viruses was not significantly different (76). Thus, M153R might influence myxoma virulence by directly regulating the course of poxviral infection. Since I expressed M153R using a vaccinia vector, and vaccinia infection has a massive effect on cellular protein expression, altering the course of the infection could explain the large number of protein expression changes observed following expression of M153R.

The second major finding from our study was that infection with vaccinia induced amino- and carboxy-terminal cleavage of the mitochondrial chaperone Hsp60. Hsp60 cleavage might be the result of expression of a specific vaccinia ORF or cellular changes induced by vaccinia infection. However, while Hsp60 cleavage was not observed following crosslinking of Fas or treatment with STS, two lines of evidence suggest that this cleavage is linked to apoptosis. First, Hsp60 is already linked to apoptosis through binding to the proapoptotic proteins Bax and Bad (205). Second, cells which did not display a loss of mitochondrial membrane potential also failed to display cleavage of Hsp60. The failure to observe cleavage of Hsp60 following crosslinking of Fas or treatment with STS might be due these stimuli inducing different apoptotic pathways than vaccinia infection. Crosslinking of Fas might also alter the apoptotic pathway induced by vaccinia infection, which could explain why it inhibited cleavage of Hsp60. Similarly, the observation that different cells use different apoptotic pathways(206,207) could explain why vaccinia infection only induced Hsp60 cleavage in HeLa cells. Interestingly, if Hsp60 cleavage is linked to apoptosis, the observation that expression of M153R

inhibits this cleavage could be explained via M153R's potential role as an apoptotic inhibitor. Thus, both major findings from our study might be linked through the inhibition of apoptosis.

Vaccinia infection does not induce complete apoptosis, due to the expression of the apoptotic inhibitor F1L (306). F1L interacts with the pro-apoptotic proteins Bax and Bad, inhibiting the release of cytochrome c (306-308). Expression of F1L creates a form of arrested apoptosis, in which apoptosis is initiated normally, but then inhibited prior to mitochondrial involvement. Thus, cleavage of Hsp60 might be the result of the specific form of apoptosis created by expression of F1L. However, in contrast to infection with vaccinia, infection with myxoma did not result in cleavage of Hsp60. Since both vaccinia and myxoma are poxviruses, they likely induce similar forms of apoptosis. Additionally, myxoma also encodes an apoptotic inhibiter, M11L, which inhibits apoptosis prior to mitochondrial involvement (202,203). Unfortunately, these experiments cannot be performed in HeLa cells since these cells are nonpermissive for myxoma infection. Thus, we are not currently able to conclude if myxoma infection fails to cause cleavage of Hsp60 due to cell type or apoptotic pathway.

The functional consequences of Hsp60 cleavage are also not presently understood. Since only a fraction of cellular Hsp60 is cleaved, it is possible that the remaining Hsp60 is still able to perform both chaperone and anti-apoptotic functions. Additionally, cleavage was primary observed in mitochondrial Hsp60, while anti-apoptotic Hsp60 is cytosolic. Thus, cleavage of Hsp60 might play only a minor role in vaccinia infection or play a significant role only late in infection once cleavage of a high percentage of Hsp60 has occured.

Quantitative Mass Spectroscopy

Since our 2D-PAGE analysis of M153R failed to identify any direct M153R substrates, I switched to an approach combining stable isotope labeling with amino acids in cell culture (SILAC)(155) and mass spectroscopy (MS). I then used this technique to test for potential substrates of K5 and MARCH-VIII.

Most proteomic studies are designed to analyze cellular processes which alter large numbers of proteins simultaneously, such as apoptosis(309,310), cellular differentiation(229,311), cellular stress(168), or proteosomal degradation(312). Our study provided a very different challenge, since expression of relatively few proteins are altered by K5 and MARCH-VIII. However, our SILAC/MS analysis revealed that CD166 (ALCAM), bone marrow stromal antigen 2 (BST2), and syntaxin-4 (STX4) were downregulated by K5, while CD44, CD81 and Bap31 were downregulated by MARCH-VIII. Importantly, this technique can be easily adapted to other systems. Thus, our results both identify novel substrates for the specific E3s tested and expand the field of quantitative proteomics allowing for the analysis of proteins with highly selective enzymatic functions, such as kinases, phosphatases, glucotransferases, ubiquitin ligases, and specific proteases.

ALCAM is a type-1 Ig superfamily protein with several known functions, including cell-cell adhesion and T cell activation (224-226). Expression of K5 resulted in ubiquitination and destruction of ALCAM via the lysosome, and ALCAM was removed from the surface of endothelial cells during lytic KSHV infection. These data suggest that ALCAM is a novel target of K5 and could play a role in increased migration and

improved immune evasion of KSHV infected cells. Compared to other costimulatory signals such as B7.2:CD28, relatively little is known about the mechanism of ALCAM costimulation through its ligand CD6. The observation that KSHV evolved immune evasion mechanisms against ALCAM, however, suggests that ALCAM plays a more important role in costimulation than previous believed. Additionally, KSHV will probably not be the only virus to target ALCAM, thus ALCAM represents a novel target for general viral immune evasion.

ALCAM is a type-1 Ig superfamily protein. Previous studies had noted that virtually all K5 substrates fell into this category, however, since this family also constituted the vast majority of proteins which had been screened as possible substrates, it was possible that the previous results were highly biased. The observation that our proteomic screen, which was relatively unbiased, also found an Ig superfamily substrate for K5, suggests that the Ig fold might play some role in K5 substrate selection, possibly by interacting with cargo receptors or trafficking proteins in the exocytic pathway.

Unlike ALCAM, STX4 is not related to previously known K5 substrates. While total STX4 levels were reduced following expression of K5, it is unknown whether STX4 is a direct K5 substrate. Interestingly, expression of most MARCH proteins relocalized STX4 to intracellular MARCH containing compartments. Thus, STX4 might also be relocalized by K5. This relocalization could result in the destruction of STX4 without it being a direct K5 target. This highlights one potential pitfall of our SILAC/MS based approach, since this technique is unable to distinguish between directly and indirectly affected proteins.

The physiological role of K5 interacting with syntaxins is unknown. As previously mentioned, one possibility is that syntaxins play a role in mediating K3- and MARCH-family substrate selection by properly localizing each K3- and MARCH protein. Previous observations that STX6 colocalized with overexpressed MARCH-II led to the conclusion that MARCH-II played a role in intracellular trafficking, by acting to correctly localize STX6 (192). This hypothesis is supported by the observation that overexpression of rat MARCH-II alters the uptake of several proteins involved in retrograde PM to endosomal trafficking, including STX6, Furin, TGN38 and TGN46. Additionally, while depletion of STX4 has no effect on the localization of MARCH-VIII (our unpublished observations), depletion of endogenous MARCH-II using stable shRNA lines of HeLa cells resulted in altered uptake of TGN38 and TGN46 as well as altered steady state localization of STX6. However, the effects noted above occurred in only ~30% of cells in a limited number of shRNA treated lines (12 out of 24 lines for TGN38, 8 out of 24 lines for TGN46 and 2 out of 24 lines for STX6). No change in either the uptake or localization of Furin was observed in any stable line. This inconsistency suggests that, while MARCH-II might play a role in endosomal trafficking, this role might not be as direct as the authors conclude.

In contrast, we hypothesize that syntaxins are one of several factors which localize MARCH proteins and that depletion of MARCH-II affects intracellular trafficking indirectly by targeting presently unknown substrates for destruction. While there is currently little supporting evidence, we prefer this hypothesis due to the consistency with previously known functions for both STX6 and MARCH-II. In our model the observed relocalization of syntaxins resulting from MARCH protein

overexpression is caused by these overexpressed MARCH proteins dragging syntaxins into intracellular vesicles, while any effects on intracellular trafficking following depletion of MARCH-II are an indirect result of another function of MARCH-II.

The final K5 substrate observed in our analysis was BST2. Interestingly, BST2 is also downregulated by MARCH-VIII. Since virtually all known MARCH substrates are immunologically relevant, newly discovered MARCH substrates also have a high probability of playing some role in the immune response. This allows for the functional characterization of proteins which were not previously known to play a role in the immune response. BST2 is a good example of this. BST2 is expressed primarily on differentiated B cells and plays a role in pre-B cell growth (218,313), however, this gene is not currently known to play an active role in the immune response. Due to the downregulation of BST2 by MARCH-VIII and K5, we hypothesize that this gene plays a previously unknown role in immune modulation. This hypothesis is supported by the finding that a large number of viral immune modulators, including K5, M153R, US2 and US11 also remove BST2 from the cell surface (105) (our unpublished observations). The observation that K5 constructs lacking a functional RING-CH domain were unable to downregulate BST2 suggests that K5 enzymatic function is required to degrade BST2, however, since a direct interaction between K5 and BST2 has not been shown, it is possible that K5 affects BST2 indirectly.

Our SILAC analysis also revealed three proteins whose expression was altered by MARCH-VIII: CD44, CD81 and Bap31. While formal demonstration has not yet been performed, CD44 and CD81 are likely direct substrates of MARCH-VII. The potential relevance of these substrates has been discussed previously. In contrast, Bap31 is

probably removed from the cell surface by binding to intracellular MARCH-VIII. As previously mentioned, depletion of Bap31 resulted in lower MARCH-VIII surface expression. Interestingly, depletion of Bap31 did not alter the vesicular localization seen for the majority of MARCH-VIII, although overexpression of MARCH-VIII relocalized Bap31 to intracellular vesicles (our unpublished observations). This observation suggests that Bap31 can interact with vesicular MARCH-VIII, but mainly plays a role in localizing MARCH-VIII from the endosomes to the plasma membrane. A second possibility is that MARCH-VIII is localized via two distinct pathways, one from the ER to the endosomes, and a second from the ER directly to the plasma membrane. This hypothesis is supported by the observation that truncations of MARCH-VIII, which do not traffic to the endosomes, are still expressed at the cell surface (191)(Appendix 1B). Interestingly, these truncations do not interact with syntaxins but are still able to interact with Bap31 (191). Thus, syntaxins might localize MARCH-VIII to the endosomes, while Bap31 might target a subset of MARCH-VIII from the ER directly to the plasma membrane.

Along with the identification of novel substrates, our analysis highlighted two important areas of quantitative proteomics. First is the need for replicate experiments. In each of our individual experiments, over half the identified proteins displayed skewed protein ratios. While this rate of inaccurate protein quantitation seems high, it is relatively comparable to rates from other laboratories (314). Unfortunately, the nature of proteomics makes validation of every identified protein difficult and expensive. Due to this problem, large unvalidated data sets are often misleading. Although I did not confirm every protein in our analysis, we concluded that the quantitation of many of these proteins was inaccurate. This conclusion is supported by the observations that K5

does not downregulate the majority of surface proteins (51), and that the subcellular location of many of these proteins makes them unlikely substrates. Attempts to reduce the inaccuracy of protein quantitation by increasing the stringency of purification(315) do not address the general inaccuracy of MS based quantitation and exclude many proteins from analysis since they are modified on peptides which cannot easily be analyzed via MS.

In contrast, I were able to demonstrate that the accuracy of protein quantitation could be greatly increased using replicate experiments. Additionally, replicate experiments allowed us to raise our proteome coverage by including proteins identified by only a single peptide. Since only around 70% of MS based analysis is reproducible (217), however, using replicate experiments might exclude potential substrates which are not consistently identified. An example of this exclusion can be seen in our failure to recover adequate peptides to several known MARCH-VIII substrates (our unpublished observations). Thus, our use of multiple replicates reduces false positives at the expense of increasing false negatives.

A second major finding of our experiments is the need for standardization of proteomics data sets. Quantitation of our data sets using different programs resulted in the identification of different potential substrates (our unpublished observations). Since many labs use different programs for data analysis, reproducibility of proteomics data sets between laboratories can be a major challenge. Thus, better software and standard methods of data analysis are required to advance the field of in quantitative MS.

Chapter 8: Future Directions

Many questions about the MARCH-family remain unanswered. The most important of these questions is which MARCH substrates are physiologically relevant. Since our SILAC/MS based technique has proven successful in discovering a physiological substrate for MARCH-IV, this technique can probably help determine physiological substrates for other MARCH proteins. To date, however, this technique has only been used to analyze MARCH-VIII. Thus, the next step in determining the function of the MARCH-family is to analyze the remaining MARCH proteins using SILAC/MS.

The most difficult part of these experiments is determining the appropriate cell line in which to test each MARCH protein. Since every cell line expresses a unique set of surface proteins, this choice makes a substantial difference in which potential substrates are identified. For example, CD44 was identified as a novel MARCH-VIII substrate through SILAC/MS analysis in HFFs. While BJAB cells express considerably higher levels of endogenous MARCH-VIII, they do not express CD44; thus, SILAC/MS analysis in these cells would not be able to identify CD44 as a substrate. Additionally, expression of a MARCH protein in different cell lines might result in different levels of MARCH expression, different MARCH subcellular localization, or recruitment of different E2s. All of these factors could alter a MARCH proteins substrate specificity, thus unique substrates might be identified in each cell line tested. Do to these factors, SILAC/MS analysis of each MARCH protein should ideally be done in multiple cell lines. While the exact cell lines will differ for each MARCH protein, some likely

candidates are HeLas, HFFs, RAJIs, BJABs, Jurkats, and THP-1s. Cell lines that express the endogenous MARCH protein can also be used to study the effect of depleting endogenous MARCH proteins with siRNA. While these experiments are difficult and expensive, targets determined this way are highly likely to represent true physiological substrates.

Since likely substrates have not been proposed for either MARCH-II or –III, these are the most interesting MARCH proteins for SILAC/MS analysis. MARCH-II is highly expressed in Jurkat T cells making this an attractive system for SILAC/MS analysis. Additionally, MARCH-II is upregulated in these cells during the course of HIV infection, however, since no substrates for MARCH-II are currently known, it is not possible to address the physiological relevance of this upregulation. Identification of MARCH-II substrates using SILAC/MS in Jurkat T cells could therefore elucidate both functions of MARCH-II and mechanisms of HIV infection. Additionally, since Jurkat cells are easily amenable to most molecular biology techniques, the mechanisms and relevance of potential substrates identified in this system can be easily addressed. MARCH-II is also expressed in HeLa cells (192). Since these cells are easily grown *in vitro*, they represent an attractive alternative system for the SILAC/MS analysis of MARCH-II. In contrast to MARCH-II, the expression of MARCH-III is not well known. Further experiments will need to be conducted to determine appropriate cell lines to analysis this MARCH protein.

Another interesting MARCH protein for SILAC analysis is MARCH-IX. MARCH-IV and –IX share virtually identical substrates, however, a non-biased approach has not been used to analyze these proteins. MARCH-IX is a better candidate for this analysis than MARCH-IV since MARCH-IX displays widespread expression in virtually

all tissues and cell lines (105). Additionally, MARCH-IX shares significant substrate specificity with members of the K3-family. Thus, novel substrates identified for MARCH-IX also represent likely targets of viral immune evasion.

The second major question remaining for the MARCH family is the mechanism of substrate selection. Since MARCH-I and –VIII are 95% identical through their RING-CH and transmembrane domains, our recent observation that MARCH-VIII downregulates CD44 and CD81 while MARCH-I does not, represents a powerful tool to dissect the mechanisms of substrate selection. The limited variability between these two proteins limits the regions which could account for this unique substrate selection. This limited variability allows for an in-depth analysis of the role of each amino acid in determining MARCH targets. While this analysis is likely to be difficult and time consuming, an understanding of how MARCH proteins select their substrates represents a major step forward for both the general scientific knowledge and practical therapeutics of the MARCH family.

Appendix 1A:

Result of Depletion of MARCH-IX on MHC-I

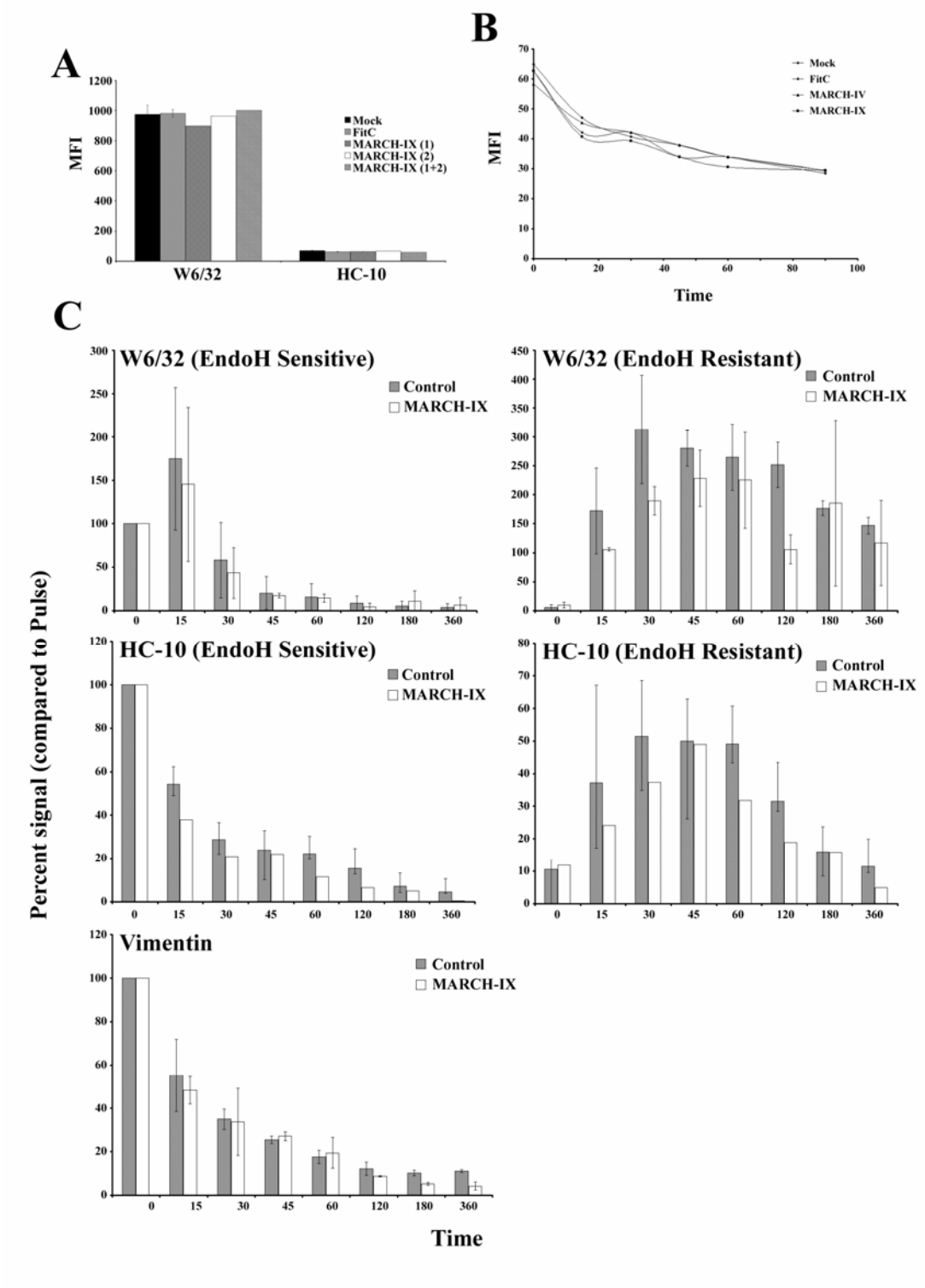

Appendix 1A: Result of Depletion of MARCH-IX on MHC-I

To determine if endogenous MARCH-IX affected the surface expression of MHC-I, HeLa cells were treated with two different siRNAs against MARCH-IX, either separately or together. $1x10^5$ HeLa cells were plated in 25mm dishes. 24 hours later, cells were transfected twice with 5µl of 20µm siRNA, six hours apart, using oligofectamine according to the manufacturer's recommendations. 72 hours after siRNA treatment, cells were harvested and the surface expression of both peptide loaded (W6/32) and unloaded (HC-10) MHC-I at the cell surface was analyzed via flowcytometry (A). No significant difference was observed in the surface expression of either peptide loaded or unloaded MHC-I over three separate experiments. To determine if endogenous MARCH-IX affected endocytosis of MHC-I, HeLa cells were treated with either scrambled siRNA or siRNA against MARCH-IV or -IX. 72 hours post-transfection, cells were transferred to 4^o and the cell surface was decorated with the anti-MHC-I antibody W6/32. Cells were then washed and returned to 37^o for the indicated times (B). At each time point, cells were harvested and the amount of W6/32 remaining at the cell surface was determined via flowcytometry. Depletion of MARCH-IX had no effect on the endocytosis rate of MHC-I in three separate experiments. To determine if endogenous MARCH-IX had any effect on the half life of MHC-I, HeLa cells were treated with MARCH-IX siRNA as above. 72 hours post-transfection, cells were labeled with S^{35} methionine/cysteine for 20 minutes and then chased in DMEM supplemented with excess cold methionine/cysteine for the indicated times. Following the chase, cells were lysed in 1% NP-40, and peptide bound (W6/32) and unbound (HC-10) MHC-I was immunoprecipitated. Precipitated material was treated with endoglycosidase H (EndoH)

overnight and then separated on a 10% SDS-PAGE gel. Following exposure to film, the abundance of both EndoH sensitive and resistant forms of MHC-I was determined at each time point using densitometry (C). The results show the average of three separate experiments. The abundance of immunoprecipitated Vimentin is shown as a control.

Appendix 1B:

Analysis of MARCH-VIII Truncations

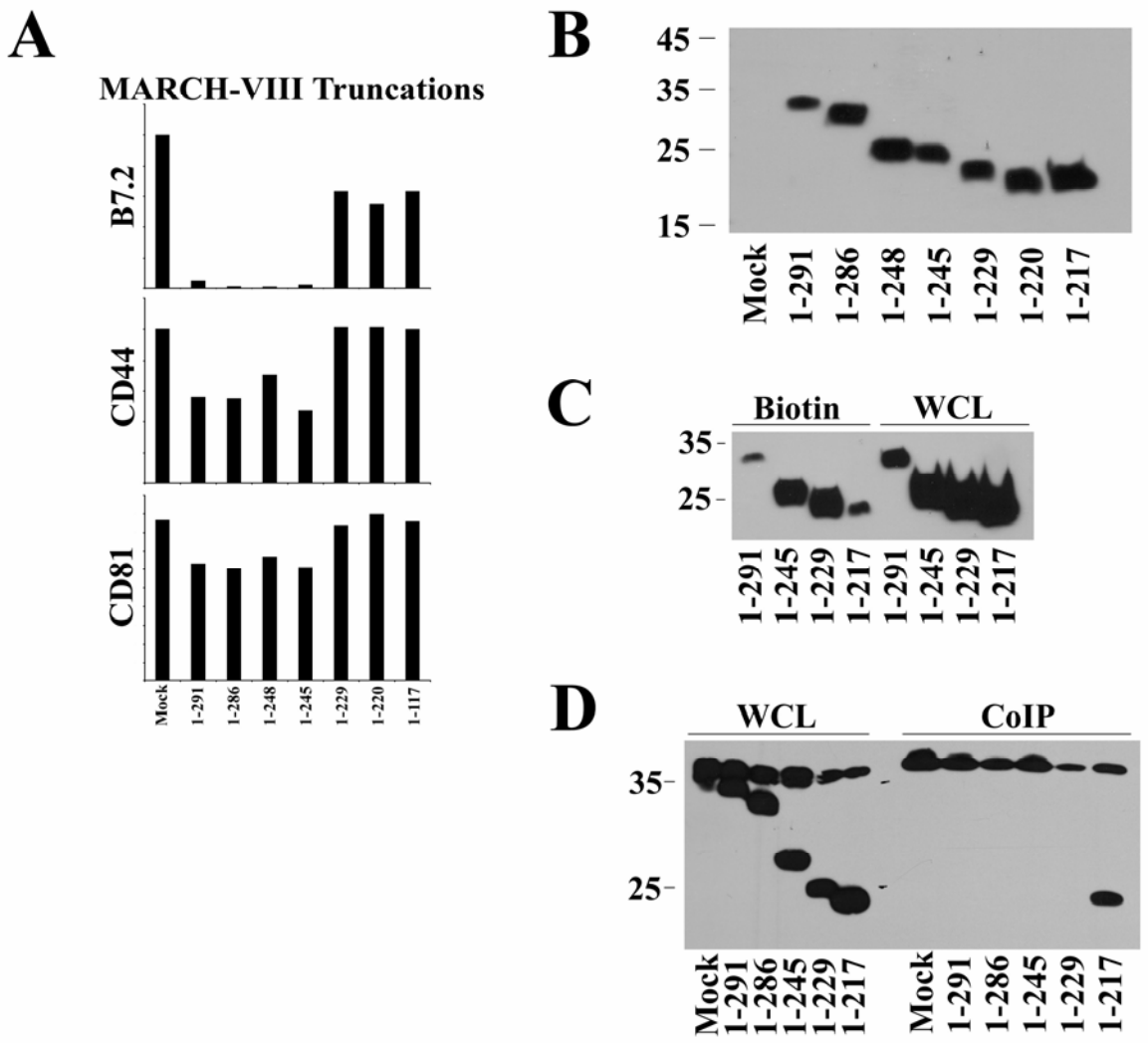

Appendix 1B: Analysis of MARCH-VIII Truncations

To determine which regions in the carboxy-terminus of MARCH-VIII were required for function, a series of carboxy-terminal truncations were constructed. Each construct is labeled according to the amino acids remaining. For example, 1-291 represents wild-type MARCH-VIII, while 1-217 represents a deletion of all 72 amino acids in MARCH-VIII's carboxy-terminus. To determine whether each truncation downregulated known substrates of MARCH-VIII, HeLa cells were transfected with constructs encoding each truncation. 24 hours post-transfection, cells were harvested and the abundance of endogenous CD44 and CD81 as well as transfected B7.2 were analyzed via flowcytometry (A). MARCH-VIII lacking the carboxy-terminal 46 amino acids (1-245) was still able to downregulate CD44, CD81 and B7.2, while constructs lacking 60 or more amino acids (1-229, 1-220, and 1-217) were unable to downregulate any of the tested substrates. To determine if this result was due a lack of expression, HeLa cells were transfected with each construct and expression of each mutant analyzed via immunoblotting with an anti-MARCH-VIII antibody (B). The results demonstrate that all carboxy-terminal truncations of MARCH-VIII are expressed at similar levels, suggesting that the failure of certain constructs to downregulate their substrates is not due to lack of expression. To determine if these constructs failed to downregulate their substrates because they were unable to traffic to the cell surface, each construct was transfected in HeLa cells. 24 hours post-transfection, the surface of transfected cells were decorated with biotin using the Cell Surface labeling and Purification kit (Pierce). Cells were then lysed and biotinylated proteins purified according to the manufacturers

recommendations. This purification resulted in the generation of two fractions, a biotin fraction, representing proteins at the cell surface, and a whole cell lysate (WCL) fraction representing intracellular proteins. Each fraction was then analyzed for the abundance of MARCH-VIII via immunoblotting with an anti-MARCH-VIII antibody (C). All carboxy-terminal truncations of MARCH-VIII are clearly observed in both the WCL lysate and biotin fractions. Thus, the failure of MARCH-VIII 1-217, 1-220, and 1-229 to downregulate their substrates is not caused by a failure of these constructs to traffic to the cell surface. To determine if the carboxy-terminal truncations of MARCH-VIII were able to form oligomers, each construct was transfected into HeLa cells along with a carboxy-terminally Flag-tagged version of wild-type MARCH-VIII. 24 hours post-transfection, cell were lysed in 1% CHAPS, and the Flag-tagged MARCH-VIII immunoprecipitated using the anti-Flag (M2) antibody (Sigma). Samples were then separated on a 10% SDS-PAGE gel and the presence of each MARCH-VIII construct was determined via immunoblotting with an anti-MARCH-VIII antibody (D Right). Expression of all constructs was confirmed by immunoblotting a WCL of each sample with an anti-MARCH-VIII antibody (D Left). Interestingly, while the Flag-tagged MARCH-VIII is clearly observed in all samples as a band running slightly above 35kDa, an interaction is only observed between this construct and a MARCH-VIII construct lacking the entire carboxy-terminus (1-217). These data suggest that the carboxy-terminus might play a role in regulating the oligomerization of MARCH-VIII.

Appendix 1C:

Generation and Testing of MARCH Antibodies

Antigen	Clone	Western	IP	IF
MARCH-I				
	2G9	Yes	No	Yes
MARCH-II				
	1D9	Yes	Yes	Yes
	4G6	Yes	Yes	Yes
MARCH-III				
	7E3	Yes	Yes	Yes
	13F9	Yes	Yes	Yes
MARCH-IV				
	6G4	No	Yes	Yes
MARCH-VIII				
	6F6	Yes	Yes	Yes
MARCH-IX				
	8G9	No	Yes	Yes
	8C10	No	Yes	Yes

Appendix 1C: Generation and Testing of MARCH Antibodies

The carboxy-terminus of MARCH-I and the amino-terminus of MARCH-II, -III, -IV, -VIII and –IX were amplified via PCR and cloned into the bacterial expression plasmid pGEX4T-1 to form amino-terminal GST fusions. Plasmids were transformed into *E coli*. (strain BL21) and protein expression induced for three hours by addition of 0.1 mM IPTG. GST fusions proteins were then purified using glutathione-sepharose beads. Purified protein was used to generate monoclonal antibodies against each MARCH protein by the VGTI antibody core. Each monoclonal antibody was then tested for reactivity against transfected MARCH protein in immunoblot, immunoprecipitation and immunoflorescence. The results of this analysis are shown in table format.

Appendix 2:

Setup for 2D-PAGE Analysis using DIGE Dyes

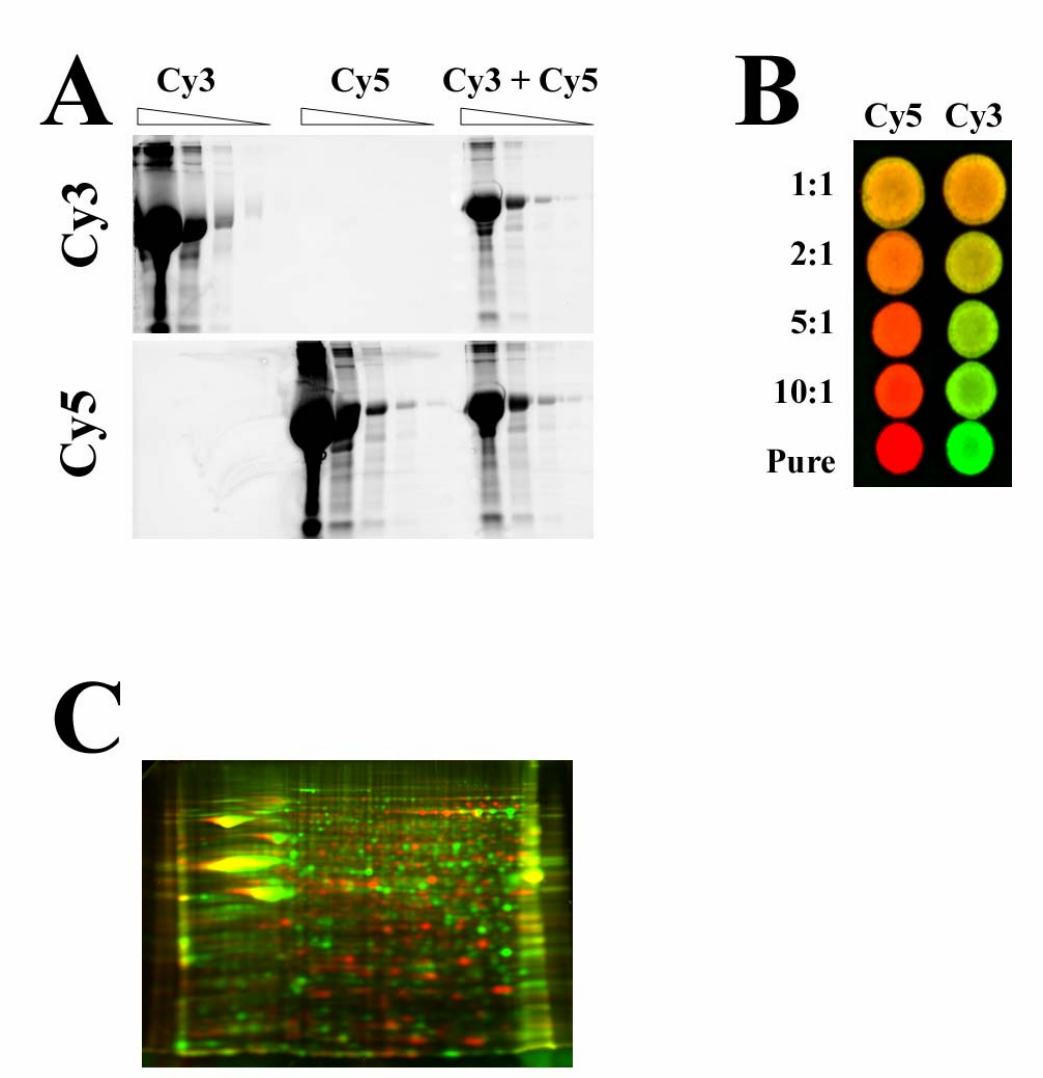

Appendix 2: Setup for 2D-PAGE Analysis using DIGE Dyes

To determine the specificity of Cy-Dyes (Amersham), BSA was labeled with either Cy3 or Cy5. Either individually labeled BSA or double labeled BSA was then separated on a 10% SDS-PAGE gel and each dye was visualized separately on a Typhoon 8600 variable mode imager (A). Individually labeled BSA is observed only in scans corresponding to the dye it was labeled with, while double labeled BSA is visualized in both scans. To determine the ability of Cy-Dyes to detect differential protein expression, BSA labeled with either Cy3 or Cy5 was combined in known ratios and 1μg of the resulting mixtures was spotted on Whatman paper. Each dye was then visualized individually (Cy3 as Green and Cy5 as Red) and the images overlaid so that differential protein expression could be observed (B). Spots with identical amounts of Cy3 and Cy5 labeled protein are visualized as yellow, while spots with different amounts of each label are visualized as either red, green or a shade of orange. To determine whether Cy-Dyes altered the molecular weight (MW) and pI of proteins during 2D-PAGE analysis, crude membrane preparations from HeLa cells were labeled with limiting amounts of either DIGE-Cy5 (Red) (Amersham), which is chemically synthesized to not alter the MW or pI of proteins regular or regular Cy-3 (Green). Following combination of both samples and separation using 2D-PAGE, the location of proteins labeled with both dyes was visualized as above. The results demonstrate that proteins labeled with Cy-Dyes and DIGE-Dyes do not migrate at the same MW and pI, suggesting that Cy-Dyes alter both the MW and pI of labeled proteins.

Appendix 3:

Abbreviations

2D-PAGE (two-dimensional polyacrylamide gel electrophoresis)

ALCAM (activated leukocyte cell adhesion molecule)

AraC (cytosine arabinoside)

β_2M (beta-2 microglobulin)

Bap31 (B-cell receptor-associated protein 31kDa)

BST2 (bone marrow stromal antigen 2)

CD (multicentric Castleman's disease)

ConA (concanamycin A)

CTL (cytotoxic T lymphocyte)

iDC (immature dendritic cell)

mDC (mature dendritic cell)

DMVEC (dermal microvascular endothelial cells)

E1 (ubiquitin activating enzyme)

E2 (Ubiquitin conjugating Enzyme)

E3 (Ubiquitin Ligase Enzyme)

ER (endoplasmic reticulum)

ERAD (ER associated degradation)

ESCRT (endosomal sorting complex required for transport)

GRAIL (Gene Related to Anergy In Lymphocytes)

HA (hemagglutinin)

HCMV (human cytomegalovirus)

HCV (Hepatitis C virus)

HECT (Homologous to E6-Associated Protein carboxy-Terminus)

HFF (human foreskin fibroblasts)

Hsp60 (heat shock protein 60kDa)

ICAT (Isotope coded affinity tagging)

Ifnγ-R (interferon-gamma receptor)

KS (Kaposi's Sarcoma)

KSHV (Kaposi's Sarcoma Associated Herpesvirus)

LANA (latency associated nuclear antigen)

LC (liquid chromatography)

MARCH (Membrane associated RING-CH)

MCMV (murine cytomegalovirus)

MHC-I (major histocompatibility complex)

MHV-68 (γ2-herpesvirus 68)

MIR (modulator of immune recognition)

MOI (multiplicity of infection)

MS (mass spectroscopy)

MVB (multivesicular body)

MW (molecular weight)

NK (natural killer)

ORF (open reading frame)

pI (isoelectric point)

PM (plasma membrane)

PMA (phorbol 12-myristate 13-acetate)

RING (Really Interesting New Gene)

SILAC (stable isotope labeling with amino acids in cell culture)

STS (staurosporine)

STX4 (syntaxin-4)

TAP (transporter of antigenic peptide)

TCA (Trichloroacedic acid)

TCR (T cell receptor)

TfR (transferrin receptor)

TGN (trans-Golgi network)

TLR (toll like receptor)

TMRE (Tetramethylrhodamine, ethyl ester, perchlorate)

Tsg101 (tumor susceptibility gene 101)

Vps (vacuolar protein **s**orting protein)

VV (vaccinia virus)

WCL (whole cell lysate)

WT (wild type)

Bibliography

1) Fields, B, Knipe, D and Howley, PM. 1996. Fields Virology. 2950.

2) Alcami, A and Koszinowski, UH. 2000. Viral mechanisms of immune evasion. Immunol Today. 21:447-55.

3) Tortorella, D, Gewurz, BE, Furman, MH, Schust, DJ and Ploegh, HL. 2000. Viral subversion of the immune system. Annu Rev Immunol. 18:861-926.

4) Xu, XN, Screaton, GR and McMichael, AJ. 2001. Virus infections: escape, resistance, and counterattack. Immunity. 15:867-70.

5) Sylwester, AW, Mitchell, BL, Edgar, JB, Taormina, C, Pelte, C, Ruchti, F, Sleath, PR, Grabstein, KH, Hosken, NA, Kern, F, Nelson, JA and Picker, LJ. 2005. Broadly targeted human cytomegalovirus-specific CD4+ and CD8+ T cells dominate the memory compartments of exposed subjects. J Exp Med. 202:673-85.

6) Spiliotis, ET, Manley, H, Osorio, M, Zuniga, MC and Edidin, M. 2000. Selective export of MHC class I molecules from the ER after their dissociation from TAP. Immunity. 13:841-51.

7) Paquet, ME, Cohen-Doyle, M, Shore, GC and Williams, DB. 2004. Bap29/31 influences the intracellular traffic of MHC class I molecules. J Immunol. 172:7548-55.

8) Levitskaya, J, Sharipo, A, Leonchiks, A, Ciechanover, A and Masucci, MG. 1997. Inhibition of ubiquitin/proteasome-dependent protein degradation by the Gly-Ala repeat domain of the Epstein-Barr virus nuclear antigen 1. Proc Natl Acad Sci U S A. 94:12616-21.

9) York, IA, Roop, C, Andrews, DW, Riddell, SR, Graham, FL and Johnson, DC. 1994. A cytosolic herpes simplex virus protein inhibits antigen presentation to CD8+ T lymphocytes. Cell. 77:525-35.

10) Ahn, K, Gruhler, A, Galocha, B, Jones, TR, Wiertz, EJ, Ploegh, HL, Peterson, PA, Yang, Y and Fruh, K. 1997. The ER-luminal domain of the HCMV glycoprotein US6 inhibits peptide translocation by TAP. Immunity. 6:613-21.

11) Jones, TR, Wiertz, EJ, Sun, L, Fish, KN, Nelson, JA and Ploegh, HL. 1996. Human cytomegalovirus US3 impairs transport and maturation of major histocompatibility complex class I heavy chains. Proc Natl Acad Sci U S A. 93:11327-33.

12) Wiertz, EJ, Jones, TR, Sun, L, Bogyo, M, Geuze, HJ and Ploegh, HL. 1996. The human cytomegalovirus US11 gene product dislocates MHC class I heavy chains from the endoplasmic reticulum to the cytosol. Cell. 84:769-79.

13) Reusch, U, Muranyi, W, Lucin, P, Burgert, HG, Hengel, H and Koszinowski, UH. 1999. A cytomegalovirus glycoprotein re-routes MHC class I complexes to lysosomes for degradation. Embo J. 18:1081-91.

14) Hengel, H, Reusch, U, Gutermann, A, Ziegler, H, Jonjic, S, Lucin, P and Koszinowski, UH. 1999. Cytomegaloviral control of MHC class I function in the mouse. Immunol Rev. 168:167-76.

15) Gold, MC, Munks, MW, Wagner, M, Koszinowski, UH, Hill, AB and Fling, SP. 2002. The murine cytomegalovirus immunomodulatory gene m152 prevents recognition of infected cells by M45-specific CTL but does not alter the immunodominance of the M45-specific CD8 T cell response in vivo. J Immunol. 169:359-65.

16) Kavanagh, DG, Gold, MC, Wagner, M, Koszinowski, UH and Hill, AB. 2001. The multiple immune-evasion genes of murine cytomegalovirus are not redundant: m4 and m152 inhibit antigen presentation in a complementary and cooperative fashion. J Exp Med. 194:967-78.

17) Kavanagh, DG, Koszinowski, UH and Hill, AB. 2001. The murine cytomegalovirus immune evasion protein m4/gp34 forms biochemically distinct complexes with class I MHC at the cell surface and in a pre-Golgi compartment. J Immunol. 167:3894-902.

18) Loch, S and Tampe, R. 2005. Viral evasion of the MHC class I antigen-processing machinery. Pflugers Arch. 451:409-17.

19) Coscoy, L and Ganem, D. 2000. Kaposi's sarcoma-associated herpesvirus encodes two proteins that block cell surface display of MHC class I chains by enhancing their endocytosis. Proc Natl Acad Sci U S A. 97:8051-6.

20) Ishido, S, Wang, C, Lee, BS, Cohen, GB and Jung, JU. 2000. Downregulation of major histocompatibility complex class I molecules by Kaposi's sarcoma-associated herpesvirus K3 and K5 proteins. J Virol. 74:5300-9.

21) Henry, M, Uthman, A, Geusau, A, Rieger, A, Furci, L, Lazzarin, A, Lusso, P and Tschachler, E. 1999. Infection of circulating CD34+ cells by HHV-8 in patients with Kaposi's sarcoma. J Invest Dermatol. 113:613-6.

22) Humphrey, RW, Davis, DA, Newcomb, FM and Yarchoan, R. 1998. Human herpesvirus 8 (HHV-8) in the pathogenesis of Kaposi's sarcoma and other diseases. Leuk Lymphoma. 28:255-64.

23) Antman, K and Chang, Y. 2000. Kaposi's sarcoma. N Engl J Med. 342:1027-38.

24) Sarid, R, Flore, O, Bohenzky, RA, Chang, Y and Moore, PS. 1998. Transcription mapping of the Kaposi's sarcoma-associated herpesvirus (human herpesvirus 8) genome in a body cavity-based lymphoma cell line (BC-1). J Virol. 72:1005-12.

25) Rivas, C, Thlick, AE, Parravicini, C, Moore, PS and Chang, Y. 2001. Kaposi's sarcoma-associated herpesvirus LANA2 is a B-cell-specific latent viral protein that inhibits p53. J Virol. 75:429-38.

26) Verma, SC, Lan, K and Robertson, E. 2007. Structure and function of latency-associated nuclear antigen. Curr Top Microbiol Immunol. 312:101-36.

27) Decker, LL, Shankar, P, Khan, G, Freeman, RB, Dezube, BJ, Lieberman, J and Thorley-Lawson, DA. 1996. The Kaposi sarcoma-associated herpesvirus (KSHV) is present as an intact latent genome in KS tissue but replicates in the peripheral blood mononuclear cells of KS patients. J Exp Med. 184:283-8.

28) Ballestas, ME, Chatis, PA and Kaye, KM. 1999. Efficient persistence of extrachromosomal KSHV DNA mediated by latency-associated nuclear antigen. Science. 284:641-4.

29) Ballestas, ME and Kaye, KM. 2001. Kaposi's sarcoma-associated herpesvirus latency-associated nuclear antigen 1 mediates episome persistence through cis-acting terminal repeat (TR) sequence and specifically binds TR DNA. J Virol. 75:3250-8.

30) Friborg, J, Jr., Kong, W, Hottiger, MO and Nabel, GJ. 1999. p53 inhibition by the LANA protein of KSHV protects against cell death. Nature. 402:889-94.

31) Lan, K, Kuppers, DA, Verma, SC and Robertson, ES. 2004. Kaposi's sarcoma-associated herpesvirus-encoded latency-associated nuclear antigen inhibits lytic

replication by targeting Rta: a potential mechanism for virus-mediated control of latency. J Virol. 78:6585-94.

32) Fujimuro, M and Hayward, SD. 2004. Manipulation of glycogen-synthase kinase-3 activity in KSHV-associated cancers. J Mol Med. 82:223-31.

33) Ottinger, M, Christalla, T, Nathan, K, Brinkmann, MM, Viejo-Borbolla, A and Schulz, TF. 2006. Kaposi's sarcoma-associated herpesvirus LANA-1 interacts with the short variant of BRD4 and releases cells from a BRD4- and BRD2/RING3-induced G1 cell cycle arrest. J Virol. 80:10772-86.

34) Gessain, A and Duprez, R. 2005. Spindle cells and their role in Kaposi's sarcoma. Int J Biochem Cell Biol. 37:2457-65.

35) Fiorelli, V, Gendelman, R, Sirianni, MC, Chang, HK, Colombini, S, Markham, PD, Monini, P, Sonnabend, J, Pintus, A, Gallo, RC and Ensoli, B. 1998. gamma-Interferon produced by CD8+ T cells infiltrating Kaposi's sarcoma induces spindle cells with angiogenic phenotype and synergy with human immunodeficiency virus-1 Tat protein: an immune response to human herpesvirus-8 infection? Blood. 91:956-67.

36) MacPhail, LA, Dekker, NP and Regezi, JA. 1996. Macrophages and vascular adhesion molecules in oral Kaposi's sarcoma. J Cutan Pathol. 23:464-72.

37) Regezi, JA, MacPhail, LA, Daniels, TE, DeSouza, YG, Greenspan, JS and Greenspan, D. 1993. Human immunodeficiency virus-associated oral Kaposi's sarcoma. A heterogeneous cell population dominated by spindle-shaped endothelial cells. Am J Pathol. 143:240-9.

38) Nadji, M, Morales, AR, Ziegles-Weissman, J and Penneys, NS. 1981. Kaposi's sarcoma: immunohistologic evidence for an endothelial origin. Arch Pathol Lab Med. 105:274-5.

39) Kraffert, C, Planus, L and Penneys, NS. 1991. Kaposi's sarcoma: further immunohistologic evidence of a vascular endothelial origin. Arch Dermatol. 127:1734-5.

40) Boshoff, C, Schulz, TF, Kennedy, MM, Graham, AK, Fisher, C, Thomas, A, McGee, JO, Weiss, RA and O'Leary, JJ. 1995. Kaposi's sarcoma-associated herpesvirus infects endothelial and spindle cells. Nat Med. 1:1274-8.

41) Davis, MA, Sturzl, MA, Blasig, C, Schreier, A, Guo, HG, Reitz, M, Opalenik, SR and Browning, PJ. 1997. Expression of human herpesvirus 8-encoded cyclin D in Kaposi's sarcoma spindle cells. J Natl Cancer Inst. 89:1868-74.

42) Martin, DF, Kuppermann, BD, Wolitz, RA, Palestine, AG, Li, H and Robinson, CA. 1999. Oral ganciclovir for patients with cytomegalovirus retinitis treated with a ganciclovir implant. Roche Ganciclovir Study Group. N Engl J Med. 340:1063-70.

43) Hayward, GS. 2003. Initiation of angiogenic Kaposi's sarcoma lesions. Cancer Cell. 3:1-3.

44) Haque, M, Ueda, K, Nakano, K, Hirata, Y, Parravicini, C, Corbellino, M and Yamanishi, K. 2001. Major histocompatibility complex class I molecules are down-regulated at the cell surface by the K5 protein encoded by Kaposi's sarcoma-associated herpesvirus/human herpesvirus-8. J Gen Virol. 82:1175-80.

45) Paulson, E, Tran, C, Collins, K and Fruh, K. 2001. KSHV-K5 inhibits phosphorylation of the major histocompatibility complex class I cytoplasmic tail. Virology. 288:369-78.

46) Haque, M, Chen, J, Ueda, K, Mori, Y, Nakano, K, Hirata, Y, Kanamori, S, Uchiyama, Y, Inagi, R, Okuno, T and Yamanishi, K. 2000. Identification and analysis of the K5 gene of Kaposi's sarcoma-associated herpesvirus. J Virol. 74:2867-75.

47) Hewitt, EW, Duncan, L, Mufti, D, Baker, J, Stevenson, PG and Lehner, PJ. 2002. Ubiquitylation of MHC class I by the K3 viral protein signals internalization and TSG101-dependent degradation. Embo J. 21:2418-29.

48) Sanchez, DJ, Coscoy, L and Ganem, D. 2002. Functional organization of MIR2, a novel viral regulator of selective endocytosis. J Biol Chem. 277:6124-30.

49) Coscoy, L, Sanchez, DJ and Ganem, D. 2001. A novel class of herpesvirus-encoded membrane-bound E3 ubiquitin ligases regulates endocytosis of proteins involved in immune recognition. J Cell Biol. 155:1265-73.

50) Duncan, LM, Piper, S, Dodd, RB, Saville, MK, Sanderson, CM, Luzio, JP and Lehner, PJ. 2006. Lysine-63-linked ubiquitination is required for endolysosomal degradation of class I molecules. Embo J. 25:1635-45.

51) Coscoy, L and Ganem, D. 2001. A viral protein that selectively downregulates ICAM-1 and B7-2 and modulates T cell costimulation. J Clin Invest. 107:1599-606.

52) Means, RE, Ishido, S, Alvarez, X and Jung, JU. 2002. Multiple endocytic trafficking pathways of MHC class I molecules induced by a Herpesvirus protein. Embo J. 21:1638-49.

53) Aravind, L, Iyer, LM and Koonin, EV. 2003. Scores of RINGS but no PHDs in ubiquitin signaling. Cell Cycle. 2:123-6.

54) Ishido, S, Choi, JK, Lee, BS, Wang, C, DeMaria, M, Johnson, RP, Cohen, GB and Jung, JU. 2000. Inhibition of natural killer cell-mediated cytotoxicity by Kaposi's sarcoma-associated herpesvirus K5 protein. Immunity. 13:365-74.

55) Mansouri, M, Douglas, J, Rose, PP, Gouveia, K, Thomas, G, Means, RE, Moses, AV and Fruh, K. 2006. Kaposi sarcoma herpesvirus K5 removes CD31/PECAM from endothelial cells. Blood. 108:1932-40.

56) Crump, CM, Xiang, Y, Thomas, L, Gu, F, Austin, C, Tooze, SA and Thomas, G. 2001. PACS-1 binding to adaptors is required for acidic cluster motif-mediated protein traffic. Embo J. 20:2191-201.

57) Simmen, T, Aslan, JE, Blagoveshchenskaya, AD, Thomas, L, Wan, L, Xiang, Y, Feliciangeli, SF, Hung, CH, Crump, CM and Thomas, G. 2005. PACS-2 controls endoplasmic reticulum-mitochondria communication and Bid-mediated apoptosis. Embo J. 24:717-29.

58) Karlhofer, FM, Ribaudo, RK and Yokoyama, WM. 1992. MHC class I alloantigen specificity of Ly-49+ IL-2-activated natural killer cells. Nature. 358:66-70.

59) Li, Q, Means, R, Lang, S and Jung, JU. 2006. Downregulation of interferon gamma receptor 1 by Kaposi's Sarcoma-Associated Herpesvirus K3 and K5. J Virol.

60) Sanchez, DJ, Gumperz, JE and Ganem, D. 2005. Regulation of CD1d expression and function by a herpesvirus infection. J Clin Invest. 115:1369-78.

61) Lorenzo, ME, Jung, JU and Ploegh, HL. 2002. Kaposi's sarcoma-associated herpesvirus K3 utilizes the ubiquitin-proteasome system in routing class major histocompatibility complexes to late endocytic compartments. J Virol. 76:5522-31.

62) Stevenson, PG, Efstathiou, S, Doherty, PC and Lehner, PJ. 2000. Inhibition of MHC class I-restricted antigen presentation by gamma 2-herpesviruses. Proc Natl Acad Sci U S A. 97:8455-60.

63) Boname, JM and Stevenson, PG. 2001. MHC class I ubiquitination by a viral PHD/LAP finger protein. Immunity. 15:627-36.

64) Boname, JM, de Lima, BD, Lehner, PJ and Stevenson, PG. 2004. Viral degradation of the MHC class I peptide loading complex. Immunity. 20:305-17.

65) Boname, JM, May, JS and Stevenson, PG. 2005. The murine gamma-herpesvirus-68 MK3 protein causes TAP degradation independent of MHC class I heavy chain degradation. Eur J Immunol. 35:171-9.

66) Lybarger, L, Wang, X, Harris, MR, Virgin, HWt and Hansen, TH. 2003. Virus subversion of the MHC class I peptide-loading complex. Immunity. 18:121-30.

67) Wang, X, Lybarger, L, Connors, R, Harris, MR and Hansen, TH. 2004. Model for the interaction of gammaherpesvirus 68 RING-CH finger protein mK3 with major histocompatibility complex class I and the peptide-loading complex. J Virol. 78:8673-86.

68) Wang, X, Herr, RA, Chua, WJ, Lybarger, L, Wiertz, EJ and Hansen, TH. 2007. Ubiquitination of serine, threonine, or lysine residues on the cytoplasmic tail can induce ERAD of MHC-I by viral E3 ligase mK3. J Cell Biol.

69) Wang, X, Ye, Y, Lencer, W and Hansen, TH. 2006. The viral E3 ubiquitin ligase mK3 uses the Derlin/p97 endoplasmic reticulum-associated degradation pathway to mediate down-regulation of major histocompatibility complex class I proteins. J Biol Chem. 281:8636-44.

70) Nishikawa, S, Brodsky, JL and Nakatsukasa, K. 2005. Roles of molecular chaperones in endoplasmic reticulum (ER) quality control and ER-associated degradation (ERAD). J Biochem (Tokyo). 137:551-5.

71) McCracken, AA and Brodsky, JL. 2003. Evolving questions and paradigm shifts in endoplasmic-reticulum-associated degradation (ERAD). Bioessays. 25:868-77.

72) Tsai, B, Ye, Y and Rapoport, TA. 2002. Retro-translocation of proteins from the endoplasmic reticulum into the cytosol. Nat Rev Mol Cell Biol. 3:246-55.

73) Jones, TR, Hanson, LK, Sun, L, Slater, JS, Stenberg, RM and Campbell, AE. 1995. Multiple independent loci within the human cytomegalovirus unique short region down-regulate expression of major histocompatibility complex class I heavy chains. J Virol. 69:4830-41.

74) Fruh, K, Bartee, E, Gouveia, K and Mansouri, M. 2002. Immune evasion by a novel family of viral PHD/LAP-finger proteins of gamma-2 herpesviruses and poxviruses. Virus Res. 88:55-69.

75) Gao, L and Qi, J. 2007. Whole genome molecular phylogeny of large dsDNA viruses using composition vector method. BMC Evol Biol. 7:41.

76) Guerin, JL, Gelfi, J, Boullier, S, Delverdier, M, Bellanger, FA, Bertagnoli, S, Drexler, I, Sutter, G and Messud-Petit, F. 2002. Myxoma virus leukemia-associated protein is responsible for major histocompatibility complex class I and Fas-CD95 down-regulation and defines scrapins, a new group of surface cellular receptor abductor proteins. J Virol. 76:2912-23.

77) Mansouri, M, Bartee, E, Gouveia, K, Hovey Nerenberg, BT, Barrett, J, Thomas, L, Thomas, G, McFadden, G and Fruh, K. 2003. The PHD/LAP-domain protein M153R of

myxomavirus is a ubiquitin ligase that induces the rapid internalization and lysosomal destruction of CD4. J Virol. 77:1427-40.

78) Hershko, A, Ciechanover, A, Heller, H, Haas, AL and Rose, IA. 1980. Proposed role of ATP in protein breakdown: conjugation of protein with multiple chains of the polypeptide of ATP-dependent proteolysis. Proc Natl Acad Sci U S A. 77:1783-6.

79) Ciechanover, A, Heller, H, Elias, S, Haas, AL and Hershko, A. 1980. ATP-dependent conjugation of reticulocyte proteins with the polypeptide required for protein degradation. Proc Natl Acad Sci U S A. 77:1365-8.

80) Hershko, A and Heller, H. 1985. Occurrence of a polyubiquitin structure in ubiquitin-protein conjugates. Biochem Biophys Res Commun. 128:1079-86.

81) Ziegenhagen, R, Goldberg, M, Rakutt, WD and Jennissen, HP. 1990. Multiple ubiquitination of calmodulin results in one polyubiquitin chain linked to calmodulin. FEBS Lett. 271:71-5.

82) Stang, E, Johannessen, LE, Knardal, SL and Madshus, IH. 2000. Polyubiquitination of the epidermal growth factor receptor occurs at the plasma membrane upon ligand-induced activation. J Biol Chem. 275:13940-7.

83) Grossman, SR, Deato, ME, Brignone, C, Chan, HM, Kung, AL, Tagami, H, Nakatani, Y and Livingston, DM. 2003. Polyubiquitination of p53 by a ubiquitin ligase activity of p300. Science. 300:342-4.

84) Nandi, D, Tahiliani, P, Kumar, A and Chandu, D. 2006. The ubiquitin-proteasome system. J Biosci. 31:137-55.

85) Reed, SI. 2006. The ubiquitin-proteasome pathway in cell cycle control. Results Probl Cell Differ. 42:147-81.

86) Huang, TT and D'Andrea, AD. 2006. Regulation of DNA repair by ubiquitylation. Nat Rev Mol Cell Biol. 7:323-34.

87) Haglund, K and Dikic, I. 2005. Ubiquitylation and cell signaling. Embo J. 24:3353-9.

88) Urbe, S. 2005. Ubiquitin and endocytic protein sorting. Essays Biochem. 41:81-98.

89) Mosesson, Y and Yarden, Y. 2006. Monoubiquitylation: a recurrent theme in membrane protein transport. Isr Med Assoc J. 8:233-7.

90) Staub, O and Rotin, D. 2006. Role of ubiquitylation in cellular membrane transport. Physiol Rev. 86:669-707.

91) Hurley, JH and Emr, SD. 2006. The ESCRT complexes: structure and mechanism of a membrane-trafficking network. Annu Rev Biophys Biomol Struct. 35:277-98.

92) Kerscher, O, Felberbaum, R and Hochstrasser, M. 2006. Modification of proteins by ubiquitin and ubiquitin-like proteins. Annu Rev Cell Dev Biol. 22:159-80.

93) Jackson, PK, Eldridge, AG, Freed, E, Furstenthal, L, Hsu, JY, Kaiser, BK and Reimann, JD. 2000. The lore of the RINGs: substrate recognition and catalysis by ubiquitin ligases. Trends Cell Biol. 10:429-39.

94) Buneeva, OA and Medvedev, AE. 2006. Ubiquitin-protein ligase parkin and its role in the development of Parkinson's disease. Biochemistry (Mosc). 71:851-60.

95) Meetei, AR, de Winter, JP, Medhurst, AL, Wallisch, M, Waisfisz, Q, van de Vrugt, HJ, Oostra, AB, Yan, Z, Ling, C, Bishop, CE, Hoatlin, ME, Joenje, H and Wang, W. 2003. A novel ubiquitin ligase is deficient in Fanconi anemia. Nat Genet. 35:165-70.

96) He, L, Lu, XY, Jolly, AF, Eldridge, AG, Watson, SJ, Jackson, PK, Barsh, GS and Gunn, TM. 2003. Spongiform degeneration in mahoganoid mutant mice. Science. 299:710-2.

97) Schindl, M, Gnant, M, Schoppmann, SF, Horvat, R and Birner, P. 2007. Overexpression of the human homologue for Caenorhabditis elegans cul-4 gene is associated with poor outcome in node-negative breast cancer. Anticancer Res. 27:949-52.

98) Honda, R, Tanaka, H and Yasuda, H. 1997. Oncoprotein MDM2 is a ubiquitin ligase E3 for tumor suppressor p53. FEBS Lett. 420:25-7.

99) Wang, X, Trotman, LC, Koppie, T, Alimonti, A, Chen, Z, Gao, Z, Wang, J, Erdjument-Bromage, H, Tempst, P, Cordon-Cardo, C, Pandolfi, PP and Jiang, X. 2007. NEDD4-1 is a proto-oncogenic ubiquitin ligase for PTEN. Cell. 128:129-39.

100) Ho, MS, Tsai, PI and Chien, CT. 2006. F-box proteins: the key to protein degradation. J Biomed Sci. 13:181-91.

101) Kee, Y and Huibregtse, JM. 2007. Regulation of catalytic activities of HECT ubiquitin ligases. Biochem Biophys Res Commun. 354:329-33.

102) Ogunjimi, AA, Briant, DJ, Pece-Barbara, N, Le Roy, C, Di Guglielmo, GM, Kavsak, P, Rasmussen, RK, Seet, BT, Sicheri, F and Wrana, JL. 2005. Regulation of Smurf2 ubiquitin ligase activity by anchoring the E2 to the HECT domain. Mol Cell. 19:297-308.

103) Huang, L, Kinnucan, E, Wang, G, Beaudenon, S, Howley, PM, Huibregtse, JM and Pavletich, NP. 1999. Structure of an E6AP-UbcH7 complex: insights into ubiquitination by the E2-E3 enzyme cascade. Science. 286:1321-6.

104) Eletr, ZM, Huang, DT, Duda, DM, Schulman, BA and Kuhlman, B. 2005. E2 conjugating enzymes must disengage from their E1 enzymes before E3-dependent ubiquitin and ubiquitin-like transfer. Nat Struct Mol Biol. 12:933-4.

105) Bartee, E, Mansouri, M, Hovey Nerenberg, BT, Gouveia, K and Fruh, K. 2004. Downregulation of major histocompatibility complex class I by human ubiquitin ligases related to viral immune evasion proteins. J Virol. 78:1109-20.

106) Huang, J, Huang, Q, Zhou, X, Shen, MM, Yen, A, Yu, SX, Dong, G, Qu, K, Huang, P, Anderson, EM, Daniel-Issakani, S, Buller, RM, Payan, DG and Lu, HH. 2004. The poxvirus p28 virulence factor is an E3 ubiquitin ligase. J Biol Chem. 279:54110-6.

107) Collin, N, Guerin, JL, Drexler, I, Blanie, S, Gelfi, J, Boullier, S, Foucras, G, Sutter, G and Messud-Petit, F. 2005. The poxviral scrapin MV-LAP requires a myxoma viral infection context to efficiently downregulate MHC-I molecules. Virology. 343:171-8.

108) Lehner, PJ, Hoer, S, Dodd, R and Duncan, LM. 2005. Downregulation of cell surface receptors by the K3 family of viral and cellular ubiquitin E3 ligases. Immunol Rev. 207:112-25.

109) Holzerlandt, R, Orengo, C, Kellam, P and Alba, MM. 2002. Identification of new herpesvirus gene homologs in the human genome. Genome Res. 12:1739-48.

110) Nicholas, J, Ruvolo, V, Zong, J, Ciufo, D, Guo, HG, Reitz, MS and Hayward, GS. 1997. A single 13-kilobase divergent locus in the Kaposi sarcoma-associated herpesvirus (human herpesvirus 8) genome contains nine open reading frames that are homologous to or related to cellular proteins. J Virol. 71:1963-74.

111) Afonso, CL, Tulman, ER, Lu, Z, Zsak, L, Kutish, GF and Rock, DL. 2000. The genome of fowlpox virus. J Virol. 74:3815-31.

112) Smith, CA, Hu, FQ, Smith, TD, Richards, CL, Smolak, P, Goodwin, RG and Pickup, DJ. 1996. Cowpox virus genome encodes a second soluble homologue of cellular TNF receptors, distinct from CrmB, that binds TNF but not LT alpha. Virology. 223:132-47.

113) Afonso, CL, Tulman, ER, Delhon, G, Lu, Z, Viljoen, GJ, Wallace, DB, Kutish, GF and Rock, DL. 2006. Genome of crocodilepox virus. J Virol. 80:4978-91.

114) Nerenberg, BT, Taylor, J, Bartee, E, Gouveia, K, Barry, M and Fruh, K. 2005. The poxviral RING protein p28 is a ubiquitin ligase that targets ubiquitin to viral replication factories. J Virol. 79:597-601.

115) Boutell, C, Sadis, S and Everett, RD. 2002. Herpes simplex virus type 1 immediate-early protein ICP0 and is isolated RING finger domain act as ubiquitin E3 ligases in vitro. J Virol. 76:841-50.

116) Chen, M and Gerlier, D. 2006. Viral hijacking of cellular ubiquitination pathways as an anti-innate immunity strategy. Viral Immunol. 19:349-62.

117) Senkevich, TG, Koonin, EV and Buller, RM. 1994. A poxvirus protein with a RING zinc finger motif is of crucial importance for virulence. Virology. 198:118-28.

118) Huang, K, Johnson, KD, Petcherski, AG, Vandergon, T, Mosser, EA, Copeland, NG, Jenkins, NA, Kimble, J and Bresnick, EH. 2000. A HECT domain ubiquitin ligase closely related to the mammalian protein WWP1 is essential for Caenorhabditis elegans embryogenesis. Gene. 252:137-45.

119) Tamai, KK and Shimoda, C. 2002. The novel HECT-type ubiquitin-protein ligase Pub2p shares partially overlapping function with Pub1p in Schizosaccharomyces pombe. J Cell Sci. 115:1847-57.

120) Mitsui, K, Nakanishi, M, Ohtsuka, S, Norwood, TH, Okabayashi, K, Miyamoto, C, Tanaka, K, Yoshimura, A and Ohtsubo, M. 1999. A novel human gene encoding HECT domain and RCC1-like repeats interacts with cyclins and is potentially regulated by the tumor suppressor proteins. Biochem Biophys Res Commun. 266:115-22.

121) Rossi, M, De Laurenzi, V, Munarriz, E, Green, DR, Liu, YC, Vousden, KH, Cesareni, G and Melino, G. 2005. The ubiquitin-protein ligase Itch regulates p73 stability. Embo J. 24:836-48.

122) Su, L, Lineberry, N, Huh, Y, Soares, L and Fathman, CG. 2006. A novel E3 ubiquitin ligase substrate screen identifies Rho guanine dissociation inhibitor as a substrate of gene related to anergy in lymphocytes. J Immunol. 177:7559-66.

123) Ayad, NG, Rankin, S, Ooi, D, Rape, M and Kirschner, MW. 2005. Identification of ubiquitin ligase substrates by in vitro expression cloning. Methods Enzymol. 399:404-14.

124) Van den Bergh, G and Arckens, L. 2005. Recent advances in 2D electrophoresis: an array of possibilities. Expert Rev Proteomics. 2:243-52.

125) Lilley, KS, Razzaq, A and Dupree, P. 2002. Two-dimensional gel electrophoresis: recent advances in sample preparation, detection and quantitation. Curr Opin Chem Biol. 6:46-50.

126) O'Farrell, PH. 1975. High resolution two-dimensional electrophoresis of proteins. J Biol Chem. 250:4007-21.

127) Afjehi-Sadat, L, Yang, JW, Pollak, A, Kim, DW, Choi, SY and Lubec, G. 2007. Structural and functional analysis of hypothetical proteins in mouse hippocampus from two-dimensional gel electrophoresis. J Proteome Res. 6:711-23.

128) Kim, Y, Nandakumar, MP and Marten, MR. 2007. Proteome map of Aspergillus nidulans during osmoadaptation. Fungal Genet Biol.

129) Jiang, X, Zhang, W, Gao, F, Huang, Y, Lv, C and Wang, H. 2006. Comparison of the proteome of isoniazid-resistant and -susceptible strains of Mycobacterium tuberculosis. Microb Drug Resist. 12:231-8.

130) Koksharova, OA, Klint, I and Rasmussen, U. 2006. [The first protein map of Synechococcus sp. strain PCC 7942]. Mikrobiologiia. 75:765-74.

131) Lei, Z, Elmer, AM, Watson, BS, Dixon, RA, Mendes, PJ and Sumner, LW. 2005. A two-dimensional electrophoresis proteomic reference map and systematic identification of 1367 proteins from a cell suspension culture of the model legume Medicago truncatula. Mol Cell Proteomics. 4:1812-25.

132) Jensen, ON. 2004. Modification-specific proteomics: characterization of post-translational modifications by mass spectrometry. Curr Opin Chem Biol. 8:33-41.

133) Chaudhary, A, Pechan, T and Willett, KL. 2007. Differential protein expression of peroxiredoxin I and II by benzo(a)pyrene and quercetin treatment in 22Rv1 and PrEC prostate cell lines. Toxicol Appl Pharmacol.

134) Rassmann, A, Henke, A, Zobawa, M, Carlsohn, M, Saluz, HP, Grabley, S, Lottspeich, F and Munder, T. 2006. Proteome alterations in human host cells infected with coxsackievirus B3. J Gen Virol. 87:2631-8.

135) Fang, C, Yi, Z, Liu, F, Lan, S, Wang, J, Lu, H, Yang, P and Yuan, Z. 2006. Proteome analysis of human liver carcinoma Huh7 cells harboring hepatitis C virus subgenomic replicon. Proteomics. 6:519-27.

136) Recktenwald, CV, Mendler, S, Lichtenfels, R, Kellner, R and Seliger, B. 2007. Influence of Ki-ras-driven oncogenic transformation on the protein network of murine fibroblasts. Proteomics. 7:385-98.

137) Melle, C, Ernst, G, Scheibner, O, Kaufmann, R, Schimmel, B, Bleul, A, Settmacher, U, Hommann, M, Claussen, U and von Eggeling, F. 2007. Identification of specific protein markers in microdissected hepatocellular carcinoma. J Proteome Res. 6:306-15.

138) Wang, X, Ni, W, Ge, X, Zhang, J, Ma, H and Cao, K. 2006. Proteomic identification of potential target proteins regulated by an ASK1-mediated proteolysis pathway. Cell Res. 16:489-98.

139) Reiter, LT, Seagroves, TN, Bowers, M and Bier, E. 2006. Expression of the Rho-GEF Pbl/ECT2 is regulated by the UBE3A E3 ubiquitin ligase. Hum Mol Genet. 15:2825-35.

140) Chang, TL, Cubillos, FF, Kakhniashvili, DG and Goodman, SR. 2004. Ankyrin is a target of spectrin's E2/E3 ubiquitin-conjugating/ligating activity. Cell Mol Biol (Noisy-le-grand). 50:59-66.

141) Stephen, AG, Trausch-Azar, JS, Ciechanover, A and Schwartz, AL. 1996. The ubiquitin-activating enzyme E1 is phosphorylated and localized to the nucleus in a cell cycle-dependent manner. J Biol Chem. 271:15608-14.

142) Gao, M, Labuda, T, Xia, Y, Gallagher, E, Fang, D, Liu, YC and Karin, M. 2004. Jun turnover is controlled through JNK-dependent phosphorylation of the E3 ligase Itch. Science. 306:271-5.

143) Kamel, A and Prakash, C. 2006. High performance liquid chromatography/atmospheric pressure ionization/tandem mass spectrometry (HPLC/API/MS/MS) in drug metabolism and toxicology. Curr Drug Metab. 7:837-52.

144) Jemal, M and Xia, YQ. 2006. LC-MS Development strategies for quantitative bioanalysis. Curr Drug Metab. 7:491-502.

145) Evans, CR and Jorgenson, JW. 2004. Multidimensional LC-LC and LC-CE for high-resolution separations of biological molecules. Anal Bioanal Chem. 378:1952-61.

146) Nagele, E, Vollmer, M, Horth, P and Vad, C. 2004. 2D-LC/MS techniques for the identification of proteins in highly complex mixtures. Expert Rev Proteomics. 1:37-46.

147) Yates, JR, 3rd, Eng, JK, McCormack, AL and Schieltz, D. 1995. Method to correlate tandem mass spectra of modified peptides to amino acid sequences in the protein database. Anal Chem. 67:1426-36.

148) Nesvizhskii, AI. 2006. Protein identification by tandem mass spectrometry and sequence database searching. Methods Mol Biol. 367:87-120.

149) Yoo, C, Patwa, TH, Kreunin, P, Miller, FR, Huber, CG, Nesvizhskii, AI and Lubman, DM. 2007. Comprehensive analysis of proteins of pH fractionated samples using monolithic LC/MS/MS, intact MW measurement and MALDI-QIT-TOF MS. J Mass Spectrom.

150) Metz, TO, Jacobs, JM, Gritsenko, MA, Fontes, G, Qian, WJ, Camp, DG, 2nd, Poitout, V and Smith, RD. 2006. Characterization of the human pancreatic islet proteome by two-dimensional LC/MS/MS. J Proteome Res. 5:3345-54.

151) Anderson, DC, Campbell, EL and Meeks, JC. 2006. A soluble 3D LC/MS/MS proteome of the filamentous cyanobacterium Nostoc punctiforme. J Proteome Res. 5:3096-104.

152) Vasilescu, J, Smith, JC, Ethier, M and Figeys, D. 2005. Proteomic analysis of ubiquitinated proteins from human MCF-7 breast cancer cells by immunoaffinity purification and mass spectrometry. J Proteome Res. 4:2192-200.

153) Matsumoto, M, Hatakeyama, S, Oyamada, K, Oda, Y, Nishimura, T and Nakayama, KI. 2005. Large-scale analysis of the human ubiquitin-related proteome. Proteomics. 5:4145-51.

154) Kirkpatrick, DS, Weldon, SF, Tsaprailis, G, Liebler, DC and Gandolfi, AJ. 2005. Proteomic identification of ubiquitinated proteins from human cells expressing His-tagged ubiquitin. Proteomics. 5:2104-11.

155) Ong, SE, Blagoev, B, Kratchmarova, I, Kristensen, DB, Steen, H, Pandey, A and Mann, M. 2002. Stable isotope labeling by amino acids in cell culture, SILAC, as a simple and accurate approach to expression proteomics. Mol Cell Proteomics. 1:376-86.

156) Gygi, SP, Rist, B, Gerber, SA, Turecek, F, Gelb, MH and Aebersold, R. 1999. Quantitative analysis of complex protein mixtures using isotope-coded affinity tags. Nat Biotechnol. 17:994-9.

157) Ross, PL, Huang, YN, Marchese, JN, Williamson, B, Parker, K, Hattan, S, Khainovski, N, Pillai, S, Dey, S, Daniels, S, Purkayastha, S, Juhasz, P, Martin, S, Bartlet-Jones, M, He, F, Jacobson, A and Pappin, DJ. 2004. Multiplexed protein quantitation in Saccharomyces cerevisiae using amine-reactive isobaric tagging reagents. Mol Cell Proteomics. 3:1154-69.

158) Ong, SE and Mann, M. 2005. Mass spectrometry-based proteomics turns quantitative. Nat Chem Biol. 1:252-62.

159) Han, DK, Eng, J, Zhou, H and Aebersold, R. 2001. Quantitative profiling of differentiation-induced microsomal proteins using isotope-coded affinity tags and mass spectrometry. Nat Biotechnol. 19:946-51.

160) Li, XJ, Zhang, H, Ranish, JA and Aebersold, R. 2003. Automated statistical analysis of protein abundance ratios from data generated by stable-isotope dilution and tandem mass spectrometry. Anal Chem. 75:6648-57.

161) Chiang, MC, Juo, CG, Chang, HH, Chen, HM, Yi, EC and Chern, Y. 2007. Systematic uncovering of multiple pathways underlying the pathology of Huntington's disease by an acid-cleavable isotope-coded affinity tag approach. Mol Cell Proteomics.

162) Chou, J, Choudhary, PK and Goodman, SR. 2006. Protein profiling of sickle cell versus control RBC core membrane skeletons by ICAT technology and tandem mass spectrometry. Cell Mol Biol Lett. 11:326-37.

163) Chen, R, Pan, S, Yi, EC, Donohoe, S, Bronner, MP, Potter, JD, Goodlett, DR, Aebersold, R and Brentnall, TA. 2006. Quantitative proteomic profiling of pancreatic cancer juice. Proteomics. 6:3871-9.

164) Pawlik, TM, Hawke, DH, Liu, Y, Krishnamurthy, S, Fritsche, H, Hunt, KK and Kuerer, HM. 2006. Proteomic analysis of nipple aspirate fluid from women with early-stage breast cancer using isotope-coded affinity tags and tandem mass spectrometry reveals differential expression of vitamin D binding protein. BMC Cancer. 6:68.

165) Leitner, A and Lindner, W. 2006. Chemistry meets proteomics: the use of chemical tagging reactions for MS-based proteomics. Proteomics. 6:5418-34.

166) Everley, PA, Krijgsveld, J, Zetter, BR and Gygi, SP. 2004. Quantitative cancer proteomics: stable isotope labeling with amino acids in cell culture (SILAC) as a tool for prostate cancer research. Mol Cell Proteomics. 3:729-35.

167) Kolkman, A, Slijper, M and Heck, AJ. 2005. Development and application of proteomics technologies in Saccharomyces cerevisiae. Trends Biotechnol. 23:598-604.

168) Gruhler, A, Schulze, WX, Matthiesen, R, Mann, M and Jensen, ON. 2005. Stable isotope labeling of Arabidopsis thaliana cells and quantitative proteomics by mass spectrometry. Mol Cell Proteomics. 4:1697-709.

169) Smith, RD. 2000. Probing proteomes--seeing the whole picture? Nat Biotechnol. 18:1041-2.

170) Gygi, SP, Corthals, GL, Zhang, Y, Rochon, Y and Aebersold, R. 2000. Evaluation of two-dimensional gel electrophoresis-based proteome analysis technology. Proc Natl Acad Sci U S A. 97:9390-5.

171) Rabilloud, T, Vuillard, L, Gilly, C and Lawrence, JJ. 1994. Silver-staining of proteins in polyacrylamide gels: a general overview. Cell Mol Biol (Noisy-le-grand). 40:57-75.

172) Piubelli, C, Fiorini, M, Zanusso, G, Milli, A, Fasoli, E, Monaco, S and Righetti, PG. 2006. Searching for markers of Creutzfeldt-Jakob disease in cerebrospinal fluid by two-dimensional mapping. Proteomics. 6 Suppl 1:S256-61.

173) Hershko, A and Ciechanover, A. 1998. The ubiquitin system. Annu Rev Biochem. 67:425-79.

174) Hicke, L. 1997. Ubiquitin-dependent internalization and down-regulation of plasma membrane proteins. Faseb J. 11:1215-26.

175) Joazeiro, CA and Weissman, AM. 2000. RING finger proteins: mediators of ubiquitin ligase activity. Cell. 102:549-52.

176) Aasland, R, Gibson, TJ and Stewart, AF. 1995. The PHD finger: implications for chromatin-mediated transcriptional regulation. Trends Biochem Sci. 20:56-9.

177) Saha, V, Chaplin, T, Gregorini, A, Ayton, P and Young, BD. 1995. The leukemia-associated-protein (LAP) domain, a cysteine-rich motif, is present in a wide range of proteins, including MLL, AF10, and MLLT6 proteins. Proc Natl Acad Sci U S A. 92:9737-41.

178) Swanson, R, Locher, M and Hochstrasser, M. 2001. A conserved ubiquitin ligase of the nuclear envelope/endoplasmic reticulum that functions in both ER-associated and Matalpha2 repressor degradation. Genes Dev. 15:2660-74.

179) Yu, YY, Harris, MR, Lybarger, L, Kimpler, LA, Myers, NB, Virgin, HWt and Hansen, TH. 2002. Physical association of the K3 protein of gamma-2 herpesvirus 68 with major histocompatibility complex class I molecules with impaired peptide and beta(2)-microglobulin assembly. J Virol. 76:2796-803.

180) McFadden, G and Murphy, PM. 2000. Host-related immunomodulators encoded by poxviruses and herpesviruses. Curr Opin Microbiol. 3:371-8.

181) Goto, E, Ishido, S, Sato, Y, Ohgimoto, S, Ohgimoto, K, Nagano-Fujii, M and Hotta, H. 2003. c-MIR, a human E3 ubiquitin ligase, is a functional homolog of herpesvirus proteins MIR1 and MIR2 and has similar activity. J Biol Chem. 278:14657-68.

182) Bishop, N and Woodman, P. 2000. ATPase-defective mammalian VPS4 localizes to aberrant endosomes and impairs cholesterol trafficking. Mol Biol Cell. 11:227-39.

183) Gossen, M and Bujard, H. 1992. Tight control of gene expression in mammalian cells by tetracycline-responsive promoters. Proc Natl Acad Sci U S A. 89:5547-51.

184) Babst, M, Katzmann, DJ, Estepa-Sabal, EJ, Meerloo, T and Emr, SD. 2002. Escrt-III: an endosome-associated heterooligomeric protein complex required for mvb sorting. Dev Cell. 3:271-82.

185) Haglund, K, Sigismund, S, Polo, S, Szymkiewicz, I, Di Fiore, PP and Dikic, I. 2003. Multiple monoubiquitination of RTKs is sufficient for their endocytosis and degradation. Nat Cell Biol. 5:461-6.

186) Bordallo, J, Plemper, RK, Finger, A and Wolf, DH. 1998. Der3p/Hrd1p is required for endoplasmic reticulum-associated degradation of misfolded lumenal and integral membrane proteins. Mol Biol Cell. 9:209-22.

187) Gardner, RG, Swarbrick, GM, Bays, NW, Cronin, SR, Wilhovsky, S, Seelig, L, Kim, C and Hampton, RY. 2000. Endoplasmic reticulum degradation requires lumen to cytosol signaling. Transmembrane control of Hrd1p by Hrd3p. J Cell Biol. 151:69-82.

188) Fang, S, Ferrone, M, Yang, C, Jensen, JP, Tiwari, S and Weissman, AM. 2001. The tumor autocrine motility factor receptor, gp78, is a ubiquitin protein ligase implicated in degradation from the endoplasmic reticulum. Proc Natl Acad Sci U S A. 98:14422-7.

189) Biederer, T, Volkwein, C and Sommer, T. 1997. Role of Cue1p in ubiquitination and degradation at the ER surface. Science. 278:1806-9.

190) Sommer, T and Jentsch, S. 1993. A protein translocation defect linked to ubiquitin conjugation at the endoplasmic reticulum. Nature. 365:176-9.

191) Bartee, E, McCormack, A and Fruh, K. 2006. Quantitative membrane proteomics reveals new cellular targets of viral immune modulators. PLoS Pathog. 2:e107.

192) Nakamura, N, Fukuda, H, Kato, A and Hirose, S. 2005. MARCH-II is a syntaxin-6-binding protein involved in endosomal trafficking. Mol Biol Cell. 16:1696-710.

193) Hoer, S, Smith, L and Lehner, PJ. 2007. MARCH-IX mediates ubiquitination and downregulation of ICAM-1. FEBS Lett. 581:45-51.

194) Ohmura-Hoshino, M, Matsuki, Y, Aoki, M, Goto, E, Mito, M, Uematsu, M, Kakiuchi, T, Hotta, H and Ishido, S. 2006. Inhibition of MHC class II expression and immune responses by c-MIR. J Immunol. 177:341-54.

195) Shan, YX, Liu, TJ, Su, HF, Samsamshariat, A, Mestril, R and Wang, PH. 2003. Hsp10 and Hsp60 modulate Bcl-2 family and mitochondria apoptosis signaling induced by doxorubicin in cardiac muscle cells. J Mol Cell Cardiol. 35:1135-43.

196) Xanthoudakis, S, Roy, S, Rasper, D, Hennessey, T, Aubin, Y, Cassady, R, Tawa, P, Ruel, R, Rosen, A and Nicholson, DW. 1999. Hsp60 accelerates the maturation of pro-caspase-3 by upstream activator proteases during apoptosis. Embo J. 18:2049-56.

197) Link, AJ, Eng, J, Schieltz, DM, Carmack, E, Mize, GJ, Morris, DR, Garvik, BM and Yates, JR, 3rd. 1999. Direct analysis of protein complexes using mass spectrometry. Nat Biotechnol. 17:676-82.

198) Keller, A, Nesvizhskii, AI, Kolker, E and Aebersold, R. 2002. Empirical statistical model to estimate the accuracy of peptide identifications made by MS/MS and database search. Anal Chem. 74:5383-92.

199) Wasilenko, ST, Meyers, AF, Vander Helm, K and Barry, M. 2001. Vaccinia virus infection disarms the mitochondrion-mediated pathway of the apoptotic cascade by modulating the permeability transition pore. J Virol. 75:11437-48.

200) Gerner, C, Frohwein, U, Gotzmann, J, Bayer, E, Gelbmann, D, Bursch, W and Schulte-Hermann, R. 2000. The Fas-induced apoptosis analyzed by high throughput proteome analysis. J Biol Chem. 275:39018-26.

201) Madesh, M, Antonsson, B, Srinivasula, SM, Alnemri, ES and Hajnoczky, G. 2002. Rapid kinetics of tBid-induced cytochrome c and Smac/DIABLO release and mitochondrial depolarization. J Biol Chem. 277:5651-9.

202) Everett, H, Barry, M, Lee, SF, Sun, X, Graham, K, Stone, J, Bleackley, RC and McFadden, G. 2000. M11L: a novel mitochondria-localized protein of myxoma virus that blocks apoptosis of infected leukocytes. J Exp Med. 191:1487-98.

203) Everett, H, Barry, M, Sun, X, Lee, SF, Frantz, C, Berthiaume, LG, McFadden, G and Bleackley, RC. 2002. The myxoma poxvirus protein, M11L, prevents apoptosis by direct interaction with the mitochondrial permeability transition pore. J Exp Med. 196:1127-39.

204) Rizzuto, R, Pinton, P, Carrington, W, Fay, FS, Fogarty, KE, Lifshitz, LM, Tuft, RA and Pozzan, T. 1998. Close contacts with the endoplasmic reticulum as determinants of mitochondrial Ca2+ responses. Science. 280:1763-6.

205) Gupta, S and Knowlton, AA. 2005. HSP60, Bax, apoptosis and the heart. J Cell Mol Med. 9:51-8.

206) Scaffidi, C, Fulda, S, Srinivasan, A, Friesen, C, Li, F, Tomaselli, KJ, Debatin, KM, Krammer, PH and Peter, ME. 1998. Two CD95 (APO-1/Fas) signaling pathways. Embo J. 17:1675-87.

207) Scaffidi, C, Schmitz, I, Zha, J, Korsmeyer, SJ, Krammer, PH and Peter, ME. 1999. Differential modulation of apoptosis sensitivity in CD95 type I and type II cells. J Biol Chem. 274:22532-8.

208) Johnson, DC and Hegde, NR. 2002. Inhibition of the MHC class II antigen presentation pathway by human cytomegalovirus. Curr Top Microbiol Immunol. 269:101-15.

209) Ziegler, H, Muranyi, W, Burgert, HG, Kremmer, E and Koszinowski, UH. 2000. The luminal part of the murine cytomegalovirus glycoprotein gp40 catalyzes the retention of MHC class I molecules. Embo J. 19:870-81.

210) Lodoen, M, Ogasawara, K, Hamerman, JA, Arase, H, Houchins, JP, Mocarski, ES and Lanier, LL. 2003. NKG2D-mediated natural killer cell protection against cytomegalovirus is impaired by viral gp40 modulation of retinoic acid early inducible 1 gene molecules. J Exp Med. 197:1245-53.

211) Kerkau, T, Bacik, I, Bennink, JR, Yewdell, JW, Hunig, T, Schimpl, A and Schubert, U. 1997. The human immunodeficiency virus type 1 (HIV-1) Vpu protein interferes with an early step in the biosynthesis of major histocompatibility complex (MHC) class I molecules. J Exp Med. 185:1295-305.

212) Willey, RL, Maldarelli, F, Martin, MA and Strebel, K. 1992. Human immunodeficiency virus type 1 Vpu protein induces rapid degradation of CD4. J Virol. 66:7193-200.

213) Garcia, JV and Miller, AD. 1992. Downregulation of cell surface CD4 by nef. Res Virol. 143:52-5.

214) Collins, KL, Chen, BK, Kalams, SA, Walker, BD and Baltimore, D. 1998. HIV-1 Nef protein protects infected primary cells against killing by cytotoxic T lymphocytes. Nature. 391:397-401.

215) Ong, SE, Foster, LJ and Mann, M. 2003. Mass spectrometric-based approaches in quantitative proteomics. Methods. 29:124-30.

216) Yates, JR, 3rd, Eng, JK and McCormack, AL. 1995. Mining genomes: correlating tandem mass spectra of modified and unmodified peptides to sequences in nucleotide databases. Anal Chem. 67:3202-10.

217) Durr, E, Yu, J, Krasinska, KM, Carver, LA, Yates, JR, Testa, JE, Oh, P and Schnitzer, JE. 2004. Direct proteomic mapping of the lung microvascular endothelial cell surface in vivo and in cell culture. Nat Biotechnol. 22:985-92.

218) Ishikawa, J, Kaisho, T, Tomizawa, H, Lee, BO, Kobune, Y, Inazawa, J, Oritani, K, Itoh, M, Ochi, T, Ishihara, K and et al. 1995. Molecular cloning and chromosomal mapping of a bone marrow stromal cell surface gene, BST2, that may be involved in pre-B-cell growth. Genomics. 26:527-34.

219) Ohtomo, T, Sugamata, Y, Ozaki, Y, Ono, K, Yoshimura, Y, Kawai, S, Koishihara, Y, Ozaki, S, Kosaka, M, Hirano, T and Tsuchiya, M. 1999. Molecular Cloning and Characterization of a Surface Antigen Preferentially Overexpressed on Multiple Myeloma Cells. Biochem. Biophys. Res. Commun. 258:583-591.

220) Kupzig, S, Korolchuk, V, Rollason, R, Sugden, A, Wilde, A and Banting, G. 2003. Bst-2/HM1.24 is a raft-associated apical membrane protein with an unusual topology. Traffic. 4:694-709.

221) Salaun, C, James, DJ, Greaves, J and Chamberlain, LH. 2004. Plasma membrane targeting of exocytic SNARE proteins. Biochim Biophys Acta. 1693:81-9.

222) Fukuda, H, Nakamura, N and Hirose, S. 2006. MARCH-III Is a novel component of endosomes with properties similar to those of MARCH-II. J Biochem (Tokyo). 139:137-45.

223) Bowen, MA, Bajorath, J, D'Egidio, M, Whitney, GS, Palmer, D, Kobarg, J, Starling, GC, Siadak, AW and Aruffo, A. 1997. Characterization of mouse ALCAM (CD166): the CD6-binding domain is conserved in different homologs and mediates cross-species binding. Eur J Immunol. 27:1469-78.

224) Gimferrer, I, Calvo, M, Mittelbrunn, M, Farnos, M, Sarrias, MR, Enrich, C, Vives, J, Sanchez-Madrid, F and Lozano, F. 2004. Relevance of CD6-mediated interactions in T cell activation and proliferation. J Immunol. 173:2262-70.

225) Hassan, NJ, Barclay, AN and Brown, MH. 2004. Frontline: Optimal T cell activation requires the engagement of CD6 and CD166. Eur J Immunol. 34:930-40.

226) Zimmerman, AW, Joosten, B, Torensma, R, Parnes, JR, van Leeuwen, FN and Figdor, CG. 2006. Long-term engagement of CD6 and ALCAM is essential for T-cell proliferation induced by dendritic cells. Blood. 107:3212-20.

227) Moses, AV, Fish, KN, Ruhl, R, Smith, PP, Strussenberg, JG, Zhu, L, Chandran, B and Nelson, JA. 1999. Long-term infection and transformation of dermal microvascular endothelial cells by human herpesvirus 8. J. Virol. 73:6892-6902.

228) Garrus, JE, von Schwedler, UK, Pornillos, OW, Morham, SG, Zavitz, KH, Wang, HE, Wettstein, DA, Stray, KM, Cote, M, Rich, RL, Myszka, DG and Sundquist, WI.

2001. Tsg101 and the vacuolar protein sorting pathway are essential for HIV-1 budding. Cell. 107:55-65.

229) Loyet, KM, Ouyang, W, Eaton, DL and Stults, JT. 2005. Proteomic profiling of surface proteins on Th1 and Th2 cells. J Proteome Res. 4:400-9.

230) Gronborg, M, Kristiansen, TZ, Iwahori, A, Chang, R, Reddy, R, Sato, N, Molina, H, Jensen, ON, Hruban, RH, Goggins, MG, Maitra, A and Pandey, A. 2006. Biomarker discovery from pancreatic cancer secretome using a differential proteomic approach. Mol Cell Proteomics. 5:157-71.

231) Blagoev, B, Kratchmarova, I, Ong, SE, Nielsen, M, Foster, LJ and Mann, M. 2003. A proteomics strategy to elucidate functional protein-protein interactions applied to EGF signaling. Nat Biotechnol. 21:315-8.

232) Neher, SB, Villen, J, Oakes, EC, Bakalarski, CE, Sauer, RT, Gygi, SP and Baker, TA. 2006. Proteomic Profiling of ClpXP Substrates after DNA Damage Reveals Extensive Instability within SOS Regulon. Mol Cell. 22:193-204.

233) Hitchcock, AL, Auld, K, Gygi, SP and Silver, PA. 2003. A subset of membrane-associated proteins is ubiquitinated in response to mutations in the endoplasmic reticulum degradation machinery. Proc Natl Acad Sci U S A. 100:12735-40.

234) Peng, J, Schwartz, D, Elias, JE, Thoreen, CC, Cheng, D, Marsischky, G, Roelofs, J, Finley, D and Gygi, SP. 2003. A proteomics approach to understanding protein ubiquitination. Nat Biotechnol. 21:921-6.

235) Saito, T, Okada, S, Yamada, E, Ohshima, K, Shimizu, H, Shimomura, K, Sato, M, Pessin, JE and Mori, M. 2003. Syntaxin 4 and Synip (syntaxin 4 interacting protein) regulate insulin secretion in the pancreatic beta HC-9 cell. J Biol Chem. 278:36718-25.

236) Chin, LS, Vavalle, JP and Li, L. 2002. Staring, a novel E3 ubiquitin-protein ligase that targets syntaxin 1 for degradation. J Biol Chem. 277:35071-9.

237) Lin, J, Miller, MJ and Shaw, AS. 2005. The c-SMAC: sorting it all out (or in). J Cell Biol. 170:177-82.

238) Gangemi, RM, Swack, JA, Gaviria, DM and Romain, PL. 1989. Anti-T12, an anti-CD6 monoclonal antibody, can activate human T lymphocytes. J Immunol. 143:2439-47.

239) Matsuki, Y, Ohmura-Hoshino, M, Goto, E, Aoki, M, Mito-Yoshida, M, Uematsu, M, Hasegawa, T, Koseki, H, Ohara, O, Nakayama, M, Toyooka, K, Matsuoka, K, Hotta, H, Yamamoto, A and Ishido, S. 2007. Novel regulation of MHC class II function in B cells. Embo J.

240) Ohmura-Hoshino, M, Goto, E, Matsuki, Y, Aoki, M, Mito, M, Uematsu, M, Hotta, H and Ishido, S. 2006. A novel family of membrane-bound E3 ubiquitin ligases. J Biochem (Tokyo). 140:147-54.

241) Tirosh, B, Iwakoshi, NN, Lilley, BN, Lee, AH, Glimcher, LH and Ploegh, HL. 2005. Human cytomegalovirus protein US11 provokes an unfolded protein response that may facilitate the degradation of class I major histocompatibility complex products. J Virol. 79:2768-79.

242) Aruffo, A, Stamenkovic, I, Melnick, M, Underhill, CB and Seed, B. 1990. CD44 is the principal cell surface receptor for hyaluronate. Cell. 61:1303-13.

243) Rubinstein, E, Le Naour, F, Lagaudriere-Gesbert, C, Billard, M, Conjeaud, H and Boucheix, C. 1996. CD9, CD63, CD81, and CD82 are components of a surface tetraspan network connected to HLA-DR and VLA integrins. Eur J Immunol. 26:2657-65.

244) Rossol, S. 1999. [Identification of CD81 protein as HCV receptor--relevance for pathogenesis and cell tropism?]. Z Gastroenterol. 37:1209-11.

245) Abache, T, Le Naour, F, Planchon, S, Harper, F, Boucheix, C and Rubinstein, E. 2007. The transferrin receptor and the tetraspanin web molecules CD9, CD81, and CD9P-1 are differentially sorted into exosomes after TPA treatment of K562 cells. J Cell Biochem.

246) Radford, KJ, Thorne, RF and Hersey, P. 1996. CD63 associates with transmembrane 4 superfamily members, CD9 and CD81, and with beta 1 integrins in human melanoma. Biochem Biophys Res Commun. 222:13-8.

247) Annaert, WG, Becker, B, Kistner, U, Reth, M and Jahn, R. 1997. Export of cellubrevin from the endoplasmic reticulum is controlled by BAP31. J Cell Biol. 139:1397-410.

248) Lambert, G, Becker, B, Schreiber, R, Boucherot, A, Reth, M and Kunzelmann, K. 2001. Control of cystic fibrosis transmembrane conductance regulator expression by BAP31. J Biol Chem. 276:20340-5.

249) Schamel, WW, Kuppig, S, Becker, B, Gimborn, K, Hauri, HP and Reth, M. 2003. A high-molecular-weight complex of membrane proteins BAP29/BAP31 is involved in the retention of membrane-bound IgD in the endoplasmic reticulum. Proc Natl Acad Sci U S A. 100:9861-6.

250) Zen, K, Utech, M, Liu, Y, Soto, I, Nusrat, A and Parkos, CA. 2004. Association of BAP31 with CD11b/CD18. Potential role in intracellular trafficking of CD11b/CD18 in neutrophils. J Biol Chem. 279:44924-30.

251) Bell, AW, Ward, MA, Blackstock, WP, Freeman, HN, Choudhary, JS, Lewis, AP, Chotai, D, Fazel, A, Gushue, JN, Paiement, J, Palcy, S, Chevet, E, Lafreniere-Roula, M, Solari, R, Thomas, DY, Rowley, A and Bergeron, JJ. 2001. Proteomics characterization of abundant Golgi membrane proteins. J Biol Chem. 276:5152-65.

252) de la Hera, A, Acevedo, A, Marston, W and Sanchez-Madrid, F. 1989. Function of CD44(Pgp-1) homing receptor in human T cell precursors. Int Immunol. 1:598-604.

253) Liu, JN, Bi, GF, Wen, PE, Yang, WH, Ren, X, Tang, TH, Xie, C, Dong, W and Jiang, GS. 2007. Down-Regulation of CD44 Contributes to the Differentiation of HL-60 Cells Induced by ATRA or HMBA. Cell Mol Immunol. 4:59-63.

254) Ibrahim, EM, Stewart, RL, Corke, K, Blackett, AD, Tidy, JA and Wells, M. 2006. Upregulation of CD44 expression by interleukins 1, 4, and 13, transforming growth factor-beta1, estrogen, and progestogen in human cervical adenocarcinoma cell lines. Int J Gynecol Cancer. 16:1631-42.

255) Sallusto, F and Lanzavecchia, A. 1994. Efficient presentation of soluble antigen by cultured human dendritic cells is maintained by granulocyte/macrophage colony-stimulating factor plus interleukin 4 and downregulated by tumor necrosis factor alpha. J Exp Med. 179:1109-18.

256) Haegel-Kronenberger, H, de la Salle, H, Bohbot, A, Oberling, F, Cazenave, JP and Hanau, D. 1998. Adhesive and/or signaling functions of CD44 isoforms in human dendritic cells. J Immunol. 161:3902-11.

257) Thankamony, SP and Knudson, W. 2006. Acylation of CD44 and its association with lipid rafts are required for receptor and hyaluronan endocytosis. J Biol Chem. 281:34601-9.

258) Szollosi, J, Horejsi, V, Bene, L, Angelisova, P and Damjanovich, S. 1996. Supramolecular complexes of MHC class I, MHC class II, CD20, and tetraspan molecules (CD53, CD81, and CD82) at the surface of a B cell line JY. J Immunol. 157:2939-46.

259) Angelisova, P, Hilgert, I and Horejsi, V. 1994. Association of four antigens of the tetraspans family (CD37, CD53, TAPA-1, and R2/C33) with MHC class II glycoproteins. Immunogenetics. 39:249-56.

260) Shoham, T, Rajapaksa, R, Boucheix, C, Rubinstein, E, Poe, JC, Tedder, TF and Levy, S. 2003. The tetraspanin CD81 regulates the expression of CD19 during B cell development in a postendoplasmic reticulum compartment. J Immunol. 171:4062-72.

261) Cherukuri, A, Shoham, T, Sohn, HW, Levy, S, Brooks, S, Carter, R and Pierce, SK. 2004. The tetraspanin CD81 is necessary for partitioning of coligated CD19/CD21-B cell antigen receptor complexes into signaling-active lipid rafts. J Immunol. 172:370-80.

262) Zhang, J, Randall, G, Higginbottom, A, Monk, P, Rice, CM and McKeating, JA. 2004. CD81 is required for hepatitis C virus glycoprotein-mediated viral infection. J Virol. 78:1448-55.

263) Akazawa, D, Date, T, Morikawa, K, Murayama, A, Miyamoto, M, Kaga, M, Barth, H, Baumert, TF, Dubuisson, J and Wakita, T. 2007. Cd81 Expression Is Important for Heterogeneous Hcv Permissiveness of Huh7 Cell Clones. J Virol.

264) Gordon-Alonso, M, Yanez-Mo, M, Barreiro, O, Alvarez, S, Munoz-Fernandez, MA, Valenzuela-Fernandez, A and Sanchez-Madrid, F. 2006. Tetraspanins CD9 and CD81 modulate HIV-1-induced membrane fusion. J Immunol. 177:5129-37.

265) Tardif, MR and Tremblay, MJ. 2005. Tetraspanin CD81 provides a costimulatory signal resulting in increased human immunodeficiency virus type 1 gene expression in primary CD4+ T lymphocytes through NF-kappaB, NFAT, and AP-1 transduction pathways. J Virol. 79:4316-28.

266) Szczesna-Skorupa, E and Kemper, B. 2006. BAP31 is involved in the retention of cytochrome P450 2C2 in the endoplasmic reticulum. J Biol Chem. 281:4142-8.

267) Ladasky, JJ, Boyle, S, Seth, M, Li, H, Pentcheva, T, Abe, F, Steinberg, SJ and Edidin, M. 2006. Bap31 enhances the endoplasmic reticulum export and quality control of human class I MHC molecules. J Immunol. 177:6172-81.

268) Stojanovic, M, Germain, M, Nguyen, M and Shore, GC. 2005. BAP31 and its caspase cleavage product regulate cell surface expression of tetraspanins and integrin-mediated cell survival. J Biol Chem. 280:30018-24.

269) Nakamura, N, Kimura, Y, Tokuda, M, Honda, S and Hirose, S. 2006. MARCH-V is a novel mitofusin 2- and Drp1-binding protein able to change mitochondrial morphology. EMBO Rep. 7:1019-22.

270) Shin, JS, Ebersold, M, Pypaert, M, Delamarre, L, Hartley, A and Mellman, I. 2006. Surface expression of MHC class II in dendritic cells is controlled by regulated ubiquitination. Nature. 444:115-8.

271) Pierre, P, Turley, SJ, Meltzer, J, Mirza, A, Steinman, R and Mellman, I. 1997. Localization and intracellular transport of MHC class II molecules in bone marrow-derived dendritic cells. Adv Exp Med Biol. 417:179-82.

272) Winzler, C, Rovere, P, Rescigno, M, Granucci, F, Penna, G, Adorini, L, Zimmermann, VS, Davoust, J and Ricciardi-Castagnoli, P. 1997. Maturation stages of

mouse dendritic cells in growth factor-dependent long-term cultures. J Exp Med. 185:317-28.

273) Pober, JS, Guild, BC and Strominger, JL. 1978. Phosphorylation in vivo and in vitro of human histocompatibility antigens (HLA-A and HLA-B) in the carboxy-terminal intracellular domain. Proc Natl Acad Sci U S A. 75:6002-6.

274) Haynes, BF, Telen, MJ, Hale, LP and Denning, SM. 1989. CD44--a molecule involved in leukocyte adherence and T-cell activation. Immunol Today. 10:423-8.

275) Shimizu, Y, Van Seventer, GA, Siraganian, R, Wahl, L and Shaw, S. 1989. Dual role of the CD44 molecule in T cell adhesion and activation. J Immunol. 143:2457-63.

276) Koppelman, B, Neefjes, JJ, de Vries, JE and de Waal Malefyt, R. 1997. Interleukin-10 down-regulates MHC class II alphabeta peptide complexes at the plasma membrane of monocytes by affecting arrival and recycling. Immunity. 7:861-71.

277) Chan, A, Baird, M, Mercer, AA and Fleming, SB. 2006. Maturation and function of human dendritic cells are inhibited by orf virus-encoded interleukin-10. J Gen Virol. 87:3177-81.

278) Termeer, C, Johannsen, H, Braun, T, Renkl, A, Ahrens, T, Denfeld, RW, Lappin, MB, Weiss, JM and Simon, JC. 2001. The role of CD44 during CD40 ligand-induced dendritic cell clustering and maturation. J Leukoc Biol. 70:715-22.

279) Khan, SA, Cook, AC, Kappil, M, Gunthert, U, Chambers, AF, Tuck, AB and Denhardt, DT. 2005. Enhanced cell surface CD44 variant (v6, v9) expression by osteopontin in breast cancer epithelial cells facilitates tumor cell migration: novel post-transcriptional, post-translational regulation. Clin Exp Metastasis. 22:663-73.

280) Marroquin, CE, Downey, L, Guo, H and Kuo, PC. 2004. Osteopontin increases CD44 expression and cell adhesion in RAW 264.7 murine leukemia cells. Immunol Lett. 95:109-12.

281) Calzolari, A, Raggi, C, Deaglio, S, Sposi, NM, Stafsnes, M, Fecchi, K, Parolini, I, Malavasi, F, Peschle, C, Sargiacomo, M and Testa, U. 2006. TfR2 localizes in lipid raft domains and is released in exosomes to activate signal transduction along the MAPK pathway. J Cell Sci. 119:4486-98.

282) Morelli, AE, Larregina, AT, Shufesky, WJ, Sullivan, ML, Stolz, DB, Papworth, GD, Zahorchak, AF, Logar, AJ, Wang, Z, Watkins, SC, Falo, LD, Jr. and Thomson, AW. 2004. Endocytosis, intracellular sorting, and processing of exosomes by dendritic cells. Blood. 104:3257-66.

283) Kovats, S, Main, EK, Librach, C, Stubblebine, M, Fisher, SJ and DeMars, R. 1990. A class I antigen, HLA-G, expressed in human trophoblasts. Science. 248:220-3.

284) Wiendl, H, Feger, U, Mittelbronn, M, Jack, C, Schreiner, B, Stadelmann, C, Antel, J, Brueck, W, Meyermann, R, Bar-Or, A, Kieseier, BC and Weller, M. 2005. Expression of the immune-tolerogenic major histocompatibility molecule HLA-G in multiple sclerosis: implications for CNS immunity. Brain. 128:2689-704.

285) Clements, CS, Kjer-Nielsen, L, Kostenko, L, Hoare, HL, Dunstone, MA, Moses, E, Freed, K, Brooks, AG, Rossjohn, J and McCluskey, J. 2005. Crystal structure of HLA-G: a nonclassical MHC class I molecule expressed at the fetal-maternal interface. Proc Natl Acad Sci U S A. 102:3360-5.

286) Liwski, RS, Chase, JC, Baldridge, WH, Sadek, I, Rowden, G and West, KA. 2006. Prolonged costimulation is required for naive T cell activation. Immunol Lett. 106:135-43.

287) Ducret, A, Nguyen, M, Breckenridge, DG and Shore, GC. 2003. The resident endoplasmic reticulum protein, BAP31, associates with gamma-actin and myosin B heavy chain. Eur J Biochem. 270:342-9.

288) Yang, M, Ellenberg, J, Bonifacino, JS and Weissman, AM. 1997. The transmembrane domain of a carboxyl-terminal anchored protein determines localization to the endoplasmic reticulum. J Biol Chem. 272:1970-5.

289) Wyllie, DH, Kiss-Toth, E, Visintin, A, Smith, SC, Boussouf, S, Segal, DM, Duff, GW and Dower, SK. 2000. Evidence for an accessory protein function for Toll-like receptor 1 in anti-bacterial responses. J Immunol. 165:7125-32.

290) Hajjar, AM, O'Mahony, DS, Ozinsky, A, Underhill, DM, Aderem, A, Klebanoff, SJ and Wilson, CB. 2001. Cutting edge: functional interactions between toll-like receptor (TLR) 2 and TLR1 or TLR6 in response to phenol-soluble modulin. J Immunol. 166:15-9.

291) Ozinsky, A, Underhill, DM, Fontenot, JD, Hajjar, AM, Smith, KD, Wilson, CB, Schroeder, L and Aderem, A. 2000. The repertoire for pattern recognition of pathogens by the innate immune system is defined by cooperation between toll-like receptors. Proc Natl Acad Sci U S A. 97:13766-71.

292) Takeuchi, O, Kawai, T, Muhlradt, PF, Morr, M, Radolf, JD, Zychlinsky, A, Takeda, K and Akira, S. 2001. Discrimination of bacterial lipoproteins by Toll-like receptor 6. Int Immunol. 13:933-40.

293) Meza, JE, Brzovic, PS, King, MC and Klevit, RE. 1999. Mapping the functional domains of BRCA1. Interaction of the ring finger domains of BRCA1 and BARD1. J Biol Chem. 274:5659-65.

294) Inouye, C, Dhillon, N and Thorner, J. 1997. Ste5 RING-H2 domain: role in Ste4-promoted oligomerization for yeast pheromone signaling. Science. 278:103-6.

295) MacKenzie, NM. 2006. New therapeutics that treat rheumatoid arthritis by blocking T-cell activation. Drug Discov Today. 11:952-6.

296) Kurhan-Yavuz, S, Direskeneli, H, Bozkurt, N, Ozyazgan, Y, Bavbek, T, Kazokoglu, H, Eksioglu-Demiralp, E, Wildner, G, Diedrichs-Mohring, M and Akoglu, T. 2000. Anti-MHC autoimmunity in Behcet's disease: T cell responses to an HLA-B-derived peptide cross-reactive with retinal-S antigen in patients with uveitis. Clin Exp Immunol. 120:162-6.

297) VanCompernolle, SE, Wiznycia, AV, Rush, JR, Dhanasekaran, M, Baures, PW and Todd, SC. 2003. Small molecule inhibition of hepatitis C virus E2 binding to CD81. Virology. 314:371-80.

298) DeLisser, HM, Christofidou-Solomidou, M, Strieter, RM, Burdick, MD, Robinson, CS, Wexler, RS, Kerr, JS, Garlanda, C, Merwin, JR, Madri, JA and Albelda, SM. 1997. Involvement of endothelial PECAM-1/CD31 in angiogenesis. Am J Pathol. 151:671-7.

299) Muraoka, N, Shum, L, Fukumoto, S, Nomura, T, Ohishi, M and Nonaka, K. 2005. Transforming growth factor-beta3 promotes mesenchymal cell proliferation and angiogenesis mediated by the enhancement of cyclin D1, Flk-1, and CD31 gene expression during CL/Fr mouse lip fusion. Birth Defects Res A Clin Mol Teratol. 73:956-65.

300) Morabito, F, Mangiola, M, Stelitano, C, Deaglio, S, Callea, V and Malavasi, F. 2003. Simultaneous expression of CD38 and its ligand CD31 by chronic lymphocytic leukemia B-cells: anecdotal observation or pathogenetic hypothesis for the clinical outcome? Haematologica. 88:354-5.

301) Dales, JP, Garcia, S, Andrac, L, Carpentier, S, Ramuz, O, Lavaut, MN, Allasia, C, Bonnier, P and Charpin, C. 2004. Prognostic significance of angiogenesis evaluated by CD105 expression compared to CD31 in 905 breast carcinomas: correlation with long-term patient outcome. Int J Oncol. 24:1197-204.

302) Grumet, FC, Hiraki, DD, Brown, BWM, Zehnder, JL, Zacks, ES, Draksharapu, A, Parnes, J and Negrin, RS. 2001. CD31 mismatching affects marrow transplantation outcome. Biol Blood Marrow Transplant. 7:503-12.

303) El-Chennawi, FA, Kamel, HA, Mosaad, YM, El-Sherbini, SM and El-Billey, NA. 2006. Impact of CD31 mismatches on the outcome of hematopoeitic stem cell transplant of HLA-identical sibling. Hematology. 11:227-34.

304) Breckenridge, DG, Stojanovic, M, Marcellus, RC and Shore, GC. 2003. Caspase cleavage product of BAP31 induces mitochondrial fission through endoplasmic reticulum calcium signals, enhancing cytochrome c release to the cytosol. J Cell Biol. 160:1115-27.

305) Maatta, J, Hallikas, O, Welti, S, Hilden, P, Schroder, J and Kuismanen, E. 2000. Limited caspase cleavage of human BAP31. FEBS Lett. 484:202-6.

306) Wasilenko, ST, Stewart, TL, Meyers, AF and Barry, M. 2003. Vaccinia virus encodes a previously uncharacterized mitochondrial-associated inhibitor of apoptosis. Proc Natl Acad Sci U S A. 100:14345-50.

307) Wasilenko, ST, Banadyga, L, Bond, D and Barry, M. 2005. The vaccinia virus F1L protein interacts with the proapoptotic protein Bak and inhibits Bak activation. J Virol. 79:14031-43.

308) Taylor, JM, Quilty, D, Banadyga, L and Barry, M. 2006. The vaccinia virus protein F1L interacts with Bim and inhibits activation of the pro-apoptotic protein Bax. J Biol Chem. 281:39728-39.

309) Hwang, SI, Lundgren, DH, Mayya, V, Rezaul, K, Cowan, AE, Eng, JK and Han, DK. 2006. Systematic characterization of nuclear proteome during apoptosis: a quantitative proteomic study by differential extraction and stable isotope labeling. Mol Cell Proteomics. 5:1131-45.

310) Thiede, B, Kretschmer, A and Rudel, T. 2006. Quantitative proteome analysis of CD95 (Fas/Apo-1)-induced apoptosis by stable isotope labeling with amino acids in cell culture, 2-DE and MALDI-MS. Proteomics. 6:614-22.

311) Romijn, EP, Christis, C, Wieffer, M, Gouw, JW, Fullaondo, A, van der Sluijs, P, Braakman, I and Heck, AJ. 2005. Expression clustering reveals detailed co-expression patterns of functionally related proteins during B cell differentiation: a proteomic study using a combination of one-dimensional gel electrophoresis, LC-MS/MS, and stable isotope labeling by amino acids in cell culture (SILAC). Mol Cell Proteomics. 4:1297-310.

312) Guerrero, C, Tagwerker, C, Kaiser, P and Huang, L. 2006. An integrated mass spectrometry-based proteomic approach: quantitative analysis of tandem affinity-purified in vivo cross-linked protein complexes (QTAX) to decipher the 26 S proteasome-interacting network. Mol Cell Proteomics. 5:366-78.

313) Goto, T, Kennel, SJ, Abe, M, Takishita, M, Kosaka, M, Solomon, A and Saito, S. 1994. A novel membrane antigen selectively expressed on terminally differentiated human B cells. Blood. 84:1922-30.

314) Villen, J, Beausoleil, SA, Gerber, SA and Gygi, SP. 2007. Large-scale phosphorylation analysis of mouse liver. Proc Natl Acad Sci U S A. 104:1488-93.

315) Warren, MR, Parker, CE, Mocanu, V, Klapper, D and Borchers, CH. 2005. Electrospray ionization tandem mass spectrometry of model peptides reveals diagnostic fragment ions for protein ubiquitination. Rapid Commun Mass Spectrom. 19:429-37.